

3.4 Non-metallic atomic adsorbates on metals and semiconductors

3.4.1 Adsorbate properties of hydrogen on solid surfaces

3.4.1.1 Introduction

Hydrogen is the most abundant chemical element in the universe. On earth and at temperatures below ~ 2000 K the thermodynamic stable form of hydrogen is dihydrogen H_2 . This simplest homonuclear diatomic molecule exhibits a strong chemical bond (bond dissociation energy 432 kJ/mol) which may be considered the prototype of covalent bonding. A survey of the physical and chemical properties of H_2 and hydrides has been given by Silvera [80Sil]. A full potential energy surface (PES) for the H_2 molecule has been calculated by Shavitt et al. [68Sha]. For a variety of reasons (hydrogen's role in heterogeneous catalysis, battery and fuel cell technology, materials science, plasma physics), its interaction with solid surfaces (preferentially metallic surfaces) has attracted and still attracts much attention in science and technology. It is useful, for chemical and energetic reasons, to distinguish the interaction of H *atoms* and that of H_2 *molecules* (which is by far more important) with these surfaces. A fairly consistent understanding of the underlying general chemical scenario has arisen from the numerous surface studies performed hitherto: The thermal H_2 molecule approaches the surface and is transiently trapped in a weakly bound precursor state. It can either reside in this state for some time or move on towards a more strongly bound state, dissociate into atoms, which then become adsorbed in a deep chemisorption potential. Depending on the thermal energy of the physisorbed molecule or chemisorbed atom compared to the depth of the adsorption potential well the hydrogen particle may be able or unable to migrate across the surface whereby also tunnelling processes can play a role. With a given layer of adsorbed hydrogen atoms formed by dissociation, also the reverse process, namely, the recombination of two individual H atoms to dihydrogen and its desorption is a likely event, especially at elevated temperatures.

The hydrogen - surface interaction may be thermally activated and will then be governed by kinetics rather than by thermodynamics. Accordingly, the field of hydrogen reaction dynamics and kinetics represents a topic of greatest scientific interest, experimentally as well as theoretically. Modern (quantum-state selective) spectroscopic techniques render the investigation and (in many cases state-selective) characterization even of ultra-short particle - surface interaction steps possible [88Zac, 90Zac].

However, once the adsorbed hydrogens (be it molecules or atoms) have been accommodated on the solid surface, the system has usually reached thermodynamic equilibrium. Depending on temperature the particles either reside in distinct adsorption sites and often form ordered two-dimensional phases (*localized* or *immobile* adsorption, preferred at low temperatures) or they can freely migrate across the surface (*delocalized* or *mobile* adsorption dominating at elevated temperatures) and then be considered within the framework of a *lattice gas* system. Of course, various transitions between these two extreme cases are conceivable, for example, particle hopping and site exchange processes. In addition, due to the light mass of H, delocalization by quantum-mechanical tunnelling may contribute to H surface diffusion, especially at very low temperatures [86Wha]. Generally, the hydrogen adsorption process can be considered a transition from an initial state (= clean, i.e., uncovered, solid surface plus an ensemble of gaseous hydrogen molecules) to a final state (= surface covered with a two-dimensional layer of adsorbed hydrogen molecules or atoms). In this scheme the solid surface must not be considered a rigid lattice of periodic adsorption sites; many studies revealed that the solid surface is a dynamic, flexible and 'soft' system that will instantaneously respond (geometrically and electronically) to the presence of hydrogen. Consequently, surface restructuring effects are the rule rather than the exception affecting both surface energetics and geometry, c.f., sects. 3.4.1.3.3. and 3.4.1.3.4.

Another noteworthy property of adsorbing hydrogen is its ability to migrate through the topmost surface layer, enter the surface-near crystal region and accommodate in subsurface and bulk sites, respectively, a process referred to as *sorption* or *absorption*. A variety of metals is known which dissolve hydrogen gas quite readily, among others Ti, V, Zr, Nb, Hf, Ta, and, most notably, Pd [67Lew, 78Wic, 79Bur]. Both subsurface and bulk absorption sites can be distinguished from the (surface) location of

adsorbed H atoms in a simple one-dimensional potential energy diagram (Fig. 1). The various potential energy wells are separated by (usually H concentration-dependent) activation barriers making the H uptake temperature dependent. A wealth of literature exists concerning the sorption properties of these metals (which cannot be covered here for the sake of space limitation); overviews are given, for example, in the monograph ‘Hydrogen in Metals’ [78Ale] and other review articles [92Sch2, 01Kir].

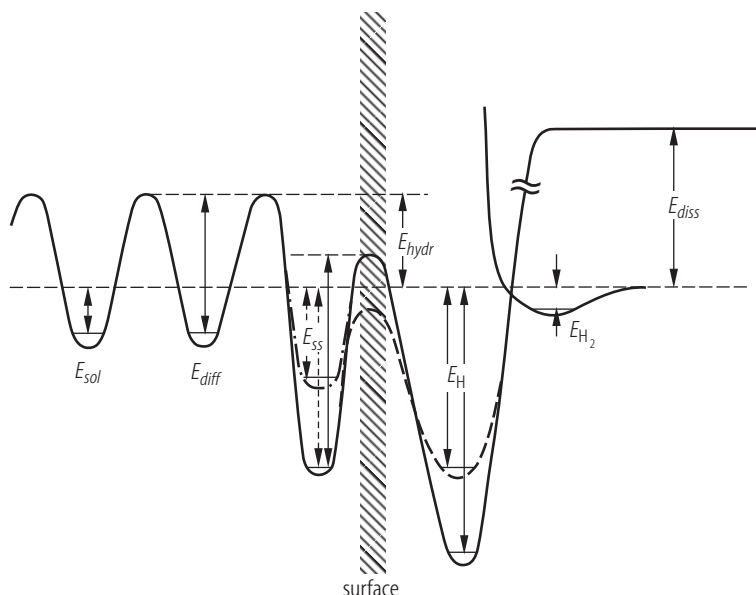


Fig. 1: One-dimensional diagram illustrating the change in potential energy of a hydrogen molecule approaching a metal surface (indicated by the hatched area). It describes the energetic situation during the following processes

- Physisorption of the H_2 molecule into a shallow potential energy minimum of depth E_{H_2}
- Dissociation of the H_2 molecule and the formation of a stable chemisorptive bond with adsorption energy E_H .
- Transport of H atoms into subsurface sites, with a coverage-dependent sorption energy E_{ss} .
- (Possible) absorption of H atoms in interstitial sites with heat of solution E_{sol} . Indicated is also the activation energy of diffusion of the respective H atoms, E_{diff} .

Probably one of the most important quantities which governs adsorption and desorption phenomena is the hydrogen surface concentration (number of atoms or molecules per m^2). The related quantity mostly used in experimental work is the hydrogen *coverage* Θ , which is usually defined as a dimensionless quantity between 0 and 1, relating the number of actually adsorbed particles (H atoms or H_2 molecules in the first layer) with the maximum number of adsorption sites (or sometimes substrate *surface* atoms per unit area):

$$\Theta_H = \frac{N_{ad}}{N_{max}} \quad (1)$$

Multiplying Θ_H with the number of substrate surface atoms, N_{max} , yields the number of the adsorbed H atoms per m^2 . Since in most cases the H-related system properties (listed in the upcoming tables) will depend on Θ_H , this quantity will be given where necessary.

This survey of hydrogen - surface interaction is organized in the following manner: We will accompany a hydrogen molecule on its way towards the surface and make a coarse distinction between (time-dependent) *kinetic* properties on the one hand and *equilibrium* phenomena consisting of (static)

energetic, structural (geometric and electronic) and vibrational properties on the other hand. In the first category (dealing with *kinetic* phenomena) we will list the available data for the *initial sticking probability*, the *frequency factor* and the *reaction-order* for desorption. Where the respective data exist we will also include activation energies for adsorption, because (as mentioned above) the adsorption *dynamics* of hydrogen has received considerable interest during the last decade, motivated by the increasingly more sophisticated (molecular beam and/or quantum-state resolved short time) experiments and calculations. In the second part we will expand on the *equilibrium* properties, namely, *kind and number of hydrogen adsorption states*, (coverage-dependent) *adsorption/ desorption energy*, *surface structure* (long-range ordered phases with and without reconstruction), *structural phase transitions*, *local adsorption site geometry* (bond length, coordination number), *vibrational frequencies*, and *electronic structure* (adsorbate-induced electronic-bonding states and work function changes). In a final chapter, a brief overview over the theoretical attempts to describe the H₂ dissociation and H chemisorption will be given.

Quite generally, the position of the respective substrate element in the periodic table will be the ordering principle of the various interaction systems, whereby the available data for elemental semiconductors and non-metallic elemental solids will be listed separately. For the sake of reliability, only those data will be considered that have been measured with clean and structurally well-defined *single crystal surfaces*. In this sense, we have tried to include most of the relevant data available in the literature, and it is possible, by comparing older with more recent data, to directly follow the progress that has been made in the respective research area during the past twenty or thirty years. Not in all instances a complete data base will be found in the columns of the tables – despite the relatively many “white spots” on the map of hydrogen properties it is deemed useful to give the citation which offers the possibility to at least look up the reference and judge on the kind and quality of the respective scientific work.

3.4.1.2 Some general principles of the hydrogen – surface interaction

Our current understanding of the interaction of hydrogen with solid surfaces is documented in several review articles [82Kno, 88Chr, 90Dav]. Most of these reviews are concerned with the interaction of hydrogen with *metal* surfaces, only in some cases also its interaction with semiconducting or insulating surfaces is addressed in sections 3.6.1 and 3.6.2 in part 3 of this Landolt-Börnstein volume III/42A, because interest in the interaction of hydrogen with these materials has arisen only during the past decade [90Hig, 90Cha, 96Hoe, 99Bal], especially in conjunction with the discovery that H atoms can lift the semiconductor's inherent surface reconstruction by selectively saturating its dangling bonds. As a consequence, the respective reconstructions are replaced by (1×1) surface phases with H termination, prominent examples being the Si(111)-(1×1)-H [91Cha] or the diamond C(111)-(1×1)-H surfaces [91Mit].

A well-known property of the hydrogen molecule is its ability to dissociate into H atoms when getting into contact with surfaces. The H atoms then can interact quite strongly with the solid leading to the process of *chemisorption* with typical binding energies ranging between 50 and ~150 kJ/mol. Further reactions that affect the chemical state of the solid may consist of dissolution, absorption and compound (hydride) formation: Hydrogen often exhibits a peculiar reactivity here because of its small size. Note that the dissociation reaction itself can proceed as a homolytic process, according to the scheme: $\text{H}_2 \leftrightarrow \text{H}^\bullet + \text{H}^\bullet$, or heterolytic, along the path: $\text{H}_2 \leftrightarrow \text{H}^+ + \text{H}^-$. On metals, the homolytic step is certainly the rule, while on (polar) semiconductor and insulating surfaces (oxides, in particular) also the heterolytic mechanism has been reported.

An electrically neutral hydrogen molecule arriving from the gas phase and getting in contact with a solid surface will first experience a (weak) van-der-Waals potential in which it is physisorbed at sufficiently low temperatures. Generally, the binding forces acting between the trapped H₂ molecule and the surface are quite small, due to the closed-shell character of H₂. The respective adsorption energies lie well below ~10 kJ/mol and resemble the condensation enthalpy of elemental hydrogen. Accordingly, temperatures around or below 20 K are required to stabilize H₂ molecules on the surface [82Avo]. However, it was shown that on otherwise active metal surfaces with special geometry, containing steps

and/or holes such as Ni(510) or Pd(210), H₂ dissociation may be kinetically hindered resulting in a chemisorbed molecular hydrogen species which can be stable up to 100...130 K [86Mar, 93Nyb, 01Sch1]. Physisorption is the only interaction if chemically inert (insulating and/or semiconducting) surfaces are exposed to hydrogen gas at low temperatures.

A completely different situation is encountered when surfaces are exposed to H *atoms*. Then a strong chemical interaction (often leading to compound, i.e. hydride, formation) is the rule. It is worth to mention here that semiconducting or insulating surfaces as well as free electron and/or noble metal surfaces (Cu, Ag, Au) [95Ham2] with their deep-lying d electron states exhibit a surprisingly small activity to dissociate H₂ molecules, in contrast to transition metal (TM) surfaces with their high density of d electron states at the Fermi level (E_F) [98Chr]. Typical transition metals (e.g., Ni, Ru, or Pt) effectively catalyze the spontaneous homolytic dissociation of dihydrogen, especially in the presence of active (defect) sites [88Ren]. It is thought that the existence of empty d electron states right at E_F allows the filled molecular orbitals of the H₂ molecule to effectively circumvent the Pauli repulsion barrier by rehybridization [88Har, 89Har]. This process is not possible with free-electron metals such as Cu, Ag, or Au because of their lack of empty d electron states right at E_F . [This matter will be taken up again in sect. 3.4.1.3.5 which is devoted to the electronic interaction between a hydrogen molecule and a metal surface]. Accordingly, the activation barriers for dissociation and chemisorption of hydrogen on these surfaces are relatively large [81Nor1]. This has motivated a whole number of studies, especially during the last two decades, to expose the respective materials either to thermally excited H₂ beams (using supersonic molecular beam techniques, often with well-defined translational and/or rovibrational quantum-states) to overcome the dissociation barrier, or to dissociate the H₂ molecules prior to adsorption in the gas phase (either by the thermal energy of a hot tungsten filament (following Langmuir's early recipe [12Lan, 14Lan, 15Lan])) or by a hydrogen RF discharge operating at a frequency of 2.450 GHz [88Bas]). By exposure to a reactive beam of H atoms, many surfaces which are inert with respect to 'normal' H₂ gas exposure can be forced to build up atomic hydrogen layers, e.g., Cu, Ag, Au, but also diamond, silicon and various alkaline, alkaline earth, and earth metals. Particularly these latter materials quite easily form salt-like (in some cases volatile) hydrides, AlH₃ being a good example [91Kon].

Within simple transition-state theory, the process of dissociation and subsequent atomic adsorption can be visualized by a two-dimensional potential hyperface [85Kno] either with an 'early' or with a 'late' activation barrier; in other words, the dissociation reaction may be supported by translational (early barrier) or vibrational excitation (late barrier) of the incoming molecule [87Pol]. The situation is illustrated by means of Fig. 2. Quantum-chemical calculations performed, e.g., with the Pd(100)/H₂ system clearly revealed the quite complex nature of the dissociation reaction as a multi-dimensional process [95Gro1, 98Gro, 99Eic]. Generally, up to 6 dimensions are considered when calculating the potential energy surfaces (PES) for the H₂ dissociation reaction. Latest experimental developments in low-temperature scanning tunnelling microscopy (STM) have made it possible to directly watch hydrogen molecules dissociating on a Pd(111) surface [03Mit2], with the interesting result that the dissociation event requires – at least for the Pd(111)/H₂ system – more than two adjacent empty adsorption sites, namely, at least three such sites, a conclusion that had been indirectly deduced from H adsorption studies on bimetallic Ru surfaces more than twenty years ago [80Shi].

After H₂ dissociation a layer of H atoms is readily built up, a process referred to as hydrogen *chemisorption*, with appreciable adsorption energies involved: The trapped H atoms reside at the bottom of a deep chemisorption potential; neighboring sites can be reached by hopping or tunnelling. While the dynamics of dissociation may be fairly complicated [03Gro] – the overall energetics can be relatively simply visualized in terms of the one-dimensional Lennard-Jones potential model (Fig. 3). It can easily be seen that the following energy balance holds

$$E_{\text{Me-H}} = \frac{1}{2}(E_{ad} + E_{diss}), \quad (2)$$

in which E_{ad} stands for the adsorption energy (i.e., depth of the adsorption potential) and E_{diss} denotes the H - H bond dissociation energy (= 432 kJ/mol). $E_{\text{Me-H}}$ is the binding energy of a single H - metal adsorptive bond. At room temperature, chemisorbed H atoms may stay for quite a while in the respective potential, since the energies involved (E_{ad}) can easily reach 100 kJ/mol or more for typical transition metals. Frequent structural consequences of these strong interaction forces are relaxation or

reconstruction phenomena of the substrate either locally, i.e., in the direct vicinity of an adsorbed atom, or by H-induced perturbations of the surface electronic structure with long-range character. Further interaction steps can include occupation of subsurface (between the topmost and second substrate layer) or bulk sites (H solution or absorption processes), or compound (hydride) formation, Pd-H being a well-known example.

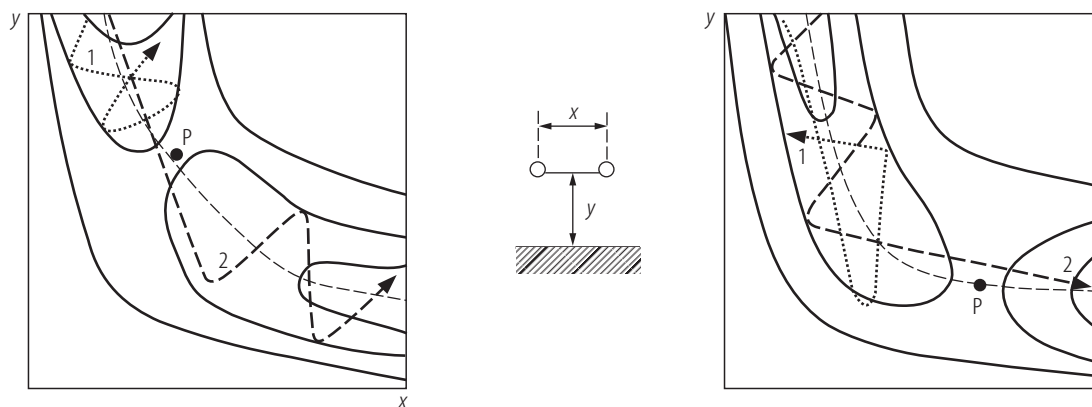


Fig. 2: Two-dimensional representation (so-called elbow plots) of the potential energy surface of the H_2 molecule interacting with an active metal surface. The coordinate x denotes the internuclear H - H distance, y the distance of the molecular entity to the surface. Several trajectories are indicated: (1) denotes a reflection trajectory (unsuccessful event) with no chemisorption, (2) a successful approach leading to dissociation. Note that the saddle point P can be located either in the 'entrance' channel relatively far away from the surface (left-hand side) or in the 'exit' channel (right-hand side). In the first case, mainly translational energy of the H_2 molecule is required for a successful passage across the barrier, while vibrational excitation is advantageous if P is located closer to the surface.

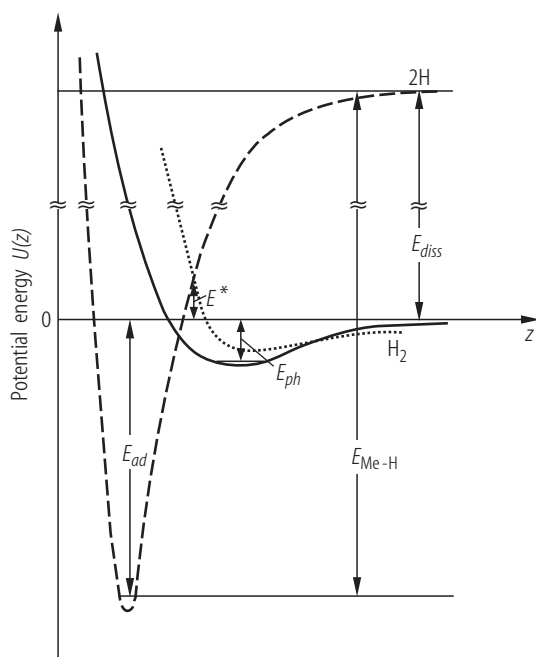


Fig. 3: One-dimensional potential energy (Lennard-Jones) diagram of a H_2 molecule interacting with an active (full line) and an inactive metal surface (dotted line). The dashed line indicates the potential energy $U(z)$ if the H_2 molecule is pre-dissociated in the gas phase (dissociation energy E_{diss}) and the two isolated, reactive, H atoms approach the surface. The deep potential energy well (E_{Me-H}) represents the energy of the metal - H bond formed (which is gained twice). While the shallow physisorption minimum E_{phys} characteristic of inactive surfaces causes the intersection between the dotted and dashed line to occur at positive energies (above zero) and, hence, leads to an activation barrier of height E^* , a deeper physisorption well pushes the respective intersection to negative energies (below zero) thus enabling a non-activated (spontaneous) dissociation (cross-over between the full and the dashed line). Accordingly, the heat of adsorption, E_{ad} , is released.

At higher temperatures, two chemisorbed H atoms will diffuse, meet each other, recombine and desorb as a H_2 molecule, leaving behind the empty surface. This process of desorption can be considered the time reverse of the adsorption process and is usually described in terms of simple kinetic models based on transition-state theory (TST). However, a correct description of the rate of desorption becomes difficult, if the adsorption and dissociation are activated processes [01Wet]. Possible accompanying

processes such as adsorbate-induced structural phase transformations, occupation of subsurface sites or bulk (sorption) phenomena can and will introduce even more severe obstacles in the endeavor to quantify the complete interaction scenario.

3.4.1.3 The interaction of hydrogen with solid surfaces: experimental data

3.4.1.3.1 Adsorption kinetics

3.4.1.3.1.1 Introductory remarks

The quantity that governs the hydrogen uptake of a given surface is the sticking coefficient s . It is understood as the probability that a gaseous particle hitting the surface will become adsorbed for a finite time rather than be immediately back-reflected into the gas phase. ‘Finite’ time means that the particle must have accommodated on the surface and lost the memory from which direction it has impinged; it varies with the depth of the interaction potential and depends on the surface temperature. Following Groß [03Gro], the decisive condition for sticking or trapping is that the particle can transfer its kinetic energy to the substrate. He defines a function $P_E(\varepsilon)$ which is the probability that an incoming particle with kinetic energy E will transfer the energy ε to the surface. If the particle transfers at least its entire gas phase kinetic energy to the surface it safely remains trapped in the adsorption potential, and the (energy-dependent) sticking probability can be expressed as

$$s(E) = \int_E^{\infty} P_E(\varepsilon) d\varepsilon \quad (3)$$

For more details on definitions of s , its coverage and temperature dependencies, precursor kinetics etc., we refer to the special literature [84Mor, 92Ren] and to the introductory chapters 1 and 2 of this Landolt-Börnstein subvolume III/42A (which you can find in parts 1 and 2, respectively). Generally, the (coverage-dependent) sticking probability can be regarded as a product of an initial, coverage-independent, but system-immanent, factor, s_0 , called the *initial sticking coefficient*, and a function $f(\Theta)$ which contains the coverage dependence. Then, using simple kinetic theory, the rate of adsorption r_{ad} becomes

$$r_{ad} = \frac{d\Theta}{dt} = s_0 \cdot f(\Theta) N_{max}^{-1} \frac{P_{H_2}}{\sqrt{2\pi m k T}} \cdot \exp\left(-\frac{E_{ad}^*}{kT}\right), \quad (4)$$

in which P_{H_2} stands for the hydrogen gas pressure, N_{max} for the maximum number of adsorbed particles, m for the absolute mass of the molecule, and E_{ad}^* for a (possibly important) activation barrier in the adsorption process to account for a temperature dependence of the sticking probability.

It is important to note here that especially *hydrogen* sticking depends quite sensitively on the physical state of the solid surface (impurities, structural features, structural defects, foreign atoms) as pointed out by Poelsema et al. [85Poe] for the system H on Pt(111) and in a comprehensive article by Rendulic and Winkler [89Ren2]. Usually, surfaces rich in defects show a much larger activity in trapping (and subsequently dissociating) H_2 molecules than smooth surfaces (smooth on the microscopic scale), the difference sometimes amounting to several orders of magnitude. In the catalytic chemist’s language these defects are known as ‘active sites’ and can strongly influence the general chemical reactivity of a given system. In the same sense, even traces of foreign atoms can hinder or enhance hydrogen sticking quite effectively. It is not trivial to detect and characterize traces of surface impurities (in the order of a few percent of a monolayer) and it is even more difficult to ascertain the short-range crystallographic order of a given surface. Therefore, the literature data available for s_0 have to be considered with some care, especially data that were obtained from surfaces whose crystallographic order and chemical cleanliness

were not properly controlled. Only in a few cases the surfaces were sufficiently well characterized, e.g., by parallel scanning tunnelling microscopy (STM) or LEED measurements. Another problem concerns temperature dependencies of the sticking – especially when the adsorption is activated. In these cases, the sticking coefficient depends sensitively on the kinetic and internal energy of the incoming hydrogen molecule, and only quantum-state selective molecular beam and coupled laser experiments can provide the necessary physical information. Using standard Boltzmann formalism, the height of the activation barrier for adsorption can nevertheless be estimated from the temperature dependence of the hydrogen uptake.

3.4.1.3.1.2 The initial sticking probability

The initial sticking coefficient of hydrogen s_0 reflects the specific energy accommodation and dissipation properties of a given hydrogen – surface interaction system. In the *zero-coverage* limit ($\Theta \rightarrow 0$) one actually considers the sticking probability of the first impinging hydrogen molecule. The energy accommodation can occur either by direct coupling of the respective molecule to the surface phonons of the heat bath of the solid or (in case of metals) by excitation of electron – hole pairs right at the Fermi level (electronic friction) [77Kno, 80Sch1, 82Sch, 97Men, 99Nie]. In a simple approximation, the impinging event is considered as a binary elastic collision between a gas particle of mass m and initial energy E_i and a fixed surface atom of mass M . Applying the rules of energy and momentum conservation, the amount of transferred energy, $\Delta E = E_i - E_f$ is described by the classical Baule expression [14Bau] (μ being the mass ratio m/M):

$$\Delta E = \frac{4\mu}{(1+\mu)^2} E_i \quad (5)$$

The respective energy is then used to heat up the phonon bath of the solid. It has been argued that with hydrogen as the lightest molecule ($m \ll M$) this phonon coupling mechanism is not as effective as it is for heavier adsorbate species [76Bre, 79Mue, 79Bre, 80Sed, 82Bre]. A principally much more complicated situation arises, if a *molecule* (such as the H_2 molecule) can or will dissociate as it hits the surface. Sophisticated multi-dimensional quantum chemical calculations are required to describe this dissociation event properly. Recent theoretical treatments revealed that dynamical steering processes (i.e. the time-dependent orientation of the incoming molecule with respect to the configuration of the substrate atoms) can decisively govern the hydrogen dissociation reaction [95Gro1, 95Gro2, 98Gro].

3.4.1.3.1.3 The coverage dependence of the sticking probability

Sticking or trapping requires at least a single empty adsorption site. As the filling of the adsorption sites proceeds, s usually decreases with coverage as accounted for by the function $f(\Theta)$ in Eq. (4). For non-dissociative adsorption (H_2 molecules at very low temperatures) and negligible lateral interactions, $f(\Theta)$ simply equals $1 - \Theta$; for dissociative adsorption (H_2 on TM surfaces) and vanishing mutual interactions, $f(\Theta) = (1 - \Theta)^2$. Formation of phases with long-range order or laterally inhomogeneous phases (islands etc.) require more complicated expressions. Furthermore, one has to take into account that impinging molecules can become transiently trapped in a weak van-der-Waals potential in which they can ‘live’ for a few microseconds and diffuse across the surface, until they find an empty adsorption site. This well-known precursor kinetics strongly affects the coverage dependence of the sticking probability and various $s(\Theta)$ relations have been derived and reported in the literature, among others by Kisliuk [57Kis, 58Kis]. More details on precursor kinetics, terms and definitions can be found in the review by King, Bowker, and Morris [84Mor]. Since trapped hydrogen molecules are usually only very weakly bound, precursor kinetics are not often observed in hydrogen adsorption experiments performed in the temperature range from 77 to 300 K, in contrast to carbon monoxide adsorption on transition metal surfaces where Kisliuk-type adsorption kinetics is almost the rule. Generally, the hydrogen sticking coefficient drops markedly

with increasing coverage. As an example, we present the $s(\Theta)$ relation for the system hydrogen on Rh(110) in Fig. 4, which shows in addition the influence of the formation of ordered H phases and a marked isotope effect [88Ehs].

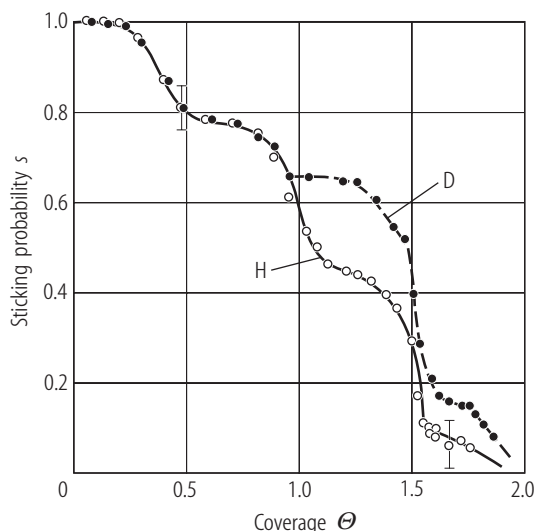


Fig. 4: Coverage dependence of the sticking probability of hydrogen and deuterium interacting with a clean rhodium(110) surface at $T = 100$ K. On this surface, hydrogen forms various phases with long-range order which apparently has some influence of the shape of the curve $s(\Theta)$ [88Ehs].

3.4.1.3.1.4 The experimental determination of sticking coefficients

Convenient means to measure initial sticking probabilities use i) direct gravimetry, e.g., by a microbalance [78Rob] or a quartz oscillator [74Bry], ii) thermal desorption [91Chr] or iii) flow methods (which have the advantage of a continuous measurement of the rate of adsorption) using calibrated capillaries or molecular beam (MB) techniques [78Eng]. A widely used method was proposed by King and Wells [72Kin], which is especially suited for single crystal samples: The gas is introduced to the system by means of a sharp molecular beam. The recipient contains two gauges, only one of which can receive molecules directly from the gas source. The other gauge measures the ambient pressure, and by comparison a simple expression for s results.

In the following tables, we have listed most of the accessible sticking coefficient data reported for *single crystalline* surfaces. The data are organized as follows: s_0 for metals (listed according to the groups of the periodic table and subdivided with respect to the crystallographic orientation), and, in a separate short section, for semi- and non-conducting chemical elements. Note, however, that for these latter systems there is only a very scarce base of reliable data.

3.4.1.3.1.5 The sticking probability of hydrogen on metal surfaces

Note that most of the measurements of Table 3.4.1.3.1.5 refer to data that have been measured in the temperature range from ~ 80 K (liquid N_2) to room temperature. One can safely assume that hydrogen adsorbs dissociatively on most transition metal (TM) surfaces in this temperature range, however, a couple of smooth, low-index TM surfaces such as Ni(100) [85Ham, 93All], Ni(111) [89Ren1], or Pt(111) [85Poe], exhibit surprisingly low hydrogen sticking coefficients, provided these surface are free of crystallographic defects or impurity atoms. Slight activation barriers of adsorption of hydrogen on these surfaces have thus been concluded; this is indicated in the table.

A somewhat different situation is encountered if the samples are exposed to H_2 gas at temperatures far below 80 K, i.e., around 10...50 K. In this case, *molecular* hydrogen adsorption competes with dissociative (atomic) adsorption (the latter may be weakly thermally activated). The residence time of the hydrogen molecules in the shallow van-der-Waals adsorption potentials usually increases with falling

temperature and may, in addition, sensitively depend on coverage, surface roughness and quantum-mechanical effects, leading to the interesting situation that the sticking probability $s(\theta)$ can indeed increase with coverage in the low-coverage regime, because molecule - molecule collisions on the surface help to provide the energy accommodation [88Wil]. Only at medium coverages a constant, θ -independent sticking due to condensation is observed [95Fri]. However, not too many measurements have been performed under these low-temperature conditions, experiments with Cu(100) at 10 K [83And, 88Wil, 93And], Pd(210) and Ni(210) at 40...50 K are examples [01Sch2]. For the latter TM surfaces indeed a competition between molecular and atomic adsorption has been observed and theoretically explained [98Mus, 01Sch1].

Metal surfaces

Surface	Surface temperature [K]	Initial sticking coefficient s_0	Remarks	Reference
V(111)	223	0.60	MB experiments, performed with deuterium	00Beu
Fe(100)	300	0.03		80Ben
Fe(100)	300	1.5×10^{-3}		91Ber2; 92Ber1
Fe(110)	150	0.16		77Boz
Fe(110)	200...450	0.15...0.18		88Kur
Fe(110)	300	1.2×10^{-2}		91Ber2
Fe(111)	300	1.6×10^{-2}		91Ber2
Fe(211)	40...200	1.0	T -dependent reconstruction	95Sch1
Co(0001)	300	0.045	activated adsorption	79Bri
Co(10-10)	100...200	>0.8	T -dependent reconstruction	94Ern
Ni(100)	120	0.06...0.1	activated adsorption	85Ham
Ni(100)	120	0.06		79Chr1
Ni(100)	250	0.19	SIMS study	88Zhu
Ni(110)	300	0.01		73McC
Ni(110)	100	0.9...1.0	T -dependent reconstruction	89Chr
Ni(110)	140	0.96	T -dependent reconstruction	82Win
Ni(110)	100	0.87	T -dependent reconstruction	85Chr
Ni(110)	155	0.1	expts. performed with deuterium	85Rob
Ni(110)	300	~0.55	MB studies with nozzle beams of different energies; mixture of activated and non-activated sites	89Ren1
Ni(111)	200	0.15 ± 0.05	absolute (volumetric) measurement	74Rin
Ni(111)	140	0.05	activated adsorption	82Win
Ni(111)	155	0.1	expts. performed with deuterium ; activated adsorption	85Rob
Ni(111)	300	<0.1; s_0 increases with beam energy	MB studies with nozzle beams of different energies; activated adsorption, barrier height ~5...10 kJ/mol	89Ren1
Ni(111)-(2×2)-2H	220	0.45	TOF-low energy recoil spectrometry	99Ito

Surface	Surface temperature [K]	Initial sticking coefficient s_0	Remarks	Reference
Ni(210)	100	~ 1		01Sch2
Cu(100)	15	0.05 at $\Theta \rightarrow 0$	MB expts. with H ₂ and D ₂	85And
Cu(100)	15	0.03 at $\Theta \rightarrow 0$; ~ 0.5 at $\Theta = 0.8$	MB expts. with D ₂ at very low T (physisorption)	88Wil
Cu(100)	10	0.27 (D ₂)	MB studies of H ₂ (D ₂) physisorption	93And
Cu(100)	218...258	2.5×10^{-13} (H ₂) 7.8×10^{-14} (D ₂)	H ₂ pressures up to 5 bar were used	93Ras
Cu(100)	300	$\sim 10^{-5}$	MB expts.	89Ang1
Cu(110)	15	0.38 (D ₂)	MB expts. with D ₂ at very low T (physisorption)	93And
Cu(110)	140	~ 0	MB expts	89Hay
Cu(110)	200	0.18 \pm 6%	TDS expts., surface exposed to H atoms	93Bis
Cu(110)	90	0.05 \pm 0.04	TDS expts.; surface exposed to H atoms	94Roh
Cu(111)	10	0.25	MB expts. With D ₂ at very low T (physisorption)	93And
Cu(111)	5...300 K	0		83Gre
Cu(111)	300	$\sim 10^{-5}$	MB expts.	89Ang1
Cu(111)	300	$< 10^{-7}$	MB expts. with D ₂	92Ret1
Nb(100)	90	0.23 (state 1) 0.056 (state 2)		74Hag
Nb(110)	300...550	0.91 \pm 0.01	T -dependent ; competing absorption	81Pic
Mo(110)	78	0.10		72Mad
Mo(110)	300	0.35	MB expts.	72Cha
Mo(110)	350	0.06	ESD expts.	89Ern
Mo(100)	300	0.7	MB expts.	72Cha
Mo(100)	210	1	TDS	92Baf
Mo(111)	300	0.7	MB expts.	72Cha
Mo(211)	100...320	0.76 \pm 0.08		94Lop
Ru(0001)	95	0.58	N species	85Feu
	173	0.03	P species precursor kinetics	
Ru(0001)	100	0.25 \pm 0.1		80Shi
Ru(0001)	250	0.1		79Sch
Ru(0001)	100	0.4		78Dan
Ru(0001)(1 \times 1)H	5	0.03	physisorption; sticking coeff. increases linearly with Θ up to 0.6 at $\Theta \approx 0.6$	95Fri
Ru(10-10)	100	1.0		89Lau
Rh(100)	100	0.53 \pm 0.05	expts. performed with D ₂	82Kim
Rh(100)	90	High		88Ric1
Rh(110)	80	0.97 \pm 0.1		88Ehs
Rh(111)	100	0.65		79Yat

Surface	Surface temperature [K]	Initial sticking coefficient s_0	Remarks	Reference
Rh(111)		0.33 (H ₂) 0.28 (D ₂)	MB expts.	99Beu
Rh(111)	180...305	0.01 ± 0.005	MB expts.; activated adsorption	96Col
Rh(311)	90	0.25		91Nic1
Rh(311)	35	0.30	theoretical analysis	99Pay
Pd(100)	170	0.5	precursor kinetics	80Beh
Pd(110)	130	0.7		83Cat1, 88He1
Pd(111)	200	0.15		76Con1
Pd(111)	100	0.5...0.6	MB studies with nozzle beams of different energies	95Beu1
Pd(111)	80	0.5		87Gdo
Pd(111)	423	0.76 ± 0.05	MB studies quantum-state resolved	97Gos
Pd(210)	90	~1		98Mus 01Sch1
Pd(311)	40...200	1		98Fri
Ag(111)	10	~1 near $\Theta = 1$ ML	HREELS data	82Avo
Ag(111)	110	~0	expts. performed with D ₂ thermal beams	95Hea
W(100)	78...300	0.077 ± 0.008 0.133 ± 0.013	β_1 state β_2 state	69Tam 70Tam
W(100)	190...900	0.50 ± 0.03	MB expts.	89Aln
W(100)	300	0.65		66Est
W(100)	300	0.51 ± 0.03 (H ₂) 0.57 ± 0.03 (D ₂)	calibrated capillary	73Mad
W(100)	300	0.56		74Bar
W(100)	170...400	0.60 ± 0.03		80Kin
W(100)	80...1000	0.90	MB study	92Ber2
W(110)	300	0.22		74Bar
W(110)	90	0.12	TDS and $\Delta\Phi$ study	97Nah2
W(111)	300	1		74Bar
W(111)	80...1000	0.85	MB study	92Ber2
W(211)	150	0.57 (β_2 state) 0.05 (β_1 state)		73Rye
Re(10-10)	100	0.7		95Mus
Ir(100)-(1×1)	200	0.18	D ₂ MB study	98Ali
Ir(100)-(5×1)	200	0.10	D ₂ MB study	98Ali
Ir(110)-(1×2)	130	7 × 10 ⁻³	β_1 state	80Ibb, 81Ibb
	130	1	β_2 state	
Ir(110)-(1×2)	130	0.007	β_1 state	81Ibb
Ir(111)	100	7 × 10 ⁻³		87Eng
Pt(100)-(1×1)	35	0.1 a ₂ state 0.03 a ₁ state	activated adsorption	91Pen2
Pt(100)-(1×1)	300	0.17		95Dix
Pt(100)-hex	78	0.15		77McC2

Surface	Surface temperature [K]	Initial sticking coefficient s_0	Remarks	Reference
Pt(100)-hex	160	0.1		93Klo
Pt(100)-hex	150	0.06		95Dix
Pt(100)-hex	122...150	0.06	MB studies using D ₂	95Pas
Pt(100)-hex	190	0.07		74Lu
Pt(100)-hex	300	0.17		75Net
Pt(110)-(1×2)	190	0.33		74Lu
Pt(110)-(1×2)	78	0.2		77McC2
Pt(110)-(1×2)	100	0.46	TDS	87Eng
Pt(110)-(1×2)	170	0.8		92She
Pt(110)-(1×2)	300	0.31		76McC
Pt(110)-(1×2)	300	0.33		72Cha
Pt(110)-(1×2)	100	0.45...0.48	MB study	89Ang2
Pt(110)-(1×2)	285	0.6	MB study, rotational state resolution	96Beu
Pt(111)	190	0.016		74Lu
Pt(111)	78	0.1	activated adsorption	77McC2
Pt(111)	150	0.1		75Chr
Pt(111)	300	0.07	MB studies	77Sal
Pt(111)	300	0.2		77McC2
Pt(111)	300	0.016		77Sch
Pt(111)	100...200	6×10^{-2} at 240 K; 4.5×10^{-2} at 90 K	increases with T ; activated adsorption	85Poe
Pt(111)	600...800	2×10^{-1}	s increases with T	79Sal
Pt(210)	78	0.4		77McC1
Pt(211)	190	0.14		74Lu
Pt(997)	120	0.34		76Chr
Au(110)-(1×2)	150	0		86Sau

3.4.1.3.1.6 Sticking and adsorption of hydrogen on bimetallic and alloy surfaces

From the viewpoint of heterogeneous catalysis, the sticking behavior of hydrogen on *alloy* and *bimetallic* surfaces deserves particular attention, because these materials are often catalytically more active than the individual metals. Hydrogen adsorption studies with both crystallographically well-defined alloy single crystal surfaces and samples consisting of epitactic films grown on single crystalline substrates have been reported, and the researchers have been interested in kinetic coefficients, adsorption/desorption energies, hydrogen vibrations, work function changes and hydrogen surface phases. Regarding the thin-film systems, so-called *surface alloys* are sometimes formed, i.e., interdiffusion of the components leads to more or less well-defined alloy phases which are restricted to the surface region. However, there is a class of metallic elements which are immiscible in the bulk and do not show noticeable surface alloying effects either. Nevertheless even marginal chemical interaction between the constituents can (and often will) modify the surface sites for adsorbing hydrogen. These systems are well-known as *bimetallic surfaces* and play a significant role in heterogeneous catalysis [83Sin, 90Cam].

Unfortunately, systematic and quantitative investigations concerning hydrogen adsorption have not been performed, due to the complexity of these materials regarding their variable surface morphology and surface chemical composition. Often, the standard surface-analytical techniques do not provide

sufficiently accurate information, although some progress has been made in the recent decade by using scanning tunneling microscopy techniques in conjunction with LEED [93Sch, 98Gau]. Quite generally, reliable kinetic (and energetic) data concerning H adsorption are rare. The respective quantities often depend in a very complex manner on surface morphology and composition. Since interdiffusion of the alloy constituents is a thermally activated process, the aforementioned properties depend sensitively on temperature and require a steady experimental control. This is particularly awkward in the course of TDS experiments (which have been carried out by many researchers), since even a single TD run may irreversibly alter both morphology and surface composition. Moreover, the hydrogen adsorbate itself (as well as other reactive adsorbates such as carbon monoxide or oxygen) may cause de-mixing and segregation of one component of the alloy, usually that component, which provides the higher interaction energy with the adsorbed H atom. This component is enriched at the surface (corrosive chemisorption). An example is provided by the Ge-on-Si(001) system [98Rud].

Regarding the ‘chemistry’ of the systems in question, the following distinction may be useful: Alloys which consist of two metals, *both of which* adsorb hydrogen readily (for example, Ni and Fe, or Pd and Pt), have to be distinguished from alloys where one of the constituents does *not* spontaneously adsorb hydrogen, examples being Cu-Ni or Cu-Pd or Au-Pt alloys. In the first case hydrogen will probably not differentiate between the two kinds of metal atoms (unless the local charge distribution will be greatly modified and differ for the two kinds of atoms so that one kind of site is favored over the other). In the second case the alloy system (with its ‘active’ and ‘inert’ atoms) can behave in three different ways: 1) Hydrogen will strictly only adsorb at and near the ‘active’ TM atom – then the system follows a coverage dependence which resembles the one of the pure metal, but the coverage is reduced to the fraction of the ‘active’ atoms. 2) Hydrogen will again only adsorb at and near the active substrate atoms, but after dissociation the H atoms can freely diffuse across the surface and adsorb also in sites provided by inactive atoms a process well-known as *spill-over* effect [88Chr, 88Con]. 3) The chemical nature of *all* sites is modified compared to the clean constituents, depending on the (surface) mole fraction and the mutual distribution of the atoms: There exist local areas (patches) consisting predominantly of active metal atoms (which exhibit almost the adsorptive properties of the clean active metal) and patches, in which ensembles of active atoms are more or less diluted by inert atoms. Here, the sticking behavior (and/or the adsorption energy) may be greatly reduced and impaired, depending on how many inert atoms are included in the respective ensemble. As mentioned above, problems of this kind are crucial in heterogeneous catalysis [69Bal]: Not only do they influence the rate of the hydrogen uptake (adsorption kinetics), but can also affect the entire energetics and electronic interaction involved in the hydrogen chemisorption reaction. The dependence of the kind and number of hydrogen binding states on the alloy composition and/or the lateral distribution of the different kinds of atoms are well known as *ensemble* and *ligand* effect [79Ert], both of which can decisively govern the activity and selectivity of surface reactions involving hydrogen.

Since there exist only quite few systematic and reliable numbers for sticking coefficients and adsorption energies (which often depend in a complicated manner on preparation and annealing conditions as mentioned above) we refrain from trying to list these numbers systematically in tables. Rather, we provide some miscellaneous information on the interaction of hydrogen with a variety of alloy or bimetallic systems for which relevant adsorptive properties have been determined. In view of the many possible binary alloy systems [58Han] and the fact that just in recent years the respective reports on binary and ternary systems have increased almost exponentially, this list is by no means complete and provides only a small (but hopefully representative) survey over the principal features.

Alloy and bimetallic surfaces

Alloy/bimetallic system	T [K]	Measured properties	Remarks	Ref.
Ag - Pt(111) Au - Pt(111)	100	TDS state at 160 K TDS state at 120 K	Ag and Au films on Pt(111); H adsorption is thermally activated	04Ogu
Ag - Ru(10–10)	80... 100	LEED, $\Delta\Phi$, TDS; $\Theta_{\text{Ag}}=0.2 \rightarrow E_{\text{des}}=73\text{kJ/mol}$; $\Theta_{\text{Ag}}=0.5 \rightarrow E_{\text{des}}=50\text{kJ/mol}$	Ag(111) films on Ru (10–10); $0.1 < \Theta_{\text{Ag}} < 1.0$	93Len

Alloy/bimetallic system	T [K]	Measured properties	Remarks	Ref.
Al - Pd(100) p(2×2)-p4g		TDS δ -state at 360 K 1 st -order, $\nu = 4 \times 10^{20} \text{ s}^{-1}$, $E_{des} = 144 \text{ kJ/mol}$ STM + HREELS $\nu_{sym} = 77 \text{ meV}$ (H in 4fold hollow)	Al films on Pd(100) form a p(2×2)-p4g surface alloy	93Oni 99Kis
Au - Ir(111)	100	TDS states at 160 and 240 K	Au films on Ir(111); H ₂ adsorbs dissociatively on Au	03Oka
Bi - Pt(111)	150	2 TDS states; Bi acts as a site blocker for H ads.	Bi films on Pt(111); $0 < \Theta_{Bi} < 1 \text{ ML}$	89Paf
Cs - Al(111) • p(2×2) $\rightarrow \Theta_{Cs} = 0.25$ • ($\sqrt{3} \times \sqrt{3}$)R30° $\rightarrow \Theta_{Cs} = 0.33$ complete Cs layer	85	TDS, HREELS, work function. Formation of CsAlH ₂ surface complex	Cs thin films on Al(111); annealing to $T > 200 \text{ K}$ \rightarrow Cs-Al surface alloys with several ordered phases	96Kon
Cu _{0.85} Pd _{0.15} (110) - (2×1) Cu _{0.85} Pd _{0.15} (110) - disordered		MB study; activated adsorption of D ₂	sticking strongly influenced by annealing	95Cot
Cu - Ru(0001)	150	TDS states at $\sim 360 \text{ K}$	thin Cu films on Ru(0001) (bimetallic system); Cu strongly suppresses H uptake	80Shi
Cu - Ru(0001)	100	TDS: Cu-induced H states at • 190 K • 220 K	thin Cu films (1 - 8 ML) on Ru(0001) with preadsorbed atomic hydrogen	85Goo
Cu - Ru(0001)	170	TDS, $\Delta\Phi$ measurement; $\Theta_{Cu} = 0.15 \rightarrow E_{des} = 166$, $s_0 = 0.29$ $\Theta_{Cu} = 0.70 \rightarrow E_{des} = 72$, $s_0 = 0.43$	thin Cu films on Ru(0001) depos. at 1080 K; expts. performed with D ₂	82Vic
Cu ₃ Pt(111) - (2×2)Pt sublattice	100	TDS 2 nd -order state	H adsorption at Pt sites	94Lin
Cu - W(100) Ag - W(100) Au - W(100)	300	H adsorption linearly blocked with Cu (Ag, Au) coverage	coinage metal films deposited on W(100) up to $\sim 2 \text{ ML}$	89Att
Fe - Al	300	D ₂ -TDS states at 500 and 820 K; desorption energy 1.57 eV	alloy films deposited on Si sample	02Che
Fe - Ru(0001)	220	D ₂ -TDS; sticking coeff. for 1 ML Fe = 0.05	Fe films on Ru(0001) (bimetallic system)	88Ega
Fe - Ti	300	TDS state at 710 K; desorption energy 2.10 eV	alloy films deposited on (400) Si	03Che
Fe - W(110) Fe - W(100)	100	TDS, LEED, for $0.12 < \Theta_{Fe} < 1.1 \text{ ML}$ 3 TD states between 250 and 500 K	Fe films on W(110) and (100) (bimetallic system)	90Ber
Fe - W(110)	90	TDS, $\Delta\Phi$, equilibrium measurements; $\Delta H_{des} = 81.6 \text{ kJ/mol}$ for $\Theta \leq 0.3$ and 125 kJ/mol at $\Theta > 0.3$; $\Theta_{max} = 0.6$; $s_0 = 0.3$ at 90 K	Fe monolayer films on W(110) annealed to 600 K prior to H ₂ adsorption	97Nah1 97Nah2
Fe - W(100)	140	3 TDS states	1 ML Fe on a W(100) surface	88Zho
Mo _{1-x} Re _x (110); x=0.05, 0.15, 0.25	<130	LEED, TDS, HREELS; losses at 48, 70, 97 (110), 155 meV H (D) for sat'n on x = 0.15 alloy	alloy single crystals; (2×2)-H, c(2×2) and (1×1) H phases depending on compos.	98Oka1
Mo _{0.75} Re _{0.25} (100), (110), (111)	130	LEED, nuclear reaction analysis; D coverages • (100) $\rightarrow \Theta_D = 2.0$ • (110) $\rightarrow \Theta_D = 0.99$ • (111) $\rightarrow \Theta_D = 2.86$	alloy single crystals	98Oka2
Ni - Cu(111)	140	UV photoemission states, electronic band structure, H-induced $\Delta\Phi$ (50 meV)	Ni monolayer film on Cu(111)	89Frau

Alloy/bimetallic system	T [K]	Measured properties	Remarks	Ref.
NiAl(110)	115	LEED, TDS, HREELS; single TD state 300...250 K with 2 nd order kinetics; $E_{des} = 52.2$ kJ/mol at low Θ_H ; 33.8 kJ/mol at high Θ_H	alloy single crystal; exposure to H atoms	95Han
NiAl(110)	190	TDS, LEED, MB techniques; H sat'n = 0.49, H-induced $\Delta\Phi$ (550 meV), activation barrier for H ₂ dissociation 0.72 eV	alloy single crystal	95Beu2
Pd - Ta(110)	100	LEED, TDS; $s_0 = 0.58$, TD states at 150, 385, 615 and 1100 K	epitactic Pd(111) films on Ta single crystal	93Hei
Pt ₈₀ Fe ₂₀ (111) p(2×2)	120	UPS, TDS; 2 TDS states shifting with H coverage: • 358...304 K • 440...406 K H-induced $\Delta\Phi = -400$ meV	alloy single crystal, strong Pt surface segregation upon annealing	92Atl
Pt _{0.5} Ni _{0.5} (111)	115	LEIS, TDS: 2 nd -order desorption, $E_{des} = 50$ kJ/mol; $s_0 = 5 \times 10^{-3}$; H-induced $\Delta\Phi = -100$ meV, nuclear reaction analysis: $\Theta_H = 2.7 \times 10^{18}$ (= 0.2 ML)	strong Pt surface segregation	94Atl
Re - Pt(111)	150	activation energy for desorption decreases with Θ_{Re} , H uptake increases with Θ_{Re}	thin Re films on a Pt(111) single crystal	88God
Sn - Pt(111) ($\sqrt{3} \times \sqrt{3}$)R30°		XPS	Sn films form a surface alloy with Pt; H binds on Pt sites only	96Jan
Sn - Pt(111) p(2×2) Sn - Pt(111) ($\sqrt{3} \times \sqrt{3}$)R30°	300	• $\Theta_{Sn} = 0.25 \rightarrow \Theta_D = 0.68$, $s_0 = 0.33$ • $\Theta_{Sn} = 0.33 \rightarrow \Theta_D = 0.51$, $s_0 = 0.18$; reduced Pt - D bond energy 232 kJ/mol	Sn films form surface alloys; no spontan. D ₂ dissociation → exposure to D atoms	98Vos
Ti - Pd(100) p(2×2)-p4g	300	2 TDS states • 355...345 K due to desorption from c(2×2) domains • 380 K due to desorption from p(2×2)-p4g patches	Ti films on Pd(100) form a Pd ₃ Ti p(2×2)-p4g surface alloy	04Tsu

3.4.1.3.1.7 The sticking on semiconducting and insulating surfaces

Compared with hydrogen-on-metal systems the available data for sticking of H₂ on non-metallic elements is scarce, for several reasons. For very shallow surface - H₂ interaction potentials the equilibrium concentration of trapped hydrogen molecules at non-cryogenic temperatures and pressures usually accessible in UHV model experiments is very small and so is the probability of H₂ dissociation under these conditions [83Sch2]. Therefore, pressures in the mbar or bar range are necessary to populate these potentials with hydrogen molecules at common temperatures. The high pressures in turn prevent the use of the standard surface (electron) spectroscopies and cause serious purity problems, since the H adsorption properties are especially altered by co-adsorption of contaminating species [90Chr]. Parallel to

‘chemical’ impurities, even traces of crystallographic defects (steps, kinks, holes etc.) may dramatically affect the dissociation probability and, hence, the hydrogen uptake. This is particularly true for semiconductor surfaces, where structural defects play a decisive role in hydrogen sticking: On vicinal Si surfaces, for example, the sticking probability (i.e., the hydrogen uptake) increases dramatically for slightly misoriented samples in that defect sites serve as adsorption conduits from which H atoms diffuse onto the rest of the surface [96Han]. In other words: H₂ molecules may become dissociated at edge atoms, kinks, steps or holes. Sticking (in conjunction with the formation of a covalent Si - H bond) is the first step towards a chemical hydrogenation reaction. On the Si(111)-(7×7) surface, for example, two main channels for this reaction have been proposed: i) direct adsorption of a H atom on the Si adatom dangling bonds and ii) breaking by H of the Si adatom back bond [91Mor, 93Bol, 96Nog]. Thus, a progressive hydrogenation of the entire surface is initiated which first leads to monomers Si - H, then to dimers Si - H₂ or trimers Si - H₃ until finally silane-like species are formed. A somewhat more detailed description of these various interaction steps of hydrogen (and other molecules) with several Si surfaces is given by Joyce and Foxon [84Joy]. Various mechanisms as to how the H₂ dissociation takes place are discussed in the literature: By means of an STM investigation a so-called ‘Si dimer’ mechanism has recently been confirmed [02Due]. Another interesting reaction path which can make molecular hydrogen dissociate on a semiconductor surface at elevated temperatures is the so-called phonon-assisted sticking, which has been deduced for H₂ on Si(111)-(7×7) [95Bra] and on Si(100)-(2×1) [95Kol1] from the increase of the sticking probability with temperature.

Of course, the shallow molecular adsorption potentials of H₂ on non-metallic surfaces can be filled with molecules by lowering the temperatures into the 5...10 K regime, and actually several studies have been carried out with physisorbed hydrogen, especially on graphite surfaces, aiming at formation of ordered phases and two-dimensional phase transitions [82Seg, 85Fre2, 87Fre, 88Cui, 89Cui] or at the mechanism of the ortho – para hydrogen conversion [83And, 97Sve]. The sticking probability under these conditions is difficult to estimate, since the phonon-assisted mechanism may not be very effective. Rather, particle scattering effects within the adsorbed H₂ layer are essential, leading to an increase of *s* with coverage, but no systematic studies of the sticking behavior of physisorbed hydrogen have been performed to our knowledge.

All in all, spontaneous dissociative hydrogen adsorption is not a very common feature on semiconductor and insulator surfaces, at least not as long as defect-free surfaces are considered. An entirely different situation exists, if H₂ molecules are pre-dissociated in the gas phase into reactive H atoms [84But]. In most of the experimental studies this is accomplished by means of a hot W filament: By choosing the temperature of the filament, the yield of H atoms can be sensitively controlled [80Sch2, 83Sch2]; the H atoms formed then react vigorously with the Si (C, Ge, GaAs, InP etc.) surfaces to mono- or dihydride compounds. Oxides exposed to H atoms may easily become reduced, leading to the formation of water and the loss of lattice oxygen, whereby the lattice is often destabilized, oxygen vacancies are being formed which provide additional reaction sites for hydrogen. However, these complex chemical processes (which are of great relevance in heterogeneous catalysis though) cannot be covered here. In the following table, we put together both the molecular and the atomic hydrogen data obtained so far for a variety of common semiconductor and insulator surfaces with emphasis on silicon and carbon (in the form of diamond). Note that many (if not all) of the clean surfaces are reconstructed, since a surface with unsaturated covalent (“dangling”) bonds is energetically inherently unstable. Well-known examples are the silicon (111) surface which is, in the clean state, (7×7) reconstructed [83Bin2], and the Si(100) surface, which reconstructs to (2×1), c(4×2), and p(2×2) surface phases [86Ham]. Much interest has been (and still is) spent to diamond single crystal surfaces and their interaction with hydrogen, owing to the technological interest in diamond thin films [02Big]. In some respect, diamond surfaces resemble silicon, for example, as far as surface reconstruction and reactivity with respect to hydrogen is concerned. In other respects, there are, of course, important differences (conductivity, hardness etc.). For more details, we refer to the exhaustive article by Pate [85Pat].

In the last decade, the interest in H₂ adsorption *dynamics* especially on Si single crystal surfaces aroused both experimentally and theoretically, and since then, a wealth of articles appeared on that subject. One particular issue is the correct theoretical description of the dissociative adsorption of H₂ at elevated temperatures and the recombinative hydrogen desorption from partially or totally hydrided

silicon single crystal surfaces, without violating the principle of detailed balancing. Due to space limitations, we cannot enter this interesting topic and refer instead to some selected references [93Wu], [94Bre], [94Kra], [95Kol2], [95Jin], [00Peh], [00Zim]. A somewhat more general overview of the Si + H interaction has been given by Oura et al. [99Our].

Comparatively few studies have been performed with Ge, but its behavior with respect to hydrogen appears to be quite similar to Si; again, mono and dihydrides are formed upon exposure to H atoms. To some extent, this is also true for the diamond surfaces.

Semiconductor and insulator surfaces

Surface	T [K]	Sticking coefficient	Remarks	Ref.
C(111) -1×1 diamond	300	~0	no adsorption of molecular hydrogen	85Pat
C(0001) -1×1 (HOPG) graphite	150	0.4 (H) 0.25...0.5 (D)	exposure to H (D) atoms	02Zec
Si single crystal surfaces in general	300	$< 10^{-6} \dots 10^{-8}$	activation barrier ca. 0.5 eV	59Law 83Sch2 90Lie1
Si(111)7×7	580 1050	2×10^{-9} 5×10^{-6}	phonon-assisted sticking; adsorption activation barrier 0.9 eV	95Bra 96Bra
Si(111)	300	$< 10^{-6}$	exposure to H ₂ molecules	83Sch2
		1.0	exposure to H atoms	
Si(100)2×1	300...900	5×10^{-6} at 300 K 1.5×10^{-5} at 630 K	sticking rises with temperature	95Kol1
Si(100)2×1	440...670	$10^{-8} \dots 10^{-4}$	adsorption at terraces; activation energy of 0.8 eV can be lowered by dynamical distortions of Si surface atoms	99Due
Si(100)2×1	300	$< 10^{-10}$ strongly T -dependent; s_0 increases to $\sim 10^{-4}$ as T approaches 750...800 K	phonon-assisted sticking only at small H coverages; at medium and larger coverages a barrier-free autocatalytic pathway exists	00Zim
Si(100) Si(111) vicinal surfaces	>50	~0.1	second harmonic generation (SHG)	96Han
Si(111)	300 1000	10^{-10} 10^{-4} ; activation barrier = 0.94±0.1 eV = 90.7 kJ/mol	sum frequency vibrational spectroscopy and SHG	01Mao
GaAs(110)	300	~1.0 up to 1 ML coverage	exposure to H atoms	87Mha
GaAs(110)	300	initially high, but decreases strongly with H coverage	exposure to H atoms. Upon H adsorption, surface changes from relaxed to unrelaxed form	99Gay

3.4.1.3.2 Kinetics of hydrogen desorption

3.4.1.3.2.1 General remarks

The rate of a desorption reaction (we consider here only *thermal* desorption processes occurring from a homogeneous surface and neglect any activation barriers in the adsorption channel) can be usually described by the Polanyi-Wigner equation (Eq. 6)

$$r_{des} = \left| -\frac{d\Theta}{dt} \right| = \nu_{(x)} g(\Theta) N_{max}^{x-1} \exp\left(-\frac{E_{des}}{kT}\right) \quad (6)$$

where ν = frequency (pre-exponential) factor, x = reaction order, E_{des} = desorption energy, N_{max} = maximum number of adsorbed particles. The function $g(\Theta)$ describes the concentration dependence of the desorption reaction. Since the ongoing desorption *reduces* the surface concentration of the adsorbate, r_{des} is defined as a negative quantity, for convenience, we consider only its absolute value here. Multiplying Eq. (6) with the inverse heating rate β^{-1} ($\beta = dT/dt$) transforms the time-dependent rate $r_{des}^{(t)}$ to a temperature-dependent rate $r_{des}^{(T)}$. Note that the standard procedure in a thermal desorption experiment is to apply a *linear* temperature program ($T(t) = T_0 + \beta t$; with $\beta = \text{const}$) which transforms Eq. (6) to

$$r_{des}^{(T)} = \left| -\frac{d\Theta}{dT} \right| = \frac{\nu(x)}{\beta} g(\Theta) N_{max}^{x-1} \exp\left(-\frac{E_{des}}{kT}\right). \quad (7)$$

This is the standard form of the Polanyi-Wigner equation and mostly used to evaluate TPD data. The pre-exponential factor and the desorption energy are system-specific quantities. Often, especially on high-index surfaces, several energetically different hydrogen binding sites may be populated; the desorption of the respective adsorbed species from the various types of sites is then governed by individual relations of the type of Eq. (7). A series of typical hydrogen thermal desorption spectra is reproduced in Fig. 5, taken from the H-on-Co(10–10) system, which shows (in addition to the 2nd order β state) a relatively sharp α state indicating H atoms bound in different surface sites [94Ern].

The coverage function $g(\Theta)$ simply equals Θ^x , with the desorption order x mostly taking the value 1 or 2. A first-order ($x = 1$) hydrogen desorption process results, if the rate-limiting step is the removal of the H_2 entity from the surface (associative desorption), which certainly applies to physisorbed H_2 . A second-order ($x = 2$) desorption mechanism implies a surface migration of the separated H atoms, a subsequent collision event of two atoms, their recombination to the molecule, and, finally, the desorption of the H_2 molecular entity. The overall reaction rate is primarily dependent on how fast the dispersed, migrating H atoms collide and recombine, whereas the desorptive removal of the molecule to the gas phase is *not* rate-limiting. Hence, the coverage function in its simplest form equals Θ^2 in this case.

3.4.1.3.2.2 The frequency factor and the order of the desorption reaction

For the physical interpretation of the pre-exponential factor ν we must again delineate between 1st and 2nd order desorption processes. In terms of transition-state theory, ν can be identified with the universal frequency factor $\frac{kT}{h}$ ($\approx 6 \times 10^{12} \text{ s}^{-1}$ at 300 K), modified with the ratio of the partition functions of the transition state and the adsorbed molecule, if necessary. If the activated complex (the H_2 entity „ready“ for desorption) and the adsorbed species have the same degrees of translational and rovibrational freedom, these partition functions cancel each other. Usually however, the transition state complex is less strongly bound to the surface and may have higher degrees of freedom; then ν may significantly exceed the value $6 \times 10^{12} \text{ s}^{-1}$. In a naive view, ν can be regarded as representing the attempt frequency to move along the direction of the desorption trajectory, i.e., away from the surface; it would then correspond to the frequency of vibration of the adsorbed particle perpendicular to the surface. Depending on the

physical state of the adsorbate prior to the desorption reaction, two extreme cases can be distinguished. i) The adsorbed atoms are completely mobile in two dimensions, then the (second-order) frequency factor ν_2 simply equals the collision frequency in the two-dimensional gas. ii) The adsorbed atoms are completely immobile, then the frequency factor corresponds to the number of available adsorption sites. Note the different units of the 1st and 2nd order frequency factor: $\nu_1 \rightarrow [\text{s}^{-1}]$; but $\nu_2 \rightarrow [\text{cm}^2 \cdot \text{s}^{-1} \cdot \text{atom}^{-1}]$. Since the configuration of the adsorbed particles changes with coverage, the frequency factor usually is coverage-dependent; this θ dependence often resembles the one encountered with the adsorption energy, the reason being the well known compensation effect [55Cre, 81Aln].

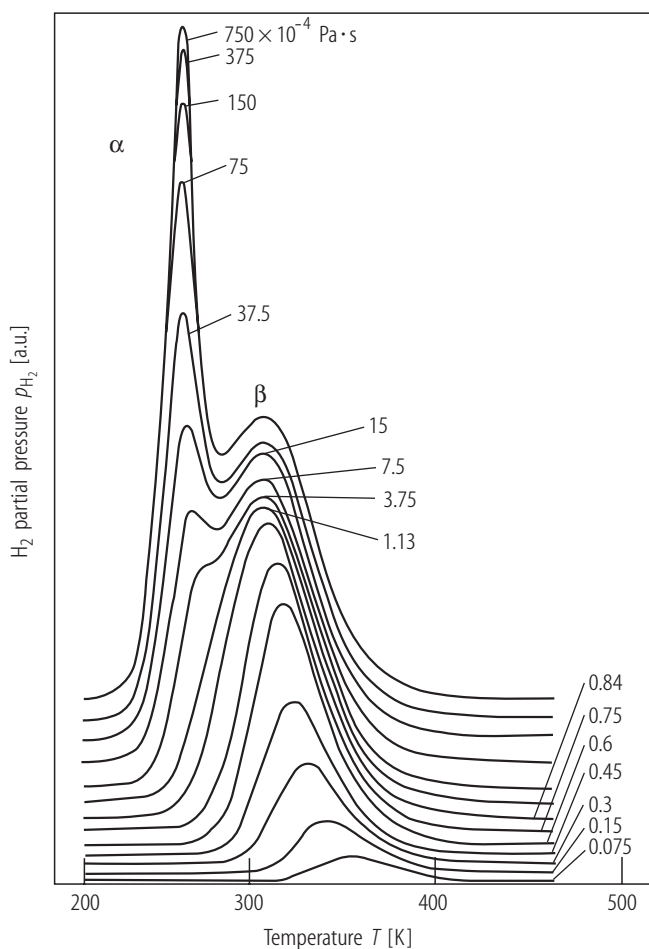


Fig. 5: A typical series of hydrogen thermal desorption spectra, obtained from a cobalt(10–10) surface exposed to increasing amounts of hydrogen gas at $T = 200$ K. Two binding states are formed: At low and medium coverages, a single β state develops with a 2nd order desorption kinetics, while at elevated coverages a sharp α shoulder state appears at lower temperatures. After [94Ern].

In the following table we have listed the available first and second-order frequency factors for hydrogen desorption from single crystal surfaces. Since H atoms often adsorb in several different binding states (denoted as α , β , γ , δ etc.) having different kinetic and energetic properties, we have also listed the respective states and their desorption temperature maximum T_{max} at the saturation coverage. Unfortunately, reliable ν data are scarce, for the same reasons mentioned in the foregoing section. In many cases it is not quite clear whether the desorption occurs via 1st or 2nd order; mostly, this information is taken from series of thermal desorption spectra, i.e. from the shift of the TD maximum with coverage, whereby a judgement of the peak position can be obscured by lateral interactions between the adsorbed particles (which can cause similar peak shifts [74Ada]). Relatively accurate frequency factors for hydrogen desorption can be determined by a so-called *line shape analysis* of TD spectra, according to evaluation ‘recipes’ developed by Bauer et al. [75Bau1] or King [75Kin]; both procedures (which are entirely equivalent) are solely based on the validity of the Polanyi-Wigner equation (Eq. 7) and explicitly consider coverage dependencies of ν and E_{des} .

We also recall from sect. 3.4.1.3.1 that there is a number of systems (including the noble metals Cu, Ag, Au, but also other ‘free electron’ metals like Be or Al) which do not spontaneously adsorb and dissociate hydrogen molecules. Accordingly, they exhibit vanishingly small sticking coefficients and practically no H uptake. Nevertheless, the interaction with hydrogen can be studied by simply exposing the respective surfaces to fluxes of H atoms or supersonic H₂ molecular beams. The respective data for the frequency factors and reaction orders etc. are included in our list, together with a brief comment.

3.4.1.3.2.3 The desorption energy as a kinetic quantity

In the context of adsorption and desorption *kinetics*, it is justified to consider the desorption energy simply as a *kinetic* quantity: As mentioned above, the particle residing at the bottom of the adsorption potential has to be supplied with this energy to be able to leave the surface; it may therefore be regarded as kind of an *activation energy* to run the desorption reaction. Fortunately, since most of the hydrogen adsorption cases involve no or only vanishingly small activation barriers, the thermal desorption experiment is well suited to map out the depths of the adsorption potential wells under equilibrium conditions; therefore the quantity ‘desorption energy’ can serve as a measure of the hydrogen - surface interaction energy, and actually many of the values listed in the compilation of sect. 3.4.1.3.3 stem from TD experiments.

To illustrate this internal correlation, we have, in the following table, listed the number of desorption states and the temperature position of the TD maxima, together with the respective frequency factors. Note that the desorption energy E_{des} refers to the actual energy that a particle must overcome to leave the potential energy well. For non-activated adsorption E_{des} actually equals the adsorption energy E_{ad} . Only in the case of activated adsorption, E_{des} consists of the adsorption energy E_{ad} , *plus* the height of the activation barrier, E_{ad}^* . Particles leaving the surface first have to surmount this ‘extra’ barrier and, accordingly, carry a certain amount of excess energy and are not necessarily in thermal equilibrium with the surface. This may significantly alter the shape of the thermal desorption curves as was proven, e.g., for hydrogen molecules desorbing from Cu(100) by Anger et al. [89Ang1]. Furthermore, the flux of the desorbing particles can exhibit directional dependencies. This shows up in a $\cos^n \theta$ distribution ($n > 1$) with a lobe perpendicular to the surface, θ being a polar angle relative to the surface normal. Measurements of these deviations from thermal equilibrium requires fairly sophisticated experimental set-ups, especially, if quantum-state resolution is attempted (combined molecular beam and/or laser spectroscopy). A brief overview is given by Zacharias [88Zac]. In some cases, *parallel* entrance channels can exist for dissociative adsorption, activated and non-activated ones. How an impinging H₂ molecule finds the easiest pathway to dissociate and chemisorb as atoms is called *dynamical steering* effect [03Gro]. Most of the common transition metal single crystal surfaces, however, provide non-activated adsorption pathways resulting in spontaneous dissociation of the incident hydrogen molecules.

3.4.1.3.2.3.1 Metal surfaces

Surface	H adsorption states + desorption temperature at sat'n [K]	Frequency factor		Remarks	Ref.
		1 st order [s ⁻¹]	2 nd order [cm ² /s]		
Be(0001)	β 470 (low Θ)		2 nd order with attractive H - H interaction	surface exposed to H atoms at 80 K	90Ray
	β 510 (high Θ)	fractional-order		activation barrier for adsorption = 0.95 eV	
Al(100)	β 345			surface exposed to H atoms	88Pau
Al(100)	β 330	close to 0 order		surface exposed to H atoms	91Win
Al(110)	β 338	fractional order		surface exposed to H atoms	91Win
Al(110)	β 315...335	fractional order		surface exposed to H atoms; H-induced surface reconstruction	92Kon
Al(111)	β 335	close to 0 order		surface exposed to H atoms	91Win

Surface	H adsorption states + desorption temperature at sat'n [K]		Frequency factor		Remarks	Ref.
			1 st order [s ⁻¹]	2 nd order [cm ² /s]		
Al(111)	β	323...334	zero order; 2×10^{13}		surface exposed to H atoms	88Mun
Al(111)	β	320...340	fractional		surface exposed to H atoms; desorption of Al-hydride	91Har
V(111)	surface bulk	330 1200	1 st order	2 nd order	MB expts. performed with D ₂ , competing bulk dissolution	00Beu
Fe(100)	β_1 β_2	~300 380		1.5×10^{-2}	TDS expts.; H saturation coverage $5.6 \times 10^{18} \text{ m}^{-2}$	80Ben
Fe(100)	β_1 β_2	290 400		2 nd order		77Boz
Fe(100)	β_1 β_2	265 355				91Ber2
Fe(100)	β_1 β_2			pseudo-1 st order		96Mer
Fe(110)	β_1 β_2	~340 ~430		2 nd order		77Boz
Fe(110)	α β_1 β_2	300 ~330 ~400		2 nd order	MB expts.	91Ber2
Fe(111)	β_1 β_2 β_3	~240 ~300 ~370		2 nd order		77Boz
Fe(111)	β_1 β_2	~260 ~350		2 nd order 2 nd order	MB expts.	91Ber2
Fe(211)	α_1 α_2 α_3 β	~210 ~230 ~265 ~340		~2 nd order	<i>T</i> -dependent reconstruction : α states on unreconstructed, β state on reconstructed surface	95Sch1
Co(0001)	β	~400		2 nd order		79Bri
Co(0001)	β_1 β_2 β_3	273 308 333			preliminary study	86Gre
Co(10-10)	α β	260 300	1 st order	2 nd order	<i>T</i> -dependent reconstruction	94Ern
Ni(100)	β_1 β_2	318 348		3×10^0		79Chr1
Ni(100)				2.5×10^{-1}		72Lap1
Ni(100)	β_1 β_2	330 370		8×10^{-2}		74Chr
Ni(100)	α_2 α_1 $\alpha (= \beta_2)$	200 270 350		5×10^{-2}		81Joh1
Ni(100)				0.4	laser-induced thermal desorption expts.	84Hal
Ni(110)	α β_1 β_2	220 290 340	fractional-order first order		<i>T</i> -dependent reconstruction	89Chr
Ni(110)	α β_1 β_2	225 290 340		initial 2 nd order		82Win
Ni(110)	α β_1 β_2			2 nd order	expts. performed with H ₂ and D ₂ molecular beams	85Rob

Surface	H adsorption states + desorp- tion temperature at sat'n [K]	Frequency factor		Remarks	Ref.
		1 st order [s ⁻¹]	2 nd order [cm ² /s]		
Ni(111)	β		2×10^{-1}		72Lap2
Ni(111)	β_1				74Chr
	β_2 360		8×10^{-2}		
Ni(111)	β_1 ca. 300			absolute (volumetric) measurements	74Rin
	β_2 360		0.15 ± 0.5		
Ni(111)	β_1 355		2×10^{-4}		79Chr1
	β_2 383		10^{-3}		
Ni(111)	β_1 290			β_1 peak position angle-dependent due to activated adsorption	86Rus
	β_2 370				
Ni(111)	β_1 325			H ₂ exposure at 170 K	86Gre
	β_2 365				
Ni(111)	α 250	1 st order		α state due to desorption from subsurface sites, filled by implantation	90Gol
	β_1 355				
	β_2 383				
Cu(100)	10...15			physisorption of H ₂ molecules after exposure to H ₂ at 4 K	82Ebe
Cu(100)	218...258 590...650 (bulk spec.)			pressures up to 5 bar were used; after extended exposures bulk desorption occurs	93Ras
Cu(100)	~270			non-equilibrium effects prevent reliable data analysis	89Angl
Cu(100)	285; 340...290		1 st order 2 nd order	exposure to H atoms surface reconstructs	91Cho
Cu(110)	330		6×10^{-6} ...0.1	exposure to H atoms; both E_{des} and ν increase with coverage	89Angl
Cu(110)			10^{-6}	exposure to H atoms	79Wac
Cu(110)	α 200 β_1 290 β_2 335			exposure to H atoms	93Bis
Cu(110)		1.6×10^{13}		data derived from H uptake curves (He scattering)	93Goe
Cu(110)	β 240 α 316	1 st order due to deconstruction		exposure to H atoms; activation barrier for deconstruction 1.02 eV	94Roh
Cu(111)	β_1 235 \pm 10 β_2 292 \pm 5			exposure to H atoms	83Gre
Cu(111)	sgl. state 310		3.3×10^{-4}	E_{des} decreases with coverage	89Angl
Zn(0001)	β 319	order $n=0.5$ due to island formation; $\nu = 6 \times 10^6$ s ⁻¹		exposure to H atoms	84Cha2
Nb(100)	state 1 120			molecular precursor; combined TDS and work function study	74Hag
	state 2 175				
Nb(110)	two surface states			foils with (110) orientation; data taken from T -dependent UV photoemission expts.	80Smi2
Nb(110)		2.75×10^{14}		H uptake measurements	81Pic
Mo(110)	β_1		10^{-2}	precursor kinetics	72Mah
	β_2		10^{-2}		
Mo(100)	β_1 290 β_2 350 β_3 450	$\sim 10^{13}$	$\sim 5 \times 10^{-2}$ 5×10^{-2}		71Han

Surface	H adsorption states + desorption temperature at sat'n [K]		Frequency factor		Remarks	Ref.
			1 st order [s ⁻¹]	2 nd order [cm ² /s]		
Mo(100)	β_1	325				92Baf
	β_2	~390				
	β_3	450				
Mo(211)	β_1	330				94Lop
	β_2	400				
	β_3	480		1...10		
Ru(0001)	β_1	320	$\sim 10^{10}$		strong decrease of E_d and ν with coverage	79Sch
	β_2	~360	$\sim 10^{17}$			
Ru(0001)	β_1	330				80Shi
	β_2	400		1×10^{-3}		
Ru(0001)	β_1	~200				78Dan
	β_2	~350		2 nd order		
Ru(0001)	β_1	330		1×10^{-2}	P state	85Feu
	β_2	390		3	N state	
Ru(0001)(1×1)H	15	1 st layer			physisorption of D ₂ , exposure at 4.8 K	95Fri
	7.5	2 nd layer	zero order			
	5.8	3 rd layer	zero order			
Ru(10–10)	α	220	10^{14}			89Lau
	β_1	258				
	β_2	287				
	β_3	350		9×10^{-3}		
Ru(11–21)	α_1	120				01Fan
	α_2	150...200				
	γ	350				
Rh(100)	β	~310		1.0×10^{-2}	expts. performed with deuterium	82Kim
	α	~140				
Rh(100)	β	290				84Ho
	α	150				85Heg
Rh(100)	β_1	~330		0.04		87Ric1
	β_2	~130				
Rh(100)	β	326				88Ric1
Rh(110)	α_1	138	10^{13}			88Ehs
	α_2	216	10^{13}			
	β	245		2 nd order		
Rh(110)	α	140			theoretical analysis	94Kre2
	β	210				
	γ	250	10^{11}			
Rh(111)	α	~140			strong decrease of E_d and ν with coverage	79Yat
	β	260		1.2×10^{-3}		
Rh(111)	300 (HD signal)			2×10^{-2}	MB experiments; activated adsorpt.	96Col
Rh(311)	α_1	120			expt. and theoretical modelling	99Pay
	α_2	170				
	γ_1	210				
	γ_2	255				
	δ	305		4×10^{11}		
Pd(100)	shoulder state	250				80Beh
	β	350	1 st order	1×10^{-2}		
Pd(100)	β	350		3.2×10^{-3}	adsorption performed at $T = 110$ K; 1 st order precursor model	90Bur

Surface	H adsorption states + desorption temperature at sat'n [K]		Frequency factor		Remarks	Ref.
			1 st order [s ⁻¹]	2 nd order [cm ² /s]		
Pd(100)	α	155			α state (caused by subsurface H) only appears at 100 K ads. temperature; H absorption likely	98Oku
	β	350				
Pd(110)	α	368		8×10^{-2}	room temperature study shoulder due to H desorption from bulk	74Con
	high T shoulder state	~680				
Pd(110)	α_1	165	1 st order		α states due to population of subsurface sites	83Beh 83Cat1 83Cat2
	α_2	220				
	β_1	~270				
	β_2	295				
Pd(110)	α_1	165	fractional-order		isothermal desorption expts. performed with deuterium	88He2
	α_2	230				
	β_1	~270				
	β_2	316				
Pd(110)	α_1	165		2 nd order	subsurface state population	88He1
	α_2	230				
	β_1	~270				
	β_2	310				
Pd(111)	300	shoulder state at ~250		8×10^{-2}		76Con1
Pd(111)	β	380			exposure at 300 K	83Ebe
Pd(111)	α	170		fractional order 2 nd order	at $T_{ad} = 80$ K only β state; for $90 < T < 140$ K $\alpha + \beta$ present	87Gdo
	β	310				
Pd(210)	α	150		2 nd order	expts. performed with deuterium α state due to D sorption in subsurface and bulk states	98Mus
	β_1	200				
	β_2	240				
	β_3	300				
Pd(311)	α	170	10^{13}		α state due to H sorption in subsurface states	99Far
	β_1	285				
	β_2	310				
Pd(311)	v (α)	170	fract. order	2 nd order	H adsorption strongly dependent on adsorption temperature (s = surface, rs = surface after lifting of (1×2) reconstruction, ss = subsurface, v = bulk)	98Fri
	ss	212	1 st order			
	rs (β_1)	280				
	s (β_2)	315				
Ag(100)	α	110			exposure to H atoms	04Kol
	(subsurface)					
	β	150		2 nd order	TD expts after exposure to H atoms	93Spr
Ag(110)	β_2	175				
	β_1	155	1 st order			
Ag(111)	β_2	191	fractional order		TD expts after exposure to H atoms	89Zho
	β_1	173				
	(shoulder)					
Ag(111)	β_2	191		2 nd order	TD expts. after exposure to H atoms. Data of [89Zho] re-examined	90Par2
	β_1	173				
	(shoulder)					
Ag(111)	β	180			expts. performed with H atoms	95Lee
Ag(111)	β	160			expts. performed with H atoms	04Kol

Surface	H adsorption states + desorption temperature at sat'n [K]		Frequency factor		Remarks	Ref.
			1 st order [s ⁻¹]	2 nd order [cm ² /s]		
Ag(111)	α	170	0 th order		subsurface species expts. performed with D atoms	95Hea
	β_1	175	fractional order			
	β_2	200	(0.5)			
Ta(110)	state 1	150			surface state surface state } bulk absorption	93Hei
	state 2	385				
	state 3	615				
	state 4	1100				
W(100)	β_1	450	10^{13}	4.2×10^{-2}	surface reconstructs under hydrogen	69Tam
	β_2	550				
W(100)	β_1	450				70Ada
	β_2	550				
W(100)	β_1	450		$10^3 \dots 10^{-5}$		84Hor
	β_2	550				
W(110)	β_1	440		1×10^{-2} 1.4×10^{-2}		71Tam
	β_2	510				
W(110)	β_1	440				81Hol
	β_2	550				
W(111)	α	130	1 st order	1×10^{-2} 1×10^{-2} 1×10^{-2} 1×10^{-2}		71Tam
	β_1	230				
	β_2	340				
	β_3	490				
	β_4	~640				
W(111)	α	135...145	1 st order	2^{nd} order 2^{nd} order 2^{nd} order 2^{nd} order	ratio of peak integrals: $\beta_1 : \beta_2 : \beta_3 : \beta_4 = 1.5 : 1.5 : 1.5 : 1$	72Mad
	β_1	230				
	β_2	340				
	β_3	490				
	β_4	~640				
W(211)	β_1	330		1×10^{-2}		73Rye
	β_2	675				
Re(0001)	shoulder	350		2^{nd} order		81Duc
	β_2	420				
Re(0001)	shoulder	420		2^{nd} order		90He
	β_2	490				
Re(10-10)	α	240	1 st order	2^{nd} order		95Mus
	β_1	300				
	β_2	470				
Ir(100)-(1×1)	α	240			MB study	98Ali
	β	400				
Ir(100)-(5×1)	β	400	zero or fractional-order 8×10^{12}		MB study	98Ali
Ir(100)-(5×1)	A	125		1 st order 2^{nd} order 2^{nd} order		00Mor
	B	240				
	C	365				
Ir(110)-(1×2)	β_1	200		2×10^{-7} 1.5×10^{-2}		80Ibb
	β_2	390				
Ir(110)-(1×2)	β_1	200				88Cha
	β_2	380				
Ir(111)	β_1	~200		2×10^{-6}	TDS	87Eng
	(shoulder only) β_2	290				

Surface	H adsorption states + desorption temperature at sat'n [K]		Frequency factor		Remarks	Ref.
			1 st order [s ⁻¹]	2 nd order [cm ² /s]		
Ir(111)	β_1	240				88Cha
	β_2	380				
Ir(111)	β_1	190				99Hag
	β_2	270		2 nd order		
Pt(100)-hex	α_1	170				74Lu
	α_2	245				
	α_3	270				
	β_1 shoulder					
	β_2	430		2 nd order		
Pt(100)-hex	β_1	~350			adsorption T -dependent: at $T_{ad} = 300$ K, two (not well resolved) TD states ($\beta_1 + \beta_2$); at $T_{ad} = 200$ K, four TD states ($\beta_1 + \beta_2 + \alpha_1 + \alpha_2$); only at 200 K deconstruction to (1×1)	81Bar3
	β_2	~410				
	α_1	~240				
	α_2	~260				
Pt(100)-hex	state 1	390	10^{13}		TDS + theoretical analysis, effects of reconstruction on H desorption considered	87Sob
	state 2 (shoulder)	350				
Pt(100)-hex	peak "2"	330				93Klo
	peak "1"	360		1.3×10^{-5}		
Pt(100)-hex	γ_1	200				95Dix
	γ_2	218				
	γ_3	240				
	α_3	366	4×10^{13}			
Pt(100)-hex	a_1	195		1×10^{-2}	TPD features complex because of T and H coverage dependent reconstruction	91Pen1
	a_2	225				
	a_3	330				
	b	375				
Pt(100)-hex	γ_1	194		4×10^{13}	TPD features complex because of T and H coverage dependent reconstruction	95Pas
	γ_2	216				
	γ_3	237				
	α_1	246				
	α_2	336				
	α_3	377				
Pt(110)-(1×2)	β_1	170				76McC
	β_2	230		1×10^{-2}		
Pt(110)-(1×2)	β_1	175		3×10^{-4}	strong coverage dependence	87Eng
	β_2	300	$10^{-4} \dots 0.3$			
Pt(110)-(1×2)	α	180				89Ang2
	β_1	~220				
	β_2	290				
Pt(110)-(1×2)	β_1	220		2 nd order		92She
	β_2	310	1 st order			
Pt(111)	β	330		2 nd order		74Lu
Pt(111)	β_1	~220				75Chr
	β_2	310		3×10^{-9}		
Pt(111)	β_1	<250				77Col1
	β_2	310				
Pt(111)			2.7×10^5		MB study; activated adsorption, barrier height 2 - 6 kJ/mol	79Sal
Pt(111)				$10^{-1} \dots 10^{-3}$	determined by He scattering expts.	81Poe

Surface	H adsorption states + desorption temperature at sat'n [K]		Frequency factor		Remarks	Ref.
			1 st order [s ⁻¹]	2 nd order [cm ² /s]		
Pt(111)				10 ⁻² ...10 ⁻⁵	D ₂ study; coverages determined by nuclear reaction analysis (NRA)	82Nor1
Pt(111)	β_1	310			β_1 shifting to lower T with increasing Θ_H	88God
	β_2	390				
Pt(211)	β_1	295				74Lu
	β_2	430		2 nd order		
Au(100)-(5×20)	β	170			exposure to H atoms at 100 K	96Iwa
Au(110)-(1×2)	β	216		0.1...0.001	exposure to H atoms at 100 K	86Sau
Au(110)-(1×2)	β	177	1 st order		exposure to D atoms at 96 K	97Luh
	α	121				

3.4.1.3.2.3.2 Semiconductor and insulator surfaces

Experimental investigations of hydrogen desorption from semiconducting and non-conducting surfaces including the determination of desorption energies and frequency factors are practically restricted to C, Si and Ge surfaces. As pointed out before, there is no spontaneous adsorption of hydrogen atoms due to the extremely low sticking probabilities; in order to accumulate H atoms on the surfaces the H₂ molecules have to be pre-dissociated by a hot W filament or by using the translationally or vibrationally excited molecules of a supersonic molecular beam. Many efforts have been made to determine the activation energy for adsorption (which includes the activation energy for H₂ dissociation) and the reaction pathway for desorption, especially for clean Si single crystal surfaces [94Kol, 00Hil]. To determine the activation energy for dissociation, often MB studies have been performed, but also kinetic studies following changes in the surface reflectivity [97Bei]. In some cases, the order of the thermal desorption reaction can provide valuable hints to the adsorption and desorption mechanism [89Sin, 94Kol]. Generally, however, the data base is again scarce. One reason here is certainly the experimental difficulty to mount and prepare these materials and to reliably measure temperatures and hydrogen atom fluxes. Nevertheless, a quite general scenario can be drawn:

In the course of the interaction of H atoms with the respective surfaces, the first step is very often the lifting of the inherent surface reconstruction(s); as the H exposure continues, hydride compounds (mono- and/or dihydrides) are formed which thermally decompose at elevated temperatures thereby chemically etching the respective surfaces as mentioned before. We recall that C, Si, and Ge surfaces can adsorb at least a full monolayer of H atoms so as to form a (1×1)-H phase which practically passivates the surfaces and gives them interesting chemical and physical properties. In many recent studies, these passivated surfaces have served as convenient templates for depositing thin films of all kinds of materials.

Semiconductor and insulator surfaces

Surface	H adsorption states + desorption temperature at sat'n [K]	Frequency factor		Remarks	Ref.
		1 st order [s ⁻¹]	2 nd order [cm ² /s]		
C(100)-2×1 diamond	1200 (low Θ_H)... 1050 (high Θ_H)	3×10^5		expts. performed with D atoms	90Ham
C(100)-2×1 diamond	1173	1 st order		atomic H inefficient to break C - C dimer bonds	92Tho
C(111)-1×1 diamond	1310	$9.5 \pm 4.0 \times 10^{13}$ at $\Theta = 0.2$ ML		expts. performed with D atoms	97Su
C(0001) graphite (HOPG)	H : 445 (flat surface) 500 + 560 (step sites) D: 490 (flat surface) 540 + 580 (step sites)	1 st order		exposure to H (D) atoms; max. coverages ~0.4...0.5	02Zec
Si(100)-2×1	795 (monohydride) 680 (dihydride)	2.2×10^{11} (H ₂) 1.3×10^{11} (D ₂) 5.6×10^{11} (D ₂)		isothermal desorption expts., H coverages of 0.06, 0.34, and 1.0 ML; TD expts. after exposure to H (D) atoms at 123 K. Desorption energy 188.3 kJ/mol for both H ₂ and D ₂	89Sin 90Sin
Si(100)-2×1	β_1 790 β_2 ~670	2×10^{15} (D ₂)	3×10^{15}	exposure to D atoms	93Flo
Si(111)-7×7	β_1 870 β_2 ~695		$1.2 \times 10^{1(\pm 1.3)}$	exposure to H and D atoms, Laser-induced thermal desorption expts.	88Koe
Si(111)	β_1 870 (small Θ) β_1 810 ($\Theta \approx 1.0$) β_2 ~695 β_3 ~650 (shoulder state)	9.7×10^{12}	136	exposure to H atoms; H coverages β_1 state $\sim 8 \times 10^{18}$ H atoms m ⁻² $\beta_{2,3}$ states $\sim 3 \times 10^{18}$ H atoms m ⁻²	83Sch2
Si(111)-7×7	β_1 820 ($\Theta_H=0.12$) shifting to 785 ($\Theta_H=0.76$)		91 ± 10	TDS and isothermal desorption measurements; desorption activation energy 266 kJ/mol; derived Si - H bond strength 343 kJ/mol	91Wis
Si(100)-2×1	β_1 795 (monohydride) β_2 ~680 (shoulder only, dihydride)	2.2×10^{12}		TDS and isothermal desorption measurements using D atoms; desorption activation energy 210 kJ/mol derived Si - H bond strength 376 kJ/mol	90Sin
Si(100)-2×1	β_1 800	5.5×10^{15}		TDS and isothermal desorption measurements; desorption energy 243 kJ/mol	91Wis
Ge(100) Ge(111)	650 (low Θ) 620 (high Θ)		2 nd order	TDS after exposure to H atoms at 300 K	84Sur
Ge(100)-2×1	493 (monohydride)	1 st order			86Pap

Surface	H adsorption states + desorption temperature at sat'n [K]	Frequency factor		Remarks	Ref.
		1 st order [s ⁻¹]	2 nd order [cm ² /s]		
Ge(100)-2×1	570 (0.4 < Θ < 1.1)	4×10^{13}		desorption energy 176 kJ/mol; pairing energy of 22 kJ/mol of Ge surface dimers	93Dev
Ge(100)-2×1	500...550 K	2.7×10^{13} (H ₂) 1.2×10^{13} (D ₂)		desorption energy 160 kJ/mol for both H ₂ and D ₂	03Lee
Ge(100)- 2×1	645...620 (0 < Θ < 1)		2 nd order	exposure to H atoms; formation of dihydride phase	84Sur
Ge(111)	645...620 (0 < Θ < 1)		2 nd order	exposure to H atoms; formation of dihydride phase	84Sur
GaAs(110)	~380...420 (0 < Θ < 1)		2×10^{-7}	exposure to H atoms, adatom - adatom interactions important desorption monitored by intensity decrease of vibrational bands with temperature	81Lue
GaAs(110)	460 (small Θ) 415 (high Θ) 480...500 K (high Θ)		2 nd order	exposure to H atoms at 250 K, desorption energy between 0.5 and 0.7 eV = 48...68 kJ/mol H coverage 3×10^{18} m ⁻²	84Mok
GaAs(001)	303 - 423	1.0×10^8		exposure to H atoms	95Qi

3.4.1.3.3 The energetics of hydrogen adsorption and desorption

3.4.1.3.3.1 General remarks

A quantity that largely characterizes a given hydrogen adsorption complex is the strength of the bond(s) formed between the adsorbed hydrogen atom (or molecule) and the surface atoms of the substrate, E_B . We have seen that in the case of non-activated associative adsorption E_B equals the adsorption energy, E_{ad} . Thermodynamically, E_{ad} simply is the energy released by the system upon adsorption and counted negatively. We recall that in the case of activated adsorption an additional activation energy of adsorption, E_{ad}^* comes into play.

When considering the adsorption energetics in general, impinging H₂ molecules can encounter two principally different situations: i) They find a clean, H free, surface and can occupy sites that are not influenced by any neighboring adsorbed particles: In this case, the *initial* adsorption energy, $E_{ad,0}$ is released by the very first molecules that dissociate and adsorb on the bare surface. ii) A H₂ molecule hits a surface which contains already adsorbed H atoms (H coverage Θ), competes for an empty dissociation site and, once the atoms have become adsorbed, they interact with the already existing neighbors. The resulting adsorption energy E_Θ usually deviates from $E_{ad,0}$. In case of attractive interactions $E_\Theta > E_{ad,0}$; for repulsive interactions (which are the rule) $E_\Theta < E_{ad,0}$. The respective difference depends, of course, on the number of interacting neighbors leading to a (more or less pronounced) *coverage dependence* of the adsorption energy, $E(\Theta)$. This kind of coverage dependence described above is induced only by the adsorbed particles; the respective effect is called *induced (a posteriori) energetic heterogeneity*. As an example, we present in Fig. 6 a typical curve which has been measured for H adsorbing on Ni(111) under extremely clean and well-defined conditions in a glass apparatus [74Rin].

However, there also exist surfaces with inherent (a priori) structural heterogeneity, characterized by energetically different adsorption sites even in the bare state. These are, for example, high-index surfaces with differently coordinated adsorption sites, steps or foreign (impurity) atoms. Exposing such a surface to hydrogen will result in a more or less subsequent filling of the energetically inequivalent sites and, hence, also in a coverage dependence of the adsorption energy.

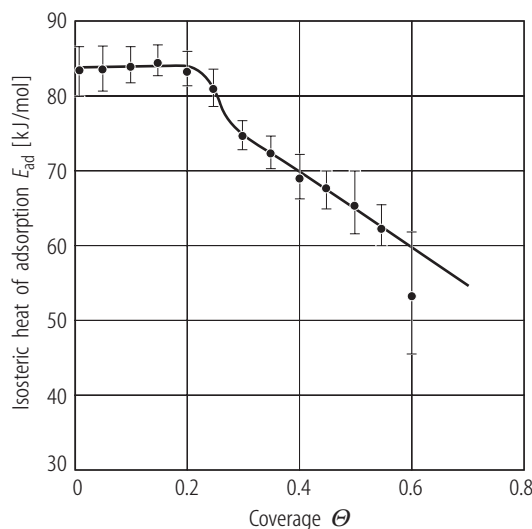


Fig. 6: Coverage dependence of the isosteric heat of adsorption (here denoted as E_{ad}) of hydrogen on a nickel(111) surface. E_{ad} has been measured volumetrically [74Rin]. Note that the coverage is given on an absolute scale. Only at lower coverages the heat of adsorption remains constant; it drops at elevated coverages due to repulsive H - H interactions.

In the following table we will mostly focus on values of the *initial* adsorption energy measured at vanishing or at least small coverages. We caution, however, that the respective measurements and data can suffer from small concentrations of impurities or inherent surface defects. It is known that especially carbon atoms can modify the hydrogen adsorption energetics to a large extent [90Chr]. Therefore it is quite important for the reliability of the tabulated energy data to carefully consider the chemical and crystallographic state of the surface under consideration as well as the vacuum conditions at which the experiments have been carried out.

A few words should be added concerning the *measurement* of hydrogen binding states and their adsorption energies and coverage dependencies. There exist *thermodynamic* and *kinetic* means to experimentally determine the adsorption energy E_{ad} . In a thermodynamic experiment, often the isosteric heat of adsorption is measured, either as an integral or a differential quantity. In this case equilibrium conditions are required (which are not always easy to establish), but then the data provide quite reliable thermodynamic information [70Cla]. For more details and definitions, we refer to the chapters 1 and 2 of this Landolt-Börnstein subvolume III/42A (which you can find in parts 1 and 2, respectively) and to the specific literature [77Hie, 69Tra]. Very convenient and relatively simple to perform are E_{ad} measurements based on thermal desorption spectroscopy (TDS, c.f., [91Chr]). Since the exponential term of the Polanyi-Wigner equation (Eq. 6) contains the desorption energy, it is straightforward to deduce this quantity from an appropriate evaluation (Arrhenius plot) of a TD data set [75Bau1, 75Kin, 83Hab].

It is also possible to measure heats released by adsorption *directly* by calorimetry. This has been employed in the early days of surface science mainly for powders [55Tra], later for gas adsorption on thin metallic (polycrystalline) films vapor-deposited from a central cathode filament consisting of the film material in question onto the inner surface of glass bulbs [70Wed]. The calorimetrically determined heats of adsorption are integral quantities, unless one admits small gas pulses and follows the development of the released heats, a procedure which requires an utmost sensitivity. Only recently direct calorimetric measurements were carried out also with metal single crystal samples, using a microcalorimeter in conjunction with a molecular beam set-up [92AIS].

In the following section we will examine the kind and number of hydrogen binding states and present data on the initial heat of adsorption as defined above. The cases of associative (molecular) and dissociative adsorption and, for the latter, in addition *non-activated* and *activated* adsorption will be distinguished. We will start with a presentation of the (scarce) data on the energetics of genuine hydrogen physisorption (requiring adsorption temperatures <10 K), sect. 3.4.1.3.3.2. Thereafter, the (numerous) scattering experiments using supersonic molecular hydrogen/deuterium beams will be dwelled upon (with emphasis on the noble metals Cu, Ag, and Au), sect. 3.4.1.3.3.3, until we will expand on the much more important atomic (dissociative) interaction of H_2 with (predominantly metal) surfaces, sect. 3.4.1.3.3.4. In the column “remarks” a comment can be found on how the energy has actually been measured.

3.4.1.3.3.2 Molecular hydrogen adsorption and physisorption phenomena

Turning to physisorption of H_2 first, it is agreed upon that physisorption is the ‘normal’ process to occur if chemically inert (insulating and/or semiconducting) surfaces are exposed to and interact with hydrogen gas at sufficiently low temperatures. We recall that free electron (alkali metal, alkaline earth and/or noble metal (Cu, Ag, Au) as well as most semiconductor) surfaces exhibit a surprisingly small activity to dissociate H atoms, in contrast to transition metal surfaces as was already pointed out in sect. 3.4.1.2. Consequently, the dissociation reaction on these latter materials is so effective that the hydrogen molecule breaks instantaneously apart even below 10 K. Hence, a normal TM surface will be immediately covered by a layer of H atoms which saturate the chemical valencies and sort of passivate the surface. Once this layer of chemisorbed H atoms is formed, H_2 molecules can merely condense on top, with enthalpies ranging below 5 kJ/mol. This was shown by Frieß et al. for H_2 interacting with a $(1\times 1)\text{-H}$ layer on top of a Ru(0001) surface [95Fri]; a series of H_2 thermal desorption spectra from their work is reproduced in Fig. 7. The strictly molecular nature of this adsorption bond can be established either by H_2/D_2 isotope exchange experiments (absence of isotopic scrambling) or by measurements of the H-H stretching vibration which should yield a frequency close to the gas phase value 4153 cm^{-1} [86Mar].

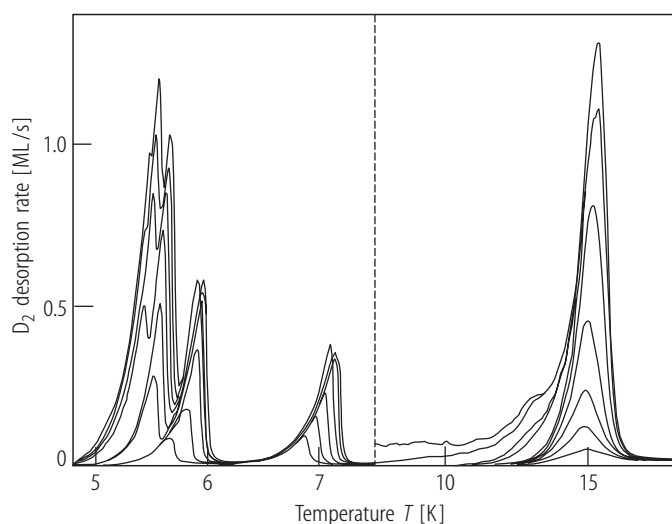


Fig. 7: Thermal desorption spectra for molecular deuterium multilayers on $(1\times 1)\text{D}/\text{Ru}(0001)$. At least five layers can be distinguished from the various TD maxima. The features right to the perpendicular dashed line belong to the first condensed D_2 layer, while the peak at 7 K stems from the 2nd layer, the one at 5.8 K to the 3rd, and the maxima below 5.5 K to the 4th and 5th layer, respectively. Note the zero order kinetics of the multilayer peaks. After Frieß et al [95Fri].

On the non-TM surfaces mentioned above and non-metallic materials such as graphite, silicon etc. hydrogen molecules merely physisorb. This means that low, in some cases very low, temperatures are required to capture the physisorbed H_2 species and keep it on the surface; even lower temperatures are needed if one wishes to detect two-dimensional molecular hydrogen phases with long-range order or the build-up of hydrogen multilayers (c.f., sect. 3.4.1.3.4). Without going into too much detail here it is simply referred to a review article [04Ptu] and some exemplary papers on H_2 adsorption on graphite(0001) covering these low-temperature phenomena [85Fre2, 88Cui].

Physisorption of hydrogen molecules

Surface	Initial adsorption energy [kJ/mol]	States and their coverage dependence $E(\Theta)$	Remarks	Ref.
Ni(111)	7.53		Physisorption energy of tritium (T_2) determined by radiotracer method between 5...30 K	73Ren
Cu(111)	2.89		MB expts., partial monolayer desorption expts.	93And
Cu(100)	2.99			
Cu(110)	2.99			
Mo(110) + H_2 ; D_2 between 1.5...30 K		extrinsic precursor states, Eden clusters	magneto-resistance expts.	92Lut
Ru(0001)(1×1)H	2.5 1 st layer 1.3 2 nd layer	5...6 states	physisorption of D_2 ; TDS expts. at 4.8 K; at least three layers can be distinguished	95Fri
Ag(111)	3.1		diffractive selective adsorption of H_2 physisorption potential	85Yu
Au(111)	1.72		HD physisorption potential as det'd by MB translational spectroscopy	86Har

3.4.1.3.3.3 Hydrogen adsorption dynamics

A special field of interest is the interaction of H_2 molecules with the free-electron metal surfaces Cu, Ag, Au. These systems have frequently been studied by means of molecular beam techniques which allow, among others, the determination of the H_2 - Cu (Ag, Au) scattering potential(s) ('selective scattering') and (by measuring the sticking probability as a function of the kinetic energy of the MB) the activation energy for dissociative adsorption. Also, the degree of vibrational and rotational excitation of the H_2 molecules and their kinetic energy is often considered and related with the dissociation/adsorption probability [94Ren, 94Hol, 00Din]. Sometimes, molecular dynamics (MD) simulations have been carried out [94Tul]. An important issue in these studies is the energy distribution among the rotational and vibrational states before and after the collision of the H_2 molecules with the surface. In some cases, 'rotational cooling' has been reported, i.e., the rotational energy distribution of the scattered molecules was only 80...90 % of the surface temperature [85Kub]. Although the dynamical behavior of hydrogen molecules interacting with surfaces is in the focus of scientific interest since many years and a wealth of investigations both experimentally and theoretically have been performed accordingly, we can only touch this topic here for the sake of space limitations.

Some special remarks may be devoted to the adsorption dynamics of hydrogen on semiconductor (silicon and germanium) surfaces. Scientists have been interested in *energetic* quantities, viz., the activation energies for adsorption and desorption and in the actual *reaction paths*, preferentially the dissociation mechanism. This topic has already been touched in sect. 3.4.1.3.1.7. and we recall the respective remarks made there. The experimental and theoretical progress, along with the technological interest in these materials, has led to an enormous increase in the number of the respective investigations. For example, the availability of scanning tunnelling microscopy made it possible to directly monitor the H_2 dissociation process on a Si surface, i.e., disentangle the individual reaction steps [91BoI2, 99Bie]. Dürr et al. directed a heated H_2 beam (temperature T) onto the surface and found with STM that the dissociated H atoms occupy Si atoms of *adjacent* dimers, and thus pairs of adjacent doubly occupied dimers are readily formed as the reaction proceeds [02Due].

Activated adsorption: Metal surfaces and elemental semiconductors

Surface	Height of barrier for adsorption [kJ/mol]	Depth of repulsive (scattering) potential [kJ/mol]	Exponent n of $\cos\theta$ distribution	Experimental technique	Remarks	Ref.
C(111) graphite		4.0 (H ₂) ($\nu=0$) 2.24 (D ₂) ($\nu=2$)		MB expts	expts. performed at 100 K with H ₂ and D ₂	80Mat
Si(100)2×1 Si(111)7×7	67 87			SHG expts.	expts. performed with D ₂	96Bra
Si(100)2×1	14.8 ($\theta_D=0.6$) 12.0 ($\theta_D=1.0$)		5.17 ($\theta_D=0.6$) 3.90 ($\theta_D=1.0$)	angle-resolved TDS	expts. performed with D ₂	93Par1 93Par2
Ni(100)	$\theta_D=0.2$		2.5...3	TDS; angular distribution + TOF mass spectrometry	expts. performed with HD and D ₂	93All
Cu(100)	21		5	angular distribution + TOF mass spectrometry of desorption		74Bal1 74Bal2
Cu(100)	66		8	angular distribution + TOF mass spectrometry of desorption	H ₂ and D ₂ permeation expts.	82Com
Cu(100)	19.3		10	supersonic MB expts.		89Ang1
Cu(100)	56.1 ($\nu=0$) 25.0 ($\nu=1$)			angular dep. of adsorption; model fitting	barrier height depends on H ₂ vibrational excitation	91Mic
Cu(110)	13		2.5	angular distribution of desorption; supersonic MB expts.		74Bal1 74Bal2
Cu(110)	67			seeded MB expts.		91Ber1
Cu(110)		2.12		MB expts; selective adsorption	six bound H ₂ states	82Per
Cu(110)			15.8	supersonic MB expts.		89Ang1
Cu(110)			7	angular distribution of desorption		89Ang1
Cu(110)	55.0 ($\nu=0$) 25.1 ($\nu=1$)			angular dep. of adsorption; model fitting	barrier height depends on H ₂ vibrational excitation	91Mic
Cu(110)	59.8 ± 6			H ₂ reactivity measurements		91Cam
Cu(110)	57.8 (H ₂)			supersonic MB expts. with H ₂ and D ₂	translational and/or vibrational excitation facilitate dissociation; late barrier found	91Hay

Surface	Height of barrier for adsorption [kJ/mol]	Depth of repulsive (scattering) potential [kJ/mol]	Exponent n of $\cos\theta$ distribution	Experimental technique	Remarks	Ref.
Cu(111)			6	angular distribution of desorption		74Ba1
Cu(111)	66		8	angular distri- bution + TOF mass spectrome- try of desorption	H ₂ and D ₂ permeation expts.	82Com
Cu(111)		2.14		MB expts.+ TOF	scattering of D ₂ and HD; selective adsorption potentials	86Har
Cu(111)			13	angular distribution of desorption		89Ang1
Cu(111)	60.0 ($\nu=0$) 22.1 ($\nu=1$)			angular dep. of adsorption; model fitting	barrier height depends on H ₂ vibrational excitation	91Mic
Cu(111)			8	angular distri- bution + TOF mass spectrome- try of desorption	H ₂ permeation expts;	82Com
Cu(111)	48...86 (H ₂ , $\nu=0$) 19...38 (H ₂ , $\nu=1$)			supersonic MB expts. with H ₂ , D ₂ , and HD + TOF expts.	strong increase of sticking probability with gas temperature indicates that both translational and vibrational excitation is important for passing the barrier	92Ret2 93Aue
Cu(310)	21			supersonic MB expts		74Ba2
Cu(110)				REMPI + TOF mass spectrometry	H ₂ permeation expts; rotat. and vibrat. state- resolved; vibrational heating observed	85Kub
Cu(111)				REMPI + TOF mass spectrometry	H ₂ permeation expts. rotat. and vibrat. state- resolved; vibrational heating observed	85Kub
Cu(111)			14	supersonic MB expts.	expts. performed with D ₂	92Ret1
Ag(110)		3.03		supersonic MB expts.		91Can
Ag(111)		3.09		MB scattering + TOF expts.	scattering of H ₂ , D ₂ and HD; selective adsorption potentials determined	83Yu
Ag(111)	26.8 \pm 0.6		8	angle-resolved TPD using D atoms		95Hea
Au(111)		≥ 2.02		MB expts.+ TOF	scattering of D ₂ and HD; selective adsorption potentials determined	86Har

3.4.1.3.3.4 Dissociative (atomic) hydrogen adsorption

The values listed in the table below were obtained by various methods at different adsorption temperatures; usually, the crystallographic structure of the surfaces in question was determined by LEED, the chemical cleanliness was controlled by Auger electron spectroscopy, XPS, or other techniques. The table includes adsorption energy data also for the inherently inactive noble metal surfaces Cu, Ag and Au. In this case, the data were mostly taken by exposing the respective surfaces to a flux of H *atoms* (formed by pre-dissociation in the gas phase or by supersonic molecular beams having sufficient thermal energy to overcome the activation barrier for dissociation). This holds for other ‘free electron’ metals, too, such as Be, Mg, Al, Ca, Zn etc., which have recently gained some interest, especially in conjunction with hydrogen storage materials and heterogeneous catalysis. Some of the respective data are also included in the following table. Although one will realize that some fields in the table do not contain numbers, the respective investigations have nevertheless *not* been omitted, because other important binding state-related properties were communicated therein, such as the *number* of states, the *temperature position* of TPD peaks or the *absolute coverage*, which may be of interest for the reader and help to get access to the H adsorption energy.

Surface	Initial adsorption energy [kJ/mol]	States and their coverage dependence $E(\Theta)$	Maximum number of H atoms adsorbed [H at/m ²] or [ML]	Remarks	Ref.
Be(0001)	92 (= activation energy to remove H from the potential well)	β	1 ML at $T = 77$ K	TD expts. after exposure to H atoms; no adsorption of H ₂ molecules for $T > 90$ K	90Ray
Al(100)		β	1 ML at $T < 90$ K	TD expts. after exposure to H atoms	88Pau
Al(100)	72.85	β	1.6 ML = 1.95×10^{19}	TD expts. after exposure to H atoms	91Win
Al(110)	69.1	β	24 ML = 2.07×10^{19}	TD expts. after exposure to H atoms	91Win
Al(111)	67.6	β	1 ML = 1.41×10^{19}	TD expts. after exposure to H atoms	88Mun
Al(111)	76.20	β	1.3 ML = 1.83×10^{19}	TD expts. after exposure to H atoms	91Win
V(111)	~63		surface 1 ML bulk	MB expts. performed with H ₂ and D ₂ , competing bulk dissolution	00Beu
Fe(100)	86.6	β_2 β_1	$2 \dots 3 \times 10^{18}$		80Ben
Fe(100)	100.4 75.4	β_2 β_1			77Boz
Fe(100)		β_2 β_1	sat'n 1.1 ML		91Ber2
Fe(100)	59.0	β_2 β_1			96Mer
Fe(110)	109 ± 5	β_2 indep. of Θ , β_1 decreases with Θ	$1.7 \times 10^{19} = 1$ ML	determined by TDS (Redhead analysis)	77Boz
Fe(110)	101.3 (H) 103.4 (D)		~0.8 ML at 200 K	isosteric heats determined by He scattering	88Kur

Surface	Initial adsorption energy [kJ/mol]	States and their coverage dependence $E(\Theta)$	Maximum number of H atoms adsorbed [H at/m ²] or [ML]	Remarks	Ref.
Fe(110)		β_2 β_1 α	0.48 ML sat'n	MB expts.	91Ber2
Fe(111)	88 75 54	β_3 β_2 β_1		determined by TDS (Redhead analysis)	77Boz
Fe(111)		β_2 β_1	1.52 ML sat'n	MB expts.	91Ber2
Fe(211)	101.3 82	β α_3 α_2 α_1	1.75 ML at 40 K	TDS analysis; surface reconstructs under hydrogen	95Sch1
Co(0001)	73 \pm 7	β	0.13 at 300 K	TDS analysis	79Bri
Co(10-10)	75.5 (80) 62	β α	1 ML (= 9.8×10^{18}) 1.5 ML at sat'n at 85 K	TDS (isosteric heat)	94Ern
Ni(100)	96.3	β_2		isosteric heat (equilibrium) measurements	74Chr
Ni(100)	96 84	β_2 β_1		TDS Redhead analysis	79Chr1
Ni(100)	89.2 69.5 49.4	' α ' state ($=\beta_2$) α_1 α_2	5.5×10^{18} at 137 K	TDS analysis	81Joh1
Ni(100)	96.2		smaller coverages (0.1 L exposure)	Laser-induced thermal desorption	84Hal
Ni(110)	88 75 30	β_2 β_1 α	1 ML 1.5 ML total at 100 K	TDS analysis; T dependent reconstruction	89Chr
Ni(110)	81.6	β_2		isosteric heat (equilibrium) measurements	71Ert
Ni(110)	90.0 (E_0) ; 98 (at $\Theta \neq 0$)	β_2		isosteric heat (equilibrium) measurements; heat <i>increases</i> with Θ due to attractive H-H interactions	74Chr
Ni(110)		β_2 β_1 α	1 ML 0.9 ML 0.4 ML total at 140 K = 2.3 ML		82Win
Ni(110)		β_2 β_1 α	1 ML = 1.14×10^{19} D at./m ² 0.5 ML total ($\alpha+\beta_1+\beta_2$) at 175 K = 1.5 ML	coverages determined by nuclear reaction analysis (NRA) using D ₂	84Jac 85Gri
Ni(110)		β_2 β_1 α	1.7 \pm 0.05 ML upon cooling in D ₂	coverages determined by nuclear reaction analysis using D ₂	87Jac1
Ni(110)	71	β_2 β_1 α		expts. performed with H ₂ and D ₂ molecular beams	85Rob
Ni(111)		β_2 β_1	1.9 \pm 0.2 $\times 10^{19}$ at 140 K = 1.0 \pm 0.1 ML total	TDS measurements	82Win
Ni(111)	95		2.7×10^{18} at 293 K	TDS analysis	72Lap2

Surface	Initial adsorption energy [kJ/mol]	States and their coverage dependence $E(\theta)$	Maximum number of H atoms adsorbed [H at/m ²] or [ML]	Remarks	Ref.
Ni(111)	96.3	β_2		isosteric heat (equilibrium) measurements	74Chr
Ni(111)	85 ± 2		4.7×10^{18} total at 100 K	isosteric heat (equilibrium) measurements	74Rin
Ni(111)	90.0 79.5	β_2 β_1		TDS analysis (Redhead)	79Chr1
Ni(111)		β_2 β_1	0.5 ML 1 ML	TDS analysis	86Rus
Cu(100)	48 ± 6 (H ₂) 56 ± 8 (D ₂)			pressures up to 5 bar were used; after extended exposures bulk uptake	93Ras
Cu(100)		single state	0.5 ML (exposure to H atoms)	non-equilibrium effects prevent a data analysis	89Ang1
Cu(100)		two states	1.03 ML	surface reconstructs (exposure to H atoms)	91Cho
Cu(110)		surface state subsurface state	0.67 ML	exposure to H atoms	86Rie
Cu(110)	45...96	single state	0.5 ML	exposure to H atoms E_{des} increases with coverage	89Ang1
Cu(110)	84.9 ± 1	single state		He scattering expts.	90Spi
Cu(110)		β_2 β_1 α	0.45 (± 0.05) ML at 140 K	exposure to H atoms; population of subsurface sites beyond 0.5 ML	93San1 93Bis
Cu(110)	59.9 ± 6 (H ₂) 65.3 ± 7 (D ₂)			exposure to H atoms; activation energy for dissociative adsorption	91Cam
Cu(110)	77.1 ± 10		1 ML at sat'n (1×1) LEED pattern	exposure to H atoms; TDS analysis	93Goe
Cu(111)		β_2 β_1	0.7 ML total at 83 K after exposure to H atoms	TDS	83Gre
Cu(111)	~84 ... ~64	single state	(exposure to supersonic MB)	E_{des} decreases slightly with coverage	89Ang1
Cu(111)			0.7 ML total at 150 K	IRAS and LEED study	89McC
Cu(111)	64.3 ± 1.3			isothermal desorption expts.	05Luo
Zn(0001)	46.5 ± 1.3	β	1 ML	exposure to H atoms; TDS analysis	84Cha2
Nb(100)	110.8 ± 12	state 2 state 1 (molecular precursor)	9×10^{18} 3.2×10^{18}	TDS analysis	74Hag
Nb(110)	105.8	two-state chemisorption		foils with (110) orientation: data derived from T dependence of UV photoemission	80Smi2
Nb(110)	61.9			kinetic uptake measurements	81Pic
Mo(110)	142.3 117.1	β_2 β_1	$\sim 7 \times 10^{18}$ $\sim 7 \times 10^{18}$ 1.3×10^{19} total at 78 K	TDS analysis	72Mah

Surface	Initial adsorption energy [kJ/mol]	States and their coverage dependence $E(\Theta)$	Maximum number of H atoms adsorbed [H at/m ²] or [ML]	Remarks	Ref.
Mo(100)	113 83.7 66.9	β_3 β_2 β_1	5×10^{18} at 78 K	TDS analysis	71Han
Mo(100)		β_3 β_2 β_1	2 ML total at 210 K	TDS; combined LEED and IR expts.	87Pry 92Baf
Mo(100)	101.3 85.8 71.6	β_3 β_2 β_1	total 2.1 ML \pm 0.2 at 100 K	combined LEED, HREELS and TDS measurements	86Zae
Mo(211)	145... 65	β_3 β_2 β_1	2 ML total at 180 K	data extracted from isobars; strong decrease of E_d with coverage	94Lop
Ru(0001)	109 44	β_2 β_1	1 ML total at 250 K; β_2 : strong decrease of E_d with coverage	TDS data plotted as isotherms	79Sch
Ru(0001)	70 43.9	β_2 β_1	0.85 ML ($= 1.3 \times 10^{19}$) at 150 K	strong decrease of E with coverage; TDS analysis	80Shi
Ru(0001)	92	β_2 β_1	1 ML ($= 1.58 \times 10^{19}$ at 100 K)	TDS analysis	78Dan
Ru(0001)	125....90 <90	β_2 (N state) β_1 (P state)		TDS data plotted as isosters	85Feu
Ru(0001)		β_2 β_1	1.02 \pm 0.05 at 200 K	TD comparison with CO (via ads. of formaldehyde)	89Sun
Ru(10–10)	82 50	β_3 β_2 β_1 α	1 ML 1.2 1.5 2.0 total (1.73×10^{19})	TDS (full line shape analysis)	89Lau
Rh(100)	79.9 \pm 1.7	β α	1 ML ($= 1.39 \times 10^{19}$) total at 100 K	expts. performed with D ₂ ; TDS analysis	82Kim
Rh(100)	108.8 \pm 3	β_1 β_2	>0.5 ML	TDS analysis	87Ric1
Rh(110)	90 (80) 53 33	β α_2 α_1	2 ML total at 80 K	TDS (isosteric equilibrium data)	88Ehs 86Chr
Rh(111)	77.8	β α	1 ML at 100 K ($= 1.58 \times 10^{19}$)	strong decrease of E_d with coverage	79Yat
Rh(111)	71.2 \pm 8	β	1 ML at 140 K	TDS and MB expts.	96Col
Rh(311)	67.5	δ γ_2 γ_1 β α	less than 1 ML	expt. + theoretical modelling	91Nic1 99Pay
Rh(311)			3...4 ML	He scattering	95Ape1 95Ape2
Pd(100)	102.6	β shoulder state	1.35 ML at 170 K	isosteric heat measurements	80Beh

Surface	Initial adsorption energy [kJ/mol]	States and their coverage dependence $E(\Theta)$	Maximum number of H atoms adsorbed [H at/m ²] or [ML]	Remarks	Ref.
Pd(100)		β α	2.5 ML at 105 K; including some bulk absorption contribution	α state (due to subsurface H) only appears at 100 K ads. temp.; H bulk absorption likely; activation energy for bulk absorption 4.6 kJ/mol	98Oku
Pd(110)	96.3 (TDS) 102.15 (isosteric heat)	β high T shoulder state ~680 K	0.5 ML at 300 K (= 4.7×10^{18})	room temperature study shoulder due to H desorption from bulk	74Con
Pd(110)	87.9 \pm 8	β_2 β_1 α_2 α_1	1.5 ML at 130 K; $\Theta > 1.5$ ML including subsurface H	population of subsurface sites	83Cat1 83Cat2 83Beh
Pd(110)	71	β_2 β_1 α_2 α_1		isothermal desorption expts. performed with deuterium	88He2
Pd(110)		β_2 β_1 α_2 α_1	$\beta_2 + \beta_1$ = surface H \approx 1.5 ML ; α_2 = 0.5 ML subsurface, α_1 = absorbed H, > 1 ML	subsurface state population	88He1
Pd(111)			1 ML	LEED expts. under stat. H ₂ pressure	73Chr1
Pd(111)	87.9 \pm 5			isosteric heat (equilibrium) measurements	74Con
Pd(111)	89.5 ~77	β shoulder state		TDS analysis; data taken at 190 K	76Con1
Pd(111)			1 ML total at 37 K	STM study	03Mit1
Pd(210)	75 \pm 10 (TDS) (90 \pm 10 isosteric heat) 63 (TDS) 45 (TDS) 38 (TDS)	β_3 β_2 β_1 α (subsurf.)	> 2 ML total at 90 K	expts. performed with deuterium; TDS and equilibrium expts.	98Mus
Pd(311)	82.9 76.2 22.2	β_2 β_1 α (subsurface)	1 ML total at 120 K	TDS analysis	99Far
Pd(311)	82.9 76.2 22.2	s (β_2) 315 K rs (β_1) 280 K ss 212 K v (α) 170 K		H adsorption strongly dependent on adsorption temperature (s = surface, rs = surface after lifting of (1 \times 2) reconstr. ss = subsurface, v = bulk)	98Fri
Ag(100)	~58	β_1 150 K α 110 K (sub-surface)		TD expts. after exposure to H (D) atoms; D ₂ - TD spectra more reproducible	04Kol

Surface	Initial adsorption energy [kJ/mol]	States and their coverage dependence $E(\Theta)$	Maximum number of H atoms adsorbed [H at./m ²] or [ML]	Remarks	Ref.
Ag(110)	41.7 ± 7 28.9 ± 3	β_2 β_1		TD expts. after exposure to H atoms	93Spr
Ag(111)	23.0 ± 1.2 (H ₂) 28.0 ± 1.2 (D ₂)	β_2 β_1		TD expts. after exposure to H atoms	89Zho
Ag(111)	43.6			expts. performed with D atoms (data of [89Zho] re-examined)	90Par2
Ag(111)			0.6 (± 0.1) ML at 100 K	TD expts. after exposure to H atoms	95Lee
Ag(111)	26.8 ± 0.6 (D ₂)		low coverages sat'n = 1.0 ± 0.3 ML	TD after exposure to D atoms	95Hea
Ta(110)			ca. 1 ML surface species; > 1 ML bulk uptake	TDS expts.	93Hei
W(100)			total 2.0 × 10 ¹⁹ H at./m ² at 300 K (= 2 ML)		66Est
W(100)	135.2 (H) 136.5 (D) 110.0 ± 1 (H) 111.4 (D)	β_2 β_1	2.5 × 10 ¹⁸ molec./m ² (0.85 ± 0.08 at 77 K) 5 × 10 ¹⁸ molec./m ²	TDS analysis	69Tam
W(100)			total 2.0 × 10 ¹⁹ H at./m ² at 300 K (= 2 ML)	King&Wells method [72Kin]	73Mad
W(100)			total 1.9 (± 0.3) × 10 ¹⁹ H at./m ²	LEED analysis	80Kin
W(100)	167.5 83.7	β_2 β_1	0.5 1.5; total 2 ML	TDS analysis	84Hor
W(100)			2 × 10 ¹⁹ H at./m ² (2ML) at 100 K	Infrared expts.	89Rif
W(110)	136.1 113 ± 5	β_2 β_1	total 0.60 ± 0.09 at 77 K	TDS analysis	71Tam
W(110)			total 9.1 × 10 ¹⁸ H at./m ² at 135 K	TDS analysis	74Bar
W(110)		β_2 β_1	total 1.5 × 10 ¹⁹ H at./m ²		81Hol
W(110)	146.4	β_2	total coverage = 1 ML = 1.42 × 10 ¹⁹ H atoms/m ²	TDS analysis; $\Delta\Phi$ measurements; isothermal desorption	97Nah2
W(111)	153.2 ± 6 127.3 ± 5 90.85 ± 3 59.0 ± 2	β_4 β_3 β_2 β_1 γ	total 1.65 ± 0.2 ML at 77 K	TDS analysis	71Tam
W(111)	129.7 ± 10 104.6 ± 10 79.5 ± 7 50.2 ± 5	β_4 β_3 β_2 β_1	total coverage = 6 × 10 ¹⁸ H at./m ²	TDS analysis	72Mad 75Sch
W(111)			total 9.4 × 10 ¹⁸ H at./m ²	TDS analysis	74Bar
W(211)	146.5 67	β_2 β_1	4.0 × 10 ¹⁸ 4.6 × 10 ¹⁸ , 8.6 × 10 ¹⁸ H at./m ² total at 110 K	TDS analysis	73Rye 73Car

Surface	Initial adsorption energy [kJ/mol]	States and their coverage dependence $E(\Theta)$	Maximum number of H atoms adsorbed [H at/m ²] or [ML]	Remarks	Ref.
Re(0001)	83.7	β with low- T shoulder	4×10^{18}	TDS analysis	81Duc
Re(0001)	134	β		TDS analysis	90He
Re(10–10)	125 80 60	β_2 β_1 α	1.63×10^{19} total at 120 K (= 2 ML)	TDS analysis	95Mus
Ir(100)-(1×1)	111.5 (TDS) 98 ± 14 (equil. data)	β α	1 ML total at 200 K	MB study using D ₂	98Ali
Ir(100)-(5×1)	85	β α	1.22 ML at 200 K	MB expts. performed with D ₂ [98Ali]	98Ali 80Ibb
Ir(100)-(5×1)	91 ± 12 ; 75 ± 12	state “C”		TDS analysis; $E(\Theta)$ decreasing with coverage	00Mor
Ir(110)-(1×2)	96.3 71.2	β_2 β_1	$2.2 (\pm 0.2) \times 10^{19}$ total at 130 K	TDS analysis	80Ibb
Ir(111)	52.8	β_2 with low- T shoulder	1.57×10^{19} total at 100 K	TDS lineshape analysis; expts. performed with D ₂	87Eng
Ir(111)		β_2 β_1	1 ML total at 90 K	TDS analysis	99Hag; 96Lau
Pt tip (111), (110), (100) orientation	67			field emission measurements	69Lew
Pt(100)-hex		β_2 β_1 shoulder α_3 α_2 α_1	4.1×10^{18} total at 135 K (= 0.63 ML)	TDS analysis	74Lu
Pt(100)-hex	62.7...66.9	one state + two substates	4.6×10^{18} total	TDS analysis	75Net
Pt(100)-hex			1.2×10^{19} total at 120 K	nuclear reaction analysis	80Nor1
Pt(100)-hex	63.2	peak “1” peak “2”	1.5×10^{19} total	TDS analysis	93Klo
Pt(100)-hex	49	α_3 γ_3 γ_2 γ_1	1.55×10^{19} total at 150 K	MB study TPD features complex because of T - and H coverage dependent reconstruction	95Dix
Pt(100)-hex	49.5 57.3 82.4	a_1 a_2 a_3 b	1.2×10^{19} total (= 1ML)	TPD features complex because of T - and H coverage dependent reconstruction	91Pen1
Pt(100)-hex	49	γ_1 γ_2 γ_3 α_1 α_2 α_3		TPD features complex because of T - and H coverage dependent reconstruction	95Pas
Pt(110)-(1×2)		β_2 β_1	4.2×10^{18} total at 125 K (= 0.47 ML)	TDS analysis	74Lu

Surface	Initial adsorption energy [kJ/mol]	States and their coverage dependence $E(\Theta)$	Maximum number of H atoms adsorbed [H at/m ²] or [ML]	Remarks	Ref.
Pt(110)-(1×2)		β_2 β_1 α	1.7 ML ($\pm 10\%$)		89Ang2
Pt(110)-(1×2)		β_2 β_1			92She
Pt(111)	73.3	β	4.1×10^{18} total at 125 K (= 0.55 ML)	TDS analysis	74Lu
Pt(111)	39.3 26.8	β_2 β_1	~1 ML	isosteric heat data; TDS analysis	75Chr
Pt(111)		β_2 β_1			77Col1
Pt(111)	65.3 ± 2			MB study; activated adsorption, barrier height 6.3 kJ/mol	79Sal
Pt(111)	71			determined by He diffraction (isosteric heat)	80Poe
Pt(111)	67 ± 7			isosteric heat data using D ₂ ; coverages determined by nuclear reaction analysis	82Nor1
Pt(111)			1 ML	He diffraction study	83Lee
Pt(111)	79.5 ± 8	β_2 β_1	1 ML (= 1.5×10^{19})	TDS analysis	88God
Pt(211)		β_2 β_1	3.3×10^{18} total at 125 K (= 0.43 ML)	TDS analysis	74Lu
Au(100)-(5×20)		β	0.3 ML at 100 K	exposure to H atoms at 100 K	96Iwa
Au(110)-(1×2)	51 ± 4	β	0.5 ML	exposure to H atoms at 100 K	86Sau
Au(110)-(1×2)	45 ± 4 31 ± 2	β α	>0.5 ML	exposure to H atoms at 96 K	97Luh

Semiconductor and Insulator Surfaces

Surface	desorption energy [kJ/mol]	states and their coverage dependence $E(\Theta)$	maximum number of H atoms adsorbed [H at/m ²] or [ML]	Remarks	Ref.
C(0001)	57.9 (H ₂)	terrace site	~0.5 ML	TDS analysis	02Zec
graphite (HOPG)	91.6 (D ₂)	terrace site	~0.5 ML		
Si(100)	238.5 196.6	β_1 β_2	1.5 ML	TDS analysis	93Flo
Si(111)-7×7	257 ± 20 (D ₂ = 247 ± 13)	β_1 state at 870 K	Si - H (D) bond energies of 346 (341) kJ/mol; H sat'n coverage = $1 \times 10^{19} \text{ m}^{-2}$	exposure to H and D atoms, Laser-induced thermal desorption expts.	88Koe
Ge(100)	145 ± 10	β state		TDS	84Sur
Ge(111)					
GaAs(001)	60 ± 8		As - H bond energy 289, Ga - H bond energy 259 kJ/mol		95Qi

3.4.1.3.4 The diffusion of adsorbed hydrogen

Surface diffusion is an important process in the interaction of hydrogen with solid surfaces in that it often governs the rate of adsorption and desorption, determines the formation of phases with long-range order and, of course, decisively affects the rate of catalytic reactions involving transfer of H atoms or H₂ molecules. Due to the limited space we will exclude bulk diffusion phenomena from our considerations, although certain metals such as Pd, V, Ti, Zr, Nb, Ta etc. can under appropriate thermodynamic conditions absorb large quantities of hydrogen which makes these materials interesting for hydrogen storage. For details on this subject as well as on a general formal description of diffusion phenomena, the reader is referred to the respective monographs and textbooks [65Jos, 78Ale]. We recall that especially Pd surfaces exhibit a variety of phenomena which involve diffusion steps, overlayer - underlayer (surface - subsurface) transitions and absorption/hydride formation processes.

Pioneering field emission work, focussing to a large extent on H surface diffusion, was performed in Gomer's laboratory [57Wor, 61Gom, 90Gom]. Morris et al. [84Mor] and Naumovets and Vedula [84Nau] reviewed the state of surface diffusion until the mid-eighties (including a description of experimental methods). More recent compilations deal with single adatom diffusion phenomena [94Ehr] or with the mechanisms of surface diffusion processes in general [02Nau, 02Ros]. A historical review is provided by Antczak and Ehrlich [05Ant]. Until the nineties, direct observation of surface diffusion by field emission techniques (either by watching the propagation of diffusion fronts or by an analysis of field emission fluctuations [82DiF]) was by far the most frequently applied and effective technique. Only in recent decades additional powerful methods were developed. In 1972 Ertl and Neumann introduced the laser-induced thermal desorption technique [72Ert], which was then further improved [86See, 86Mak1, 87Mak1, 87Mak2]: This method is based on the 'hole refilling' phenomenon: A focused laser beam illuminates a well-defined patch on the surface with an energy just sufficient to thermally desorb all the particles in that area. The refilling of the hole from the unperturbed surrounding is then followed as a function of time by subsequently fired laser pulses. The refilling signal is then fitted to expressions derived from Fick's second law. However, this technique in its simple form bears some disadvantages; among others, it is difficult to deduce directional and coverage dependencies [92Man]. Mak and George have published a simplified method to determine the coverage dependence of surface diffusion coefficients [86Mak2]. In the nineties, optical diffraction of laser beams [92Zhu, 97Cao], He atom scattering [99Gra], or scanning tunneling microscopy [96Zam, 96Tro, 97Win] were used to follow surface diffusion. A real breakthrough was achieved by applying the STM techniques: A direct counting and subsequent statistical analysis of the number of migrating N (O) atoms on a Ru surface as a function of time revealed much insight into the principal surface hopping, diffusion, and lateral ordering phenomena at and around room temperature. However, in order to watch diffusing *hydrogen atoms* with their much larger diffusion rate, considerably lower temperatures are necessary; a possible solution is provided by performing STM observations in combination with inelastic electron tunneling (IETS) in a 4 K-STM [97Sti, 98Sti]. For more details about this exciting technique and its application to hydrogen adsorption systems, the internet site <http://www.physics.uci.edu/~wilsonho/stm-iets.html> is recommended for reading.

As was first convincingly shown by Gomer, the diffusion of H (D, T) atoms can be subdivided into 'classical' diffusion (with discrete thermally activated hopping events) and quantum diffusion in which the light H (D, T) atoms behave as wave-like quantum particles and propagate by tunneling processes, without any thermal activation barrier [80DiF, 82DiF]. This latter behavior becomes immediately evident, if one follows the temperature dependence of the diffusion coefficient $D(T)$ [87Aue]. The temperature dependence of the classical surface diffusion is commonly described in the form of an Arrhenius equation

$$D(T) = D_0 \exp\left(-\frac{E_{diff}}{kT}\right) \quad (8)$$

with D_0 = pre-exponential factor [$\text{cm}^2 \text{s}^{-1}$], and E_{diff} = activation energy for diffusion [kJ/mol] which corresponds to the lateral hopping barriers between adjacent adsorption sites. For stationary diffusion, $D(T)$ can be expressed from Fick's first law as the ratio of the particle flux through the concentration front and the actual concentration gradient at time t . Likewise, the diffusion progress is described by the

mean square displacement of a particle, according to Einstein's equation, which also contains the diffusion coefficient:

$$\sqrt{\langle x^2 \rangle} = \sqrt{2Dt} \quad (9)$$

Another frequently used expression is based on random walk events between fixed sites and combines the pre-exponential factor D_0 , the jump length a and the vibrational frequency parallel to the surface, ν , via

$$D_0 = \frac{1}{4} a^2 \nu. \quad (10)$$

Of course, depending on the surface structure and corrugation, there may exist 'easy' and 'difficult' pathways for diffusion; hence, the diffusion coefficient is usually strongly direction-dependent. Most of the experiments focus on a determination of the activation energies for diffusion and the diffusion coefficients, whereby, as mentioned above, the 'classical' regime must be delineated from quantum diffusion. As a rule of thumb, the activation energy of diffusion is between one fifth and one tenth of the depth of the chemisorption potential. One can define the lifetime τ_s of a particle adsorbed in a specific site s on the surface; it is related to the diffusion energy by the expression

$$\tau_s = \tau_{s,0} \exp\left(\frac{E_{diff}}{kT}\right) \quad (11)$$

Apparently, the particle's residence time in a certain site depends sensitively on the thermal energy (temperature) of the surface; $E_{diff} \geq 10 kT$ means actually immobile particles, whereas the case $E_{diff} < kT$ enables a free motion of the adatoms across the surface.

The space limitations do not allow us to further expand on both experimental and theoretical investigations on hydrogen diffusion. There exist numerous theoretical articles dealing with diffusive H motion on surfaces, most of them focusing on the interesting non-thermally activated quantum tunneling processes [85Fre1, 98Bae].

In the following table we have compiled some diffusion coefficients and diffusion energies for a variety of hydrogen adsorption systems. As can be seen, there are not too many hydrogen adsorption systems that have been investigated; a strong preference exists for tungsten(110) which has been scrutinized in Gomer's laboratory [57Gom, 80DiF, 82DiF, 84Wan, 85Tri, 85Wan, 86Tri1, 86Tri2, 87Aue].

Surface	Temperature range [K]	Diffusion coefficient D_0 [cm ² /s]	Diffusion energy E_{diff} [kJ/mol]	Experimental method and remarks	Reference
Ni(100) (tip)	240...300		29.3 ± 4	field electron emission, front diffusion	57Wor
Ni(100)	223...283	$3 \times 10^{13} \text{ s}^{-1}$ pre-exponential factor for hopping frequency	16.7 ± 2	laser-induced thermal desorption	85Geo
Ni(100)	211 236 263	$2.1 (\pm 0.2) \times 10^{-7}$ $7 (\pm 0.2) \times 10^{-7}$ $1.5 (\pm 0.3) \times 10^{-6}$	17.6	laser-induced thermal desorption of D atoms	86Mul
Ni(100)	140...250	8×10^{-6} (Θ -indep.) (H) 2×10^{-5} (low Θ)(D) 2×10^{-4} (high Θ)(D) 10^{-12} (H, D)	13.4 (H) 15.1 (D), with little Θ dependence ~ 0	field emission fluctuation technique quantum tunneling	91Lin

Surface	Temperature range [K]	Diffusion coefficient D_0 [cm^2/s]	Diffusion energy E_{diff} [kJ/mol]	Experimental method and remarks	Reference
Ni(100)	170...200	1.1×10^{-6} (H) 5×10^{-5} (D)	14.6 (H) 20.9 (D)	linear optical diffraction technique. At 170 K, transition from activated tunneling to classical thermal diffusion	92Lee 92Zhu
	120...170	1.5×10^{-9} (H) 9×10^{-10} (D)	5.0 (H) 4.39 (D)		
Ni(111)	13...20	2.8×10^{-4} , hopping frequency $= 3 \times 10^{12} \text{ s}^{-1}$	0.84	physisorbed tritium (T_2) molecules; radiotracer method	73Ren
Ni(111)	140...250	3×10^{-4} (low Θ) (H) 7×10^{-2} (mid Θ) (H)	12.5 (low Θ) (H) 16.7 (high Θ) (H) 14.2 (low Θ) (D) 18.4 (high Θ) (D)	field emission fluctuation technique; below ~140 K quantum tunneling sets in	91Lin
	< 140	$\sim 10^{-10}$	0		
Ni(111)	110...240	2.8×10^{-3} (H); 3.4×10^{-3} (D);	18.9 (H) 21.0 (D)	optical grating method plus laser-induced thermal desorption	97Cao
	65...110	2.4×10^{-7} (H); 1.6×10^{-8} (D)	10.1 (H) 10.1 (D)		
Cu(100)	65...80 (classical thermal diffusion)	hopping frequency $\nu = 10^{12.9} \text{ s}^{-1}$ (H) $\nu = 10^{12.7} \text{ s}^{-1}$ (D)	19.0 ± 0.4 (H) 18.7 ± 0.4 (D)	direct STM observations in conjunction with inelastic tunneling spectroscopy:	00Lau
	$9 < T < 60$	10^{-19}		quantum tunneling of single H atoms	
Ru(0001)	260...330	6.3×10^{-4} at $\Theta = \text{low}$	16.7 ± 2	laser-induced thermal desorption	86Mak1
	230...270	7.9×10^{-4} Θ -independent	15.5 ± 2 Θ -independent	$0.15 < \Theta < 0.78$ strong decrease of D_0 for surface contamination with sulfur or carbon	87Mak1 87Mak2 88Bra
Rh(111)	150...300	8×10^{-2} for $0.02 < \Theta < 0.4$	15.5 (low Θ) (H) 18.0 (high Θ) (H) 18.2 (low Θ) (D) 20.5 (high Θ) (D)	laser-induced thermal desorption of H and D	88See
Rh(111)	186...216	H: 6.5×10^{-3} at $\Theta = 0.3$ 5.9×10^{-4} at $\Theta = 0.8$	H: 13.4 ± 2 at $\Theta = 0.3$ 11 ± 2 at $\Theta = 0.8$	laser-induced thermal desorption	92Man
		D: 5.7×10^{-4} at $\Theta = 0.4$ 7.1×10^{-4} at $\Theta = 0.8$	D: 13.8 ± 2 $(0.3 < \Theta < 0.9)$		
W(100)	>220 (activ. regime)	$10^{-5} \dots 10^{-7}$	16.7...29.3	field emission fluctuation technique; for $T < 200$ K coexistence of two diffusion regimes due to fluctuations caused by single atoms and by collective modes	95Dan
	140...220 <140 (tunneling)	$10^{-9} \dots 10^{-10}$	4.2...8.4		
W(110) (tip)	180...300		21.8..24.7 \pm 4 39.7 at very low coverage	field electron emission, front diffusion	57Gom

Surface	Temperature range [K]	Diffusion coefficient D_0 [cm^2/s]	Diffusion energy E_{diff} [kJ/mol]	Experimental method and remarks	Reference
W(110)	143...200	5×10^{-5} (H)	20.0 ± 1.5 (H) 20.3 ± 1.5 (D)	field emission fluctuation technique; tunneling dominates below 140 K	80DiF
	<140	7.83×10^{-8}	0; (tunnel probability $P = 8.69 \times 10^{-5}$)		82DiF
	<130	4×10^{-13} ... 10^{-12} , depending on θ .			
W(110)	> ~ 100 (thermal regime)	coverage $\theta = 0.1$: 1.7×10^{-7} (H) 3.5×10^{-5} (D) 3.3×10^{-3} (T);	coverage $\theta = 0.1$: 17.1 (H) 16.5 (D) 20.1 (T)	field emission fluctuation technique	85Wan
		coverage $\theta = 0.3$: 1.7×10^{-7} (H) 3.5×10^{-5} (D) 3.3×10^{-3} (T);	coverage $\theta = 0.3$: 19.2 (H) 19.6 (D) 20.7 (T)		
		coverage $\theta = 0.6$: 1.7×10^{-7} (H) 3.5×10^{-5} (D) 3.3×10^{-3} (T);	coverage $\theta = 0.6$: 19.7 (H) 20.3 (D) 22.3 (T)		
		coverage $\theta = 0.9$: 1.7×10^{-7} (H) 3.5×10^{-5} (D) 3.3×10^{-3} (T)	coverage $\theta = 0.9$: 21.5 (H) 22.4 (D) 24.4 (T)		
W(211)	80...250	9×10^{-5} (H)	31 (H)	field emission fluctuation technique; H coverage $\theta = 0.5$	88Dan
		5×10^{-6} (D)	27.6 (D)		
		(along channels);	(along channels);		
		8×10^{-6} (H)	27.2 (H)		
	<167...190	2×10^{-6} (D)	25.5 (D)	non thermally activated tunneling dominates	
		(across channels)	(across channels)		
		6×10^{-14} (H)	0		
		5×10^{-14} (D)	0		
		(along channels)			
		4×10^{-14} (H)	0		
		3×10^{-14} (H)	0		
		(across channels)			
Pt tip (111), (110), (100) orientation	4.2...320	9×10^4	18.8 (H)	field emission – direct observation of moving H front	69Lew
Pt(111)	200...250	3×10^4 at $\theta = 10^{-3}$	50.2 at $\theta = 0.001$	laser-induced thermal desorption	86See
		0.5 at $\theta = 0.33$	29.3 at $\theta = 0.33$		

3.4.1.3.5 The structure of adsorbed hydrogen phases

In the following section, the wealth of data which has so far been accumulated for hydrogen phases with long-range order will be reviewed. The vast majority of these phases consists of *atomically* adsorbed hydrogen and the quantities of interest are i) the coordination number of the local site (terminal, long or short bridge, threefold hollow (octahedral or tetrahedral)) of the adsorbed H atom, and ii) the Me-H bond length (chemical bonding to the adjacent substrate atoms). Often, also layer distances have been determined, which are, of course, geometrically related to the Me-H bond lengths; for the sake of brevity, these data are not included in the following tables, but easily available from the respective references. If necessary, these data (as all surface structural information) can be taken from the NIST structural compilation, vers. 5.0 (NIST = National Institute of Standards and Technology), accessible from the internet under the address <http://www.nist.gov/srd/nist42.htm>. Since mostly diffraction methods were

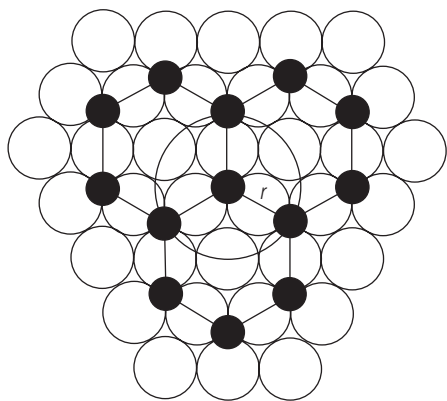
used for structure determination, in particular low-energy electron diffraction (LEED), to some extent also He atom scattering (HAS), the prerequisite for such a structural analysis is the formation of a hydrogen phase with *long-range order*, which, in turn, is governed by attractive or repulsive mutual H-H interaction forces. The respective ‘extra’ diffraction intensities reflect the degree of order, and the scattering amplitude depends, as usual, on the atomic scattering factor and the position of the H atom(s) in the surface unit mesh. Since a hydrogen atom is a very weak scatterer for electrons and, furthermore, exhibits forward scattering, i.e., large scattering amplitudes in the direction towards the bulk, low LEED intensities of true H superstructures are expected [74Pen, 77Ton]. More details on the specifics of low-energy electron diffraction at H layers can be found elsewhere [79Chr2, 88Oed, 93Mue, 96Hei]. It is worth to mention that in many cases the ‘extra’ LEED intensities of H adsorbed layers are larger than predicted from kinematic theory. The chemical interaction between atomic hydrogen and the surface atoms causes systematic displacements of the latter leading to phenomena of *multilayer relaxation* (a modification of the layer distances perpendicular to the surface) or surface *reconstruction* (the substrate atoms move laterally to new periodic sites giving rise to new diffraction features). Local buckling effects of the substrate atoms varying with the periodicity of the adsorbed H lattice can substantially reinforce the diffraction features. Careful surface-structure analyses performed over the last decades have shown that H-induced alterations of the substrate atom positions are the rule rather than the exception. The following table therefore contains a column in which H-induced surface reconstructions will be listed and commented. Another remark is worthwhile in this context: Some of the 5d electron metals of the third row of the periodic table reconstruct even in the clean state, for example the (100) and (110) surfaces of Ir, Pt, and Au. Since the respective reconstructed surfaces exhibit a complicated structure (which is nevertheless seen by the adsorbing H atoms), we have cited, in a separate line, the respective clean surface structure analysis. Note that under certain conditions the exposure of these reconstructed surfaces to hydrogen can lead to a lifting of the reconstruction, a process referred to as (H-induced) ‘deconstruction’.

As mentioned above, He atom diffraction (HAS) is used in a variety of cases for structure determination. Although this atom beam diffraction is the most sensitive method it actually probes only the integral surface corrugation. From this, the H adsorption site and possible first-layer reconstruction(s) must be extracted. Note that subsurface structural changes also enter the corrugation function. Problems and benefits of atom diffraction are covered in various articles [80Rie, 82Eng, 94Rie].

In many cases, valuable information about the local coordination of an adsorbed H atom can arise from analyses of vibrational properties of the H - substrate complex. Especially for metal and semiconductor surfaces, high-resolution electron energy loss spectroscopy (HREELS) has often been employed for this purpose, since both the number and frequencies of the vibrational bands, in conjunction with the electron scattering geometry, provides hints to the local symmetry of the adsorption site. Therefore, the following table also contains – where available – information on the local H - metal geometry obtained by HREELS. Note that a separate section (3.4.1.3.5) is devoted to H-induced vibrations at surfaces.

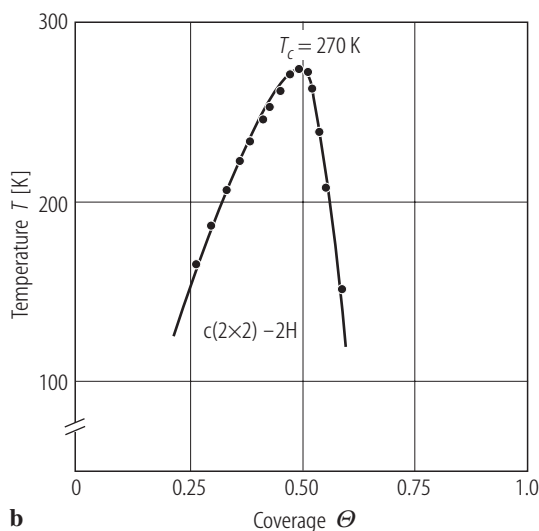
A solid data basis exists concerning both the formation of (H) adsorbate phases with long-range order and phase transitions occurring between the respective H phases. As pointed out in sect. 3.4.1.3.3.1, the long-range order within these phases is determined by the mutual interaction forces between the adsorbed particles (H atoms or, in case of physisorption, H₂ molecules), in relation to their thermal energy content, kT . Accordingly, low temperatures are always beneficial to establish long-range order and to render an observation of this order possible. Indeed, several ordered H phases could only be detected at liquid N₂ temperature or below (Pd(111)/H [86Fel] and Ru(0001)/H [91Sok] being prominent examples). The formation of ordered H overlayers on metals has also been dealt with *theoretically*, whereby calculations regarding kind and magnitude of the H - H interaction forces are in the focus of the interest [86Mus]. An exciting field in this context is, of course, the experimental determination and theoretical modelling of phase diagrams (e.g., in the temperature - coverage plane) of ordered H adsorbed layers using the tools of statistical mechanics [78Dan, 79Dom2] and Monte Carlo simulations [83Roe]. This includes the determination of phase boundaries, critical temperatures, critical exponents, and the classification of the order - disorder or order - order phase transitions. Almost a textbook example here is the (2×2)-2H superstructure (with honeycomb symmetry) formed by the Ni(111)+H system at half a monolayer H coverage, which has stimulated much experimental [79Chr2] and theoretical work [79Dom1, 82Kin,

84Nag1, 84Nag2, 86Mus, 86Roe, 90Ein]. The structure and the respective phase diagram are reproduced as Fig. 8. However, in the context of this data collection we must refrain from any further attempt to expand on all the phase diagrams (which are often quite complicated) and to list the lateral interaction energies (which may be attractive or repulsive, strictly pairwise or three-body related, long-range or oscillatory, depending on the nature of the metal and its crystallographic orientation). Just with hydrogen, these lateral interaction forces have often quantum-chemical origin and exhibit oscillatory character, as pointed out by Koutecký [58Kou], Grimley [67Gri1, 67Gri2, 73Gri] and Einstein et al. [73Ein, 79Ein].



a

Fig. 8a: The famous ‘honeycomb’ structure formed by H atoms chemisorbed on a Ni(111) surface below $T = 273$ K giving rise to a $c(2 \times 2)$ LEED pattern. The distance between two H neighbors equals $r = \frac{a_0}{3} \sqrt{6} = 2.87 \text{ \AA}$.



b

Fig. 8b: The formation of the $c(2 \times 2)$ structure requires a H coverage of 0.5 monolayers; lower or larger H surface concentrations impair or even prevent its formation, leading to the phase diagram shown.

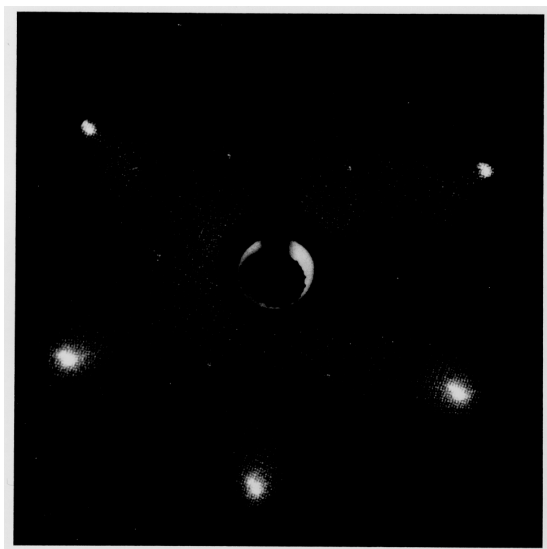


Fig. 9: Photograph of the $(\sqrt{3} \times \sqrt{3})R30^\circ$ structure formed by molecular hydrogen adsorbed on a graphite surface. The H-induced ‘extra’ spots have a much lower intensity than the graphite spots and are hardly visible as an internal hexagon. After Seguiné and Suzanne [82Seg].

Concerning ordered phases of *molecular* hydrogen, only very few (although quite rich and interesting) data are available in the literature, mainly concerning H₂ physisorption on graphite surfaces [82Seg, 89Cui, 87Fre]. Besides LEED, heat capacity measurements and neutron diffraction techniques were used for long-range order detection and analysis. A comprehensive overview is given by Suzanne [03Suz] in sect. 3.6.1 and Wiechert [03Wie] in sect. 3.6.2 of part 3 of this Landolt-Börnstein volume III/42A. So far no complete structure determination of the bond geometry of physisorbed H₂ molecules has been performed. It is worth to mention that the LEED intensities arising from the ordered H₂ phases are as low as expected from kinematic theory [82Seg]. An example is provided in Fig. 9 taken from Seguiné's and Suzanne's work on H on graphite(0001): The LEED pattern gives a convincing impression of the diffraction intensity differences between the graphite substrate and the ordered H₂ overlayer.

3.4.1.3.5.1 Metal surfaces

Surface	Ordered H phase	Coverage [ML] and/or [H atoms/m ²]	Critical temp. [K]	Experimental method	H-substrate bond distance [Å]	Coordination	Remarks	Reference
Be(0001)	($\sqrt{3}\times\sqrt{3}$) R30° honeycomb at $T = 130$ K	0.67 - 1.0	<270	LEED I,V analysis	1.53 ± 0.2	3-fold	exposure to H atoms; Be 'vacancy' structure in a honeycomb array: each vacancy is decorated by 3 tilted bridge-bonded H atoms	96Stu; 99Poh
Mg(0001)	no H superstructure at $T > 100$ K			LEED HREELS			exposure to H atoms; surface hydride phase is formed below 425 K; surface does not reconstruct under hydrogen	91Spr 94Spr
Al(100)	no H superstructure at $T < 280$ K; p(1×1)	1.0		LEED HREELS		1-fold (terminal) H species; 2-fold (bridge) species	exposure to H atoms	88Pau
Al(110)	(1×2) _{rec} after annealing at 150 K		ca. 330	LEED, HREELS		2-fold (short bridge) and 1-fold (terminal)	surface reconstruction of PR or MR type; exposure to H atoms	92Kon
Al(111)				HREELS		1-fold (terminal) below 150K; 2-fold site for $T > 150$ K;	formation of AlH ₃ at $T > 150$ K	91Kon
Ti(0001)	(1×1) _H			LEED, ARUPS	1.8...1.9			80Fei2
Cr(110)	p(2×2) streaky (1×1)	~1.0		LEED, ARUPS	1.6...1.7		adsorption at 80 K	88Kom
Fe(100)	no H superstructure at 140 K			LEED				77Boz

Surface	Ordered H phase	Coverage [ML] and/or [H atoms/m ²]	Critical temp. [K]	Experimental method	H-substrate bond distance [Å]	Coordination	Remarks	Reference
Fe(100)	no H super-structure at 140 K			HREELS		4-fold		96Mer
Fe(110)	p(2×1)	0.5	245	LEED	1.75 ± 0.05	2-fold		77Boz
	=c(2×2)	0.5		LEED		long-bridge		85Mor1
	(2×2)-2H	0.5	80	LEED	1.84	3-fold, H atom radius 0.58 Å	local buckling reconstruction; expts. at 40 K	82Imb; 92Nic 85Mor1 93Ham1 82Imb
	(3×1)-2H =(3×3)-6H (1×1)	0.67 1.0 = 1.7 × 10 ¹⁹ m ⁻²	265	LEED				
Fe(110)				HREELS	1.94	2-fold (short bridge)	expts. performed at 130 K	81Bar1
Fe(111)	no H super-structure at 135 K			LEED				77Boz
Fe(211)	c(2×6)-8H	0.67	140	LEED		unknown	metastable	90Sch
	(2×1)p1g1	1.00	180	LEED			metastable	
	c(2×6)-16H	1.33	180	LEED			metastable	
	c(2×4)-12H	1.50	80	LEED			annealing reqd.	95Sch1
	(1×2)-3H	1.50	170	LEED			<i>T</i> -dept. PT annealing reqd.	
	c(2×6)-20H	1.67	<40	LEED			<i>T</i> -dept. PT	95Sch1
	(1×3)-5H	1.67	>40	LEED				95Sch1
	(1×1)-2H	2.00	60	LEED				
	(1×2)-rec	0.2 - 1.2		LEED			missing-row (1×2) reconstruction of all phases for <i>T</i> > 280 K	90Sch 95Has
Co(0001)	no H super-structure at 300 K			LEED				79Bri
Co(10-10)	c(2×4)-4H	0.50	270	LEED		3-fold		94Ern
	(2×1)-2H	1.00	290	HREELS		3-fold		
	p2mg (1×2)	1.50					missing-row or pairing-row reconstruction	
Ni(100)	no H super-structure at 300 K; none at 120 K			LEED				74Chr
Ni(100)	quasi-ordered p(2×2)-H	0.25		LEED		4-fold	HREELS	78And2
	p(1×1)	1.0				4-fold	HREELS	86Kar
Ni(100)	no H super-structure at 120 K			LEED				79Chr1
Ni(100)	(1×1)	1.0		He diffraction	1.95...2.0		expts. performed at 100...200 K	83Rie1

Surface	Ordered H phase	Coverage [ML] and /or [H atoms/m ²]	Critical temp. [K]	Experimental method	H-substrate bond distance [Å]	Coordination	Remarks	Reference
Ni(100)	(1×1)	1.0		He transmission ion channeling		4-fold; D-Ni layer distance = 0.5 Å	expts. performed with deuterium	85Ste
Ni(110)	(2×1)=(1×2) streak			LEED			H-induced reconstruction	62Ger
Ni(110)	(2×1) (1×2) (1×2) streak		120 K >220	LEED				74Tay
Ni(110)	(1×2) streak	>1.00		LEED			at 300 K	74Chr
Ni(110)	(2×3)-1D c(2×6) c(2×4) c(2×6) c(2×6) (2×1)-2H p2mg (1×2)-3H (1×2)-streak	0.33 0.33 0.50 0.67 0.83 1.00 1.5	<175 <175 <220 >220	LEED LEED			metastable metastable metastable metastable metastable metastable pairing-row reconstr. below $T = 220$ K missing-row reconstr.	84Pen
Ni(110)	(1×2)-3H			LEED analysis			expts. performed at 150 K, missing-row reconstruction assumed	84Jon
Ni(110)	(2×1)-2H (1×2)-3H (1×2) streak	1.0 1.5	220	LEED			expts. performed with deuterium at $T = 175$ K	87Jac1
Ni(110)	(2×6) (2×6) (2×1)-2H (1×2)-3H (1×2)	0.6 0.8 1.0 1.2-1.6	 >220	He diffraction			metastable metastable metastable metastable reconstructed disordered phase	81Eng 82Eng
Ni(110)	c(2×6) c(2×4) c(2×6) c(2×6) (2×1)-2H (1×2)-3H	0.33 0.5 0.67 0.83 1.0 1.5	<220	He diffraction			metastable metastable metastable metastable metastable	83Rie2 85Rie
Ni(110)	(2×1)-2H	1.00		LEED analysis	1.72 ± 0.05	3-fold; H atom radius = 0.47 ± 0.05 Å	metastable	87Rei1
Ni(110)	(1×2)-3H	1.5	<220	LEED analysis			pairing-row reconstruction	87Kle1
Ni(110)	(2×1)-2H (1×2)-3H (1×2)-streak	1.0 1.5	<220 >220	HREELS		3-fold		85DiN

Surface	Ordered H phase	Coverage [ML] and/or [H atoms/m ²]	Critical temp. [K]	Experimental method	H-substrate bond distance [Å]	Coordination	Remarks	Reference
Ni(110)	(2×1)-2H (1×2)-3H	1.0 1.5	<220 <220	HREELS		3-fold two types of 3-fold sites	3-fold modified row-pairing	89Voi
Ni(110)	(1×2)-streak		>220	LEED, time-of-flight + Ne recoil scattering			missing-row reconstruction	91Rou
Ni(110)	(1×2)-streak	≤1 (5L exposure)	300	STM			missing/added-row reconstruction	91Nic2
Ni(110)	(1×2)-3H	1.5	<220	X-ray photoelectron diffraction			pairing-row reconstruction	92Kna
Ni(110)	(1×2)-streak		>220	He diffraction			missing-row reconstruction	93Far
Ni(110)	(2×1)-2H (1×2)-3H (1×2)-streak			STM			Ni-H strings; mechanism of H-induced missing row reconstruction elucidated	04Ale
Ni(111)	(2×2)			LEED				69Ber
Ni(111)	(2×1)=(2×2)	0.3-0.6		LEED				78Beh
Ni(111)	(2×2)-2H honeycomb	0.5	270	LEED analysis at T = 120 K	1.84 ± 0.06	3-fold; bcc and hcp sites H atom radius = 0.59 ± 0.06 Å	protonic band structure discussed	79Chr2
Ni(111)	(2×2)-2H (1×1)-H	0.5 1.0 ± 0.1		transmission ion channeling		two kinds of 3-fold sites	expts. performed with D ₂ exposure to D atoms	88Mor
Ni(111)	(2×2)-2H honeycomb	0.5		He diffraction	1.86 ± 0.07	both types of 3-fold sites		91Gro
Ni(111)	(2×2)-2H	0.5		LEED analysis	1.73 ± 0.08	3-fold; H atom radius = 0.49 ± 0.08 Å	additional local surface reconstruction (local buckling)	93Ham1
Ni(210)	no H superstructure at 90 K			LEED				01Sch2
Cu(100)	p(2×2)p4g /pgg (4√2×4√2) R45°	1.03		LEED LEED			H-induced reconstruction obs. with D at 83 K; exposure to H(D) atoms	91Cho

Surface	Ordered H phase	Coverage [ML] and /or [H atoms/m ²]	Critical temp. [K]	Experimental method	H-substrate bond distance [Å]	Coordination	Remarks	Reference
Cu(110)	(1×2)*			LEED, He diffraction			subsurface reconstruction at 300 K transforms to (1×2)* at 240 K exposure to H atoms	86Rie
	(1×2)							
Cu(110)	(1×2)			Neutral impact collision ion spectroscopy (NICISS)			missing-row reconstruction; (1×2)* phase [ref. 86Rie] could not be confirmed	90Spi
Cu(110)	(1×3)	0.2....0.8	100	LEED, HREELS			reconstructed	92Mor
	(1×2)					tilted 3-fold sites	reconstructed exposure to H atoms	
Cu(110)	(1×4)	0.25	80	He diffraction			exposure to H atoms	93Goe
	(1×3)	0.33	120					
	(1×2)	0.50	100					
	(1×1)		120					
	(1×2)rec	0.5	>140				missing-row reconstr.	
Cu(110)	(1×2)	0.5		LEED, TDS, UPS			exposure to H atoms	93Sanl
	(1×2)						missing or added row reconstruction	
Cu(110)	(1×3)rec	0.12 - 0.4		LEED				94Roh
	(1×2)rec	0.5					missing or added row reconstruction	
Cu(110)	(1×2)rec	0.5		LEIS	1.54 ± 0.09	3-fold (2 1 st layer + 1 2 nd layer atoms)	missing-row reconstruction	98Mij
Cu(111)	(2×2)	0.5	186	LEED, RAIRS, HREELS		2-fold bridge site	exposure to H atoms	89McC
	(3×3)	0.67 ?						
Cu(111)	(2×2)	0.5 0.67	100	LEED			exposure to D atoms Θ= 0.67 max. H coverage determined by nuclear re-action analysis (NRA)	96Lee
Mo(100)	IC(4×2)	~0.1	~200	LEED		modified	complicated phase diagram; H-driven	79Est
	c(2×2)	0.2-0.3	~210			2-fold	surface reconstructions	80Bar
	(4×2)	0.12-0.28	>200				(periodic distortions)	87Pry
	IC c(2×2)	0.3-0.28	<200				partially involved ;	80Ben
	(3×2)	0.3-0.4				bridge sites	several T-dependent phase transitions	
	IC(2×2)	0.4-0.55	>200					
	(2×2)	0.5-0.75						
	(1×1)-2H	>0.8						

Surface	Ordered H phase	Coverage [ML] and/or [H atoms/m ²]	Critical temp. [K]	Experimental method	H-substrate bond distance [Å]	Coordination	Remarks	Reference
Mo(100)	c(2×2)	<0.2		LEED, HREELS		modified 2-fold bridge sites	H-induced reconstr. below $\Theta = 0.2$; T -dependent phase transitions	86Zae
	(4×2)	<0.2						
	(3×2)	sat'n = 2.1 ± 0.2 H:Mo = 2 ML						
Mo(110)	(2×2)	~0.5		LEED, HREELS		quasi-3fold, intermediate long-bridge site	H-induced surface reconstr.	97Oka
	(1×1)	>0.5						
Mo(110)	(2×2)-2H	0.5	200	LEED	1.93	3-fold hollow	H-induced buckling; honeycomb struct.; H atom radius = 0.57 Å (2×2) and 0.65 Å (1×1) phase	87Alt 97Arn1
	(1×1)-H	1.0		LEED		3-fold hollow		
Mo(111)	(1×1)-3H	3.0		LEED analysis	1.90 ± 0.03	3-fold hollow H atom radius = 0.51 ± 0.03 Å		99Arn
Mo(211)	(1×1)	<1.0	360	LEED, HREELS		2-fold	H driven reconstr.	93Lop
	(1×2)	>1.0				3-fold		
Ru(0001)	($\sqrt{3} \times \sqrt{3}$)R30°	0.33	74.5	LEED			phase diagram determined	91Sok 93San2
	p(2×1)	0.50	68.0					
	(2×2)-3H	0.75	71.0					
Ru(0001)	p(2×1)	0.50	68	LEED analysis	2.0 ± 0.2	3-fold fcc site	+ buckling and pairing reconstruction; H atom radius = 0.75 ± 0.2 Å	92Hel
Ru(0001)	disordered	1.0		VLEED analysis	1.91 ± 0.06	3-fold fcc site; H atom radius = 0.56 Å	expts. performed at 170 K; no subsurface H adsorption	87Lin 86Feu
						3-fold hollow	expts. performed at 170 K	83Bar
Ru(10-10)	c(8×2) = "(1×2)split"	1.0	150	LEED, HREELS			expts. performed at 100 K	89Lau
	(1×2)	1.2	220					
	c(2×2)-3H	1.5	200					
	(1×1)-2H	$2.0 = 1.73 \times 10^{19}$	150					
Ru(10-10)	c(2×2)-3H	1.5		LEED analysis	2.01 ± 0.40 1.95 ± 0.60 1.91	H atom radius = 0.65... 0.70 Å	quasi-3-fold site; slight buckling and lateral displacement effects	98Doe
	(1×1)-2H	$2.0 = 1.73 \times 10^{19}$						

Surface	Ordered H phase	Coverage [ML] and/or [H atoms/m ²]	Critical temp. [K]	Experimental method	H-substrate bond distance [Å]	Coordination	Remarks	Reference
Ru(11-21)	no H-induced super-structure (1×1)?			HREELS LEED		pseudo-3-fold sites + 4-fold site		01Fan
Rh(100)	(1×1) = no H super-structure at 100 K	1.0 = 1.39 × 10 ¹⁹		LEED				82Kim
Rh(100)	(1×1)	1.0		HREELS		4-fold hollow		87Ric1
Rh(100)	(1×1)	1.0		HREELS	1.64	4-fold hollow	CO coadsorption study	88Ric2
Rh(110)	(1×3)-H (1×2)-H (1×3)-2H (1×2)-2H	0.33 0.50 0.67 1.0		LEED			$\Theta_{(1\times 2)-2H}$ has been corrected to contain 3 H atoms/unit cell: → $\Theta_{(1\times 2)-3H} = 1.5$	86Chr 88Ehs
Rh(110)	(1×1)-2H (1×3)-H (1×2)-H (1×3)-2H (1×2)-2H	2.0 0.33 0.50 0.67 1.0 (1.5)	130 140 >180 >160	LEED			$\Theta_{(1\times 2)-2H}$ has been corrected to contain 3 H atoms/unit cell: → $\Theta_{(1\times 2)-3H} = 1.5$	90Nic 91Nic2 89Mic
Rh(110)	(1×1)-2H	2.0 = 1.96 × 10 ¹⁹	>100					
Rh(110)	(1×n); n = 1, 2, 3)			HREELS		quasi-3-fold		94Mue
Rh(110)	(1×3)-H	0.33		LEED analysis	1.86 ± 0.1	3-fold (two 1 st and 1 2 nd layer Rh atom)	slight local reconstruction (shift-buckling); H atom radius = 0.52 ± 0.1 Å	89Leh
Rh(110)	(1×3)-H	0.33		He diffraction	1.76	quasi-3-fold		91Par
Rh(110)	(1×2)-H	0.50		LEED analysis	1.87 ± 0.1	quasi 3-fold; H atom radius = 0.53±0.1 Å	H-induced shift-buckling reconstruction	89Puc
Rh(110)	(1×2)-H	0.5		He diffraction		3-fold	H - Rh top layer distance = 0.82±0.1 Å	90Par1
Rh(110)	(1×2)-3H	1.0		LEED analysis	1.87... 1.93	3 non-equivalent quasi-3-fold sites	H-induced reconstruction; H atom radius = 0.5 ± 0.1 Å	89Mic
Rh(110)	(1×1)-2H	2.0		LEED analysis			Rh's multilayer relaxation almost entirely removed by adsorbed H	87Nic

Surface	Ordered H phase	Coverage [ML] and/or [H atoms/m ²]	Critical temp. [K]	Experimental method	H-substrate bond distance [Å]	Coordination	Remarks	Reference
Rh(110)	(1×1)-2H	2.0		LEED analysis	1.84 ± 0.2	quasi-3-fold	H atom radius = 0.50 ± 0.2 Å	88Oed
Rh(110)	(1×1)-2H	2.0		He diffraction	1.85 ± 0.1	quasi-3-fold		91Par 91Kir
Rh(111)	(1×1)-H	1.0		LEED				78Cas
Rh(111)	(1×1)-H	1.0		HREELS			quantum motion of H atoms assumed	86Mat
Rh(111)	(1×1)-H	1.0		He diffraction			phonon dispersion curves measured	95Wit
Rh(111)	(1×1)-H	1.0		He diffraction			$T_{ad} = 160$ K	96Col
Rh(311)	(1×3)-H (1×2)-H (1×3)-2H (1×2)	0.33 0.50 0.67 ~1.0 = 8.34 × 10 ¹⁸	90 - 250	LEED			H-induced reconstr.; (1×2) cannot be saturated; population of subsurface sites	91Nic1 90Lie2
Rh(311)	(1×3)-H (1×2)-H (1×3)-2H (1×2)-2H rec	0.33 0.50 0.67 ~1.0	185 ± 5	LEED		quasi 3-fold	complete phase diagram for H/Rh(311) det'd	93Ham2
Rh(311)	c(1×1) c(1×3) cp(1×1) c(1×3) p(1×1)rec p(1×1)rec	1.0 3...4 2...3		He diffraction	1.92 ± 0.1	quasi 3-fold hollow	c(1×1) = 1 st ordered phase → $s_0 = 1$	95Ape1 95Ape1 95Ape2 96Ape
Rh(311)	c(1×1)rec	1.0		He diffraction				95Ape2
Pd(100)	c(2×2) (1×1)-H	0.5 1.0 = 1.32 × 10 ¹⁹	260	LEED		4-fold hollow	phase diagram determined	80Beh
Pd(100)	c(2×2) (1×1)-H	0.5 1.0 ± 0.1		transmission channeling	1.97 2.00		expts. performed with deuterium	87Bes
Pd(100)	c(2×2) p(1×1)	0.5 1.0		He diffraction	2.05 2.00			84Rie
Pd(100)	c(2×2) p(1×1)	0.5 1.0 ± 0.1		HREELS		4-fold hollow		82Nor1 83Nyb
Pd(110)	(2×1)-2H- p2mg (1×2)-3H (1×2)-streak	1.0 1.5 >1.5	180	LEED			H-induced reconstr. H-induced reconstr. formation of subsurface H	83Cat2 83Beh
Pd(110)	(1×2)-3H	1.5	120	Ion scattering			H-induced pairing-row reconstruction	86Nie
Pd(110)	(1×2)-3H	1.5		LEED analysis			row-pairing reconstruction	87Kle1 87Kle2
Pd(110)	(2×1)-2H- p2mg (1×2)-3H (1×2)-streak	1.0 1.5 >1.5		LEED			H-induced recon. formation of subsurface H	88He1

Surface	Ordered H phase	Coverage [ML] and/or [H atoms/m ²]	Critical temp. [K]	Experimental method	H-substrate bond distance [Å]	Coordination	Remarks	Reference
Pd(110)	(2×1)-2H	1.0		He diffraction		quasi 3-fold	H-induced recon. formation of subsurface H PR H-induced rec. + subsurface H	83Rie3
	(1×2)-3H	1.5						
Pd(110)	(2×1)-2H	1.0		LEED analysis	2.00 ± 0.1	quasi 3-fold: two 1 st layer atoms, one 2 nd layer atom	H atom radius = 0.6 ± 0.1 Å	87Sko
Pd(110)	(2×1)-2H	1.0		HREELS		quasi-3-fold		89Ell
	(1×2)-3H	1.5				quasi 3-fold		
Pd(110)	(2×1)-2H			HREELS		quasi-3-fold	quantum-delocalized H	96Tak
Pd(110)	(2×1) + (1×2)-3H (1×2)streak	1...1.5 ML	150 300	STM			pairing-row reconstruction missing/added-row reconstruction	95Yos
Pd(110)	(1×3) (1×2)-MR	lower higher θ	300	STM			evidence of H-induced missing-row reconstr's	96Kam
Pd(111)	(1×1)-H	1.0		LEED			expts. performed at 300 K	73Chr1
Pd(111)	(√3×√3)R30° -H	0.33	85	LEED		3-fold + octahedral sub-surface sites	phase diagram determined; subsurface site population (theory)	85Fel 86Fel 87Daw
	(√3×√3)R30° -2H	0.67	105					
Pd(111)	(√3×√3)R30° -H	0.33		He diffraction		3-fold	quantum delocalization of H assumed	91Hsu
	(√3×√3)R30° -2H	0.67						
Pd(111)	(1×1)-H	1.0		LEED analysis	1.78 - 1.80	3-fold fcc	partial occupation of single 3-fold hollow fcc site + up to 60% subsurface (octahedral) sites	89Fel
	(√3×√3)R30° -2H	0.67	82					
Pd(111)	(√3×√3)R30° -H	0.33		STM		3-fold	H adsorption, diffusion and ordering followed by direct observation	03Mit1 03Mit2
	(√3×√3)R30° -2H+	0.67						
Pd(111)	(1×1)-H	1.0		LEED		sites with three different coordinations: A, B, C	population of surface + subsurface sites	98Mus1
	no H super-structure	3...4						

Surface	Ordered H phase	Coverage [ML] and/or [H atoms/m ²]	Critical temp. [K]	Experimental method	H-substrate bond distance [Å]	Coordination	Remarks	Reference
Pd(210)	no H super-structure	3...4		LEED		sites with three different coordinations: A, B, C	expt. + theory population of surface + subsurface sites	01Sch1 02Lis
	no H super-structure	1 ML	<100	HREELS			(co)adsorption of <i>molecular</i> H ₂	01Sch1
Pd(311)	(2×1)H	0.25	170	He dif-		4-fold	thermally activated	99Far
	(2×1)2H	0.50	170	fraction,		4-fold	transition surface H →	
	(2×1)3H	0.75	170	HREELS		3-fold	subsurface H	
	c(1×1)2H	1.0	170				subsurface H in octahedral sites	
Ag(100)	diffuse (2×2)			LEED			surface exposed to H atoms; H-induced reconstruction	04Kol
Ag(110)	sequence of ordered phases; c(4×4) at sat'n		<170	He diffraction			expts. performed with D atoms	89Can
Ag(110)				He diffraction			determination of interaction potentials; no H ₂ chemisorption	91Can
Ag(110)	(1×4)	0.20		LEED,		tilted 3-fold	H lattice gas structures accompanied by weak Ag reconstruction	93Spr
	(1×3)	<0.5		HREELS				
	(2×6)	0.5-0.75						
	(2×2) = mixture of (2×1)2H + (1×2)	1.0						
	(1×2) rec	1.5					row-pairing reconstruction	
Ag(111)	(2×2) mixed (2×2) and (3×3) (4×4)		~110	LEED			expts. performed with D atoms	95Hea
							surface reconstruction likely	
Ag(111)	(2×2)	0.5	140	LEED,		3-fold	expts. performed with H and D atoms; (3×3) phase induced by LEED beam. H phase diagram det'd.	94Lee
	mixed (2×2) and (3×3)	>0.5		HREELS			(2×2) phase accompanied by Ag surface reconstruction	95Lee
Ta(100)	(1×1)-H	1.0		LEED analysis, HREELS	1.92... 1.94	3-fold hollow	H atom radius = 0.5...0.6 Å	04Yam

Surface	Ordered H phase	Coverage [ML] and/or [H atoms/m ²]	Critical temp. [K]	Experimental method	H-substrate bond distance [Å]	Coordination	Remarks	Reference
W(100)	c(2×2) = (√2×√2)R45°						clean surface (√2×√2) R 45° reconstructed (zig-zag chains)	88Alt 81Bar2
	c(2×2)-H followed by complex series of LEED patterns indicating IC phases	0.25 1.0 = 1.002 × 10 ¹⁹				2-fold (bridge) sites	reconstruction in a dimer-like arrangement H/W(100) phase diagram involving C/IC transitions	77Deb 79Deb 86Wil 81Bar1
	(1×1)	≥ 1.7 × 10 ¹⁹ ≥ 1.5 ML						78Bar1 66Est
W(100)	(√2×√2)R45°	0		LEED			clean surface reconstructed; dimer-surface reconstruction, expts. at 300 K	80Kin
	c(2×2)	0.04 - 0.22						
	c(2×2)-H split ½-order	0.22 - 0.36						
	streaked ½ order	0.3-0.48					bridge complexes are formed + W surface atom displacements occur	
	streaks + 1/5-order beams	0.8-1.0						
	disordered (1×1) (1×1)-H	1.0-<2.0 2.0						
W(100)		0 ... 1.0		HREELS		Θ-dependent occupation of two sites		76Fro
	(1×1)	2.0				2-fold (bridge)		
W(100)	(1×1)-H	2.0 ± 0.3		LEED electron-stimulated desorption (ESD)				66Est 73Mad
W(100)	(√2×√2) = c(2×2)-H (1×1)	<0.5 2.0		HREELS		bridge sites	two-state reconstruction (tilted dimer model)	83Did
W(100)	(1×1)-2H	2.0		LEED analysis	1.97 ± 0.04	2-fold (bridge)		85Pas

Surface	Ordered H phase	Coverage [ML] and/or [H atoms/m ²]	Critical temp. [K]	Experimental method	H-substrate bond distance [Å]	Coordination	Remarks	Reference
W(100) clean	($\sqrt{2}\times\sqrt{2}$)R45° = c(2×2)-H	0		LEED analysis			precise crystallography of clean reconstructed surface. Clean: zigzag rows; with H: dimer model. position of H atoms not determined	92Sch1
	c(2×2)-H phase= ($\sqrt{2}\times\sqrt{2}$)R45°	<0.5						
W(100)	c(2×2)H	0.4 = 4 × 10 ¹⁸		HREELS	1.95 ± 0.05	bridge sites on a reconstructed surface		78Bar2
W(100)	c(2×2)	0.3		RAIRS, LEED			accurate and detailed vibrational investigation	86Arr
	c(2×2)-H split ½-order	0.3-0.5						
	streaked ½ order; streaks + 1/5-order beams; disordered (1×1)	0.6-1.9						
	(1×1)-2H	2.0						
W(100)	c(2×2)-H rec	< 0.5		VLEED	1.73		reconstructed surface	86Her
	p(1×1)-H	1.0			1.96		relaxed surface	
W(100)	c(2×2)	<0.5		RAIRS (reflection-absorption IR)		bridge sites (pinched and anti-pinched)		89Rif
W(110)	p(2×1)	0.5						78Gon
	(2×2)	0.75						
	p(1×1)	1.0						
W(110)				angle-resolved UV photo-emission (ARUPS) HREELS		bridge or distorted bridge		82Bla
W(110)	(1×2)	<0.5	>200	LEED			clean surface unreconstructed; H-induced surface reconstruction (lateral shift = registry shift)	86Chu
	(2×2)	>0.5	>250					
W(110)	p(2×1)	1.0		VLEED	2.09	3-fold	two inequivalent H sites sequentially occupied	86Her
W(110)	(1×1)	1.0		LEED analysis		3-fold ; H atom radius = 0.66 Å	high quality data; <i>no</i> H-induced registry shift!	97Arn2 97Arn3

Surface	Ordered H phase	Coverage [ML] and/or [H atoms/m ²]	Critical temp. [K]	Experimental method	H-substrate bond distance [Å]	Coordination	Remarks	Reference
W(110)	(2×1) (2×2) (1×1)	<0.75 1.0		HREELS			quasi-3-fold in between the long bridge and short-bridge site H liquid like with 1-D ordering	94Bal
W(110)	p(2×1) p(2×2) p(1×1)	0.4...0.5 0.4...0.8 1.0		LEED			phase diagram: careful TDS and LEED θ calibrations reveal systematic θ differences	97Nah1
W(211)		8×10^{18} = 1 ML		Time-of-flight and recoiling spectro-metry		3-fold trough site		89Gri
Re(0001)	no H super-structure			LEED			expts. performed at 300 K	81Duc
Re(0001)	(2×2) with missing spots	0.25	~300	LEED			LEED pattern visible between 110...300 K	90He
Re(10-10)	c(2×2)-3H (1×1)-2H	1.5 = 1.22×10^{19} 2.0		LEED				95Mus
Re(10-10)	c(2×2)-3H (1×1)-2H	1.5 = 1.22×10^{19} 2.0		LEED analysis	1.85 ± 0.4	2 H atoms in quasi 3-fold + 1 H atom in a 2-fold (bridge) site	H atom radius = 0.47 ± 0.4 Å	98Doe
Ir(100)-(1×5)	clean surface	0		LEED			clean surface hexagonally reconstructed	85Bic
Ir(100)-(1×5)	(1×3) (1×3)+(1×1)	sat'n		LEED			the reconstruction is affected by H. (1×3) phase is metastable	00Mor
Ir(100)-(1×5)	(1×3) (1×3)streaky	sat'n		LEED analysis			(1×3) phase is stabilized by H; (1×3) phase reconstr.; it contains 3 Ir atoms + layer rumpling	01Sau
Ir(110)-(1×2)	clean surface	0		LEED LEED analysis			clean surface (1×2) reconstructed reconstruction of missing-row type with layer relaxation (paired rows in 2 nd and buckled rows in 3 rd layer)	73Chr2 86Cha
Ir(110)-(1×2)	no H super-structure for $T > 130$ K			LEED			clean surface MR-reconstructed	80Ibb
Ir(110)-(1×2)				HREELS		3-fold hollow	clean surface MR-reconstructed	88Cha

Surface	Ordered H phase	Coverage [ML] and/or [H atoms/m ²]	Critical temp. [K]	Experimental method	H-substrate bond distance [Å]	Coordination	Remarks	Reference
Ir(111)	no H super-structure for $T > 130$ K			LEED				87Eng
Ir(111)				HREELS		3-fold hollow		88Cha
Ir(111)	no H super-structure			HREELS		1-fold (terminal site bonding) at larger coverages	quantum delocalized H motion at low coverages	99Hag
Pt(100)-(5×20)	clean surface	0.00		LEED		hexagonal arrangement of top Pt layer	clean surface hex. and hex.-rot reconstructed, respectively, depending on T	79Hei 81Van1 81Van2
Pt(100)-(5×20)	no H super-structure			LEED			hex reconstruction can be lifted to (1×1) phase by H adsorption at $T < 200$ K	81Bar3
Pt(100)-(5×20)	no H super-structure	$1.54 \pm 0.1 \times 10^{19}$ $= 1.20 \pm 0.08$ ML		Rutherford back-scattering			reconstruction only <i>partially</i> lifted by H adsorption	81Nor2
Pt(100)-(5×20)	no H super-structure			LEED			hex-rot reconstruction only <i>partially</i> lifted by H adsorption; critical coverage = 2.8×10^{18} H atoms/m ²	93Klo
Pt(100)-(5×20)	no H super-structure at 35 K			LEED			at 35 K no removal of (5×20) reconstruction by H, heating to 100 K necessary to lift reconstruction	91Pen1 91Pen2
Pt(100)-(5×20)	no H super-structure at 300 K (1×1)			LEED			no structural change after H ₂ dosing.	95Hu
				LEED analysis			(1×1) phase obtained after dosing to H atoms at 300 K. (1×1) = disordered Pt, H atoms neglected	
Pt(100)-(5×20)	no H super-structure at and below 250 K	1.0 at 120 K = 1.28×10^{19} H atoms/m ²		He diffraction			hex reconstruction is not removed below 250 K; H atoms cause charge redistribution at the (1×1) surface	95Rom
Pt(110)-(1×2)	clean surface	0		LEED			clean surface (1×2) reconstructed	81Ada
				Field ion microscopy			reconstruction of missing-row type with layer relaxation	85Kel

Surface	Ordered H phase	Coverage [ML] and/or [H atoms/m ²]	Critical temp. [K]	Experimental method	H-substrate bond distance [Å]	Coordination	Remarks	Reference
Pt(110)-(1×2)	clean surface	0		LEED analysis			surface (1×2)- and/or (1×3) reconstructed. Reconstruction of missing-row type	88Fer1 88Fer2
Pt(110)-(1×2)	no H super-structure			LEED, TDS		deep trough sites populated first	H adsorption into (111) microfacets	87Eng 88Duc
Pt(110)-(1×2)	no H super-structure			MB expts.			H adsorption into (111) microfacets	89Ang2
Pt(110)-(1×2)	no H super-structure			LEED, W.F. measurements			two different sites (H sits in diatomic Pt clusters)	92She
Pt(110)-(1×2)	no H super-structure			He diffraction (HAS)	1.8	2-fold (bridge) sites; H atoms below the topmost Pt rows	Pt atom relaxation changes by H adsorption	90Kir
Pt(110)-(1×2)	no H super-structure			Tensor-LEED (+ DFT calc.)		2-fold (bridge) sites; confirmation of HAS data [90Kir]	relaxation of Pt - Pt layer distance changes with H coverage	04Zha
Pt(111)	no H super-structure at $T > 150$ K (1×1)-H phase likely	0.8 ± 0.4 at 150 K		LEED			slight lattice expansion due to H deduced from LEED (I,V) data	75Chr
Pt(111)	no H super-structure	1.1×10^{19} = 0.733 ML		Rutherford back-scattering + nuclear reaction analysis			slight outward relaxation under hydrogen	80Dav 82Nor1
Pt(111)	no H super-structure			HREELS		3-fold hollow		79Bar
Pt(111)	no H super-structure			HREELS	1.93	2-fold + 3-fold	(theory to HREELS)	84Say1
Pt(111)	(1×1)-H at 160 K	1.0		He diffraction		3-fold (C _{3v}) (hcp-type)	corrugation changes slightly with (1×1)-H layer; confirmed by calculations of [84Bat]	83Lee
Pt(111)	(1×1)-H			Low-energy ion recoil Scattering (LERS)	1.78 ± 0.08	3-fold fcc type	kind of site differs from Lee's work [83Lee]	86Koe
Pt(111)	(1×1)-H			Ion channeling	1.9 ± 0.1	3-fold fcc type		99Lui

Surface	Ordered H phase	Coverage [ML] and/or [H atoms/m ²]	Critical temp. [K]	Experimental method	H-substrate bond distance [Å]	Coordination	Remarks	Reference
Pt(111)	no H superstructure at 85 K	<0.75		HREELS			H atoms quantum delocalized, several vibrational bands resolved	02Bad
Pt(111)	(1×1)-H	1 ± 0.05		HREELS, TPD		3-fold hollow fcc-site	H is quantum delocalized; expts. performed at 85 K	03Bad
Pt(111)	no H superstructure	0.25		DFT theory			3-fold fcc site; H is quantum delocalized	01Kae
Au(100)-c(26×68); phase often incorrectly described as (5×20)	clean surface	0		LEED analysis			complicated hexagonal reconstruction of top layers	81Van1
Au(100)-(5×20)	incomplete (1×1)	0.3		LEED			exposure to H atoms; after large H exposures incomplete (1×1) + faint remanent (5×20) phase: H-induced deconstr.	96Iwa
Au(110)-(1×2)	clean surface	0		STM			missing-row reconstruction with (111) facets	83Bin1
Au(110)-(1×2)	clean surface	0		LEED analysis			clean surface missing-row reconstructed (2 nd layer row-pairing + 3 rd layer buckling)	85Mor2
Au(110)-(1×2)	no H-induced ordered phase	0.5		LEED			exposure to H atoms. (1×2) reconstruction not lifted	86Sau
Au(111)	clean surface	0		STM			clean surface reconstructed	90Bar
Au(111) (thin film grown on Ir(111))				LEED, TDS			dissociative H ₂ adsorption claimed	03Oka

3.4.1.3.5.2 Semiconductor and insulator surfaces

The surface structure of semiconductors (especially of the elemental semiconductors Si and Ge) has been of interest since the early days of Surface Science. It has been found that practically all of these materials reconstruct spontaneously, the reason being the covalent bonding chemistry which forces cleaved surface bonds to bend and to form dimers thus enabling a lowering of the surface free energy. The most famous example is certainly the silicon(111) surface which usually reconstructs to a complicated (7×7) surface phase whose structure could unequivocally be resolved only by combined electron diffraction [85Tak] and STM studies in the eighties and nineties [83Bin2, 91Bol1, 91Bol2, 91Mor]. For the same chemical reason, also the Si(100) surface is (2×1) reconstructed in the clean state, the driving force being the formation of both a σ bond and a weak π bond between the two silicon atoms in each dimer [85Tro].

Less was known at this time about how adsorbed hydrogen could modify these structures until the possibility of chemically ‘etching’ Si surfaces by H containing solutions (ammonium fluoride NH_4F etc.) was discovered leading to almost perfect (1×1) surface phases in which each cleaved Si - Si bond was saturated by a H atom. The same perfect surfaces could be obtained, if the Si surfaces were exposed to molecular hydrogen at elevated temperatures ($T \approx 900$ K), because the sticking probability increases very much with temperature [99Mao]. Since then a feverish activity to prepare, characterize and technologically use these smooth and chemically inert surfaces began which led to an enormously distended literature. About the same time, the *chemical* origin of this ‘deconstruction’ behavior was acknowledged, and related phenomena were reported also for Ge and C and some compound semiconductor surfaces. However, here we can only briefly review some of the exemplary articles.

Semiconductor and insulator surfaces

Surface	Ordered H phase or H-induced reconstructed phase	Coverage [ML] and /or [H atoms/ m^2]	Experimental method	Remarks	Ref.
C(100)-diamond	clean surface	0	LEED	reconstruction with two (2×1) domains	77Lur
C(100)-diamond	1×1 and 2×1		LEED, electron-stimulated desorption	thermally driven reconstruction from 1×1 to 2×1 ; H-C-H surface dimers are present	90Ham
C(100)-diamond	2×1 -H	mono-hydride	LEED I,V analysis	(Tensor-LEED) dimer model, dimer length = 1.60 \AA	99Wan
C(111) graphite	$(\sqrt{3}\times\sqrt{3})\text{R}30^\circ$ incommensurate phases	$<1\text{ML}$ $>1\text{ML}$	LEED	physisorbed H_2 , HD, D_2 on graphite single crystals; phases and phase transitions	89Cui
C(111)- 1×1 diamond	clean surface	0	LEED-I,V	surface atoms have bulk position with small relaxation	82Yan
C(111)- 1×1 to 2×1 transition		$\leq 1 \text{ ML}$	LEED ESDIAD	thermally induced (1×1) -to- (2×1) phase transition in the presence of hydrogen	88Ham
C(111)- 2×1 diamond	clean surface	0	LEED-I,V LEED	reconstruction with two (2×1) domains	82Yan 90Ham
Si(100) 2×1 c(2×4) p(2×2)	clean surface	0	STM	dimer-type reconstruction with buckled and non-buckled dimers, stabilized by defects	85Tro 86Ham
Si(100)	(3×1)	H-saturation, H:Si atom ratio 3:2	LEED, high-resolution IR	alternating monohydride and dihydride unit cells responsible for (3×1) phase	85Cha1
Si(111) 7×7	clean surface	0	STM TED (transmission electron diffraction)	clean surface reconstructed in a complex manner with corner holes and adatoms to yield a (7×7) repetition unit	83Bin2 91Mor 85Tak
Si(111) 7×7	(7×7) -H	fully H-covered surface (1 H /Si atom)	kinematic LEED	adsorbed H atoms form triangular Si islands with $[-1-12]$ step boundaries	81McR

Surface	Ordered H phase or H-induced reconstructed phase	Coverage [ML] and /or [H atoms/m ²]	Experimental method	Remarks	Ref.
Ge(111) (2×1) c(2×8)	clean surface	0		clean surface reconstructed either in (2×1) or in c(2×8) phase	81Cha
Ge(111)	(1×1)-H	fully H-covered surface	LEED I,V analysis	Negligible influence of adsorbed H atoms on Ge LEED intensities. Slight contraction of 1 st -to -2 nd layer distance	87Imb
GaAs(001) (2×4) c(8×2)	clean surface	0	LEED, STM	surface As terminated. Dimer vacancy structure responsible for 4-fold periodicity in [110] direction top layer is based on rectangular units.	87Cha 88Pas 90Bie 95Ave
c(4×4)				reconstruction still not fully understood	01Nag
GaAs(001) c(4×4)	disordered (1×1) at 323 K c(2×2) + c(4×2) at T > 423 K	H covered surface	reflection high-energy electron diffraction (RHEED)	disordered (1×1) phase = AsH _x clusters centered phases: H adsorbed on surface Ga atoms, H-induced loss of As	04Kha
GaAs(110)	clean surface	0	TOF-ion scattering spectroscopy	clean surface relaxed, 1 st As layer located above the Ga layer	97Gay

3.4.1.3.6 Vibrational modes of adsorbed hydrogen

Vibrational spectroscopy is extremely helpful in determining both the structure and coordination of a given H - substrate adsorbate complex, but also in gaining information about the strength of the respective H - substrate bond potential [87Ham]. In contrast to LEED or other diffraction techniques it has the advantage to be applicable also to systems which do not possess long-range order. As far as experimental means to measure vibrational frequencies is concerned, classical (reflection - absorption) infrared techniques (IRAS or RAIRS) and high-resolution electron energy loss spectroscopy (HREELS) are common techniques, whereby especially the latter method has been frequently employed for H-induced surface vibrations. An example concerning the system H on Pt(111) taken from the work of Badescu et al. [03Bad] is presented in Fig. 10. For theoretical and experimental details we refer to review articles and monographs on this subject [85Hol; 86Ueb; 80Wil, 77Fro, 82Iba].

Another experimental technique to probe surface vibrations is (inelastic) helium atom scattering (HAS), which has, for example, extensively been used in the laboratory of J.-P. Toennies (Göttingen) to study phonon dispersion curves, but also for probing vibrations of adsorbed hydrogen [94Ben]. Although HAS gives very high resolution, the magnitude of the possible momentum transfer is small, in contrast to the aforementioned HREELS technique. Internal vibrations of adsorbed molecules can also be excited by a method called Inelastic Electron Tunneling Spectroscopy (IETS). This is known since 1966 when vibrational spectra were obtained for the first time from molecules adsorbed at the buried metal - oxide interface of a metal - oxide - metal tunneling junction [66Jak]. However, this 'buried state' usually causes a complex local environment of the probed molecule and restricted the applicability of IETS for quite a while. Yet, recent developments of STM technology allowed the monitoring of vibrational properties even of single molecules under very well defined local conditions – these molecules are adsorbed on metal surfaces and reside at the tunneling gap between the STM tip and the surface. In this way, Ho and coworkers succeeded in obtaining IET spectra, e.g., from single acetylene molecules adsorbed on a Cu(100) surface [98Sti] and more recently also from H atoms adsorbed on the same surface [00Lau]. In a different laboratory, the electrical conductivity of a single H₂ molecule trapped in a tunnel junction between Pt electrodes held at 4.2 K could even be measured [02Smi].

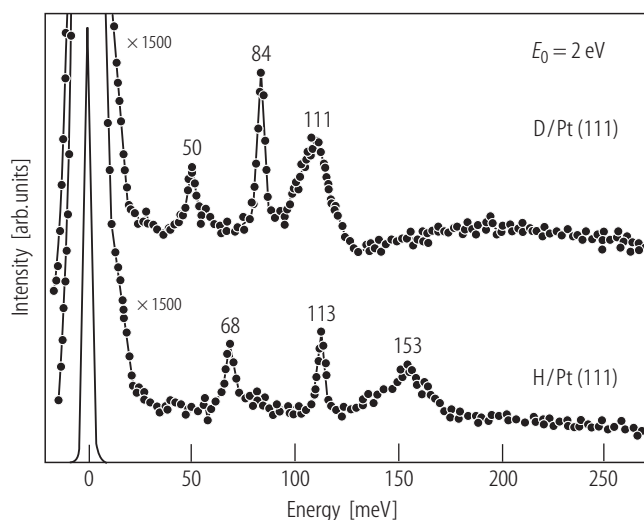


Fig. 10: Vibrational loss spectra obtained from a full monolayer of H (D) atoms adsorbed on a platinum(111) surface at 85 K, obtained with a primary electron beam energy of 2 eV and a resolution better than 1 meV. Note the shift of the vibrational bands between the H and D spectra, due to the isotope mass difference. After Badescu et al. [02Bad].

Nevertheless, the classical ‘integral’ vibrational spectroscopies have been and still are widely applied, and most of the data collected here refer to either IRAS or HREELS experiments. It is, perhaps, worth to mention that a real breakthrough in the performance of low-energy electron spectrometers has been reached during the past two decades in that the energy resolution along with the signal-to-noise ratio could be improved almost by a factor of ten [91Iba]. In the data listing below, the vibrational energies are given in both wave numbers [cm^{-1}] and millielectronvolts [meV]. In the context of our compilation, only a few peculiarities of HREELS concerning its application to hydrogen adsorbed layers [90Ste] are to be mentioned: A frequent problem is the comparatively small cross section for dipole scattering of adsorbed H atoms leading to weak loss signals and unsatisfactory signal-to-noise ratio. Often, off-specular measurements allow to discriminate between dipole-excited and impact-excited loss features, because the cross section for dipole excitations drops sharply away from the specular reflection. Especially H parallel modes cannot be dipole-excited due to the surface selection rule. If they are, however, impact-active, they can well be detected in off-specular measurements.

In addition, the H-substrate bond lengths are usually quite short, in other words, the H atom is often more or less ‘immersed’ in the surface (sometimes below the image-charge plane) making any dipole excitation difficult. On the other hand, vibrational loss studies of adsorbed hydrogen can benefit from the large mass difference between the H and the D isotope in that isotopic shifts of the vibrational frequencies are large (downshift by a factor of $\sqrt{2} \approx 1.42$) and relatively easy to determine. In this respect, true H - substrate vibrations (which always exhibit this downshift, if the experiments are carried out with deuterium) can be distinguished from substrate phonons and/or protonic band excitations whose band positions do not shift under deuterium.

There is still another interesting peculiarity of electron energy loss spectroscopy performed with adsorbed H: Electronic excitations of surface states of metal substrates can be quite sensitively modified by adsorbed hydrogen as demonstrated by strong changes of the energy dependence of the low-energy electron reflectivity due to hydrogen. By adjusting the primary electron beam energy accordingly (to fall together with a reflectivity *minimum*), the electron beam can be kind of coupled into the surface quite effectively, resulting in a largely enhance sensitivity for detecting H vibrations [84Con, 86Con1].

A different (but also H-specific) phenomenon is the occurrence of a so-called *giant phonon anomaly* for the H-on-W(110) (and Mo(110)) adsorption system, first detected by Hulpke and Lüdecke by means of HAS in 1992 [92Hul1, 92Hul2, 93Hul], which since then has stimulated a lot of experimental and theoretical work on surface phonons and the effect of adsorbed (and absorbed) H on the lattice dynamics of the respective substrates [96Bal and references cited therein]. Not only in that respect, one will find that the adsorption system ‘H on tungsten’ represents (besides, perhaps H on nickel) the most frequently and most thoroughly studied subject, not only concerning H - surface vibrational excitations, but also regarding structural, kinetic, and thermodynamic properties.

Before listing the data material available for H - surface vibrational frequencies, some other short remarks may be useful. H atoms bound to a single atom are excited in the 2200...1600 wave number range; edge-bridging H atoms lead to absorption bands between 1400 and 800 cm^{-1} ; triply coordinated hydrogen should yield absorption features at even lower wave numbers [72Kae]. The energetic position of a H-induced vibrational band, the number of detectable modes and their angular and azimuthal dependence are important properties, since they provide (via symmetry selection rules) conclusive information about the local symmetry properties of a given H adsorption complex. For details, we refer to the monograph by Ibach [82Iba].

Finally, there is an issue which comes up from time to time when dealing with adsorbed hydrogen and electron energy loss spectroscopy – the concept, whereupon adsorbed H atoms can (or even must) be considered as quantum particles which are delocalized as atomic bands. In other words, the H atoms can perform *quantum motion*. This idea was first proposed and discussed in 1979 via an atomic band model, in which the motion of the H atoms is represented by wave functions localized normal to the surface, but delocalized along the surface [79Chr2]. Some years later Puska et al. calculated the band energy levels and wave functions of the chemisorbed H atoms on Ni using the effective medium theory [83Pus, 85Pus]. Since then, evidence of quantum delocalized chemisorbed hydrogen has been reported several times, e.g., for H on Rh(111) [86Mat], H on Pd(111) [91Hsu], H on Pd(110) [96Tak], H on Cu(110) [92Ast], and, most recently, H on Pt(111) [02Bad], whereby HREELS and helium diffraction, respectively, were used for detecting and confirming the respective evidence. The state of the art has been reviewed by Nishijima et al. [05Nis].

3.4.1.3.6.1 Metal surfaces

Surface	H coverage [ML] at T [K]	Observed frequencies or loss bands [cm^{-1}] [meV]		Vibrational mode assignment and coordination	Remarks	Refe.
Be(0001)	0 - 0.38	1492	185	Be - H stretch (bridge site)	exposure to H atoms at 80 K	90Ray
	0.4...0.74	532 1274 1371 1468	66 158 170 182	more trigonal (tilted bridge) site	<i>single</i> site occupation at low coverages	
Mg(0001)		887	107...121	bridge site of Mg - hydride phase assumed;	exposure to H atoms at 110 K; Mg surface hydride phase	91Spr 94Spr
		742 1315	92 163	perpendicular Mg - H mode parallel Mg - H mode (H adsorption in a single fcc or hcp 3-fold site)	metastable up to 425 K dipole active losses	
Al(100)	$T < 90$ K	750 1125 1750	93 139 217	Al-H bending mode bridge-bonded H terminal Al-H stretching mode	exposure to H atoms	88Pau
	280 K	1825	226	ordered islands of terminal H		
Al(110)		1900	236		exposure to H atoms	85Thi
Al(111)		831 1653 1895	103 205 235	occupation of 'multiple' sites	exposure to H atoms at 100 K	88Mun
Al(111)	1.0 at 85 K	A 800	99	bending mode (terminal H)	exposure to H atoms	91Kon
		B 1700	211	stretching mode (terminal H)	AlH_3 molecules	
		C 1200	149	stretching mode (bridged H)	preformed at surface	

Surface	H coverage [ML] at T [K]	Observed frequen- cies or loss bands [cm ⁻¹] [meV]		Vibrational mode assignment and coordination	Remarks	Refe.
Fe(100)	low coverage (β_2 state)	700	87	stretching mode 4-fold hollow site		96Mer
	high coverage (β_1 state)	1000	124	asymmetric site within the 4- fold hollow		
Fe(110)		1060 spe- cular	132	Fe - H stretching mode	adsorption at 300 K	81Barl
		880 non- specular	109	Fe - H asymmetric stretching mode H located in the short bridge		
Co(10–10)	< 0.5 (c(2×4) phase)	468	58	two types of 3-fold coordinated sites	expts. performed at 100 K; measure- ments performed in two perpendicular azimuthal directions exploiting surface symmetry selection rules	94Ern
		605	75			
		1089	135	quasi-3-fold site (hcp-type) ν_1 = perpendicular Co - H stretching mode ν_2 = parallel Co - H mode ν_3 = non-dipole active (impact) parallel mode		
		1169	145			
	1.0 ML (2×1)p2mg phase	580	$72 = \nu_1$			
		1122	$143 = \nu_2$			
(1×2)-rec	904	$112 = \nu_3$ ν_3 only visible along [0001] azimuth				
	609	$76 = \nu_1$				
	984	$122 = \nu_2$				
	1205	$150 = \nu_3$				
Ni(100)	quasi- ordered p(2×2)H at Θ =0.25 ML	581 ± 8	72 ± 1	Ni - H symmetric stretching vibration	expts. performed at 200 K	78And2
	0.5 ML	597 ± 8	74 ± 1	H in a 4-fold hollow (‘center’) site		
Ni(100)	<0.1	629	78	adsorption into defects	expts. performed at 80 K	86Kar
	<0.5	532+629	66 +78	vibr. motion in dilute disordered phase		
	sat’n (~1 ML) at 80 K	629	78	Ni - H stretch in (1×1) H phase		
Ni(100)	1.0 ML (= (1×1)-H)	645 700...850	80 87...105	symmetric stretching mode asymmetric stretching mode	collective asym- metric mode with large dispersion	02Oku
Ni(110)	low Θ	650 1060	81 131	low-symmetry bridge site short bridge site(s)	expts. performed at 100 K dipole active modes	84Oll
	medium Θ	610 940	76 117			
	after heating to >300 K	640 930	79 115	modes change due to (1×2)streak reconstruction		

Surface	H coverage [ML] at T [K]	Observed frequencies or loss bands [cm ⁻¹] [meV]		Vibrational mode assignment and coordination	Remarks	Refe.
Ni(110)	$\theta < 0.4$	573 1057	71 131	symmetric Ni - H stretch asymmetric Ni - H stretch H atoms in quasi 3-fold site	expts. performed either at 150 K to study the metastable lattice gas phases or at 230 K to induce the H-induced (1×2)streak reconstruction;	82DiN 85DiN
	$0.4 < \theta < 1$		mixed			
	$\theta = 1.0$	573 1057	71 131	symmetric stretching mode asymmetric stretching mode		
	$\theta > 1.1$	613 944	76 117	symmetric stretching mode asymmetric stretching of H in a 3-fold site		
	$\theta = 1.5$ (T = 150 K)	613 944 1129	76 117 140 (weak)	symmetric stretching mode asymmetric stretching of H in a 3-fold site with distortion	modes dipole-active	
	$\theta < 0.4$ at 230 K	573 1057	71 131			
	1.0 at 230 K		mixed 140 (weak)	H in a lower coordinated site		
Ni(110)	1 ML = (2×1)-2H	637 1049	79 130	low-symmetry short bridge sites	expts. performed between 100..300 K modes dipole-active	85Jo
	1.5 ML = (1×2)3H	613 944 1210	76 117 150	low-symmetry short bridge sites + high-symmetry short- bridge sites		
	(1×2)streak for $T > 220$	~645 944 1129	~80 117 140	distorted + undistorted surface patches with local structures as (2×1) + (1×2)		
Ni(110)	1 ML = (2×1)-2H phase	560...640	69...79	species 1	exposure at 100 K; HREELS measurements momentum-resolved. Two H sites each with C _s symmetry in the (2×1)-2H phase identical sites with quasi-3-fold symmetry occupied (species 1)	89Voi 87Leh
		870...910 (off- specular)	108...113	species 1; ν polarized parallel to Ni rows		
		1100 ([1-10] azimuth)	136	species 1		
		620...640	77...79	species 1		
	1.5 ML = (1×2)-3H	1100 ([001] azimuth)	136	species 1	in the (1×2)-pairing- row reconstructed surface likewise sites with local quasi 3- fold symmetry are occupied (species 2)	
		610...635	76...79	species 1		
		560...710 (off- specular)	69...88	species 1		
		1035-40	128...129	species 1		
		890...930	110...115	species 2		
		1210-40 ([1-10] azimuth)	150...154	species 2		
		635	79	species 1		
		1035	128	species 1		
		450 (off- specular)	56	species 2		
		930	115	species 2		
		1210-40	150...154	species 2		

Surface	H coverage [ML] at T [K]	Observed frequencies or loss bands [cm ⁻¹] [meV]		Vibrational mode assignment and coordination	Remarks	Refe.
Ni(111)	all coverages	710	88	original interpretation : perpendicular Ni - H stretch (site « A » = hcp)	expts. performed at 170 K; both modes non-dipole active	80Ho
		1121	139	perpendicular Ni - H stretch (site « B » = fcc)) later interpretation : 88 = symmetric Ni - H stretch (perpendicular mode) ; 139 = asymmetric Ni - H stretch (parallel mode)		
Ni(111)	1 ML surf.	955	118	symmetric Ni - H stretch	exposure to <i>atomic</i> H at 80...100 K; after prolonged exposure crystal contains embedded (bulk) H	91Joh
		1170	145	antisymmetric Ni - H stretch		
		800	99	vibration due to embedded H		
	1 ML surf. + 1 ML bulk	955	118	symmetric Ni - H stretch		
		1170	145	antisymmetric Ni - H stretch		
Ni(111)	0.05...0.5	726	90	asymmetric Ni - H stretch	H ₂ exposure at 100 K	97Yan
		1048	130	symmetric Ni - H stretch associated with (2×2) honeycomb structure		
	>0.5	726	90			
		927	115			
		1129	140			
	1.0	927	115	correlated with (1×1)-H structure		
		1129	140			
Ni(111)	0.5 (= c(2×2))	732	91	antisymmetric Ni - H stretch	H ₂ exposure at 90 K	03Oku
		774	96	in two different 3-fold sites		
	honey-comb	1054	131	symmetric Ni - H stretch in		
		1094	136	two different 3-fold sites		
		1250	155	indicate delocalization of excited vibrational states		
		1390	172			
		2180	270			
	1.0 (= 1×1 phase)	954	118	overtone of ν_s		
		1170	145	asymmetric Ni - H stretch		
		1744	216	symmetric Ni - H stretch		
Ni(311)	very low θ	444	55	bending (parallel) mode (H species 1)	exposure to H ₂ at 100 K	96Sch
		1202	149	stretching (perpendicular) mode (H species 1) (species 1 = H in a 3-fold site =(111)-facet)		
	low and medium θ	347	43	bending mode (H species 2)		
		452	56	bending mode (H species 1)		
		726	90	stretching mode (H species 2)		
		1202	149	stretching mode (H species 1) (species 2 = H in a 4-fold site =(100)-facet)		
	high θ	282	35	bending mode (H species 2)		
		524	65	bending mode (H species 1)		
		686	85	stretching mode (H species 2)		
		887	110	bending mode (H species 3)		
		1000	124	stretching mode (H species 3)		
		1250	155	stretching mode (H species 3) (H species 3 = 3-fold sites in the grooves of (110)-surface)		

Surface	H coverage [ML] at T [K]	Observed frequencies or loss bands [cm ⁻¹] [meV]		Vibrational mode assignment and coordination	Remarks	Refe.
Ni(510)	low and medium θ	645	80	wagging mode	expts. performed at 100 K	88Mar
		847	105	asymmetric Ni - H stretch		
		1113	138	symmetric Ni - H stretch of low-symmetry short-bridge site located at the terrace steps (3-fold symmetry)		
		387	48	component of the asymm. (parallel) mode (4-fold symmetry site on the terrace)		
		589	73	symmetric (perpendicular) stretch of H in 4-fold (terrace) sites		
	high θ	766 + 1242	95 + 154	H adsorbed at step sites (low- symmetry long-bridge site)	surface reconstr. cannot be excluded	
Cu(100) + H ₂	1 ML of physi- sorbed H ₂ molecules	363	45	rot. trans. $J = 0 \rightarrow J = 2$	expts. performed with H ₂ , D ₂ , and HD molecules condensed at 15 K	83And 97Sve
		581	72	rot. trans. $J = 1 \rightarrow J = 3$		
		4178	518	rot.+vibr. trans. $\nu = 0 \rightarrow \nu = 1 +$ $J = 0 \rightarrow J = 2$		
		4516	560	rot.+vibr. trans. $\nu = 0 \rightarrow \nu = 1 +$ $J = 1 \rightarrow J = 3$		
		4734	587	rot.+vibr. trans. $\nu = 0 \rightarrow \nu = 1 +$ $J = 1 \rightarrow J = 3$		
Cu(100)	low θ	565	70	H in a 4-fold hollow site	expts. performed with atomic H at 83 K	91Cho
	high θ (1.03 ML)	468	58	modified 4-fold hollow site	high θ leads to surface reconstr. of	
		565	70		p4g or pgg type;	
		948	117.5	bridge-bonded H	losses dipole-active	
Cu(110)		548	68	long-bridge site	exposure to H atoms	87Bad
		653	81	4-fold hollow site		
	$T > 140$ K	750	93		disordered H	
	(=1×2) rec	944+871 1129	117+108 140		adsorption	
Cu(110)	$\theta < 0.2$	620	77	symmetric stretch (species 1)	exposure to H atoms at 100 K	90Hay
	= (1×1)			symmetric stretch (species 2)		
	$T < 140$ K			in long-bridge + 4-fold sites		
	$\theta > 0.2$	620 +	77 +	alternative assignment:		
	= (1×3)	shoulder	shoulder	H in quasi-3-fold sites		
	$T < 140$ K	at 505	at 63			
Cu(110)		950	118			
	$0.1 < \theta < 1$	765	95	symmetric mode		
	(1×2) MR-	950	118	asymmetric mode: H in a		
	recon- structed surface	1150	143	tilted trigonal site with mirror plane parallel to [001] azimuth		
Cu(110)	≤ 0.33	637	79	parallel mode	exposure to H (D)	92Ast
	= (1×3)	952	118	perpendicular mode	atoms at 110 K	
	phase			H in quasi-3-fold site, ν polarized in [1-10] mirror plane	delocalization of low-density H atoms (protonic band structure)	

Surface	H coverage [ML] at T [K]	Observed frequen- cies or loss bands [cm ⁻¹] [meV]		Vibrational mode assignment and coordination	Remarks	Refe.	
Cu(111)	0.5...0.67 ?	1040	129	symmetric stretching of H in 2-fold (bridge) site	exposure to H atoms at 150 K. Use of RAIRS + HREELS technique	89McC	
		1150-70	143-145	1 st overtone of deformation mode of H in a 2-fold site			
Cu(111)	0.67 = (3×3) phase	770	95	frustrated parallel translational modes of H in 3-fold sites	RAIRS measurements; 1151 cm ⁻¹ [89McC] mode <i>not</i> observed	95Lam	
		1040	129				
Nb(100)	sat'n	944	117	H in tetrahedral sites just below the surface	expts. performed at 300 K ? H-induced losses ex- hibit inhomogene- ous broadening; hint to occupation of ine- quivalent subsurface sites	86Li	
		1049	130				
Mo(100)		555 (at 270 K)	69	Mo - H bending mode	expts. performed at 80 K and at 270 K; losses between 400...600 and 700...900 cm ⁻¹ due to Mo phonons	86Zae	
		1025	127	} Mo - H stretching modes			
		1220	151				
		1260	156				
Mo(100)	low θ (0.08) = (5×2)at 120 K	1220	151	ν_1 mode of H in a short bridge site	RAIRS expts.	87Pry	
	low θ (0.35)= (4×2) at 250 K	1205	149	H on a shorter bridge site on reconstructed Mo surface			
	high θ (2.0 ML) = (1×1)-2H phase at 100 K	1020	126	symmetric stretch (ν_1): all H atoms in bridge sites			
		1300	161	asymmetric Fano line to the overtone of the wagging mode of Mo - H - Mo structure			
Mo(100)	sat'n = (1×1)-2H	1016	126	symmetric stretch	Surface infrared	88Reu	
		1302	161	overtone of wagging mode	spectroscopy (SIRS) expts		
Mo(110)	<0.5 beginning (2×2)	710	88	antisymmetric stretching mode	low θ losses due to reconstructed (2×2) (rippled) surface	97Oka	
		1097	136	symmetric stretching mode of H atoms in quasi trigonal (3- fold) sites			
	intermedi- ate θ (2×2)	798	99		108 meV loss due to (1×1) island nucleation		
		871	108 (only in [1-10] azimuth)				
	$\theta > 0.5$ (1×1) phase; sat'n = 1 ML	1226	152		high θ losses due to H-saturated (1×1) phase; fully H-covered (110) surface ex- hibits a giant phonon anomaly, see, e.g., [92Hu11]		
		798	99				
		1226	152				

Surface	H coverage [ML] at T [K]	Observed frequen- cies or loss bands [cm ⁻¹] [meV]		Vibrational mode assignment and coordination	Remarks	Refe.
Mo(211)	$\Theta < 1$ ML: no H superstr.	1250- 1323	155...164	two types of binding sites symmetric stretch of 2-fold (bridge-bonded) H	expts. performed at 200 K	93Lop
	$\Theta > 1$ ML: (1×2) phase exists up to sat'n (= 2.0 ML)	750 1323	93 164	symmetric stretch of H in 3- fold coordinated site symmetric stretch of 2-fold (bridge-bonded) H	(1×2) phase due to H-induced PR reconstruction; no protonic bands	
	Ru(0001)	sat'n = 1 ML	847 1113	105 138	symmetric Ru-H stretch asymmetric Ru-H stretch	
Ru(0001)	sat'n (~ 1 ML)	823 1137	102 = ν_1 141 = ν_2 three weak ad- ditional losses at	Ru - H parallel mode Ru - H perpendicular mode	expts. performed at 115 K strong dependence of electron reflectivity on H coverage	84Con
		1549 1960 2274	192 = ν_3 243 = ν_4 282 = ν_5	} overtones + combination modes		
Ru(0001)	< 0.3	686	85	perpendicular Ru - H stretching mode ; H in 3-fold hollow site	expts. performed at 90 K; two kinds of adsorbed H species, depending on coverage	94Shi
	1.0	726 823 1137	90 102 141	3-fold site with reduced symmetry		
Ru(0001)	0...1 ML	820 1137	102 141	doubly degenerate parallel Ru - H mode perpendicular Ru - H stretching mode	expts. performed at 170 K; only one kind of adsorbed H spec- ies reported	04Kos
Ru(10–10)	0.7...1.0 (= c(8×2) phase)	847 1145	105 142	parallel Ru - H mode perpendicular Ru - H mode (site A)	expts. performed at 100 K azimuthal dependences of losses suggest C _s site symmetry of quasi 3- fold site(s) "A" and "B"	89Lau
	1.2...1.3 (= (1×2) phase)	(355) 847 1210	(44) 105 150	phonon ? ($\nu_H = \nu_D$) parallel mode (site A) perpendicular mode (site A)		
	1.5 (c(2×2)-3H phase)	621 847 1290- 1331	77 105 160...165			
	2.0 ((1×1)- 2H phase)	621 774 847 shoulder 1057 1145- 1226 1355	77 96 105 shoulder 131 142...152 168	parallel mode (site B) parallel mode (site B) parallel mode (site A) perpendicular mode (site B) perpendicular mode (site A) perpendicular mode (site B)	additional occupation of quasi-3-fold site "B" in the high- coverage phase	

Surface	H coverage [ML] at T [K]	Observed frequen- cies or loss bands [cm ⁻¹] [meV]		Vibrational mode assignment and coordination	Remarks	Refe.	
Ru(10–10)	1.0 ML	169	21	Ru phonon mode	expts. performed at 90 K; excitation cross section strongly dependent on primary electron energy. Quantum motion at small coverages due to wide protonic band	93Gru	
		218	27	parallel mode (site A)			
		323	40	parallel mode (site A)			
	2.0 ML	1210	150	perpendicular mode (site A)			
		629	78	parallel mode (site B)			
		807	100	parallel mode (site B)			
	1032	128	perpendicular mode (site B)				
Ru(11–21)	small coverages < 0.12 L (γ - TD state)	500	62	parallel mode (site 1)	expts. performed at 90 K	01Fan	
		742	92	parallel mode (site 1)			
		1169	145	perpendicular mode (site 1) (site 1 = pseudo-3-fold “A”)			
	medium coverages < 0.17 L (β TD state)	516	64	parallel mode (site 2)	all modes dipole- active		
		927	115	parallel mode (site 2)			
		1290	160	perpendicular mode (site 2) (site 2 = pseudo-3-fold “B”)			
	high cover- ages (α -TD state)	339	42	parallel mode (site 3)			
		742	92	perpendicular mode (site 3) (site 3 = quasi-4-fold)			
	Rh(100)	0.4 ML sat’n = 1 ML	565	70			ν_1 = Rh - H perpendicular stretch 1 st overtone of ν_1 H in a 4-fold hollow site doubly degenerate parallel mode (impact-active)
			661	82			
1226			152				
1113			138				
Rh(100)	sat’n = 1 ML = 1.39 $\times 10^{19}$	528 \pm 4	65.5 \pm 0.5	ν_{asym}	expts. performed at 90 K	88Ric1	
		661 \pm 2.5	82.0 \pm 0.3	ν_{sym}			
		1008 \pm 16	125 \pm 2	} overtones			
		1105 \pm 32	137 \pm 4				
		1242 \pm 16	154 \pm 2				
		1395 \pm 16	173 \pm 2				
		1557 \pm 16	193 \pm 2				

Surface	H coverage [ML] at T [K]	Observed frequen- cies or loss bands [cm ⁻¹] [meV]		Vibrational mode assignment and coordination	Remarks	Refe.	
Rh(110)	0.3...0.5 (=(1×3) + (1×2) phases)	444..	460	55...57	ν_1 (A' symmetry)	expts. performed at 100 K in the two azimuthal directions [1–10] and [001]; excitation strongly dependent on impact energy due to surface resonances	94Mue
		532		66	ν_2 (A'' symmetry (impact m.))		
		694		86	ν_3 (A' symmetry) = perpendicular Rh - H mode (quasi-3fold hollow sites)		
		984		122	combin. mode ($=\nu_1 + \nu_2$)		
		1024		127	overtone (2 ν_2)		
		1145		142	combin. mode ($=\nu_1 + \nu_3$)		
		1234		153	combin. mode ($=\nu_2 + \nu_3$)		
		1355		168	overtone (2 ν_3)		
	$\theta > 0.5$ (non- primitive H phases: (1×2)-2H + (1×3)-2H)	403		50	ν_1 (A ₁ +B ₁ symmetry)		
		871		108	ν_2 (B ₂ + A ₂ symmetry)		
		694		86	ν_3 (A ₁ +B ₁ symmetry)		
		1048		130	combin. mode ($=\nu_1 + \nu_3$)		
		1153		143	combin. mode ($=\nu_1 + \nu_2$)		
		1420		176	overtone (2 ν_3)		
		1532		190	combin. mode ($=\nu_2 + \nu_3$)		
		Rh(111)	0.4...1 ML	450		56	trans. from ground-state band to 1 st excited (E) band
660				82			
750				93	trans. from ground-state band		
1050				130	to A_1^1 (750 cm ⁻¹) and A_1^2 (1050 cm ⁻¹) bands		
0.6...1.0	470			58	transitions from ground-state to excited protonic bands		
	750			93			
	1100			136			
	1450			180			
Rh(311)	0.05	452		56	species I	due to the 'open' geometry, a complicated vibrational scenario arises; three H species I, II and III can be distinguished with increasing exposure	97Far
	0.1...0.5	1226...50		152 (155)	species I + II		
		444 (565)		55 (70)			
		887		110			
		1250		155			
	0.5...0.8	1613		200	species I + II + III		
		258		32			
		444 (508)		55(63,70)			
		887		110			
	0.8...1.0	1250		155	species I + II + III		
		1613		200			
		290 (218)		36 (27)			
		444. 492,		55, 61, 72			
	1...>1.3	1250		155			
		1613		200			
		323		40			
484			60				
710			88				
927			115				
	1290		160				
	1613		200				

Surface	H coverage [ML] at T [K]	Observed frequencies or loss bands [cm ⁻¹] [meV]		Vibrational mode assignment and coordination	Remarks	Refe.
Pd(100)	0.08 ML	486	60.2	symmetric Pd - H stretching vibration (H in a 4-fold hollow site)	expts. performed at 80 K	82Nyb 83Nyb
	0.59 ML (c(2×2))	502	62.2			
	0.96 ML ((1×1)-H)	512	63.5			
Pd(110)	1 ML (= (2×1)-2H phase)	790 968	98 120	parallel Pd - H mode perpendicular Pd - H stretch mode of H located in quasi-3- fold sites reconstruction leads to enhanced linewidth (only slightly modified H-Pd sites)	expts. performed at 100 K	89Eil
	1 ML ((1×2)-3H phase)	790 968 (line broadening)	98 120			
Pd(110)	low coverages (0.04..0.4)	702...718 774...807 976...984	87...89 (weak) 96...100 121...122	in the low-coverage region the observed bands can reflect transitions from protonic ground-state to excited bands	expts. performed at 90 K; loss peak positions shift with coverage	96Tak
Pd(111)	medium H coverages (2 L exposure)	774 1000	96 124	ν_1 = parallel Pd - H stretch ν_2 = perpendicular Pd - H stretch of H bound in 3-fold hollow site	expts. performed at 120 K; evidence of strong H-induced surface resonances	86Con1 86Con2
Pd(210)	low...high coverages	444 694...726	55 86...90	limited resolution prevents a precise assignment. Broad losses indicate various Pd - H coordinations	expts. performed at 120 K HREELS insensitive to subsurface H	98Mus1
Pd(311)	0.25 ML (= (2×1)-H phase)	452	56	parallel mode (4-fold site)	expts. performed at 120 K; activated population of subsurface sites. Octahedral subsurface sites identified	98Sch 99Far
		686	85	perpendicular mode (4-fold s.)		
		758	94	parallel mode (3-fold site)		
		968	120	perpendicular mode (3-fold s.)		
	0.5 ML	403 ~686 ~726 1016	50 ~85 ~90 126	slight θ -dependent band shifts		
Ag(110)	0.1...1 ML	484	60	parallel mode	exposure to H atoms at 100 K H atoms localized; no evidence of quantum motion	93Spr
		847	105	perpendicular mode (H in tilted trigonal sites with C_s symmetry)		
Ag(111)+ H ₂	1 ML	395	49	$J'=0 \rightarrow J'=2$ transition	physisorption of molecular hydrogen at $T = 10$ K	82Avo
		4187	518	$\nu = 0 \rightarrow \nu = 1 + J'=0 \rightarrow J' = 0$ transition		
		4533	562	$\nu = 0 \rightarrow \nu = 1 + J'=0 \rightarrow J' = 2$ transition		
Ag(111)	0.1 < θ < 1	702	87 (off- specular)	parallel mode (impact active)	delocalized (protonic band) motion ruled out	95Lee
		855	106	perpendicular mode (dipole active) Ag - H stretch		
Ta(100)	sat'n at 300 K (~1 ML)	1129	140	Ta - H stretching vibration (superposition of symmetric stretch (= A_1) and antisymmetric stretch (= E) with $\Delta E = 15$ meV)	broad single loss at all coverages assumed to consist of two peaks; no H-induced reconstruction	04Yam

Surface	H coverage [ML] at T [K]	Observed frequencies or loss bands [cm ⁻¹] [meV]		Vibrational mode assignment and coordination	Remarks	Refe.
W(100)	$\Theta < 0.5$	1251	155	on-top site (β_2 -hydrogen) bridge sites exclusively occupied	expts. performed at 300 K in specular direction; occupation equilibrium of two different sites, depending on H coverage	76Fro
	$\Theta \geq 0.5$	1049	130			
		1251	155			
	$\Theta > 0.7$	1049	130			
		1251	155 weak			
	$\Theta = 2$	1049	130			
W(100)	$\Theta < 0.5$	1282 \pm 8	159 \pm 1	W - H bending mode (β_2 -TD-state)	expts. performed at $T < 350$ K in specular direction; evidence of <i>atomic</i> nature of adsorbed H species	77Adn
	$\Theta = 1.2$	637	79 weak			
	$\Theta = 2$	1065 \pm 8	132 \pm 1			
W(100)	$\Theta = 2$ ($= 2 \times 10^{19}$ at/m ² (sat'n))	1049	130 spec.	symmetric W - H stretch (A_1) in 2-fold (bridge) site	expts. performed at 300 K in both specular and off-specular direction	78Ho
		645	80 o-sp.	ν_2 = parallel (bending) mode		
		1049	130 o-sp.	ν_1 = symm. stretch (2-fold s.)		
		1290	160 o-sp.	ν_3 = asym. stretch (2-fold s.)		
		2097	260 o-sp	overtone of symm. stretch ($2\nu_1$)		
W(100)	0.5 (= c(2×2)H phase)	484	60	ν_2 = bending mode (2-fold s.)	expts. performed at 300 K; consideration of H-induced surface reconstruction; detection-angle dependent measurements	78Bar2 80Will
		1008	125	ν_1 = symm. stretch (2-fold s.)		
		1250	155	ν_3 = asym. stretch (2-fold site)		
			+ weak overt.	(local site geometry affected by surface reconstruction)		
	2.0 (= (1×1)-2H phase)	645	80	ν_2 = bending mode (2-fold s.)		
		1049	130	ν_1 = symm. stretch (2-fold s.)		
W(100)	0.1...1.0	1250	155...	ν_1 = symm. stretch (2-fold s.)	expts. performed at 150 K and at 300 K; consideration of displacive W surface reconstruction; confirmation of tilted dimer model	83Did
		1049	130 (specular)	moves from 155 to 130 meV as Θ increases from 0.1 to 1.		
		444...645	55...80	$\nu_2 = \nu_{wag}$ wagging mode shifts from 55 to 80 meV for $\Theta \rightarrow 1$		
		1008	125	ν_1 = symm. stretch (2-fold s.)		
		1210...90	150...160	ν_3 = asym. stretch (2-fold site)		
W(100)	sat'n = (1×1)-2H	1070	133	symmetric stretch	high-resolution infrared spectroscopy expts.	85Cha2
		1270	157	overtone of wagging mode		
W(100)	sat'n = (1×1)-2H	1069	133	symmetric stretch	Surface infrared spectroscopy (SIRS) expts.	88Reu
		1269	157	overtone of wagging mode		
W(100)	0...2.0 ML at 100 K	1100 ($\Theta = 1.4$)	136	ν_1 = W ₂ - H symm. stretch	RAIRS expts.	89Rif
		1070	133	ν_1 = W ₂ - H symm. stretch		
		1260	156	2 ν_2 = overtone wagging md.		
		($\Theta = 1.65$..2.0)				

Surface	H coverage [ML] at T [K]	Observed frequencies or loss bands [cm ⁻¹] [meV]		Vibrational mode assignment and coordination	Remarks	Refe.	
W(110)	0.1...1 ML	767	95	symmetric stretch of H in 2-fold (bridging) site		77Bac	
		1267	157	symmetric stretch of H in atop sites (?). A later reconsideration suggested H in sites with higher coordination (2-fold and/or quasi-3-fold)		80Jay	
W(110)	p(2×1)	113	14	substrate phonon	specular and off-specular experiments at 110 K with momentum resolution; emphasis on the phonon dispersion curves.	94Bal	
		213	26	} 3-fold hollow site likely		W - H vibrational modes for three coverages were followed through k space.	96Bal
		539...550	67...68				
		768...774	95...96				
		1252...56	155...156	perpendicular W - H mode			
	(2×2)	214	27	substrate phonon	In the (1×1) phase, H is adsorbed in a two-dimensional quasi liquid-like phase		
		621	77	} 3-fold hollow site(s)			
		736	91				
		884	110			perpendicular W - H mode	
		1222	152	perpendicular W - H mode (two kinds of H species)			
	p(1×1)	1327	165				
		197	24	substrate phonon			
		continuum below					
		850	105				
		1300	161	sharp W - H mode			
W(111)	$\theta > 0.1$ ML	1291 (broad)	160	H in sites with higher coordination (2-fold and/or quasi-3-fold)		77Bac 80Jay	
Re(10–10)	$\theta < 0.9$	379...484	47...60	Re phonons	expts. performed at 120 K in two perpendicular directions of scattering plane	98Mus2	
		645...669	80...83	H species 1 (C _{2v} symmetry)			
		1347	167				
	1.5 (c(2×2)-3H)	379...484	47...60	H species 1 + species 2 (C _s symm.)			
		669	83				
		936	116				
	2.0 (1×1)-2H	1347	167	H species 3 (C _s symmetry)			
		645	80				
		903	112				
		1000	124				
1347	167						
Ir(110)-(1×2)		590	73	H in a quasi-3-fold site	expts. performed at 170 K	88Cha	
		(2025)	(251)		<u>note:</u> a strong vibration around 2025 cm ⁻¹ – compare Hagedorn's study [99Hag] – was observed, but assigned as Ir - C=O stretching mode caused by slight CO impurities		

Surface	H coverage [ML] at T [K]	Observed frequencies or loss bands [cm ⁻¹] [meV]		Vibrational mode assignment and coordination	Remarks	Refe.
Ir(111)	medium Θ	560 (2025)	69 (251)	H in a 3-fold site	expts. performed at 170 K <u>note:</u> the observed strong vibration around 2025 cm ⁻¹ was assigned as Ir - C=O stretching mode	88Cha
Ir(111)	<0.4 ML	525	65	excitation into delocalized protonic bands	expts. performed at 90 K	99Hag
	>0.44 ML	2030	252	Ir - H mode (terminal site)		
Pt(110)-(1×2)	low Θ	790 1137 1549	98 141 192	? symmetric stretch parallel mode perpendicular to rows (H in 2-fold bridge at bottom of missing-row trough)	besides the (1×2)-MR reconstruction a (1×4) reconstructed surface was observed	91Ste
	high Θ (sat'n)	540 669 1202	67 83 149	symmetric mode locally 3-fold sites at edges of (1×2) rows		
Pt(111)	low Θ and high Θ (up to 0.7 ML)	550 1230	68 153	symmetric Pt - H stretching asymmetric Pt - H stretching (vibration perpendicular and parallel for H in a 3-fold coordinated site)	expts. performed at ≥ 90 K; specular and off-specular to distinguish dipolar and impact contributions	79Bar 84Say1 84Say2
Pt(111)	1 ML = 1.49×10^{19} ; well-ordered (1×1) phase	540 903 1234	67 112 153	asymmetric Pt - H stretching symmetric Pt - H stretching overtone + combination loss $\nu_{asy}^{0 \rightarrow 2}$ and $(\nu_{asy} + \nu_{sym})$ (unresolved)	expts. performed at 85 K and 170 K; evidence for soft parallel modes	87Ric2
Pt(111)	$\Theta \leq 0.75$ ML	250 395 548	31 49 broad 68	bands are due to transitions between protonic bands of delocalized H atoms	expts. performed at 85 K. At lower Θ , the bands at 112 and 153 [87Ric2] are <i>not</i> detected. Strong evidence of H atomic band structure (delocalized H motion)	02Bad
Pt(111)	$\Theta = 0.8 \dots 1.0$ ML	548 911 1234	68 113 153	symmetric stretching mode hybride mode with both in-plane and dipole character symmetric stretching mode (H in the 3-fold hollow (fcc) site)	expts. performed at 85 K	03Bad

3.4.1.3.6.2 Semiconductor and insulator surfaces

The vibrational properties of H-covered semiconductor surfaces, silicon in particular, have been extensively studied since the early days of high-resolution electron-energy loss spectroscopy. An overview of this early work is given by Froitzheim [77Fro]; further aspects of the HREELS technique and its application to semiconductor studies (excitation of phonons etc.) can be taken from Ibach's monograph [82Iba]. The status of hydrogen interaction with elemental and compound semiconductors up to 1986, mainly in the view of vibrational loss spectroscopy, is given in a report by Schaefer [86Sch]. In more

recent years, also other techniques, mainly infrared spectroscopy, second harmonic generation or sum frequency generation spectroscopy have increasingly been exploited to determine the vibrational bands of interest. In the nineties, the upcoming technological interest in diamond films, coatings and tools has motivated a whole wealth of studies into the properties of H-covered C_{dia} surfaces, and the degree of hydrogenation, surface roughnesses etc. were frequently investigated also by HREELS. For space limitations, however, only some of the more important data are listed in the subsequent table.

Surface	H coverage [ML] at T [K]	Observed frequencies or loss bands [cm ⁻¹] [meV]		Vibrational mode assignment and coordination	Remarks	Reference
C(111) (diamond)	1 ML at 300 K	1290 2903	160 360	C - H rocking mode C - H stretching mode	atomic hydrogen exposure on as polished C crystals	85Pat
C(111) (diamond)	1 ML (1×1) H terminated	2830	351	stretching vibration of C - H bonds with top C atoms	Infrared-visible sum frequency generation (SFG)	92Chi
C(111)-1×1 (diamond)	terminated with meth- yl (CH ₃) groups	1000 to 1450	124 to 180	mixed modes of C - H bending vibrations and/or substrate phonons	exposure to H plasma; impact scattering important	93Aiz
		2839	352	C - H stretching mode of sp ³ hybridized bonding		
C(100)-2×1 (diamond)	terminated with C - H bond (mono- hydride)	1000 to 1450	124 to 180	mixed modes of C - H bending vibrations and/or substrate phonons	exposure to H plasma; impact scattering important	93Aiz
		2928	363	C - H stretching vibration		
C(100)-1×1 C(111) (diamond)	H terminated	650 to 1690	80 to 210	phonon modes and C - H bending vibrations	exposure to H plasma	93Lee
		2930	363	C - H stretching vibration		
C(100)-2×1 (diamond)	1 ML (H saturated)	1250 2440 2920 3600	155 303 362 446	C - H bending mode overtone of 1250 cm ⁻¹ mode C - H stretching mode overtone, multiple losses	exposure to H plasma	94Tho
C(100)-2×1 (diamond)	H terminated	823 968 1097 1202 1258 2903 2919	102 120 136 149 156 360 362	phonons off-specular only phonons off-specular only phonons phonons symmetric and antisymmetric C - H stretching modes	exposure to H atoms, HREELS study	03Tha1 03Tha2
C(0001) HOPG graphite	sat'n coverage at 300 K (0.5 ML)	1210 2650 640 1950 850 1580	150 329 79 242 105 196	C - H bending mode C - H stretching mode C - D bending mode C - D stretching mode surface phonon surface phonon	exposure to H (D) atoms	02Zec
Si(100)	H- terminated	630 2080	78 258	monohydride bending (scissor) mode monohydride stretching vibr.	exposure to H atoms at 500 K	84But
Si(111)-7×7	H- terminated	630 900	41 112	dihydride wagging mode dihydride bending (scissor) mode	exposure to H atoms at 140 K	84But
		2080	258	monohydride stretching vibr.		
Si(100)-2×1	1 ML (mono- hydride)	2087.5 2098.8	259 260.2	Si - H stretching modes	exposure to H (D) atoms; surface IR study	84Cha3

Surface	H coverage [ML] at T [K]	Observed frequencies or loss bands [cm ⁻¹] [meV]		Vibrational mode assignment and coordination	Remarks	Reference
Si(100)-2×1	mono- hydride phase	645 2097	80 260	Si - H wagging mode Si - H stretching mode	exposure to H atoms	86Sch
Si(100)-1×1	dihydride phase	645 915 2097	80 113.5 260	Si - H wagging mode Si - H ₃ scissor mode Si - H stretching mode		
Si(100)	1 ML (1×1) H terminated	400 490 520 650 910 2105	50 61 64.5 80 113 261.5	possibly several phonon bands scissor mode of SiH ₂ Si - H ₂ stretching vibration	surface prepared by etching in a 40% ammonium fluoride solution	91Dum
Si(100)-2×1	ca. 1 ML	2084 2094 2104 2114 2127 2089	258.4 259.6 261 262 263.7 259	parallel component vertical component = symm. stretching mode of mono- hydride (lower H exposures) dihydride stretching modes trihydride (larger exposures) of occupied dimer phase monohydride stretching mode (only feature at very large exposures)	exposure to atomic hydrogen (high-resolution surface IR spectroscopy)	99Niw
Si(111)	less than 1 ML	630 900 2100	78 112 260	Si - H bending mode SiH ₂ , SiH ₃ wagging and rocking modes Si - H ₂ bending mode with bond angle changes Si - H stretching mode	exposure to atomic hydrogen	81Wag
Si(111)-2×1 (7×7)	ca. 1 ML	460; 919 968 2258	57; 114 120 280	phonon + phonon overtone Si - H stretching vibration	freshly cleaved surf. exposure to H atoms after annealing to 623 K	83Fro
Si(111)-7×7	0 ...sat'n	637 879 2080 (smaller expos.) 637 879 2077 (medium exp's) 2097 (large exp's)	79 109 258 79 109 257.5 260	Si - H bending mode Si - H ₂ scissor mode Si - H stretching mode Si - H bending mode Si - H ₂ scissor mode Si - H stretching mode Si - H stretching mode	exposure to H atoms at 300 K; heating to 650...750 K causes minor shifts in frequency and intensity of the three characteristic vibrational bands	83Kob
Si(111)-7×7	H sat'n	637 887 2089	79 110 259	Si - H bending mode Si - H ₂ scissor mode Si - H stretching mode	exposure to H atoms	84Fro
Si(111)-2×1	H sat'n → (1×1) LEED phase	613 806.5 2073	76 100 257	Si - H bending mode Si - H ₂ scissor mode Si - H stretching mode	exposure to H atoms at 300 K. Quenching of Si phonon modes	86Sch

Surface	H coverage [ML] at T [K]	Observed frequencies or loss bands [cm ⁻¹] [meV]		Vibrational mode assignment and coordination	Remarks	Reference
Si(111)	1 ML (1×1) H terminated	520 636 795 2085	64.5 79 98 258.5	substrate phonon bending mode of the monohydride Si - H stretch mode	all losses disappear at 750 K due to H ₂ desorption	91Dum
Si(111)	1 ML (1×1) H terminated	626.7 2083.7	77.7 258.4	doubly degenerate bending mode stretching vibration of the surface Si - H bond	transmission IR spectroscopy with vicinal H/Si(111) surfaces	02Cau
Ge(100)	(2×1) H terminated	532 1976	66 245	Ge - H bending mode Ge - H stretching mode	exposure to H atoms	86Pap
GaAs(110)	1 ML	1890 (H) 1380 (D) 2150 (H) 1660 (D)	234 171 267 206	Ga - H stretching mode Ga - D stretching mode As - H stretching mode As - D stretching mode	exposure to H (D) atoms	81Lue
GaAs(001) c(2×8) (1×6) reconstr.	1 ML	1950 - 2150 1835 1875	242 - 267 228 232	arsenic hydride vibrations vibrations due to two terminal Ga hydrides	exposure to H atoms between 303 and 433 K. IR reflectance spectroscopy	95Qi
GaAs(001) • c(4×4) • (2×4) • (2×6) • (4×2)	(1×1)-H → (1×4) 					

3.4.1.3.7 Electronic states of adsorbed hydrogen and photoemission spectroscopy

The geometrical structures of H adsorbate layers listed in sect. 3.4.1.3.3 reflect nothing but the consequences of the electronic (quantum-chemical) interaction of a hydrogen molecule with the respective substrate. The following paragraph(s) will be devoted to this interaction and finally lead up to a (short) presentation of current theories and models to adequately describe this interaction. In section 3.4.1.3.7 we will review data that have basically been obtained by (UV) photoelectron spectroscopy (UPS). UPS actually maps the electronic states of a solid surface and their adsorbate-induced changes occurring in the substrate's conduction and valence band energy region ($0 < E < 50$ eV), whereby the interaction of hydrogen with *conducting* (metallic) surfaces is in the focus of the scientific interest. Section 3.4.1.3.8 then samples the H-induced work function data.

A few remarks may be helpful to understand the principles of the quantum-chemical interaction of a H_2 molecule with a solid surface; for the sake of simplicity we will consider again *metallic* surfaces here. In this description, we will largely follow the informative exposition given by Harris [88Har]. When an unperturbed H_2 molecule with its large covalent binding energy of 4.7 eV and the comparatively quite close H - H bond distance of 0.74 Å is approaching a metal surface, say, a nickel (100) surface, it is first attracted by a weak van-der-Waals interaction potential. Since the energetically more favorable situation consists in a cleaved H - H bond and the formation of two stable Ni - H bonds (c.f., Eq. (2)) the system faces the difficulty that the typical distances between two metal (Ni) atoms are a factor of ~ 3 larger (Ni - Ni distance = 2.49 Å) than the internuclear spacing in H_2 , in other words, the proton - proton distance has to be stretched quite considerably to match the Ni - Ni distance and make the two Ni - H bonds. The decisive quantity to be considered here is the (multi-dimensional) potential-energy surface (PES) which determines the transition (and the trajectories) of the incoming H_2 molecule to the final equilibrium situation where two adsorbed H atoms exist on the metal surface. The accurate calculation of both the PES and the hydrogen trajectories is among the most prominent tasks of hydrogen chemisorption theory. For the $H_2/Mg(0001)$ system, Nørskov et al. [81Nor1, 87Nor] have calculated the one-electron density of states and the total binding energy for a H_2 molecule approaching this surface using the effective medium theory [80Nor2, 82Nor3]. As repeatedly mentioned in the previous sections, the shallow van-der-Waals potential is separated from the deep chemisorption well by a more or less pronounced activation energy barrier which must be overcome to reach the chemisorbed state and to minimize the total energy of the combined system. According to Harris [88Har], this activation barrier has the following origin: The unperturbed H_2 molecule is a closed-shell entity possessing a filled and very compact $1\sigma_g$ molecular orbital (MO). As it approaches the surface, interference between this $1\sigma_g$ MO and the metallic (sp) wave functions results in the well known Pauli repulsion: The necessary orthogonalization of the involved MOs pulls up their energies. As the molecule gets closer to the surface, this rise in energy continues until, for energetic reasons, a dramatic change in the system's configuration can take place, namely, the dissociation of the H_2 molecule. Since only with transition metals the sp and d wave functions share a common Fermi level, the far-reaching and diffuse metallic sp orbitals (which are especially affected) can avoid the Pauli repulsion by 'escaping' to unfilled (but energetically equivalent) d orbitals and thus offer the H_2 molecule a trajectory of minimum potential energy and a much smaller activation barrier for dissociation [88Har]. Of course, in a more detailed view the spatial orientation of the H_2 molecule relative to the surface must be considered on its way into its adsorbed state, which requires a full dynamical treatment (i.e., inclusion of time-dependent phenomena). Accordingly, an increasing number of calculations taking care of dynamical quantum processes have been performed in recent years; for more details, which are beyond the scope of this presentation, it is referred to the special literature [95Dar, 96Gro]. We simply point to the respective calculations performed by Wilke and Gross who successfully treated the adsorption dynamics of the $H_2/Pd(100)$ system as a six-dimensional problem and introduced the dynamical *steering effect* already mentioned in the introduction [96Wil]. Returning to Nørskov's treatment of the $H_2/Mg(0001)$ system [81Nor1], which gives an idea about possible broadenings and downshifts of the involved hydrogenic MO's along the reaction coordinate, c.f., Fig. 11, one immediately realizes that the adsorptive bonding of a H atom on a metal usually causes redistribution(s) of metallic electron density and can even lead to the formation of discrete electronic states especially in the

conduction band region: These can be viewed as localized quantum levels formed by the overlap and, hence, chemical bond, of metallic and hydrogenic (1s) electron states.

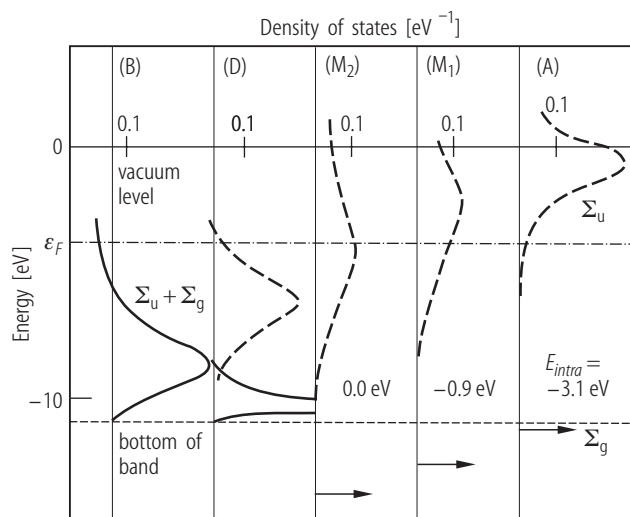


Fig. 11: One-electron density of states (1/eV) for a hydrogen molecule approaching a magnesium(0001) surface along the reaction coordinate. The capital letters in the top indicate extrema on the potential energy surface. From right to left, the practically unperturbed gaseous H₂ molecule (P) feels a slight activation barrier (A) for entering the physisorbed state (outer part of the well M₁, inner part of the well M₂). At the same time, the molecular orbitals (MO) of the H₂ molecule 1σ_g and 2σ_u^{*} begin to downshift and broaden. As the molecule further approaches the Mg surface, a large barrier for dissociation occurs (D), and only after passing this barrier two separated H atoms can exist on the surface in a bridge position (B). After Nørskov et al. [81Nor1].

The respective changes in the electron density of states in the valence band region of the solid surface can be probed particularly well with the experimental technique of photoelectron spectroscopy. This has been demonstrated many times especially for carbon monoxide chemisorption, but also for the adsorption of hydrogen on metal surfaces. Without entering any details of the experimental set-up and theory (which can be obtained from the literature [78Feu, 86Woo]) the standard experiment is performed having vacuum UV light (generated by means of a noble gas discharge lamp (He, Ne)) incident on the (H covered) sample and collecting the emitted photoelectrons in an energy-dispersive analyzer. One then obtains the so-called energy distribution curves (EDCs) of the photoelectrons which mirror the electron density of states of the probed surface region. Much more detailed information on the surface electronic band structure is, of course, available, if these measurements are performed in a momentum-resolved manner ('angle-resolved' UV photoelectron spectroscopy, ARUPS [75Plu, 92Kev]): Then the surface Brillouin zone (SBZ) can be mapped and band dispersion curves of the H-induced state (which mostly is derived from the hydrogenic 1s orbital) be followed in *k*-space. This yields most valuable information on the energy dispersion and symmetry of the electronic states involved in the H adsorptive binding, but sheds also light on the proximity of the adsorbed H atoms in a given structure: Phases with high density should result in a larger band dispersion than H phases with wide mutual H - H distances. Furthermore, due to the often significant energy dependence of the cross sections for the respective electronic excitations it is advantageous to perform the experiments at a synchrotron storage facility, where a high flux of photons with continuously variable energy is available.

While UPS measurements only probe the occupied states in the region at and below the Fermi level, Bremsstrahlung isochromat spectroscopy (BIS), better known as 'inverse photoemission' (IPE) provides access also to the density of unoccupied states in the energy region between the Fermi and the vacuum level [83Dos], but the literature data base concerning unoccupied H-induced electronic states is still small. Furthermore, it is remarkable that photoemission measurements (especially when performed at a synchrotron storage ring) are seldom combined with other surface spectroscopic techniques. This may sometimes introduce uncertainty as far as surface cleanliness, accuracy of H coverages and population of binding states is concerned.

In the following table, the H-induced electronic levels found in UPS measurements performed with metal and semiconductor surfaces are listed. Most of the data were obtained by angle-integrated measurements; in those cases, where angle-resolution is provided, we will add a respective comment.

3.4.1.3.7.1 Metal surfaces

Surface	H coverage, H phases	Tem- pera- ture [K]	Photon energy of incident light $h\nu$ [eV]	Position of H- induced photo- emission state(s) below the Fermi energy E_F [eV] at normal emission	Band dispersion; band width (1s-derived band(s))	Remarks, mode of measurement etc.	Ref.
Ti(0001)	(1×1)H (all coverages)		22	1.3 at Γ point 4.5...7 (6.9 eV at Γ point)	H-induced surface state (no dispersion) H 1s derived band	angle-integrated and angle-resolved UPS measurements using synchrotron radiation	80Fei2
Cr(110)		300		new energy loss at 16 eV below E_p (E_p = energy of primary electron beam)	H-induced emission peak	secondary electron emission study (SES), in combi- nation with electron loss spectroscopy	80Sak 81Kat
Cr(110)	$\Theta = 0.25$ (p(2×2) phase) $\Theta = 0.88$ and $\Theta = 1$ ((1×1)H str phase)	80	25	2.5 at Γ point only 5.5 7.8 at Γ point	H-induced surface state weak and broad dispersion of ~2.8 eV in [001] azimuth	ARUPS; at low Θ H-induced levels with very small dispersion only	88Kom
Fe(100)	$\Theta \approx 1$ (sat'n)	140	40.8	5.6	broad 1s- derived band	angle-integrated UPS	77Boz
Fe(110)	(2×1)-H = c(2×2) ($\Theta = 0.5$) (3×1)-2H = (3×3-6H ($\Theta = 0.67$))	80		7.9 at Γ point 8.2 at Γ point	H 1s-derived state, upward dispersion by ~1.5 eV in [1-10] and by ~1 eV in [001] azimuth H 1s-derived state, upward dispersion by ~0.9 eV in [1-10] and by ~1.6 eV in [001] azimuth	ARUPS measurements using synchrotron radiation	91Mar
Fe(111)	sat'n	140	40.8	5.6	broad 1s- derived band	angle-integrated UPS	77Boz
Co(0001)	0.6 ML	170.. .300	21.2 40.8	1.7 (sp-like surface state) 7.2 at Γ point	 H 1s split-off state	angle-integrated UPS H 1s state shows 'some' dispersion	86Gre

Surface	H coverage, H phases	Tem- pera- ture [K]	Photon energy of incident light $h\nu$ [eV]	Position of H- induced photo- emission state(s) below the Fermi energy E_F [eV] at normal emission	Band dispersion; band width (1s-derived band(s))	Remarks, mode of measurement etc.	Ref.
Co(10–10)	(2×1)-2H ($\Theta = 1$)	100	45	~ 6	downward dispersion by ~ 0.3 eV	ARUPS	90Ern
				~ 8	upward dispersion by ~ 1 eV		
	(1×2)-3H	100	19.7	~ 5.6	downward dispersion by ~ 0.5 eV		
				~ 9.0	upward dispersion by ~ 3 eV		
Ni(100)	$\Theta = 1.0$	160	fixed photon energy of 9.3 eV (CaF ₂ photon detector)	1.3 above E_F	formation of sp-derived surface resonance	IPE, angle- integrated UPS	87Rei2
Ni(110)	?	78	21.2	~ 5.8	width ~ 3 eV	angle-integrated UPS	77Dem
Ni(110)	(1×2)-3H ($\Theta = 1.50$)	80	30 eV	9.0 at Γ point		ARUPS at synchrotron	87Kom
Ni(110)	(1×2)-3H ($\Theta = 1.50$)	100	19	7.5...8 at Γ point	upward dispersion by ~ 4 eV in [1–10] dir.; upward dispersion by ~ 5 eV in [001] dir.	ARUPS	88Chr 90Ern
Ni(110)	(1×2)-3H ($\Theta = 1.50$)	80	30	9 at Γ point	upward dispersion by 3.1 eV in [1–10] dir., almost no dispersion in [001] dir.	ARUPS	87Kle1
Ni(110)	(1×2)-3H ($\Theta = 1.50$)	90	fixed pho- ton ener- gy of 9.4 eV (SrF ₂ photon detector)	set of new surface states (A, B ₁ , B ₂ , B ₃) ca. 1 eV, 0.2 eV, 2.1 eV, 4.5 eV above E_F	formation of sp-derived surface resonances	IPE; angle-resolved measurements provide the dispersion of unoccupied bands in the SBZ	90Ran
Ni(111)	(2×2)-2H ($\Theta = 0.50$)	200	21.2 26.9	5.9	width ~ 2.5 eV	angle-integrated UPS	76Con2
Ni(111)	medium Θ larger Θ	78.... 300	21.2	5.8	width ~ 3 eV	angle-integrated UPS	77Dem

Surface	H coverage, H phases	Tem- pera- ture [K]	Photon energy of incident light $h\nu$ [eV]	Position of H- induced photo- emission state(s) below the Fermi energy E_F [eV] at normal emission	Band dispersion; band width (1s-derived band(s))	Remarks, mode of measurement etc.	Ref.
Ni(111)	small coverages (~ 0.1 ML)	300	13...22	0.25	surface state of Ni; blue- shifted with H	ARUPS sp-orbitals dominate in the H-Ni(111) bonding	79Him
	sat'n		22	6.2	H surface resonance between 1...7 eV below E_F		
Ni(111)	0.5...0.6 ML	140	24 35	4.9 (vanishes at $\theta < 0.5$)	position of split-off state strongly θ dependent	ARUPS, momentum-resolved	86Gre 81Ebe
	1 ML (sat'n)	~ 100	40	9.0 at Γ point	H split-off state disperses between 5 and 9 eV; hints to admixture of Ni 3d states		
Ni(111)	medium	160	fixed photon energy 9.3 eV	no H-induced extra emission above E_F		IPE	88Rei
Cu(100)	from submono- layers to multilayers	4	30, 35, 40 eV at syn- chrotron	9.2 1 st layer 10.2 multi- layer H ₂ film		exposure to H ₂ ; physisorption of H ₂ molecules	82Ebe
Cu(110)	0.45 ML	100	IPE: fixed photon energy 9.4 eV (SrF ₂); UPS: $h\nu =$ 16.85 eV	-1.9...1.3 0.5	unoccupied surface state shifts with θ to 1.3 eV above E_F occupied surface state	exposure to H atoms IPE + UPS (angle- resolved) H-induced (1 \times 2) reconstruction produces shifts of Cu surface states	93San1
Cu(111)	medium	<200		6.2	H 1s-derived bonding state	ARUPS	83Gre
Nb(100)		150.. 754	21	5.1...4.6 (states B+C) ~ 7 (state A, weak)	normal emission	ARUPS at synchrotron. From T dependence of H states H subsur- face/bulk absorption processes inferred	88Fan
Nb(110)	0.1...sat'n	300	21.2 16.8	5.4 (large)	H derived state, disappears for $T > 700$ K	angle-integrated UPS	80Smi2

Surface	H coverage, H phases	Temperature [K]	Photon energy of incident light $h\nu$ [eV]	Position of H-induced photo-emission state(s) below the Fermi energy E_F [eV] at normal emission	Band dispersion; band width (1s-derived band(s))	Remarks, mode of measurement etc.	Ref.
Ru(0001)	medium θ	200	11...50	3.7 8.1 at Γ point	extrinsic surface state weak and broad, H 1s-derived split-off state from Ru d-band, dispersing from 5.9 (K point) to 8.1 eV (Γ point)	ARUPS, spectra contain final state bands	85Hof
		300		'invisible'			
Pd(111)	medium θ	200	26.9 40.8	6.5	decrease in the d band emission intensity	angle-integrated UPS	76Chr
Pd(111)	medium θ	80	21.2	6.4	width 1.5 eV; dramatic loss of Pd d-band intensity	angle-integrated UPS	77Dem
Pd(111)	1 ML (1 \times 1)-H phase	\sim 100	30, 40, 50	1.2 3.1 7.9 at Γ point 6.4 at M point 5.9 at K point	normal emission H 1s split-off state disperses between 5.9 and 7.9 eV.	ARUPS at synchrotron	83Ebe 81Ebe 86Gre
		300		no visible state			
Ag(111)	saturation	100	40.8	7.3	H 1s split-off state	angle-integrated UPS exposure to D atoms	89Zho
Ag(111)	0.5 ML (2 \times 2) LEED phase	100		2.5 8.5 broad	only observable in off-normal directions	angle-resolved UPS at 100 K after exposure to H atoms at synchrotron	00Lee
Ce(0001)	100 - 500 L	300	21.2	4.2	Ce - H solid solution phase	angle-resolved UPS	Ros86
	>500 L	300		3.4	Ce-dihydride formation		
Gd(0001) [epitactic films grown on W(110)]	0...20 L	120; 300		3.8	formation of one H monolayer after 3 L	ARUPS using synchrotron rad.	93Li
Gd(0001) [epitactic films grown on W(110)]	0.4 L	300	16.85	4.0	normal emission	ARUPS study using NeI rad.	98Get

Surface	H coverage, H phases	Temperature [K]	Photon energy of incident light $h\nu$ [eV]	Position of H-induced photo-emission state(s) below the Fermi energy E_F [eV] at normal emission	Band dispersion; band width (1s-derived band(s))	Remarks, mode of measurement etc.	Ref.
Ta(110)	exposures up to 7 L (medium Θ)	300 ?	14...30	2.2 6.5	at normal emission bonding state between H 1s orbital and metal d orbitals	angle-integrated UPS at synchrotron	83Mur
W(100)	$0 < \Theta < \text{sat}$		21.2 16.8	1.2...1.5 3.6 5.7	considerable coverage dependence of peak positions	angle-integrated UPS	75Plu
W(100)	sat'n ($\Theta = 2$)	300 ?	13...20	4.3 6.5 (+ H-induced doublet between 0 and 2 eV below E_F)	H band with odd parity H band with even parity	polarization-dependent ARUPS	78And1
W(110)	low $\Theta(\beta_2)$ high $\Theta(\beta_1)$	300	10.2	2.8 4.0	normal emission	angle-integrated UPS	73Feu
W(110)	low $\Theta(\beta_2)$ high $\Theta(\beta_1)$	300	21.2 16.8	2.0 4.0, further H-induced resonances at 0.5; 1; 3; 6; 7 eV below E_F	normal emission; H-induced bands show only little dispersion	ARUPS band dispersion curves measured along two azimuths	81Hol
W(110)	low Θ $\Theta > 0.5 \text{ ML}$ 1 ML (sat'n)	42		clean W states (1, 1.5, 3.5 eV below E_F) affected 3.5 6...9	normal emission only excited for E -vector parallel to [1-10] direct. H split-off state	polarization-dependent ARUPS at synchrotron. Band dispersion (between 6 and 9 eV) determined. Reduction in surface symmetry for $\Theta > 0.5$.	82Bla
W(110)	sat'n	300	21.2	2.0 3.8 6.0	peak positions independent of H coverage	angle-integrated UPS	82Wen
W(110)	low (unreconstructed surface) high (reconstructed surface)	80	42 60	~2.5 3.8...4 4.8 9.0 (at Γ point) ~2.5 ~4.0 9.3...7.0	9 eV state disperses to 6.8 eV at N point	ARUPS at synchrotron	93Aiu
W(111)	high Θ	300	10.2	1.7 2.8 strong	normal emission	angle-integrated UPS	73Feu

Surface	H coverage, H phases	Tem- pera- ture [K]	Photon energy of incident light $h\nu$ [eV]	Position of H- induced photo- emission state(s) below the Fermi energy E_F [eV] at normal emission	Band dispersion; band width (1s-derived band(s))	Remarks, mode of measurement etc.	Ref.
W(111)	0.39		18...20	~6 (broad) at Γ point	H split-off state, dis- persion from 4.5 to 6 eV	ARUPS at synchro- tron, polarization dependent, momen- tum resolved	82Cer
Pt(111)	medium Θ	80	21.2	7.3	width 1.5 eV	angle-integrated UPS	77Dem
Pt(111)	medium Θ	<200	21.2	no distinguishable H-induced state	strong suppr- ession of d band emission	angle-integrated UPS	77Col2
Pt(111)	medium Θ	140	40	9.4 at Γ point	H 1s split-off state	angle-integrated UPS	81Ebe

3.4.1.3.7.2 Semiconductor and insulator surfaces

Surface	H coverage, H phases	Tem- pera- ture [K]	Photon energy of incident light $h\nu$ [eV]	Position of H- induced photo- emission state(s) below the Fermi level [eV] at normal emission	Band dispersion; band width (1s-derived band(s))	Remarks, mode of measurement etc.	Ref.
C(111)	(1×1) terminated	300	21.22	no distinct 'extra' signals; as unrecon- structed surface			85Pat
C(100) - 2×1 reconstructed (diamond)	likely mono- hydride terminated + CH ₂ and		21.22 40.8	no distinct 'extra' signals; the H-termin- ated surfaces show negative electron affinity (NEA)→ vacu- um level lies be- low the conduc- tion band mini- mum		XPS, UPS	96Die
C(100)-1×1	CH ₃ groups					exposure to H atoms necessary to form (1×1) phase	
C(100)-2×1 (diamond)	mono- hydride terminated surface	300	21.22	the H-termin- ated surfaces show NEA	broad featu- res between 5 and 15 eV below E_F	UPS + ab-initio theory	94Wei
Si(100)-2×1 Si(111)-2×1		300	21.22	11.1 below E_{vac}		ads. H removes the 'dangling-bond' surface state	74Iba
Si(100)-2×1 Si(100)-1×1	mono- hydride + dihydride phase	300	21.22	10 below E_{vac} 12 below E_{vac} near 10 12 below E_{vac}		low H exposures: (2×1) persists; at larger H exposur- es: (1×1) phase forms	76Sak

Surface	H coverage, H phases	Temperature [K]	Photon energy of incident light $h\nu$ [eV]	Position of H-induced photo-emission state(s) below the Fermi level [eV] at normal emission	Band dispersion; band width (1s-derived band(s))	Remarks, mode of measurement etc.	Ref.
Si(100)-2×1	mono-hydride + dihydride phase	300..600	21.22 40.8	10.0 below E_{vac} 14.7 below E_{vac} 8.0 below E_{vac} 9.2 below E_{vac} 10.0 below E_{vac} 11.5 below E_{vac} 13.9 below E_{vac}	exposure at 300 K monohydride features, after exposure at 523 K	exposure to H atoms; UPS + tight-binding and extended Hückel calculations	84Cir
Si(111)-1×1	H saturated	300	21.22	10 below E_{vac} 12 below E_{vac} (after gentle exposure) 11 below E_{vac} 15 below E_{vac} (excessive H exposure)		exposure to H atoms new trihydride state (questioned, however, by [82But] who ascribed the states to oxygen contaminations)	75Pan
Si(100)-2×1 Si(111)-7×7	mono - to dihydride coverage	300	40.8	10 below E_{vac} 12 below E_{vac} 10 below E_{vac}	monohydride enhanced s-like bulk state enhanced → dihydride	exposure to H atoms; little dependence on crystallographic orientation	84But
Si(111)	mono-hydride (low θ); mono + dihydride (larger θ)	300		5.3 7.3 6.2	monohydride monohydride dihydride	exposure to H atoms; all surface states disappear with H coverage	90Kou
Si(111)-7×7	low exposure (mono-hydride ?)			5.6 7.6		combined exptl. and theor. study	95Sta
Si(111)-1×1	H-terminated	300	32	4.3 (sharp) 9 (broad)	surface resonance contrib, from bulk sp band	ARUPS at synchrotron	00Gal
Ge(100)-2×1	exposed to H ₂ plasma	430..460	21.22	5.6	(2×1) H phase, no dispersion	atomic H through RF plasma; ARUPS	92Cho
Ge(100)-2×1	fully H covered	300	14, 17	4.4...5.5 4.5...5.5	dispersion of ~1 eV. H-induced surface states	ARUPS at synchrotron	94Lan
Ge(111)-2×1	fully H covered	300	21.22	4.9 12.8		UPS	75Row
Ge(111)-2×1 Ge(111)-c(2×8)	(1×1)	300	21.22 16.85	4	4...5 (width = 1eV)	ARUPS; H deconstructs surface to (1×1); two surface states disappear with H	82Bri
Ge(111)-c2×8	(1×1)-H	300	29...60	no specific H-induced feature		ARUPS at synchrotron	85Wac

Surface	H coverage, H phases	Tem- pera- ture [K]	Photon energy of incident light $h\nu$ [eV]	Position of H- induced photo- emission state(s) below the Fermi level [eV] at normal emission	Band dispersion; band width (1s-derived band(s))	Remarks, mode of measurement etc.	Ref.
Ge(113)	(1×1)	300	11.8 (Ar) 21.22 (HeI) 16.67 (NeI)	5.5		exposure to H atoms; ARUPS	95Sch2
GaAs(110)	H- terminated (1 ML)	300	21.22	0.12 below valence band edge		photon emission yield spectroscopy	87Mha
GaAs(110)	H- terminated (1 ML)	300	21.22 40.8	3.7...4 below upper valence band edge		exposure to H atoms, ARUPS	94Ple
				6.8	H atoms on top of As sites		

3.4.1.3.8 Hydrogen-induced work function changes

Another property which reflects the electronic interaction between the hydrogen adsorbate (atoms or molecules) and the solid surface is the change of the work function as the adsorption proceeds. Since it cannot be the intention of this data compilation to provide a fundamental theory of the work function – the reader is referred to textbooks or review articles [49Her; 58Sim; 69Riv; 79Hoe] – we only make some short introductory remarks and will add comments on special features characteristic of hydrogen adsorption, such as H-induced structural phase transformations and their influence on the work function. Furthermore, we refer to the contribution of K. Jacobi about work function changes in in section 4.2 in part 2 of this Landolt-Börnstein volume III/42A [02Jac].

In a very general and simple view, any chemical surface complex formed between an adsorbed H atom and the underlying atom(s) of the substrate can be thought of as a tiny dipole carrying a dipole moment μ with either the negative or the positive end pointing away from the surface. The amount of charge located on each dipole thereby depends on the polarization of the chemical bond(s) within the respective adsorption complex and, hence, reflects the differences in electron affinity of the adsorbate (H or H₂ in our case) and the substrate atom(s) involved in the bonding. The overall work function change $\Delta\phi$ produced by a surface layer of adsorbed dipoles (density σ [particles/m²]) each having a dipole moment μ_0 [A s m] can simply be modelled by a plate capacitor carrying the charge q^+ and q^- separated by the plate distance d . This leads to the well-known Helmholtz equation

$$\Delta\Phi = 4\pi \Theta N_{\max} \mu_0 f^*; \quad f^* = \frac{1}{4\pi\epsilon_0}. \quad (12)$$

μ_0 is thereby the dipole moment of an individually adsorbed particle at vanishing coverage, ϵ_0 the dielectric constant (8.85×10^{-12} As V⁻¹m⁻¹), f^* a conversion factor from cgs to SI system, N_{\max} the maximum number of adsorption sites per unit area, and Θ the coverage. It is assumed that the (imaginary) plane of electroneutrality is within the adsorbate layer; if it is defined with respect to the image charge plane within the substrate surface, an emerging electron must do work only against half of the adlayer potential, and the factor 4 reduces to a factor of 2. In principle, this equation allows the determination of the dipole moment of an individual adsorption complex, if the absolute coverage is known. From μ_0 , in turn, the dipole length l or the charge separation between the two ends of the dipole could be derived. Note that the Helmholtz equation in this simple form does not consider depolarization effects which

usually come into play as the coverage increases and the adsorbate dipoles interact with each other. Then, a more refined relation has to be used, for example, the Topping equation [27Top] which contains a coverage dependence of μ and the polarizability of the adsorbed molecule [86Woo, 91Chr]. Experimentally, depolarization effects show up in the coverage dependence of the work function change, $\Delta\Phi(\Theta)$, which is linear only at small coverages. If defect (for example, step) sites with a different dipole moment are involved and preferentially occupied, the $\Delta\Phi(\Theta)$ relation may even run through a minimum or maximum as it was found for a stepped Pt(111) surface, c.f., Fig. 12 [76Chr]. The same is true, if in the course of the adsorption sites of different local charge transfer become populated, or the surface undergoes reconstruction at a critical hydrogen coverage.

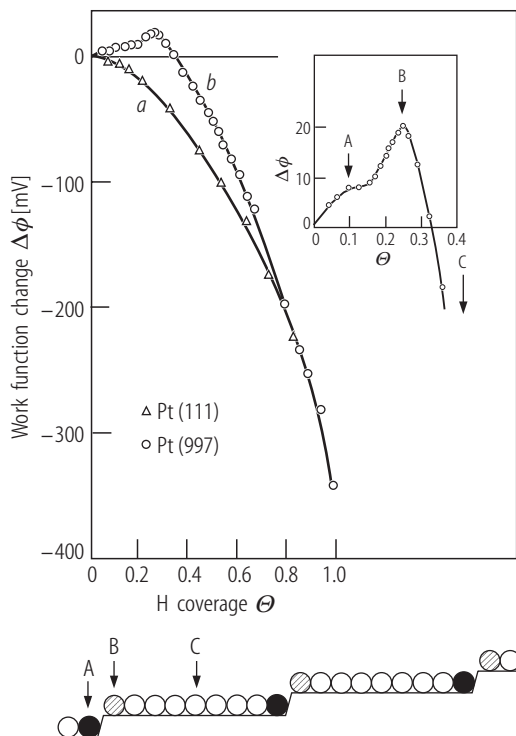


Fig. 12: The H-induced work function change, $\Delta\Phi$, as a monitor of adsorption into geometrically different surface sites. Shown is the coverage dependence of H adsorption on a flat (curve a) and on a stepped (curve b) Pt(111) surface (sketch of the structure in the bottom with different types of sites indicated as A, B, and C). While $\Delta\Phi$ decreases monotonically on the flat Pt(111) surface (occupation of terrace sites), an initial $\Delta\Phi$ increase observed with the stepped surface is attributed to preferential adsorption into step sites. After Christmann and Ertl [76Chr].

For atomic H chemisorption on most of the TM surfaces the negative end of the dipole is pointing away from the surface causing generally a work function increase. Only few metal surfaces (Fe(110), W(110) and Pt(111)) show the inverse behavior. According to the following table, the H-induced $\Delta\Phi$ increase ranges from some 10 meV (for Ru(0001)) to almost 1 eV for H on various 'open' TM surfaces (Rh(110)). The amount of charge transferred from the metal to the H atom is usually less than 1/10 of the elementary charge, e_0 . In cases where the adsorption of hydrogen is accompanied by a surface reconstruction, some care has to be taken in interpreting H-induced work function changes, since the displacement or shifts of substrate atoms can (and usually will) alter the electric surface situation and contribute to $\Delta\phi$ as well.

Turning to the few cases where the work function change due to *molecular* hydrogen adsorption was determined one can safely state that adsorbed H_2 molecules are positively polarized, i.e., a net charge seems to flow from the adsorbed molecule to the surface, giving rise to a decrease of $\Delta\Phi$. Examples are the (210) faces of Ni and Pd, where the work function decreases between 300 and 500 meV upon H_2 adsorption [01Sch1; 01Sch2].

As far as the experimental tools to measure H-induced work function changes are concerned, we simply note that most of the standard methods can be employed, photoemission spectroscopy, Kelvin probe or diode methods being the most frequently used ones. For more details, we refer to the respective literature [49Her, 59Cul, 86Woo, 91Chr].

Finally, it should be emphasized that the work function change caused by hydrogen is probably one of the most sensitive monitors of surface cleanliness. In his scientific life, the author of this contribution has measured a whole variety of H-on-metal systems and has always recognized that even traces of impurities (carbon, sulfur, phosphorus etc.) can cause a dramatic loss in the H-induced $\Delta\Phi$; as a rule of thumb, one could even state that a surface which gives the larger work function change upon adsorbing a given amount of H is the cleaner surface.

Work function changes caused by adsorption of hydrogen

Surface	H coverage, H phases	Temperature [K]	Work function change at saturation [meV] (values in parentheses calculated)	Method (CPD = contact potential difference)	Initial dipole moment [D]	Remarks	Ref.
Be(0001)	0...1 ML	90	-440	HREELS analyser in RF mode		$\Delta\Phi$ exhibits a minimum at -560 meV at $\Theta = 0.4$ ML	90Ray
Mg(0001)	sat'd hydride phase	110	-950 \pm 70	HREELS analyser in RF mode		exposure to H atoms; surface hydride is formed	91Spr
Ti(0001)	(1 \times 1)		(200)	photoemission			80Fei2
Fe(100)		140	+75	CPD (Kelvin probe)			77Boz
Fe(110)	(1 \times 1)	140	-85 \pm 5	CPD (Kelvin probe)	-0.032	$\Delta\Phi$ exhibits a small minimum (-55 meV) at completion of β_2 TD state	77Boz
Fe(111)		140	+310 (annealing required)	CPD (Kelvin probe)			77Boz
Co polycryst. films	$5.5 \times 10^{19} \text{ m}^{-2}$ $8.0 \times 10^{19} \text{ m}^{-2}$	78	+225 (negatively polar. species) -200 (ca.) (positively polarized species)	CPD (static capacitor)			76Dus
Co(10-10)	c(2 \times 4) ($\Theta = 0.5$) (2 \times 1)-2H ($\Theta = 1.0$) (1 \times 2)-3H ($\Theta = 1.5$)	85	 $\approx +200$ -122 total +85 at sat'n	CPD (Kelvin probe)	0.0137	$\Delta\Phi(\Theta)$ exhibits a maximum (207 meV) at 1.1 ML, then drops to 85 meV at saturation	94Ern
Ni(100)	$0 < \Theta < 0.5$	273	+170	CPD (Kelvin probe)		$\Delta\Phi$ linear with Θ up to $\Theta = 0.5$	74Chr
Ni(100)	$0 < \Theta < 0.8$	150	+96	CPD (Kelvin probe)	0.049	linear increase of $\Delta\Phi$ with Θ , maximum at $\Theta = 0.5$, followed by decrease to 40 meV at $\Theta = 0.8$	79Chr1
Ni(110) (1 \times 2)MR phase	$\Theta < 1.5$	<170	+580			$\Delta\Phi(\Theta)$ linear with break at $\Theta = 0.5$ (2 \times 1)-phase	74Tay
Ni(110)	$\Theta < 1.5$	273	+530	CPD (Kelvin probe)			74Chr

Surface	H coverage, H phases	Temperature [K]	Work function change at saturation [meV] (values in parentheses calculated)	Method (CPD = contact potential difference)	Initial dipole moment [D]	Remarks	Ref.
Ni(110), (1×2) PR reconstr. Phase	$0 < \Theta < 1.5$	120	+510 ($\Theta = 1$: $\Delta\Phi = 250$ meV)	CPD (Kelvin probe)	0.06 ($0 < \Theta < 1$) 0.12 ($1 < \Theta < 1.5$)	$\Delta\Phi(\Theta)$ linear with positive break at $\Theta = 1$ due to reconstruction	89Chr
Ni(111)	$0 < \Theta < 0.5$	273	+195	CPD (Kelvin probe)		$\Delta\Phi$ linear with Θ	74Chr
Ni(111)	$0 < \Theta < 0.9$ up to $\Theta = 0.5$ adsorption into c(2×2) honey-comb structure	110	+165	CPD (Kelvin probe)	0.029	linear increase of $\Delta\Phi$ with Θ , maximum at $\Theta = 0.5$, followed by decrease to 80 meV at $\Theta = 0.9$	79Chr2
Cu(100)		10	−200 (H ₂)	electron beam retardation mode		linear decrease of $\Delta\Phi$ with Θ_H	83And
Cu(100)		10	−120 (H ₂) −145 (D ₂)	electron beam retardation mode		surface exposed to molecular hydrogen; study of physisorbed H ₂ molecules (1 ML = 0.65×10^{19} molec./m ²)	88Wil
Cu(100)	$0 < \Theta < 1$ p4g-reconstr. phase	170	−250	CPD (Kelvin probe)		exposure to H atoms	91Cho
Cu(110)	(1×3) (1×2)	90	<150	CPD (Kelvin probe)		exposure to H atoms	87Bad
Cu(110)	(1×2)	100	−150 at 100 K ($\Theta_H < 0.4$); +250 at 200 K	photoemission		exposure to H atoms; $\Delta\Phi$ exhibits strong T dependence $\Delta\Phi > 0$ includes MR reconstruction.	93San1
Cu(110)	(1×3) (1×2)	115	+120	CPD (Kelvin probe)		exposure to H atoms $\Delta\Phi(\Theta)$ exhibits an initial increase of 25 meV, followed by a shallow minimum and final increase to 120 meV	94Roh
Nb(100)	sat'n = 2×10^{19} /m ²	90	+540		−0.0022 (state 1) −0.141 (state 2)	state 1 = molecular precursor) state 2 = atomic H, coverage associated with state 2 = 9×10^{18} /m ²	74Hag
Nb(110)	sat'n Θ	300	<100	UPS (width of spectrum)			80Smi2
Mo(100)	(4×2) c(2×2) sat'n (1.0)	240 <160 160-240	+500 step +600 plateau > +1200			$\Delta\Phi(\Theta)$ exhibits a plateau due to (4×4) or c(2×2) phase, but continuous increase otherwise	79Est

Surface	H coverage, H phases	Temperature [K]	Work function change at saturation [meV] (values in parentheses calculated)	Method (CPD = contact potential difference)	Initial dipole moment [D]	Remarks	Ref.
Mo(110)	$\theta < 0.1$ $\theta = 0.5$ $\theta > 0.6$	350	-20 +100 +110 (sat'n)	CPD (retarding field diode method)		$\Delta\Phi(\theta)$ exhibits a small initial minimum (20 meV), then a rise up to 0.5 ML.	89Ern
Mo(211)	$0 < \theta < 2$	100	+960 at $\theta = 1$ decrease by 280 to 680 at $\theta = 1.75$, rise to ~1000 near sat'n	CPD (diode method using LEED electron gun)	0.17 ± 0.01	$\Delta\Phi(\theta)$ linear with H coverage up to $\theta = 1$	94Lop
Ru(0001)	small θ medium and high θ (~1 ML)	100.. 150	+25 (negative "N" species) - 10...- 30 (positive "P" species)	CPD (Kelvin probe)	0.006..... 0.01	$\Delta\Phi(\theta)$ first increases, forms a maximum of ~30 meV, then decreases to negative values between - 10 and - 30 meV, depending on T	85Feu
Ru(10-10)	$0 < \theta < 1$ $1 < \theta < 1.2$ $\theta = 1.5$ $\theta = 2$ (sat'n)		+ 420 + 360 + 390 + 250	CPD (Kelvin probe)	0.12 -0.08	$\Delta\Phi(\theta)$ linear up to $\theta = 1$, subsequent decrease by ~50 meV, minimum at $\theta = 1.25$, increase by 20 meV to second maximum at $\theta = 1.5$	89Lau
Rh(111)	$\theta = 1 = 1.58 \times 10^{19}$	130	+50	UV photoemission			95Wit
Rh(110)	$\theta = 2$	100	+930	CPD (Kelvin probe)	0.027 (p(1×2)) 0.12 (1×3)-3H 0.13 (1×1)-2H	linear increase of $\Delta\Phi(\theta)$ through form'n of 1×3, 1×2, 1×3-2H phases; stronger increase with 1×2-3H	88Ehs
Pd(100)	$\theta_{c(2 \times 2)} = 0.5$; $\theta_{max} = 1.4$	170	+200	CPD (Kelvin probe)	0.021	linear increase of $\Delta\Phi(\theta)$ with positive break at $\theta = 1.0$	80Beh
Pd(110)		300	+360	CPD (Kelvin probe)		$\Delta\Phi(\theta)$ includes contributions due to (1×2) reconstruction	74Con
Pd(110)	$\theta_{max} = 1.5$ + subsurface states	130	+325	CPD (Kelvin probe)	0.0714	$\Delta\Phi(\theta)$ includes contributions due to (1×2) reconstruction	83Cat1, 83Cat2
Pd(110)	$\theta_{max} = 1.5$ + subsurface states	138	+300	CPD (Kelvin probe)		$\Delta\Phi(\theta)$ includes contributions due to (1×2) reconstruction	88He1
Pd(111)		300	+180	CPD (Kelvin probe); UPS cut-off			74Con 83Ebe
Pd(210)	$\theta_{max} > 3$ ML	120	+160	CPD (Kelvin probe)		$\Delta\Phi(\theta)$ strongly T dependent: $T_{ad} < 120$ K causes lower $\Delta\Phi_{max}$, competition of a molecularly adsorbed H_2 species with reverse dipole moment	98Mus

Surface	H coverage, H phases	Temperature [K]	Work function change at saturation [meV] (values in parentheses calculated)	Method (CPD = contact potential difference)	Initial dipole moment [D]	Remarks	Ref.
Pd(311)			+280 ± 10		0.093		99Far
Ag(110)	(1×4) (1×3) (2×6) (2×2)	100	+220 at sat'n (1 ML)	EELS analyzer in RF mode		exposure to H atoms	93Spr
Ag(111)		100	−170	UV photo-emission		exposure to H atoms	89Zho
Ag(111)	(2×2) (3×3) ($\Theta = 0.5-0.6$)	100	+320	electron beam retardation (HREELS)	0.18	exposure to H atoms, at high Θ , $\Delta\Phi \sim \Theta^n$ ($n < 1$)	95Lee
Gd(0001)	$\Theta = 1$	300	−200	UV photo-emission	−0.062	$\Delta\Phi(\Theta)$ linear with H coverage	93Li
W(100)	sat'n	300	+880			$\Delta\Phi(\Theta)$ linear with H coverage	66Arm
W(100)	sat'n = $10^{19}/\text{m}^2$		+900	CPD (retarding field diode method)			66Est
W(100)	$\Theta = 2$	330	+900	CPD (retarding field method)	0.21		73Mad
W(100)	$\Theta = 1$	130	+940	CPD (Kelvin probe)			74Bar
W(100)	sat'n	300	+900			inflection at 160, knee at 270 meV no inflection	78Bar1
W(100)	$0 < \Theta < \text{sat'n}$	300	+960	(CPD) electron reflection		initial linear increase, shoulder at 270 meV, discontinuity at 350 meV, linear increase up to sat'n	86Her
W(110)	$\Theta = 1$	300	−500				72Plu
W(110)	$\Theta = 1$	130	−500	CPD (Kelvin probe)			74Bar
W(110)	$\Theta = 1$	90	−500	CPD (Kelvin probe)		careful study; exposure dependence exhibits a small irregularity after 2 L; TDS- and LEED derived coverages differ slightly	97Nah1 97Nah2
W(110)	$\Theta = 1$ (sat'n)	300	−450	UPS			82Wen
W(110)	$0 < \Theta < \text{sat'n}$	300	−480	(CPD) electron reflection			86Her
W(111)	$\Theta = 0.2$ $\Theta = 0.6 \dots 0.8$ $\Theta = 1$ (sat'n)	130	−20 (β_4 state) +150 ($+\beta_{3+2}$ state) +280 ($+\beta_1$ state)	CPD (Kelvin probe)			74Bar
W(211)	$\Theta = 1$	110	300 at sat'n	CPD (Kelvin probe)		$\Delta\Phi(\Theta)$ exhibits a maximum (600 meV) at 0.5 ML	73Rye
W(211)	$\Theta = 1$	130	300 at sat'n	CPD (Kelvin probe)		$\Delta\Phi(\Theta)$ exhibits a maximum (600 meV) at 0.5 ML	74Bar

Surface	H coverage, H phases	Temperature [K]	Work function change at saturation [meV] (values in parentheses calculated)	Method (CPD = contact potential difference)	Initial dipole moment [D]	Remarks	Ref.
Re(10–10)	$\Theta = 0.9$ $\Theta > 0.9$	120	+370 –220, final value at sat'n = +150 meV	CPD (Kelvin probe)	0.1 ± 0.04	$\Delta\Phi(\Theta)$ exhibits a maximum (370 meV) at 0.9 ML	95Mus
Pt(100)-(5×20)	$0 < \Theta < 1$	100	+70 (state b) –370 (states $a_1 + a_2$)	CPD (Kelvin probe)		$\Delta\Phi(\Theta)$ runs through a maximum. Complex T dependence due to activated reconstruction/deconstruction phenomena	91Pen1
Pt(110)-(1×2)	$\Theta = 0.9$	120	+300 at $\Theta = 0.3$ –500 at sat'n ($\Theta = 0.9$)	CPD (retarding field using electron gun)	+0.12 –0.17	$\Delta\Phi(\Theta)$ exhibits a maximum (300 meV) at $\Theta = 0.3$	87Eng
Pt(110)-(1×2)	$0 < \Theta < 1$	170	+150 at $\Theta = 0.1$; –600 at sat'n ($\Theta = 1$)	MEM-LEED		$\Delta\Phi(\Theta)$ exhibits a maximum (150 meV) at $\Theta = 0.1$	92She
Pt(111)	$\Theta < 1.0$	150	–230	CPD (Kelvin probe)	–0.036	$\Delta\Phi \sim \Theta^n$ ($n = 1.33$)	75Chr
Ir(110)(1×2)	$\Theta = 0.3$ $\Theta > 0.85$	140	+300 in β_2 sites –300 in β_1 sites	CPD (retarding field using electron gun)	+0.14	$\Delta\Phi$ increases monotonously up to $\Theta = 0.3$, then decreases again to $\Delta\Phi_{final} = 0$	80Ibb
Au(100)	$\Theta = 0.3$	100	–200	CPD (retarding field method)		exposure to H atoms	96Iwa

3.4.1.4 The interaction of hydrogen with solid surfaces: theory

3.4.1.4.1 General remarks

In the following section, a brief survey shall be given over theoretical descriptions of hydrogen interaction with solid surfaces. It is thereby not attempted to draw detailed comparisons between the experimentally determined and the theoretically derived quantities and judge on the quality or benefits of a given theoretical modelling; rather a list of H - surface interaction systems will be compiled for which theoretical calculations exist. In a coarse distinction, these theoretical treatments may be regarded to focus 1) on the H₂ - surface interaction *dynamics* (prediction of dissociation pathways and rates, kinetic coefficients (sticking probabilities, frequency factors), activation energies etc.) and potential energy surfaces (PES), and 2) on the (*equilibrium*) binding energies, adsorption site geometries, long-range order phases (lateral interaction energies) as well as H-induced electronic states, vibrational frequencies and work function changes. For each of these two theoretical goals we will present a listing of available theoretical reports, and as in the tables before, the H interaction systems will be compiled according to the position of the element in the periodic table. In a separate column comments, for example concerning the *kind* of the theoretical treatment applied, will be added. For this purpose it is necessary to supply the reader with a short list of the currently used abbreviations, together with references from which basic information concerning the details and procedures of the respective treatments can be obtained.

Beginning with the early work by Koutecký [65Kou], Grimley [71Gri] and Schrieffer and Gomer [71Sch], the theoretical description of the H chemisorption has seen huge progress in the past twenty

years in that the initially relatively crude models and approximations were step by step improved to a much more sophisticated level. This was also very much supported by the unbelievable development of the computing facilities and available program codes. A real breakthrough was attained by applying the density functional theory, and many of the modern theoretical treatments are actually based on DFT methods. We emphasize again that it cannot be the intention of this chapter to recall all the theoretical concepts, instead, the reader is referred to the extended special literature in that field [60Gri, 78Mus, 79Gri, 79Mes, 80Smi1, 83Sch1, 83Gri, 85Mus, 03Gro]. The available reports can be further subdivided into two basic groups: There are many articles which focus on one or two distinct H adsorption systems only and calculate their respective specific properties. In the other category a certain theoretical model is applied to H chemisorption on whole classes of surfaces; in these articles, usually many adsorption systems are covered to demonstrate the merits of the respective theoretical approach. A brief separate table is devoted to these latter reports, again subdivided into general reports dealing with H₂ adsorption *dynamics* and those rather focussing on *equilibrium* properties.

Listing of abbreviations used in theoretical treatments of H - surface interaction

Abbreviation	Full name	Reference
ASED-MO	(semi-empirical) atom superposition and electron delocalization molecular orbital theory	97Iri
BEBO	Bond Energy Bond Order	91Ben
TBA	Tight-binding approach	71Gri; 94Har
FPLAPW	Full-potential linear augmented plane wave	95Bla; 96Koh
DFT	Density functional theory	64Hoh; 65Koh; 75Yin; 90Dre; 89Par
GGA	Generalized gradient approximation (often in conjunction with PW91 density functional)	92Per; 93Ham; 95Ham1; 96Per
GGC	Generalized gradient correction	
LDA	Local-density functional approximation	64Hoh, 65Koh
LSD	Local spin density	
DOS	Density of states	
RHF	Restricted Hartree-Fock	
EHT	Extended Hückel theory	
EMT	Effective medium theory	80Nor2; 82Nor2
TST	Transition state theory	66Joh
CT	Classical trajectories	
CHAIN	CHAIN method	92Lio
HF	Hartree-Fock	
LEPS	Valence-bond method based on work by London, Eyring, Polanyi, and Sato	29Lon; 31Eyr; 55Sat
FP-LMTO	Full-potential linear muffin-tin orbital	
CI	Configurational interaction	
CEM	Corrected effective medium theory	87Kre
MC	Monte Carlo calculations	
PW91	Density functional developed by Perdew and Wang	91Per
CVT	Canonical variational theory	86Lau; 88Tru
MINDO	Modified intermediate neglect of differential overlap	85Cla
PP	Pseudopotential method	82Coh
LCGTO	Linear combination of Gaussian type orbitals	79Dun
Car-Parinello	combination of molecular dynamics and density functional theory	85Car
VASP	Vienna ab-initio simulation package	93Kre1; 93Kre2; 94Kre1; 98Eic

3.4.1.4.2 General theories for hydrogen adsorption**3.4.1.4.2.1 Theories covering the adsorption dynamics (more general reports)**

Applied theory	Remarks	Reference
DFT	Electron-hole pair excitation and dissociative sticking	97Men
	Electron-hole pair excitation and dissociative sticking	82Sch
CI-SCF	Potential energy surfaces of MH ₂ clusters (M = Co, Fe, Cu)	84Sie
Band model	Quantum diffusion of H on metal surfaces	86Wha
EMT	Adiabatic PES for H ₂ interaction with Ni and Cu surfaces	89Nor
Model PES	Dissociation of a H ₂ and vibrational - translational energy transfer	89Har
Model PES	2D-PES (combination of Morse fct. + Gaussian barrier) influence of PES topology on H ₂ dissociation on metals	90Hal 90Nie
EMT	6D-PES for H ₂ molecules interacting with (111) and (110) surfaces of Cu and Ni	92Eng
SCF / jellium	H ₂ molecules in interaction with Al, Mg, Na. Calculation of PES	81Joh2
Overlap expansion of unperturbed wave functions	H ₂ physisorption on noble metal surfaces	85Nor

3.4.1.4.2.2 Theories covering equilibrium properties (more general reports)

Applied theory	Remarks	Reference
EMT	H interaction with various 3d, 4d, and 5d metals; trends in H chemisorption energies	84Nor
Spin-density functional formalism	H chemisorption on simple (sp electron) metals	78Hje
Cluster + muffin-tin	Ordering of H layers on various metal surfaces	86Mus
Anisotropic EMT	H ₂ interaction with Cu, Ag, Au and Al surfaces	90Kar
SC-LAPW	H bond distances and vibrational frequencies on close-packed metal surfaces	87Fei3
Various (review)	Chemisorption on metals (preference on hydrogen)	78Mus
Various (review)	Chemisorption on metal surfaces	90Nor
TBA and others	Indirect interactions between two H atoms	67Gri1; 67Gri2 58Kou; 73Ein
Various (review)	Order-disorder phase transitions in adsorbed H layers	78Dom
self-consistent DFT	H ₂ dissociation on Au, Cu, Ni, Pt	95Ham2
scheme according to Zaremba & Kohn [77Zar]	H ₂ physisorption potential on simple metals with focus on Al surfaces	86Nor
Spin-unrestricted screened Hartree-Fock method	location of H atoms and adsorption energies for (110) faces of Al, Cu, Ni, and NiAl	96Cas

3.4.1.4.3 Theories covering specific interaction systems**3.4.1.4.3.1 Equilibrium properties**

Surface	Theory describing surface equilibrium properties	Remarks	Reference
Li ₂	model ab-initio study	reaction of hydrogen with Li ₂ clusters, activation energies, transition states, reaction energies	86Rag
Li(110) Li(100)	Many-body perturbation theory	location and binding energy of H on Li _n clusters, n = 2...10	88Ray
Li(111)	SCF cluster calculations; many-body perturbation theory	location and binding energies of H on Li _n clusters (n = 3...10)	90Hir
Li(100)	DFT	location of H atoms, electronic structure of H monolayer	95Bir
Be(0001)	SC ab initio cluster calc.	location and bond energies of H atoms on a Be ₁₀ cluster	75Bau2
Be(0001)	SC ab initio cluster calc.	location of adsorbed H atoms on Be ₃₆ clusters	83Bag
Be(0001)	ab initio HF SCF calcul.	location of H atoms, Be - H bond strength, electronic structure for Be slabs	84Ang
Be(0001)	ab initio PP method + DFT supercell geometry	location of adsorbed H atoms, H - Be vibrational frequencies, H - Be bond energies	89Lam
Be(0001)	cluster calc. RHF	location of H atom, bond distances, binding energies	89Mar
C(100)	Slab-MINDO	H adsorption geometry, total energy (H chemisorption energies)	91Zhe
C(100) C(110) C(111)	parametrized tight-binding model	band structure, total energies, relaxed surface geometries, densities of states, C - H vibrations; extensive calculation	94Dav
C(100)	DFT + GGA	H phase formation as a function of chemical potential (coverage), vibrational frequencies of C - H bonds	02Ste
C(111)-1×1-H	plane-wave pseudopotential calc's	calculation of surface relaxations due to H adsorptive bonding	93Stu
C(111)	ab-initio LDF calculations, MD calc'ns	geometry of hydrogenated diamond surfaces	98Ker
C(111) graphite	MC calculations	simulation of adsorption isotherms for H ₂ adsorbed on graphite at 77 K	99Dar
Na(100) Na(110)	Kohn-Sham calc. + 1 st -order perturbation	H - Na binding energies, H - Na bond lengths, H - Na vibrational frequencies	79Hje
Mg(0001)	Kohn-Sham calc. + 1 st -order perturbation	H - Mg binding energies, H - Mg bond lengths, H - Mg vibrational frequencies	79Hje
Mg(0001)	SCF LDA + exchange and correlation	PES for H ₂ ; activation barriers, electronic states	81Nor1
Al(100)	SCF jellium + pseudopotentials	location of adsorbed H atoms, bond distances, charge densities	76Gun

Surface	Theory describing surface equilibrium properties	Remarks	Reference
Al(100) Al(110) Al(111)	Kohn-Sham calc. + 1 st -order perturbation	H - Al binding energies, H - Al bond lengths, H - Al vibrational frequencies	79Hje
Si(100)	tight-binding and EHT calc.	H - Si surface states, H - Si bonding configuration	84Cir
Si(111)-7×7	EHT, DOS calculations	H - Si bonding configuration, dangling bonds, surface states	95Sta
Si(100)	Cluster calc's: DFT + ab initio pseudo-potentials	energetics of Si _x H _y clusters (x = 9, 15, 21; y = 12, 16, 20)	99Pen
Si(111) Ge(111)	realistic tight-binding calcul.	surface energy bands and local density of states of H atoms bound to Si (Ge) surface atoms	76Pan
Si(100)-1×1	self-consistent LDA	H - Si bonding geometry; surface charge distributions	77App
Si(111)	self-consistent pseudopotential	H - Si bonding configuration, formation of mono-, di-, and trihydride	77Ho
Si(111), Ge(111)	ab initio slab + local DFT	H - Si bond energies, substrate geometry, H - Si vibrational frequencies	88Kax
Si(111)-7×7	first principles local density total-energy + atomic force calculations	H-on-Si adsorption geometry; surface electronic structure	93Ye
Si(111)-7×7	first-principles total-energy pseudopotential calc's	Si - H binding energies for H adsorbed in different locations; H-induced charge transfers	95Lim
Si(111)-(1×1)H	ab-initio LCAO HF (slab geometry)	H - Si bonding nature, atomic energies, polarization of the Si charge densities, charge transfers, surface geometry and relaxation	00Car
Al(110)	DFT + GGA	potential-energy curves, H dipole moment	93Ham2
Ti(0001)	SC-LCAO	location of H atoms in (1×1) layer, H-induced electronic states and work function effects	80Fei1 80Fei2
Fe(100)	MINDO	location of H atoms, binding energy, charge densities and vibrational frequencies on a Fe ₁₂ cluster	83Bly
Fe(100)	CEM	location of adsorbed H atoms, binding energies, Fe-H bond lengths, binding energies, adsorbate-induced surface relaxation	90Rae
Fe(100)	SC-LAPW	location and bond length of H atoms in a (1×1)-2H geometry	87Fer
Fe(110)	ab initio CI on embedded cluster surface model	location of adsorbed H atoms, adsorption energies, H - Fe bond length, vibrational frequencies	95Cre
Fe(110)	CEM	location of adsorbed H atoms, binding energies, Fe-H bond lengths, binding energies, adsorbate-induced surface relaxation	90Rae
Fe(110)	EHT + ASED-MO cluster method	bonding situation of H in a Fe vacancy, Fe - H bond strength, decohesion phenomena induced by H	99Jua
Fe(110)	Spin-polarized DFT, GGA, PAW	location of adsorbed H atoms (coverage-dependent), charge densities, long-range order, binding energies, diffusion barriers, work function changes $\Delta\Phi$. The authors predict a $\Delta\Phi$ increase, while experimentally a decrease was observed [77Boz]	03Jia

Surface	Theory describing surface equilibrium properties	Remarks	Reference
Fe(110)	lattice gas model: transfer matrix scaling and MC methods	phase diagrams, correlation function and critical exponents of ordered H phases	82Kin
Fe(100) Fe(110) Fe(111)	CFISO-BEBO	heats of molecular hydrogen desorption, radius of adsorbed H atoms	83Pas
Co(0001)	DFT and FP-LAPW	location of adsorbed H atoms, 3-fold site predicted	99Kli
Co(0001)	Semi-empirical SC tight-binding model	role of H chemisorption in surface magnetism	00Pic
Ni ₂	Ab initio	dissociation pathway	76Mel
Ni(100)	Tight-binding LCAO	location of H atoms, adsorption energy, electronic density of states	76Fas1 76Fas2
Ni(100)	HF	binding energies, bond distance, vibrational frequencies for H on Ni ₂₀ cluster	79Upt
Ni(100)	EMT	location of H atoms, binding energies, vibrational frequencies	82Nor3
Ni(100)	Cluster calculations	dissociation path and energy barriers	84Sie
Ni(100)	Self-consistent spin-polarized calculations	location of H atoms, bond distances, vibrational frequencies of seven-layer Ni(100) film with p(1×1)-H monolayer	85Wei
Ni(100)	first-principles calc's using a model potential	location of H atoms, Ni - H bond distance, vibrational frequencies, Ni - H binding energy	
Ni(100)	Total-energy DFT	location of H atoms, Ni - H bond length, adsorption energy of p(1×1) H layer	85Umr
Ni(100)	All electron cluster calculations with ECP	location of H atom, binding energies of Ni ₄ and Ni ₅ cluster	87Pan
Ni(100); Ni(110); Ni(111)	Spin-polarized gradient-corrected DFT	H adsorption energies, H - H interactions, diffusion barriers; location of adsorbed H atoms including consideration of (2×2)-2H phase	00Kre2
Ni(111)	EMT	location of H atoms, binding energies, vibrational frequencies	82Nor3
Ni(111)	Lattice gas model with 6 NN interactions	phase diagram of c(2×2) honeycomb H phase	84Nag2
Ni(111)	Lattice gas model, transfer matrix finite scaling	phase diagram of c(2×2) honeycomb H phase	86Roe
Ni(111)	Cluster calculation; ab initio valence orbital CI	location of adsorbed H atoms, H - Ni binding energies and bond lengths, work function changes	88Yan
Ni(111)	DFT, GGA	location of adsorbed H atoms, adsorption energies, electronic states	96Pau
Ni(111)	DFT and FP-LAPW	location of adsorbed H atoms, H-induced electronic states	99Kli
Ni(111)	DFT-GGA-PW91	location of adsorbed H atoms including subsurface sites, H binding energy, vibrational frequencies	03Gre

Surface	Theory describing surface equilibrium properties	Remarks	Reference
Cu(100)	Classical trajectory and quantal calcul.	physisorption of H ₂	86DeP
Cu(110)	DFT + GGA, VASP	PES, location of adsorbed H atoms, adsorption energy, Cu - H bond lengths	00Bae
Cu(111)	DFT + GGA, VASP	PES, location of adsorbed H atoms, adsorption energy, Cu - H bond lengths	00Bae
Zn(0001)	ab-initio CI embedding	location of adsorbed H atoms on a Zn ₁₂ cluster, binding energies	90Cre
Ge(111)	ab initio slab + local DFT	H - Ge bond energies, substrate geometry, H - Ge vibrational frequencies	88Kax
Ge(111)-(1×1)H	ab-initio LCAO HF (slab geometry)	H - Ge bonding nature, atomic energies, polarization of the Ge charge densities, charge transfers, surface geometry and relaxation	00Car
Mo(100)	SC PP	electronic structure of H layer, energy levels, work function effects	79Ker
Mo(100)	EMT	equilibrium geometry; 3D adiabatic PES, vibrational modes	90Lou
Mo(111)	DFT	location of adsorbed H atoms, on 5-, 7-, and 9-layer Mo slabs; H - Mo distances	99Arn
Ru(0001)(1×1)H	LAPW	structure, bond lengths, vibrational frequencies	87Fei1
Ru(0001)	PP + LDA	location of H atoms, H - Ru adsorption energy, vibrational frequencies, work function changes, H-induced electronic states	89Cho
Rh(100)	DFT, LDA, FP-LMTO	H - Rh adsorption energies, location of H atoms, work function changes	94Wil1 94Wil2
Rh(100)	ab-initio LDF + GGC	H ₂ orientation during dissociation; H adsorption site, H - Rh bond distances, 6D-PES	96Eic 97Eic 98Eic
Rh(111)	FP-LMTO	location of adsorbed H atoms, adsorption energy, work function change	97Löb
Rh(111)	DFT-GGA-PW91	PES, location of H atoms, vibrational properties	04Lai
Pd clusters	CAS-MCSCF	PES for H ₂ dissociation; dissociation barriers; H bonding geometry for Pd ₃ clusters	95Dai
Pd(100) Pd(110) Pd(111)	DFT + GGA	H adsorption sites, H phases, work function changes, diffusion barriers	98Don
Pd(100)	EAM	H - H lateral interactions, location of H atoms, H - Pd binding energy	90Ein
Pd(100)	Tight-binding + generalized phase-shift	electronic structure of interacting H atoms, pairwise and trio interactions, location of H atoms	90Sta
Pd(100)	DFT, LDA, FP-LMTO	H - Pd adsorption energies, location of H atoms, work function changes	94Wil1 94Wil2
Pd(100)	DFT, FP-LAPW, GGA	PES for H ₂ dissociation, location of H atom	96Will
Pd(100)	DFT+GGA, VASP	H ₂ orientation during dissociation; H adsorption energy, H - Pd bond distances, 6D-PES	97Eic 98Eic
Pd(110)	LCGTO-MCP-LSD cluster calc's	2D-PES, location of adsorbed H atoms, H - Pd binding energy, H - Pd bond lengths, H-induced changes of the electronic structure	90Pap
Pd(110)	DFT + LDA; DFT + GGA + pseudo-potentials	H-induced reconstruction, location of adsorbed H atoms	97Don2 98Led

Surface	Theory describing surface equilibrium properties	Remarks	Reference
Pd(111)	SC-pseudo-potential mixed-basis method	location of H atoms, H - Pd bond lengths, surface electronic structure, bonding and antibonding electronic states	79Lou1 79Lou2
Pd(111)	SC-pseudo-potential c'Ins	density of states, electronic character of Pd - H bond, location of subsurface H atoms	84Cha1
Pd(111)	EAM	location of surface and subsurface H atoms, H phases, critical temperatures	87Daw
Pd(111)	Quantum-mechanical transition state theory	surface diffusion constant for H and D	93Ric
Pd(111)	DFT, GGA	location of adsorbed H atoms, adsorption energies, electronic states	96Pau
Pd(111)	FP-LMTO	location of adsorbed H atoms, adsorption energy, work function change	97Löb
Pd(111)	DFT + GGA	dissociation pathways of H ₂ ; location of H atoms, H - Pd binding energies	97Don1
Pd(111)	DFT + GGA	binding energies and geometric locations of adsorbed H atoms, bond distances	99Pal
Pd(111)	DFT + LDA; DFT + GGA	2D - PES, dissociation pathway, location of H atoms, subsurface hydrogen probabilities	97Ols
Pd(111)	periodic band structure calc. + DFT + GGA	3D - PES; Pd - H adsorption energies, location of adsorbed H atoms, vibrational frequencies, ordered H phases and H - H interactions	98Lov
Pd(210)	DFT + GGA, plane waves, ultrasoft pseudo-potentials	location of H and H ₂ , H - Pd bond lengths, H and H ₂ - Pd binding energies, PES	02Lis
Ag(100)	DFT+GGA, VASP	H ₂ orientation during dissociation; H adsorption energy, H - Ag bond distances, 6D-PES, activation barrier	97Eic 98Eic
Ag(111)	DFT - LCGTO-LSD	physisorption of H ₂ on Ag _n clusters, n = 5, 7, 10, 12; dissociation of H ₂	91Mij
Ag(111)	Classical trajectory and quantal calcul.	physisorption of H ₂	86DeP
W(100)	Extended Hückel MO theory	relative H - W bonding energies, preferred H adsorption sites; energy barriers for surface diffusion	73And
W(100)	LCAO	electronic states of 16-layer W slab with (1×1) H phase	76Smi
W(100)	Ab initio LAPW	H bonding geometry, vibrational frequencies, dipole moments	86Bis
W(100)	Ab initio plane wave pseudo-potential, GGA	PES for H ₂ dissociation, location of H atoms, H - W binding energy	96Whi
W(100)	EMT	equilibrium geometry; 3D adiabatic PES	90Lou
W(110)	CEM	location of adsorbed H atoms, binding energies, bond lengths of atoms, adsorbate-induced surface relaxation	90Rae
W(211)	EMT	location of adsorbed H atoms in equilibrium	89Gri
Re(0001)	DFT-GGA	binding energies and geometric locations of adsorbed H atoms, bond distances	99Pal
Pt clusters	CAS-MCSCF	PES for H ₂ dissociation; dissociation barriers; H bonding geometry for Pt ₃ clusters	95Dai

Surface	Theory describing surface equilibrium properties	Remarks	Reference
Pt(111)	LAPW	structure, bonding location, vibrational frequencies of H monolayer	87Fei2
Pt(111)	DFT	six-dimensional PES for H ₂ interaction	02Ols
Pt(111)	DFT-GGA-PW91	H binding site, binding energy, diffusion barriers (comparative study of various atomic adsorbates)	05For
Pt(111)	pseudopotential planewave DFT	H binding energy, H adsorption geometry	00Pap

3.4.1.4.3.2 Theories covering dynamic properties of specific systems

Surface	Applied theory or theoretical concept	Remarks	Ref.
Mg(0001)	SCF LDA + exchange and correlation	PES for H ₂ ; activation barriers, electronic states, dissociation path	81Nor1
Si(100)	ab initio calculations	PES, transition state calculations	93Wu
Si(100)	ab-initio quantum dynamics calc.	dynamics of coupled H ₂ + Si surface system; sticking coefficients, adsorption barriers	96Kra
Si(100)	DFT + LDA	PES of H ₂ interacting with Si(100), calc. of activation energy for adsorption and desorption	95Peh
Si(100)-2×1	DFT using 1-dimer and 3-dimer cluster models	adsorption/desorption energetics; activation barriers	01Tok
Si	5 D quantum reaction dynamics study	H ₂ dissociation dynamics, energy-dependent sticking coefficients, activation barriers	00Hil
Si(111)	MC transition-state theory methods	activation barriers for H ₂ adsorption, preexponential factors, PES	85Noo
Ni(100)	quantum-mechanical study (restricted 2D model)	H ₂ dissociation dynamics	87Jac2
Ni(100)	LEPS ; TST with multidimensional semiclassical transmission coefficients	reaction rates and kinetic isotope effects for H ₂ and D ₂ dissociation	89Tru
Ni(100)	S-matrix Kohn technique	6D PES (with consideration of cartwheel and helicopter degree of freedom)	93Saa
Ni(100)	Surrogate Hamiltonian method [97Bae]	quantum diffusion of H and D atoms	98Bae
Ni(100)	delocalized EMT	PES of H ₂	86Lee
Ni(100)	spin-polarized gradient-corrected DFT	six-dimensional PES ; dissociation and sticking of H ₂ molecules	00Kre1
Ni(110)	delocalized EMT	PES of H ₂	86Lee
Ni(110)	LEPS; CVT-TST with multidimensional semiclassical transmission coefficients	reaction rates and kinetic isotope effects for H ₂ and D ₂ dissociation	89Tru
Ni(110)	spin-polarized gradient-corrected DFT	six-dimensional PES; dissociation and sticking of H ₂ molecules	00Kre1
Ni(111)	delocalized EMT	PES of H ₂	86Lee
Ni(111)	LEPS; TST with multidimensional semiclassical transmission coefficients	Reaction rates and kinetic isotope effects for H ₂ and D ₂ dissociation	89Tru
Ni(111)	Spin-polarized gradient-corrected DFT	six-dimensional PES; dissociation and sticking of H ₂ molecules	00Kre1
Cu(100)	LEPS approach	PES for H ₂	78Gre
Cu(100)	Delocalized EMT	PES for H ₂	86Lee
Cu”(100)”	accurate PES from CI calcul. of H ₂ – Cu cluster	relaxation dynamics of vibrationally excited H ₂ on 4-fold Cu sites	89Cac
Cu(100)	Wave packet calc. + ab initio PES	PES for H ₂	89Han

Surface	Applied theory or theoretical concept	Remarks	Ref.
Cu(100)	first principles total energy calc.; Car-Parinello approach, LDA + GGA	PES for H ₂	94Whi
Cu(100)	DFT	six-dimensional PES for H ₂	02Ols
Cu(110)	LEPS approach	PES for H ₂	78Gre
Cu(110)	Delocalized EMT	PES for H ₂	86Lee
Cu(110)	Mixed quantum-classical approach	H ₂ dissociation quantum-state-resolved, PES	94Kum
Cu(111)	Reaction path description + model Hamiltonian	PES for H ₂	91Küc
Cu(111)	LEPS approach	PES for H ₂	78Gre
Cu(111)	Quantum dynamic study	PES for H ₂ , sticking probability as a function of quantum state numbers	94Dai
Cu(111)	DFT – GGA	5D-PES for H ₂	94Gro
Cu(311)	LEPS approach	PES for H ₂	78Gre
Zn(0001)	LEPS approach	quasi-classical trajectories for H ₂ interaction with Zn; sticking probability	90Cre
Mo(100)	EMT	3D adiabatic PES	90Lou
Rh(100)	ab-initio LDF + GGC	H ₂ orientation during dissociation; H adsorption site	96Eic
Pd(100)	DFT-GGA-LAPW	6D-PES, H ₂ dissociation	96Will
Pd(100)	DFT	6D-PES, H ₂ sticking	95Gro1 97Gro
Ag(111)	DFT - LCGTO-LSD	physisorption of H ₂ on Ag _n clusters, n = 5, 7, 10, 12; PES for dissociation of H ₂	91Mij
W(100)	EMT	3D adiabatic PES	90Lou
Pt(111)	CT; Gaussian weighting, TST, CHAIN method	ab initio PES, dynamics of H ₂ desorption; late barrier position	05Per
Pt(111)	DFT	six-dimensional PES for H ₂	99Ols 02Pij 02Ols
Pt(111)	DFT + GGA	six-dimensional PES for H ₂ and D ₂	04Vin

3.4.1.5 List of acronyms

ARUPS	angle-resolved UV photoelectron spectroscopy
BIS	Bremsstrahlung isochromat spectroscopy
CAS-MCSCF	complete active space multiconfiguration self-consistent field
CFSO-BEBO	crystal field surface orbital-bond energy bond order
CPD	contact potential difference
EAM	embedded atom method
ECP	effective core potential
EDC	energy distribution curve
EELS	electron energy loss spectroscopy
EHT	extended Hückel theory
ESD	electron-stimulated desorption
GGA	generalized gradient approximation
HAS	He atom scattering
hex	hexagonal
HOPG	highly-oriented pyrolytic graphite
HREELS	high-resolution electron energy loss spectroscopy
IC	incommensurate
IETS	inelastic electron tunneling spectroscopy

IPE	inverse photoemission
IR	Infrared
IRAS	Infrared absorption spectroscopy
LCAO	Linear combination of atomic orbitals
LCGTO	linear combination of Gaussian-type orbital
LDF	local density functional
LEED	low energy electron diffraction
LEIS	low energy ion scattering
LEIS	low-energy ion recoil scattering
MB	molecular beam
MCP	model core potential
MD	molecular dynamics
MEM-LEED	mirror electron microscope LEED
MO	molecular orbital
MR	missing row (reconstruction)
NEA	negative electron affinity
NICIS	neutral impact collision ion spectroscopy
NIST	National Institute of Standards and Technology
NN	next neighbor
NRA	nuclear reaction analysis
PAW	projector-augmented wave (formalism)
PES	photoelectron spectroscopy
PR	pairing row (reconstruction)
PT	phase transition
PW91	Perdew-Wang code from 1991
RAIRS	reflection-absorption infrared spectroscopy
REMPI	resonance-enhanced multi-photon ionization
RF	retarding field
RHEED	reflected high energy electron diffraction
SBZ	surface Brillouin zone
SC	self consistent
SCF	self-consistent field
SES	secondary electron emission study
SFG	Infrared-visible sum frequency generation
SHG	second harmonic generation
SIMS	secondary ion mass spectroscopy
SIRS	surface infrared spectroscopy
STM	scanning tunneling microscopy
TD(S)	thermal desorption (spectroscopy)
TED	transmission electron diffraction
TM	transition metal
TOF	time-of-flight
TPD	temperature-programmed desorption
UHV	ultra high vacuum
UPS	ultraviolet photoemission spectroscopy
UV	ultraviolet
VASP	Vienna ab-initio simulation package
VLEED	very low energy electron diffraction
WF	work function
XPS	X-ray photoelectron spectroscopy

3.4.1.6 References

- 12Lan Langmuir, I.: J. Am. Chem. Soc. **34** (1912) 860; 1310
 14Bau Baule, B.: Ann. Phys. **44** (1914) 145.
 14Lan Langmuir, I., Mackey, G.M.J.: Am. Chem. Soc. **36** (1914) 1708.
 15Lan Langmuir, I.: Am. Chem. Soc. **37** (1915) 417.
 27Top Topping, J.: Proc. R. Soc. (London) A **114** (1927) 67.
 29Lon London, F.: Z. Elektrochem. **35** (1929) 552.
 31Eyr Eyring, H., Polanyi, M.: Z. Phys. Chem. (Leipzig) B **12** (1931) 279.
 49Her Herring, C., Nichols, M.H.: Rev. Mod. Phys. **21** (1949) 185.
 55Cre Cremer, E.: Adv. Catal. Relat. Subj. **7** (1955) 75.
 55Sat Sato, S.: J. Chem. Phys. **23** (1955) 529.
 55Tra Trapnell, B. M. W.: *Chemisorption*, Butterworth, London 1955
 57Gom Gomer, R., Wortman, R., Lundy, R.: J. Chem. Phys. **26** (1957) 1147.
 57Kis Kisliuk, P.J.: J. Phys. Chem. Solids **3** (1957) 95.
 57Wor Wortman, R., Gomer, R., Lundy, R.: J. Chem. Phys. **27** (1957) 1099.
 58Han Hansen, M., *Constitution of Binary Alloys*, 2nd ed: McGraw-Hill, New York 1958
 58Kis Kisliuk, P.J.: J. Phys. Chem. Solids **5** (1958) 78.
 58Kou Koutecký, J.: Trans. Faraday Soc. **54** (1958) 1038.
 58Sim Simon, H., Suhrmann, H.: *Der lichtelektrische Effekt und seine Anwendungen*, Springer-Verlag Berlin Göttingen Heidelberg, 2.Aufl. 1958
 59Cul Culver, R.V., Tompkins, F.C.: Adv. Catal. Relat. Subj. **11** (1959) 67.
 59Law Law, J.T.: J. Chem. Phys. **30** (1959) 1568.
 60Gri Grimley, T.B.: Adv. Catal. Relat. Subj. **12** (1960) 1.
 60Jos Jost, W. *Diffusion in Solids, Liquids, Gases*, 3rd printing with addendum, Academic Press New York 1960
 61Gom Gomer, R.: *Field emission and Field ionization*, Harvard University Press, Cambridge 1961
 62Ger Germer, L.H., MacRae, A.U.: J. Chem. Phys. **37** (1962) 1382.
 64Hoh Hohenberg, P., Kohn, W.: Phys. Rev. **136** (1964) B864.
 65Jos Jost, W.: *Diffusion*, 4th printing 1965, Academic Press, New York
 65Koh Kohn, W., Sham, L.J.: Phys. Rev. **140** (1965) A1133.
 65Kou Koutecký, J.: Adv. Chem. Phys. **9** (1965) 85.
 66Arm Armstrong, R.A.: Can. J. Phys. **44** (1966) 1753.
 66Est Estrup, P.J., Anderson, J.: J. Chem. Phys. **45** (1966) 2254.
 66Jak Jaklevic, R.G., Lambe, J.: Phys. Rev. Lett. **17** (1966) 1139.
 66Joh Johnston, H. S.: *Gas Phase Reaction Rate Theory*, (Ronald Press New York 1966)
 67Gri1 Grimley, T.B.: Proc. Phys. Soc. (London) **90** (1967) 751.
 67Gri2 Grimley, T.B.: Proc. Phys. Soc. (London) **92** (1967) 776.
 67Lew Lewis, F. A.: *The Palladium – Hydrogen System*, Academic Press, London 1967
 68Sha Shavitt, I., Stevens, R.M., Minn, F.L., Karplus, M.: J. Chem. Phys. **48** (1968) 2700.
 69Bal Balandin, A.A.: Adv. Catal. Relat. Subj. **19** (1969) 1.
 69Ber Bertolini, J. C., Dalmai-Imelik, G.: Colloquium International CNRS, Paris 1969, p.135
 69Lew Lewis, R., Gomer, R.: Surf. Sci. **17** (1969) 333.
 69Riv Rivière, J. C.: *Work function: Measurements and Results*, in: Solid State Surface Science, Vol. 1, (M. Green, ed.), Dekker New York 1969, p.179
 69Tam Tamm, P.W., Schmidt, L.D.: J. Chem. Phys. **51** (1969) 5352.
 69Tra Tracy, J.C., Palmberg, P.W.: J. Chem. Phys. **51** (1969) 4852.
 70Ada Adams, D.L., Germer, L.H.: Surf. Sci. **23** (1970) 419.
 70Cla Clarke, A.: *The Theory of Adsorption and Catalysis*, Academic Press New York 1970
 70Tam Tamm, P.W., Schmidt, L.D.: J. Chem. Phys. **52** (1970) 1150.
 70Wed Wedler, G.: *Chemisorption*, Verlag Chemie Weinheim 1970
 71Ert Ertl, G., Küppers, D.: Ber. Bunsenges. Phys. Chem. **75** (1971) 1017.
 71Gri Grimley, T.B.: Ber. Bunsenges. Phys. Chem. **75** (1971) 1005.
 71Han Han, H.R., Schmidt, L.D.: J. Phys. Chem. **75** (1971) 227.

- 71Sch Schrieffer, J.R., Gomer, R.: Surf. Sci. **25** (1971) 315.
- 71Tam Tamm, P.W., Schmidt, L.D.: J. Chem. Phys. **54** (1971) 4775.
- 72Cha Chappell, R., Hayward, D.O.: J. Vac. Sci. Technol. **9** (1972) 1052.
- 72Ert Ertl, G., Neumann, M.: Z. Naturforsch. A **27** (1972) 1607.
- 72Kae Kaesz, H.D., Saillant, R.B.: Chem. Rev. **72** (1972) 231.
- 72Kin King, D.A., Wells, M.G.: Surf. Sci. **29** (1972) 454.
- 72Lap1 Lapujoulade, J., Neil, K.S.: Surf. Sci. **35** (1972) 288.
- 72Lap2 Lapujoulade, J., Neil, K.S.: J. Chim. Phys. **57** (1972) 3535.
- 72Mad Madey, T.E.: Surf. Sci. **29** (1972) 571.
- 72Mah Mahnig, M., Schmidt, L.D.: Z. Phys. Chem. NF **80** (1972) 71.
- 72Plu Plummer, E.W., Bell, A.E.: J. Vac. Sci. Technol. **9** (1972) 583.
- 73And Anders L.W., Hansen, R.S., Bartell, L.S.: J. Chem. Phys. **59** (1973) 5277.
- 73Car Cartier, P.G., Rye, R.R.: J. Chem. Phys. **59** (1973) 4602.
- 73Chr1 Christmann, K., Ertl, G., Schober, O.: Surf. Sci. **40** (1973) 61.
- 73Chr2 Christmann, K., Ertl, G.: Z. Naturforsch. A **28** (1973) 1144.
- 73Ein Einstein, T.L., Schrieffer, J.R.: Phys. Rev. B **7** (1973) 3629.
- 73Feu Feuerbacher, B., Fitton, B.: Phys. Rev. B **8** (1973) 4890.
- 73Gri Grimley, T.B., Torrini, M.: J. Phys. C **6** (1973) 868.
- 73Mad Madey, T.E.: Surf. Sci. **36** (1973) 281.
- 73McC McCarthy, J., Falconer, J., Madix, R.J.: J. Catal. **30** (1973) 235.
- 73Ren Renard, M., Deloche, D.: Surf. Sci. **35** (1973) 487.
- 73Rye Rye, R.R., Barford, B.D., Cartier, P.G.: J. Chem. Phys. **59** (1973) 1693.
- 74Ada Adams, D.L.: Surf. Sci. **42** (1974) 12.
- 74Bal1 Balooch, M., Stickney, R.E.: Surf. Sci. **44** (1974) 310.
- 74Bal2 Balooch, M., Cardillo, M.J., Miller, D.R., Stickney, R.E.: Surf. Sci. **46** (1974) 358.
- 74Bar Barford, B.D., Rye, R.R.: J. Chem. Phys. **60** (1974) 1046.
- 74Bry Bryson, C.E., Cazcarra, V., Levenson, L.L.: J. Vac. Sci. Technol. **11** (1974) 411.
- 74Chr Christmann, K., Schober, O., Ertl, G., Neumann, M.: J. Chem. Phys. **60** (1974) 4528.
- 74Con Conrad, H., Ertl, G., Latta, E.E.: Surf. Sci. **41** (1974) 435.
- 74Hag Hagen, D. I., Donaldson, E.E.: Surf. Sci. **45** (1974) 61.
- 74Iba Ibach, H., Rowe, J.E.: Surf. Sci. **43** (1974) 481.
- 74Lu Lu, K.E., Rye, R.R.: Surf. Sci. **45** (1974) 677.
- 74Pen Pendry, J. B: *Low-energy Electron Diffraction*, Academic Press New York 1974
- 74Rin Rinne, H: *Absolutmessungen der Adsorption von Wasserstoff an der Nickel(111)Fläche und an ultradünnen Nickelfilmen*, Dissertation, Technische Universität Hannover 1974
- 74Tay Taylor, T.N., Estrup, P.J.: J. Vac. Sci. Technol. **11** (1974) 244.
- 75Bau1 Bauer, E., Bonczek, F., Poppa, H., Todd, G.: Surf. Sci. **53** (1975) 87.
- 75Bau2 Bauschlicher Jr., C.W., Liskow, D.H., Bender, C.F., Schaefer II, H.F.: J. Chem. Phys. **62** (1975) 4815.
- 75Chr Christmann, K., Ertl, G., Pignet, T.: Surf. Sci. **54** (1975) 365.
- 75Fro Froitzheim, H., Ibach, H., Lehwald, S.: Phys. Lett. A **55** (1975) 247.
- 75Kin King, D.A.: Surf. Sci. **47** (1975) 384.
- 75Net Netzer, F.P., Kneringer, G.: Surf. Sci. **51** (1975) 526.
- 75Pan Pandey, K.C., Sakurai, T., Hagstrum, H.D.: Phys. Rev. Lett. **35** (1975) 1728.
- 75Plu Plummer, E. W: in: *Interactions on Metal Surfaces* (R. Gomer, ed.), Springer, Berlin-Heidelberg.-New York 1975, p.143
- 75Row Rowe, J.E.: Solid State Commun. **17** (1975) 673.
- 75Sch Schmidt, L. D: in: *Interactions on Metal Surfaces* (R. Gomer, ed.), Springer, Berlin-Heidelberg.-New York 1975, p.78
- 75Yin Ying, S.C., Smith, J.R., Kohn, W.: Phys. Rev. B **11** (1975) 1483.
- 76Bre Brenig, W., Schönhammer, K.: Z. Phys. B **24** (1976) 91.
- 76Chr Christmann, K., Ertl, G.: Surf. Sci. **60** (1976) 365.
- 76Con1 Conrad, H: *Wechselwirkung von Gasen mit einer Pd(111) Oberfläche*, Dissertation, Ludwig-Maximilians-Universität München 1976, p.110 ff

- 76Con2 Conrad, H., Ertl, G., Küppers, J., Latta, E.E.: Surf. Sci. **58** (1976) 578.
- 76Dus Duś, R., Lisowski, W.: Surf. Sci. **61** (1976) 635.
- 76Fas1 Fassaert, D.J.M., van der Avoird, A.: Surf. Sci. **55** (1976) 291.
- 76Fas2 Fassaert, D.J.M., van der Avoird, A.: Surf. Sci. **55** (1976) 313.
- 76Fro Froitzheim, H., Ibach, H., Lehwald, S.: Phys. Rev. Lett. **36** (1976) 1549.
- 76Gun Gunnarsson, O., Hjelmberg, H., Lundqvist, B.I.: Phys. Rev. Lett. **37** (1976) 292.
- 76McC McCabe, R.W., Schmidt, L.D.: Surf. Sci. **60** (1976) 85.
- 76Mel Melius, C.F., Moskowitz, J.W., Mortola, A.P., Baillie, M.B., Ratner, M.A.: Surf. Sci. **59** (1976) 279.
- 76Pan Pandey, K.C.: Phys. Rev. B **14** (1976) 1557.
- 76Sak Sakurai, T., Hagstrum, H.D.: Phys. Rev. B **14** (1976) 1593.
- 76Smi Smith, N.V., Mattheiss, L.F.: Phys. Rev. Lett. **37** (1976) 1494.
- 77Adn Adnot, A., Carette, J.-D.: Phys. Rev. Lett. **39** (1977) 209.
- 77App Appelbaum, J.A., Hamann, D.R., Tasso, K.H.: Phys. Rev. Lett. **39** (1977) 1487.
- 77Bac Backx, C., Feuerbacher, B., Fitton, B., Willis, R.F.: Phys. Lett. A **60** (1977) 145.
- 77Boz Bozso, F., Ertl, G., Grunze, M., Weiss, M.: Appl. Surf. Sci. **1** (1977) 103.
- 77Col1 Collins, D.M., Spicer, W.E.: Surf. Sci. **69** (1977) 85.
- 77Col2 Collins, D.M., Spicer, W.E.: Surf. Sci. **69** (1977) 114.
- 77Deb Debe, M.K., King, D.A.: Phys. Rev. Lett. **39** (1977) 708.
- 77Dem Demuth, J.E.: Surf. Sci. **65** (1977) 369.
- 77Fro Froitzheim, H.: in *Electron Spectroscopy for Surface Analysis*, (H. Ibach, ed.), Springer, Berlin 1977, p. 205
- 77Hie Hiemenz, P. C: *Principles of Colloid and Surface Chemistry*, M. Dekker New York 1977, p.338 ff
- 77Ho Ho, K.M., Cohen, M.L., Schlüter, M.: Phys. Rev. B **15** (1977) 3888.
- 77Kno Knowles, T.R., Suhl, H.: Phys. Rev. Lett. **39** (1977) 1417.
- 77Lur Lurie, P.G., Wilson, J.M.: Surf. Sci. **65** (1977) 453.
- 77McC1 McCabe, R. W., Schmidt, L. D., Proc. 7th Intern. Vacuum Congr: Vol. 2 (1977), p. 120
- 77McC2 McCabe, R.W., Schmidt, L.D.: Surf. Sci. **65** (1977) 169.
- 77Sal Salmeron, M., Gale, R.J., Somorjai, G.A.: J. Chem. Phys. **67** (1977) 5324.
- 77Sch Schwarz, J.A., Polizotti, R.S., Burton, J.J.: Surf. Sci. **67** (1977) 10.
- 77Ton Tong, S.Y., van Hove, M.A.: Phys. Rev. B **16** (1977) 1459.
- 77Zar Zaremba, E., Kohn, W.: Phys. Rev. B **15** (1977) 1769.
- 78Ale Alefeld, G: Völkl, J. (eds.), *Hydrogen in Metals*, Springer-Verlag, Berlin, Vol. 1 and 2, 1978
- 78And1 Anderson, J., Lapeyre, G.J., Smith, R.J.: Phys. Rev. B **17** (1978) 2436.
- 78And2 Andersson, S.: Chem. Phys. Lett. **55** (1978) 1853.
- 78Bar1 Barker, R.A., Estrup, P.J.: Phys. Rev. Lett. **41** (1978) 1307.
- 78Bar2 Barnes, M.R., Willis, R.F.: Phys. Rev. Lett. **41** (1978) 1729.
- 78Beh Behm, R.J., Christmann, K., Ertl, G.: Solid State Commun. **25** (1978) 763.
- 78Cas Castner, D.G., Sexton, B.A., Somorjai, G.A.: Surf. Sci. **71** (1978) 519.
- 78Dan Danielson, L.R., Dresser, M.J., Donaldson, E.E., Dickinson, J.T.: Surf. Sci. **71** (1978) 599.
- 78Dom Domany, E., Schick, M., Walker, J.S., Griffiths, R.B.: Phys. Rev. B **18** (1978) 2209.
- 78Eng Engel, T.: J. Chem. Phys. **69** (1978) 373.
- 78Feu Feuerbacher, B., Fitton, B: Willis, R. F. (eds.), *Photoemission and the Electronic Properties of Surfaces*, Wiley, Chichester, New York 1978
- 78Gon Gonchar, V.V., Kanash, O.V., Naumovets, A.G., Fedorus, A.G.: JETP Lett. **28** (1978) 330.
- 78Gre Gregory, A.R., Gelb, A., Silbey, R.: Surf. Sci. **74** (1978) 497.
- 78Hje Hjelmberg, H.: Phys. Scr. **18** (1978) 481.
- 78Ho Ho, W., Willis, R.F., Plummer, E.W.: Phys. Rev. Lett. **40** (1978) 1463.
- 78Mus Muscat, J.P., Newns, D.M.: Prog. Surf. Sci. **9** (1978) 1.
- 78Pri Prince, R.M., Floyd, G.R.: Surf. Sci. **74** (1978) 342.
- 78Rob Roberts, M. W., McKee, C. S: *Chemistry of the Metal – Gas Interface*, Oxford University Press, Oxford UK, 1978, p. 256

- 78Wic Wicke, E., Brodowsky, H: in: *Hydrogen in Metals*, Vol. II (G. Alefeld & J. Völkl, eds.), Springer, Berlin-Heidelberg-New York 1978, p. 73 ff.
- 79Bar Baro, A.M., Ibach, H., Bruchmann, H.D.: *Surf. Sci.* **88** (1979) 384.
- 79Bre Brenig, W.: *Z. Phys. B* **36** (1979) 81.
- 79Bri Bridge, M.E., Comrie, C.M., Lambert, R.M.: *J. Catal.* **58** (1979) 28.
- 79Bur Burch, R: *Chemistry and Physics of Solids and Interfaces*, Specialist Periodical Report No.9, The Chemical Society, London 1979, p. 1 ff.
- 79Chr1 Christmann, K.: *Z. Naturforsch. A* **34** (1979) 22.
- 79Chr2 Christmann, K., Behm, R.J., Ertl, G., van Hove, M.A., Weinberg, W.H.: *J. Chem. Phys.* **70** (1979) 4168.
- 79Deb Debe, M.K., King, D.A.: *Surf. Sci.* **81** (1979) 193.
- 79Dom1 Domany, E., Schick, M.: *Solid State Commun.* **30** (1979) 331.
- 79Dom2 Domany, E., Schick, M.: *Phys. Rev. B* **20** (1979) 3828.
- 79Dun Dunlap, B. I., Connolly, J. W., Sabin, J. R: *J. Chem. Phys.* **71** (1979) 3386; 4993.
- 79Ein Einstein, T.L.: *Surf. Sci.* **84** (1979) L497.
- 79Ert Ertl, G: in: *The Nature of the Surface Chemical Bond* (Rhodin, T. N. & Ertl, G. eds), North-Holland Amsterdam 1979, p. 325
- 79Est Estrup, P.J.: *J. Vac. Sci. Technol.* **16** (1979) 635.
- 79Gri Grimley, T. B.: in: *The Nature of the Surface Chemical Bond*, (Rhodin, T. N., and Ertl, G: eds), North-Holland Amsterdam, 1979, Ch. 1
- 79Hei Heilmann, P., Heinz, K., Müller, K.: *Surf. Sci.* **83** (1979) 487.
- 79Him Himpel, F.J., Knapp, J.A., Eastman, D.E.: *Phys. Rev. B* **19** (1979) 2872.
- 79Hje Hjelmberg, H.: *Surf. Sci.* **81** (1979) 539.
- 79Hoe Hölzl, J., Schulte, F. K: in: *Springer Tracts in Modern Physics*, Vol. 85 (1979), Springer-Verlag Berlin Heidelberg New York
- 79Ker Kerker, G.P., Yin, M.T., Cohen, M.L.: *Phys. Rev. B* **20** (1979) 4940.
- 79Lou1 Louie, S.G.: *Phys. Rev. Lett.* **40** (1979) 1525.
- 79Lou2 Louie, S.G.: *Phys. Rev. Lett.* **42** (1979) 476.
- 79Mes Messmer, J. P., in: *The Nature of the Surface Chemical Bond*, (Rhodin, T. N., and Ertl, G: eds) North-Holland Amsterdam 1979
- 79Mue Müller, H., and Brenig, W.: *Z. Phys. B* **34** (1979) 165.
- 79Sal Salmeron, M., Gale, R.J., Somorjai, G.A.: *J. Chem. Phys.* **70** (1979) 2807.
- 79Sch Schwarz, J.A.: *Surf. Sci.* **87** (1979) 525.
- 79Upt Upton, T.H., Goddard III, W.A.: *Phys. Rev. Lett.* **42** (1979) 472.
- 79Wac Wachs, I., Madix, R.J.: *Surf. Sci.* **84** (1979) 375.
- 79Yat Yates Jr., J.T., Thiel, P.A., Weinberg, W.H.: *Surf. Sci.* **84** (1979) 427.
- 80Bar Barker, R.A., Semancik, S., Estrup, P.J.: *Surf. Sci.* **94** (1980) L162.
- 80Beh Behm, R.J., Christmann, K., Ertl, G.: *Surf. Sci.* **99** (1980) 320.
- 80Ben Benziger, J., Madix, R.J.: *Surf. Sci.* **94** (1980) 119.
- 80Dav Davies, J.A., Jackson, D.P., Norton, P.R., Posner, D.E., Unertl, W.N.: *Solid State Commun.* **34** (1980) 41.
- 80DiF DiFoggio, R., Gomer, R.: *Phys. Rev. Lett.* **44** (1980) 1258.
- 80Fei1 Feibelman, P.J., Hamann, D.R.: *Phys. Rev. B* **21** (1980) 1385.
- 80Fei2 Feibelman, P.J., Hamann, D.R., Himpel, F.J.: *Phys. Rev. B* **22** (1980) 1734.
- 80Ho Ho, W., DiNardo, N.J., Plummer, E.W.: *J. Vac. Sci. Technol.* **17** (1980) 134.
- 80Ibb Ibbotson, D.E., Wittrig, T.S., Weinberg, W.H.: *J. Chem. Phys.* **72** (1980) 4885.
- 80Jay Jayasooriya, U.A., Chesters, M.A., Howard, M.W., Kettle, S.F.A., Powell, D.B., Sheppard, N.: *Surf. Sci.* **93** (1980) 526.
- 80Kin King, D.A., Thomas, G.: *Surf. Sci.* **92** (1980) 201.
- 80Mat Mattera, L., Rosatelli, F., Salvo, C., Tommasini, F., Valbusa, U., Vidali, G.: *Surf. Sci.* **93** (1980) 515.
- 80Nor1 Norton, P.R., Creber, D.K., Davies, J.A.: *J. Vac. Sci. Technol.* **17** (1980) 149.
- 80Nor2 Nørskov, J.K., Lang, N.D.: *Phys. Rev.* **21** (1980) 2131.

- 80Poe Poelsema, B., Mechttersheimer, G., Comsa, G., Proc. IVth Int. Conf. Solid Surfaces and IIIrd ECOSS, eds. Degras, D. A & Costa, M: (Cannes 1980), p. 834
- 80Rie Rieder, K.H., Engel, T.: Phys. Rev. Lett. **45** (1980) 824.
- 80Sak Sakisaka, Y., Kato, H., Nishijima, M., Onchi, M.: Solid State Commun. **36** (1980) 353.
- 80Sch1 Schönhammer, K., Gunnarsson, O.: Phys. Rev. B **22** (1980) 1629.
- 80Sch2 Schulze, G: *Die Adsorption von Wasserstoff auf reinen Silizium-Spaltflächen*, Dissertation, Universität Hannover, 1980
- 80Sed Sedlmair, R., Brenig, W.: Z. Phys. B **36** (1980) 245.
- 80Shi Shimizu, H., Christmann, K., Ertl, G.: J. Catal. **61** (1980) 412.
- 80Sil Silvera, I.F.: Rev. Mod. Phys. **52** (1980) 393.
- 80Smi1 Smith, J.R: (ed.), *Theory of Chemisorption*, Topics in Current Physics, Vol 19, Springer, Berlin-New York 1980
- 80Smi2 Smith, R.J.: Phys. Rev. B **21** (1980) 3131.
- 80Wil Willis, R.F., ed: *Vibrational Spectroscopy of Adsorbates*, Springer Series in Chemical Physics, Springer, Berlin 1980
- 81Ada Adams, D.L., Nielsen, H.B., Van Hove, M.A., Ignatiev, A.: Surf. Sci. **104** (1981) 47.
- 81Aln Alnot, M., Cassuto, A.: Surf. Sci. **112** (1981) 325.
- 81Bar1 Baró, A.M., Erley, W.: Surf. Sci. **112** (1981) L759.
- 81Bar2 Barker, R.A., Estrup, P.J.: J. Chem. Phys. **74** (1981) 1442.
- 81Bar3 Barateau, M.A., Ko, E.I., Madix, R.J.: Surf. Sci. **102** (1981) 99.
- 81Cha Chadi, D.J., Chiang, C.: Phys. Rev. B **23** (1981) 1843.
- 81Duc Ducros, R., Housley, M., Piquard, G., Alnot, M.: Surf. Sci. **108** (1981) 235.
- 81Ebe Eberhardt, W., Greuter, F., Plummer, E.W.: Phys. Rev. Lett. **46** (1981) 1085.
- 81Eng Engel, T., Rieder, K.-H.: Surf. Sci. **109** (1981) 140.
- 81Hol Holmes, M.W., King, D.A.: Surf. Sci. **110** (1981) 120.
- 81Ibb Ibbotson, D.E., Wittrig, T.S., Weinberg, W.H.: Surf. Sci. **110** (1981) 294.
- 81Joh1 Johnson, S., Madix, R.J.: Surf. Sci. **108** (1981) 77.
- 81Joh2 Johansson, P.K.: Surf. Sci. **104** (1981) 510.
- 81Kat Kato, H., Sakisaka, Y., Nishijima, M., Onchi, M.: Surf. Sci. **107** (1981) 20.
- 81Lue Lüth, H., Matz, R.: Phys. Rev. Lett. **46** (1981) 1652.
- 81McR McRae, E.G., Caldwell, C.W.: Phys. Rev. Lett. **46** (1981) 1632.
- 81Nor1 Nørskov, J.K., Houmøller, A., Johansson, P.K., Lundqvist, B.I.: Phys. Rev. Lett. **46** (1981) 257.
- 81Nor2 Norton, P.R., Davies, J.A., Creber, D.K., Sitter, C.W., Jackman, T.E.: Surf. Sci. **108** (1981) 205.
- 81Pic Pick, M.A.: Phys. Rev. B **24** (1981) 4287.
- 81Poe Poelsema, B., Mechttersheimer, G., Comsa, G.: Surf. Sci. **111** (1981) L728.
- 81Van1 Van Hove, M.A., Koestner, R.J., Stair, P.C., Biberian, J.P., Kesmodel, L.L., Bartos, I., Somorjai, G.A.: Surf. Sci. **103** (1981) 189.
- 81Van2 Van Hove, M.A., Koestner, R.J., Stair, P.C., Biberian, J.P., Kesmodel, L.L., Bartos, I., Somorjai, G.A.: Surf. Sci. **103** (1981) 218.
- 81Wag Wagner, H., Butz, R., Backes, U., Bruchmann, D.: Solid State Commun. **38** (1981) 1155.
- 82And Andersson, S., Harris, J.: Phys. Rev. Lett. **48** (1982) 545.
- 82Avo Avouris, Ph., Schmeisser, D., Demuth, J.E.: Phys. Rev. Lett. **48** (1982) 199.
- 82Bla Blanchet, G.B., DiNardo, N.J., Plummer, E.W.: Surf. Sci. **118** (1982) 496.
- 82Bre Brenig, W.: Z. Phys. B **48** (1982) 127.
- 82Bri Bringans, R.D., Höchst, H.: Phys. Rev. B **25** (1982) 1081.
- 82But Butz, R., Memeo, R., Wagner, H.: Phys. Rev. B **25** (1982) 4327.
- 82Cer Cerrina, F., Anderson, J.R., Lapeyre, G.R., Bisi, O., Calandra, C.: Phys. Rev. B **25** (1982) 4949.
- 82Coh Cohen, M.L.: Phys. Scr. T **1** (1982) 5.
- 82Com Comsa, G., David, R.: Surf. Sci. **117** (1982) 77.
- 82DiF DiFoggio, R., Gomer, R.: Phys. Rev. B **25** (1982) 3490.
- 82DiN DiNardo, N.J., Plummer, E.W.: J. Vac. Sci. Technol. **20** (1982) 890.

- 82Ebe Eberhardt, W., Cantor, R., Greuter, F., Plummer, E.W.: Solid State Commun. **42** (1982) 799.
- 82Eng Engel, T., and Rieder, K.H. in: *Structural Studies of Surfaces*, Springer Tracts in Modern Physics, Vol 91 (1982), p.55
- 82Iba Ibach, H., Mills, D. L.: *Electron Energy Loss Spectroscopy and Surface Vibrations*, Academic Press, New York 1982
- 82Imb Imbihl, R., Behm, R.J., Christmann, K., Ertl, G., Matsushima, T.: Surf. Sci. **117** (1982) 257.
- 82Kim Kim, Y., Peebles, H.C., White, J.M.: Surf. Sci. **114** (1982) 363.
- 82Kin Kinzel, W., Selke, W., Binder, K.: Surf. Sci. **121** (1982) 13.
- 82Kno Knor, Z. in: *Catalysis* Vol.3, (J.R. Anderson and M. Boudart eds.), Springer, Berlin 1982, p.231
- 82Nor1 Norton, P.R., Davies, J.A., Jackman, T.E.: Surf. Sci. **121** (1982) 103.
- 82Nor2 Nørskov, J.K.: Phys. Rev. B **26** (1982) 2875.
- 82Nor3 Nørskov, J.K.: Phys. Rev. Lett. **48** (1982) 1620.
- 82Nyb Nyberg, C., Tengstål, C.G.: Solid State Commun. **44** (1982) 251.
- 82Per Perreau, J., Lapujoulade, J.: Surf. Sci. **122** (1982) 341.
- 82Sch Schönhammer, K., Gunnarsson, O.: Surf. Sci. **117** (1982) 53.
- 82Seg Seguire, J.L., Suzanne, J.: Surf. Sci. **118** (1982) L241.
- 82Vic Vickerman, J.C., Christmann, K.: Surf. Sci. **120** (1982) 1.
- 82Wen Weng, S.-L.: Phys. Rev. B **25** (1982) 6188.
- 82Win Winkler, A., Rendulic, K.D.: Surf. Sci. **118** (1982) 19.
- 82Yan Yang, W.S., Sokolov, J., Jona, F., Marcus, P.M.: Solid State Commun. **41** (1982) 191.
- 83And Andersson, S., Harris, J.: Phys. Rev. B **27** (1983) 9.
- 83Bag Bagus, P.S., Schaefer III, H.F., Bauschlicher Jr., C.W.: J. Chem. Phys. **78** (1983) 1390.
- 83Bar Barteau, M.A., Broughton, J.Q., Menzel, D.: Surf. Sci. **133** (1983) 443.
- 83Beh Behm, R.J., Penka, V., Cattania, M.G., Christmann, K., Ertl, G.: J. Chem. Phys. **78** (1983) 7486.
- 83Bin1 Binnig, G., Rohrer, R., Gerber, Ch., Weibel, E.: Surf. Sci. **131** (1983) L379.
- 83Bin2 Binnig, G., Rohrer, R., Gerber, Ch., Weibel, E.: Phys. Rev. Lett. **50** (1983) 120.
- 83Bly Blyholder, G., Head, J., Ruetz, F.: Surf. Sci. **131** (1983) 403.
- 83Cat1 Cattania, M.G., Christmann, K., Penka, V., Ertl, G.: Gazz. Chim. Ital. **113** (1983) 433.
- 83Cat2 Cattania, M.G., Penka, V., Behm, R.J., Christmann, K., Ertl, G.: Surf. Sci. **126** (1983) 382.
- 83Did Didham, E.F.J., Allison, W., Willis, R.F.: Surf. Sci. **126** (1983) 219.
- 83Dos Dose, V.: Prog. Surf. Sci. **13** (1983) 225.
- 83Ebe Eberhardt, W., Louie, S.G., Plummer, E.W.: Phys. Rev. B **28** (1983) 465.
- 83Fro Froitzheim, H., Lammering, H., Günter, H.-L.: Phys. Rev. B **27** (1983) 2278.
- 83Gre Greuter, F., Plummer, E.W.: Solid State Commun. **48** (1983) 37.
- 83Gri Grimley, T. B. in: *The Chemical Physics of Solid Surfaces and Heterogeneous Catalysis*, Vol. 2, Elsevier, Amsterdam 1983, Ch. 5, p.333 ff
- 83Hab Habenschaden, E., Küppers, J.: Surf. Sci. **138** (1983) L147.
- 83Kob Kobayashi, H., Edamoto, K., Onchi, M., Nishijima, M.: J. Chem. Phys. **78** (1983) 7429.
- 83Lee Lee, J., Cowin, J.P., Wharton, L.: Surf. Sci. **130** (1983) 1.
- 83Mur Murgai, V., Wenig, S.-L., Strongin, M., Ruckman, M.W.: Phys. Rev. B **28** (1983) 6116.
- 83Nyb Nyberg, C., Tengstål, C.G.: Phys. Rev. Lett. **50** (1983) 1680.
- 83Pas Pasco, R.W., Ficalora, P.J.: Surf. Sci. **134** (1983) 476.
- 83Pus Puska, M.J., Nieminen, R.M., Chakraborty, B., Holloway, S., Nørskov, J.K.: Phys. Rev. Lett. **51** (1983) 1083.
- 83Rie1 Rieder, K.H., Wilsch, H.: Surf. Sci. **131** (1983) 245.
- 83Rie2 Rieder, K.H.: Phys. Rev. B **27** (1983) 7799.
- 83Rie3 Rieder, K.H., Baumberger, M., Stocker, W.: Phys. Rev. Lett. **51** (1983) 1799.
- 83Roe Roelofs, L.D., Hu, G.Y., Ying, S.C.: Phys. Rev. B **28** (1983) 6369.
- 83Sch1 Scheffler, M., Bradshaw, A. M. in: *The Chemical Physics of Solid Surfaces and Heterogeneous Catalysis*, Vol. 2, Elsevier, Amsterdam 1983, Ch. 3, p.252 ff
- 83Sch2 Schulze, G., Henzler, M.: Surf. Sci. **124** (1983) 336.
- 83Sin Sinfelt, J. H.: *Bimetallic Catalysis*, Wiley & Sons, New York 1983

- 83Yu Yu, C.-F., Whaley, K.B., Hogg, C.S., Sibener, S.J.: Phys. Rev. Lett. **51** (1983) 2210.
- 84Ang Angonoa, G., Koutecký, J., Ermoshkin, A.N., Pisani, C.: Surf. Sci. **138** (1984) 51.
- 84Bat Batra, I.P., Barker, J.A., Auerbach, D.J.: J. Vac. Sci. Technol. A **2** (1984) 943.
- 84But Butz, R., Oellig, E.M., Ibach, H., Wagner, H.: Surf. Sci. **147** (1984) 343.
- 84Cha1 Chan, C.T., Louie, S.G.: Phys. Rev. B **30** (1984) 4153.
- 84Cha2 Chan, L., Griffin, G.L.: Surf. Sci. **145** (1984) 165.
- 84Cha3 Chabal, Y.J., Raghavachari, K.: Phys. Rev. Lett. **53** (1984) 282.
- 84Cir Ciraci, S., Butz, R., Oellig, E.M., Wagner, H.: Phys. Rev. B **30** (1984) 711.
- 84Con Conrad, H., Scala, R., Stenzel, W., Unwin, R.: J. Chem. Phys. **81** (1984) 6371.
- 84Fro Froitzheim, H., Köhler, U., Lammering, H.: Surf. Sci. **149** (1984) 537.
- 84Hal Hall, R.B., DeSantolo, A.M.: Surf. Sci. **137** (1984) 421.
- 84Ho Ho, P., White, J.M.: Surf. Sci. **137** (1984) 117.
- 84Hor Horlacher Smith, A., Barker, R.A., Estrup, P.J.: Surf. Sci. **136** (1984) 327.
- 84Jac Jackman, T.E., Davies, J.A., Norton, P.R., Unertl, W.N., Griffiths, K.: Surf. Sci. **141** (1984) L313.
- 84Jon Jones, G.J.R., Onuferko, Julia H., Woodruff, D.P., Holland, B.W.: Surf. Sci. **147** (1984) 1.
- 84Joy Joyce, B. A., Foxon, C. T., in: *Chemical Kinetics – Vol. 19 ‘Simple Processes at the Gas – Solid Interface’* (Bamford, C.H., Tipper, C.F.H., Compton, R.G: eds.), Elsevier Amsterdam 1984, Ch. II, p. 181
- 84Mok Mokwa, W., Kohl, D., Heiland, G.: Phys. Rev. B **29** (1984) 6709.
- 84Mor Morris, M.A., Bowker, M., King, D.A., in: *Chemical Kinetics – Vol. 19 ‘Simple Processes at the Gas – Solid Interface’* (Bamford, C.H., Tipper, C.F.H., Compton, R.G: eds.), Elsevier Amsterdam 1984, Ch. I
- 84Nag1 Nagai, K.: Surf. Sci. **136** (1984) L14.
- 84Nag2 Nagai, K., Ohno, Y., Nakamura, T.: Phys. Rev. B **30** (1984) 1461.
- 84Nau Naumovets, A.G., Vedula, Y.S.: Surf. Sci. Rep. **4** (1984) 365.
- 84Nor Nordlander, P., Holloway, S., Nørskov, J.K.: Surf. Sci. **136** (1984) 59.
- 84Oll Ollé, L., Baró, A.M.: Surf. Sci. **137** (1984) 607.
- 84Pen Penka, V., Christmann, K., Ertl, G.: Surf. Sci. **136** (1984) 307.
- 84Rie Rieder, K.H., Stocker, W.: Surf. Sci. **148** (1984) 139.
- 84Say1 Sayers, C.M.: Surf. Sci. **143** (1984) 411.
- 84Say2 Sayers, C.M., Wright, C.J.: J. Chem. Soc. Faraday Trans. I **80** (1984) 1217.
- 84Sie Siegbahn, P.E.M., Blomberg, M.R.A.: J. Chem. Phys. **81** (1984) 1373.
- 84Sur Surnev, L., Tikhov, M.: Surf. Sci. **138** (1984) 40.
- 84Wan Wang, S.C., Gomer, R.: Surf. Sci. **141** (1984) L304.
- 85And Andersson, S., Wilzén, L., Harris, J.: Phys. Rev. Lett. **55** (1985) 2591.
- 85Bic Bickel, N., Heinz, K.: Surf. Sci. **163** (1985) 435.
- 85Car Car, R., Parrinello, M.: Phys. Rev. Lett. **55** (1985) 2471.
- 85Cha1 Chabal, Y., Raghavachari, K.: Phys. Rev. Lett. **54** (1985) 1055.
- 85Cha2 Chabal, Y.J.: Phys. Rev. Lett. **55** (1985) 845.
- 85Chr Christmann, K., Chehab, F., Penka, V., Ertl, G.: Surf. Sci. **152/153** (1985) 356.
- 85Cla Clark, T.: *A Handbook of Computational Chemistry: A Practical Guide to Chemical Structure and Energy Calculations* (Wiley, New York, 1985)
- 85DiN DiNardo, N.J., Plummer, E.W.: Surf. Sci. **150** (1985) 89.
- 85Fel Felter, T.E., Stulen, R.H.: J. Vac. Sci. Technol. **3** (1985) 1566.
- 85Feu Feulner, P., Menzel, D.: Surf. Sci. **154** (1985) 465.
- 85Fre1 Freed, K.F.: J. Chem. Phys. **82** (1985) 5264.
- 85Fre2 Freimuth, H., Wiechert, H.: Surf. Sci. **162** (1985) 432; **178** (1986) 716.
- 85Geo George, S.M., DeSantolo, A.M., Hall, R.B.: Surf. Sci. **159** (1985) L425.
- 85Goo Goodman, D.W., Yates Jr., J.T., Peden, C.H.F.: Surf. Sci. **164** (1985) 417.
- 85Gri Griffiths, K., Norton, P.R., Davies, J.A., Unertl, W.N., Jackman, T.E.: Surf. Sci. **152/153** (1985) 374.
- 85Ham Hamza, A.V., Madix, R.J.: J. Phys. Chem. **89** (1985) 5381.
- 85Heg Hegde, R.I., White, J.M.: Surf. Sci. **157** (1985) 17.

- 85Hof Hofmann, P., Menzel, D.: *Surf. Sci.* **152/153** (1985) 382.
- 85Hol Hollins, P., Pritchard, J.: *Prog. Surf. Sci.* **19** (1985) 275.
- 85Jo Jo, M., Onchi, M., Nishijima, M.: *Surf. Sci.* **154** (1985) 417.
- 85Kel Kellog, G.L.: *Phys. Rev. Lett.* **55** (1985) 2168.
- 85Kno Knor, Z., in: *Physics of Solid Surfaces 1984*, Proceedings of the 3rd Symposium on Surface Physics, Smolenice Castle, Czechoslovakia, J.Koukal, ed: Elsevier Amsterdam 1985, p.781
- 85Kub Kubiak, G.D., Sitz, G.O., Zare, R.N.: *J. Chem. Phys.* **83** (1985) 2538.
- 85Mor1 Moritz, W., Imbihl, R., Behm, R.J., Ertl, G., Matsushima, T.: *J. Chem. Phys.* **83** (1985) 1959.
- 85Mor2 Moritz, W., Wolf, D.: *Surf. Sci.* **163** (1985) L655.
- 85Mus Muscat, J.P.: *Prog. Surf. Sci.* **18** (1985) 59.
- 85Noo NoorBatcha, I., Raff, L.M., Thompson, D.L.: *J. Chem. Phys.* **83** (1985) 1382.
- 85Nor Nordlander, P., Holmberg, C., Harris, J.: *Surf. Sci.* **152/153** (1985) 702.
- 85Pas Passler, M.A., Lee, B.W., Ignatiev, A.: *Surf. Sci.* **150** (1985) 263.
- 85Pat Pate, B.B.: *Surf. Sci.* **165** (1985) 81.
- 85Poe Poelsema, B., Verheij, L.K., Comsa, G.: *Surf. Sci.* **152/153** (1985) 496.
- 85Pus Puska, M.J., Nieminen, R.M.: *Surf. Sci.* **157** (1985) 413.
- 85Rie Rieder, K.H., Stocker, W.: *Surf. Sci.* **164** (1985) 55.
- 85Rob Robota, H.J., Vielhaber, W., Lin, M.C., Segner, J., Ertl, G.: *Surf. Sci.* **155** (1985) 101.
- 85Ste Stensgaard, I., Jakobsen, F.: *Phys. Rev. Lett.* **54** (1985) 711.
- 85Tak Takayanagi, K., Tanishiro, Y., Takahashi, S., Takahashi, M.: *Surf. Sci.* **164** (1985) 367.
- 85Thi Thiry, P.A., Pireaux, J.J., Liehr, M., Caudano, R.: *J. Vac. Sci. Technol. A* **3** (1990) 1439.
- 85Tri Tringides, M., Gomer, R.: *Surf. Sci.* **155** (1985) 254.
- 85Tro Tromp, R.M., Hamers, R.J., Demuth, J.E.: *Phys. Rev. Lett.* **55** (1985) 1303.
- 85Umr Umrigar, C., Wilkins, J.W.: *Phys. Rev. Lett.* **54** (1985) 1551.
- 85Wac Wachs, A.L., Miller, T., Hsieh, T.C., Shapiro, A.P., Chiang, T.-C.: *Phys. Rev. B* **32** (1985) 2326.
- 85Wan Wang, S.C., Gomer, R.: *J. Chem. Phys.* **83** (1985) 4193.
- 85Wei Weinert, M., Davenport, J.W.: *Phys. Rev. Lett.* **54** (1985) 1547.
- 85Yu Yu, C.F., Whaley, K.B., Hogg, C.S., Sibener, S.J.: *J. Chem. Phys.* **83** (1985) 4217.
- 86Arr Arrecis, J.J., Chabal, Y.J., Christman, S.B.: *Phys. Rev. B* **33** (1986) 7906.
- 86Bis Biswas, R., Hamann, D.R.: *Phys. Rev. Lett.* **56** (1986) 2291.
- 86Cha Chan, C.-M., Van Hove, M.A.: *Surf. Sci.* **171** (1986) 226.
- 86Chr Christmann, K., Ehsasi, M., Block, J.H., Hirschwald, W.: *Chem. Phys. Lett.* **131** (1986) 192.
- 86Chu Chung, J.W., Ying, S.C., Estrup, P.J.: *Phys. Rev. Lett.* **56** (1986) 749.
- 86Con1 Conrad, H., Kordesch, M.E., Stenzel, R.W., Sunjić, U., Trninić-Radja, B.: *Surf. Sci.* **178** (1986) 578.
- 86Con2 Conrad, H., Kordesch, M.E., Scala, R., Stenzel, W.: *J. Electron Spectrosc. Relat. Phenom.* **38** (1986) 289.
- 86DeP DePristo, A. E., Lee, C.-Y., Hutson, J. M.: *Surf. Sci.* **169** (1986) 451.
- 86Fel Felter, T.E., Foiles, S.M., Daw, M.S., Stulen, R.H.: *Surf. Sci. Lett.* **171** (1986) L379.
- 86Feu Feulner, P., Pfnür, H., Hofmann, P., Menzel, D.: *Surf. Sci.* **173** (1986) L576.
- 86Gre Greuter, F., Strathy, I., Plummer, E.W., Eberhardt, W.: *Phys. Rev. B* **33** (1986) 736.
- 86Ham Hamers, R.J., Tromp, R.M., Demuth, J.E.: *Phys. Rev. B* **34** (1986) 5343.
- 86Har Harten, U., Toennies, J.P., Wöll, Ch.: *J. Chem. Phys.* **85** (1986) 2249.
- 86Her Herlt, H.-J., Bauer, E.: *Surf. Sci.* **175** (1986) 336.
- 86Kar Karlsson, P.-A., Mårtensson, A.-S., Andersson, S., Nordlander, P.: *Surf. Sci.* **175** (1986) L759.
- 86Koe Koeleman, B.J.J., de Zwart, S.T., Boers, A.L., Poelsema, B., Verheij, L.K.: *Phys. Rev. Lett.* **56** (1986) 1152.
- 86Lau Lauderdale, J.G., Truhlar, D.G.: *J. Chem. Phys.* **84** (1986) 1843.
- 86Lee Lee, C.-Y., DePristo, A.E.: *J. Chem. Phys.* **85** (1986) 4161.
- 86Li Li, Y., Erskine, J.L., Diebold, A.C.: *Phys. Rev. B* **34** (1986) 5951.
- 86Mak1 Mak, C.H., Brand, J.L., Deckert, A.A., George, S.M.: *J. Chem. Phys.* **85** (1986) 1676.
- 86Mak2 Mak, C.H., George, S.M.: *Surf. Sci.* **172** (1986) 509.

- 86Mar Mårtensson, A.S., Nyberg, C., Andersson, S.: Phys. Rev. Lett. **57** (1986) 2045.
- 86Mat Mate, C.M., Somorjai, G.A.: Phys. Rev. B **34** (1986) 7417.
- 86Mul Mullins, D.A., Roop, B., White, J.M.: Chem. Phys. Lett. **129** (1986) 511.
- 86Mus Muscat, J.P.: Phys. Rev. B **33** (1986) 8136.
- 86Nie Niehus, H., Hiller, Chr., Comsa, G.: Surf. Sci. **173** (1986) L599.
- 86Nor Nordlander, P., Holmberg, C., Harris, J.: Surf. Sci. **175** (1986) L753.
- 86Pap Papagno, L., Shen, X.Y., Anderson, J., Schirripa Spagnolo, G., Lapeyre, G.J.: Phys. Rev. B **34** (1986) 7188.
- 86Rag von Ragué Schleyer, P., Pople, J.A.: Chem. Phys. Lett. **129** (1986) 475.
- 86Rie Rieder, K.H., Stocker, W.: Phys. Rev. Lett. **57** (1986) 2548.
- 86Roe Roelofs, L.D., Einstein, T.L., Bartelt, N.C., Shore, J.D.: Surf. Sci. **176** (1986) 295.
- 86Ros Rosina, G., Bertel, E., Netzer, F.P.: Phys. Rev. B **34** (1986) 5746.
- 86Rus Russell Jr., J.N., Chorkendorff, I., Lanzillotto, A.-M., Alvey, M.D., Yates Jr., J.T.: J. Chem. Phys. **85** (1986) 6186.
- 86Sau Sault, A.G., Madix, R.J., Campbell, C.T.: Surf. Sci. **169** (1986) 347.
- 86Sch Schaefer, J.A.: Surf. Sci. **178** (1986) 90.
- 86See Seebauer, E.G., Schmidt, L.D.: Chem. Phys. Lett. **123** (1986) 129.
- 86Tri1 Tringides, M., Gomer, R.: Surf. Sci. **166** (1986) 419.
- 86Tri2 Tringides, M., Gomer, R.: Surf. Sci. **166** (1986) 440.
- 86Ueb Ueba, H.: Prog. Surf. Sci. **22** (1986) 181.
- 86Wha Whaley, K.B., Nitzan, A., Gerber, R.B.: J. Chem. Phys. **84** (1986) 5181.
- 86Wil Willis, R.F.: Ber. Bunsenges. Phys. Chem. **90** (1986) 190.
- 86Woo Woodruff, D. P., Delchar, T. A: *Modern Techniques of Surface Science*, Cambridge University Press, Cambridge 1986, p. 162
- 86Zae Zaera, F., Kollin, E.B., Gland, J.L.: Surf. Sci. **166** (1986) L149.
- 87Alt Altman, M., Chung, J.W., Estrup, P.J., Kosterlitz, J.M., Prybyla, J., Sahu, D., Ying, S.C.: J. Vac. Sci. Technol. A **5** (1987) 1045.
- 87Aue Auerbach, A., Freed, K.F., Gomer, R.: J. Chem. Phys. **86** (1987) 2356.
- 87Bad Baddorf, A.P., Lyo, I.-W., Plummer, E.W., Davis, H.L.: J. Vac. Sci. Technol. A **5** (1987) 782.
- 87Bes Besenbacher, F., Stensgaard, I., Mortensen, K.: Surf. Sci. **191** (1987) 288.
- 87Cha Chadi, D.J.: J. Vac. Sci. Technol. A **5** (1987) 834.
- 87Cho Chou, M.Y., Chelokowski, J.R.: Phys. Rev. Lett. **59** (1987) 1737.
- 87Daw Daw, M.S., Foiles, S.M.: Phys. Rev. B **35** (1987) 2128.
- 87Eng Engstrom, J.R., Tsai, W., Weinberg, W.H.: J. Chem. Phys. **87** (1987) 3104.
- 87Fei1 Feibelman, P.J., Hamann, D.R.: Surf. Sci. **179** (1987) 153.
- 87Fei2 Feibelman, P.J., Hamann, D.R.: Surf. Sci. **182** (1987) 411.
- 87Fei3 Feibelman, P.J., Hamann, D.R.: J. Vac. Sci. Technol. A **5** (1987) 424.
- 87Fer Fernando, G.W., Wilkins, J.W.: Phys. Rev. B **35** (1987) 2995.
- 87Fre Freimuth, H., Wiechert, H., Lauter, H.J.: Surf. Sci. **189/190** (1987) 548.
- 87Gdo Gdowski, G.E., Felter, T.E., Stulen, R.H.: Surf. Sci. **181** (1987) L147.
- 87Ham Hamann, D.R.: J. Electron Spectrosc. Relat. Phenom. **44** (1987) 1.
- 87Imb Imbihl, R., Demuth, J.E., Himpsel, F.J., Marcus, P.M., Thompson, W.A.: Phys. Rev. B **36** (1987) 5037.
- 87Jac1 Jackman, T.E., Griffiths, K., Unertl, W.N., Davies, J.A., Gürtler, K.H., Harrington, D.A., Norton, P.R.: Surf. Sci. **179** (1987) 297.
- 87Jac2 Jackson, B., Metiu, H.: J. Chem. Phys. **86** (1987) 1026.
- 87Kle1 Kleinle, G., Penka, V., Behm, R.J., Ertl, G., Moritz, W.: Phys. Rev. Lett. **58** (1987) 148.
- 87Kle2 Kleinle, G., Skottke, M., Penka, V., Ertl, G., Behm, R.J., Moritz, W.: Surf. Sci. **189/190** (1987) 177.
- 87Kom Komeda, T., Sakisaka, Y., Onchi, M., Kato, H., Masuda, S., Yagi, K.: Phys. Rev. B **36** (1987) 922.
- 87Kre Kress, J. D., DePristo, A. E: J. Chem. Phys. **87** (1987) 4700; **88** (1988) 2596.
- 87Leh Lehwald, S., Voigtländer, B., Ibach, H.: Phys. Rev. B **36** (1987) 2446.

- 87Lin Lindroos, M., Pfnür, H., Feulner, P., Menzel, D.: Surf. Sci. **180** (1987) 237.
- 87Mak1 Mak, C.H., Brand, J.L., Koehler, B.G., George, S.M.: Surf. Sci. **191** (1987) 108.
- 87Mak2 Mak, C.H., Koehler, B.G., Brand, J.L., George, S.M.: J. Chem. Phys. **87** (1987) 2340.
- 87MHa M'Hamed, O., Proix, F., Sébenne, C.: Semicond. Sci. Technol. **2** (1987) 418.
- 87Nic Nichtl, W., Bickel, N., Hammer, L., Heinz, K., Müller, K.: Surf. Sci. **188** (1987) L729.
- 87Nor Nørskov, J.K., Stoltze, P.: Surf. Sci. **189** (1987) 91.
- 87Pan Panas, I., Siegbahn, P., Wahlgren, U.: Chem. Phys. **112** (1987) 325.
- 87Pol Polanyi, J.C.: Science **236** (1987) 680.
- 87Pry Prybyla, J.A., Estrup, P.J., Ying, S.C., Chabal, Y.J., Christman, S.B.: Phys. Rev. Lett. **58** (1987) 1877.
- 87Rei1 Reimer, W., Penka, V., Skottke, M., Behm, R.J., Ertl, G., Moritz, W.: Surf. Sci. **186** (1987) 45.
- 87Rei2 Reimer, W., Fink, Th., Küppers, J.: Surf. Sci. **186** (1987) 55.
- 87Ric1 Richter, Lee J., Ho, W.: J. Vac. Sci. Technol. A **4** (1987) 453.
- 87Ric2 Richter, Lee J., Ho, W.: Phys. Rev. B **36** (1987) 9797.
- 87Sko Skottke, M., Behm, R.J., Ertl, G., Penka, V., Moritz, W.: J. Chem. Phys. **87** (1987) 6191.
- 87Sob Sobyannin, V.A., Zhdanov, V.P.: Surf. Sci. **181** (1987) L163.
- 88Alt Altmann, M.S., Estrup, P.J., Robinson, I.K.: Phys. Rev. B **38** (1988) 5211.
- 88Bas Bassi, D.: in: *Atomic and Molecular Beam Methods* (G. Scoles, ed.), Oxford University Press, Oxford 1988
- 88Bra Brand, J.L., Deckert, A.A., George, S.M.: Surf. Sci. **194** (1988) 457.
- 88Cha Chakarov, D.V., Marinova, Ts.S.: Surf. Sci. **204** (1988) 147.
- 88Chr Christmann, K.: Surf. Sci. Rep. **9** (1988) 1.
- 88Con Conner, Jr., W. C.: in: *Hydrogen Effects in Catalysis* (Z. Páal and P. G. Menon, eds.), M.Dekker, New York 1988, Ch. 12, p.311 ff
- 88Cui Cui, J., Fain, S.C., Freimuth, H., Wiechert, H., Schildberg, H.P., Lauter, H.J.: Phys. Rev. Lett. **60** (1988) 1848.
- 88Dan Daniels, E.A., Lin, J. C., Gomer, R.: Surf. Sci. **204** (1988) 129.
- 88Duc Ducros, R., Fusy, J.: Surf. Sci. **207** (1988) L943.
- 88Ega Egawa, C., Iwasawa, Y.: Surf. Sci. **195** (1988) 43.
- 88Ehs Ehsasi, M., Christmann, K.: Surf. Sci. **194** (1988) 172.
- 88Fan Fang, B.-S., Ballentine, C.A., Erskine, J. L.: Surf. Sci. **204** (1988) L713.
- 88Fer1 Fery, P., Moritz, W., Wolf, D.: Phys. Rev. B **38** (1988) 7275.
- 88Fer2 Fery, P., Moritz, W., Wolf, D.: Z. Kristallogr. **182** (1988) 87.
- 88God Godby, D. J., Somorjai, G.A.: Surf. Sci. **204** (1988) 301.
- 88Ham Hamza, A.V., Kubiak, G.D., Stulen, R.H.: Surf. Sci. **206** (1988) L833.
- 88Har Harris, J.: Appl. Phys. A **47** (1988) 63.
- 88He1 He, J.-W., Harrington, D.A., Griffiths, K., Norton, P.R.: Surf. Sci. **198** (1988) 413.
- 88He2 He, J.-W., Norton, P.R.: Surf. Sci. **195** (1988) L199.
- 88Kax Kaxiras, E., Joannopoulos, J.D.: Phys. Rev. B **37** (1988) 8842.
- 88Koe Koehler, B.G., Mak, C.H., Arthur, D.A., Coon, P.A., George, S.M.: J. Chem. Phys. **89** (1988) 1709.
- 88Kom Komeda, T., Sakisaka, Y., Onchi, M., Kato, H., Suzuki, S., Edamoto, K., Aiura, Y.: Phys. Rev. B **38** (1988) 7349.
- 88Kur Kurz, E. A., Hudson, J. B.: Surf. Sci. **195** (1988) 15; 31.
- 88Mar Mårtensson, A.-S., Nyberg, C., Andersson, S.: Surf. Sci. **205** (1988) 12.
- 88Mor Mortensen, K., Besenbacher, F., Stensgaard, I., Wampler, W.R.: Surf. Sci. **205** (1988) 433.
- 88Mun Mundenar, J.M., Murphy, R., Tsuei, K.D., Plummer, E.W.: Chem. Phys. Lett. **143** (1988) 593.
- 88Oed Oed, W., Puchta, W., Bickel, N., Heinz, K., Nichtl, W., Müller, K.: J. Phys. C **21** (1988) 237.
- 88Pas Pashley, M.D., Haberern, K.W., Friday, W., Woodall, J.M., Kirchner, P.D.: Phys. Rev. Lett. **60** (1988) 2176.
- 88Pau Paul, J.: Phys. Rev. B **37** (1988) 6164.
- 88Ray Ray, A.K., Hira, A.S.: Phys. Rev. B **37** (1988) 9943.

- 88Rei Reimer, W., Fink, Th., Küppers, J.: *Surf. Sci.* **193** (1988) 259.
- 88Ren Rendulic, K.D.: *Appl. Phys. A* **47** (1988) 55.
- 88Reu Reutt, J.E., Chabal, Y.J., Christman, S.B.: *Phys. Rev. B* **38** (1988) 3112.
- 88Ric1 Richter, L.J., Germer, T.A., Sethna, J.P., Ho, W.: *Phys. Rev. B* **38** (1988) 10403.
- 88Ric2 Richter, L.J., Germer, T.A., Ho, W.: *Surf. Sci.* **195** (1988) L182.
- 88See Seebauer, E.G., Kong, A.C.F., Schmidt, L.D.: *J. Chem. Phys.* **88** (1988) 6597.
- 88Tru Truong, T.G., Truhlar, D.G.: *J. Chem. Phys.* **88** (1988) 6611.
- 88Wil Wilzén, L., Andersson, S., Harris, J.: *Surf. Sci.* **205** (1988) 387.
- 88Yan Yang, H., Whitten, J.L.: *J. Chem. Phys.* **89** (1988) 5329.
- 88Zac Zacharias, H.: *Appl. Phys. A* **47** (1988) 37.
- 88Zho Zhou, X.-L., Yoon, C., White, J.M.: *Surf. Sci.* **203** (1988) 53.
- 88Zhu Zhu, X.-Y., Akhter, S., Castro, M.E., White, J.M.: *Surf. Sci.* **195** (1988) L145.
- 89Aln Alnot, P., Cassuto, A., King, D.A.: *Surf. Sci.* **215** (1989) 29.
- 89Ang1 Anger, G., Winkler, A., and Rendulic, K.D.: *Surf. Sci.* **220** (1989) 1.
- 89Ang2 Anger, G., Berger, H.F., Luger, M., Feistritz, S., Winkler, A., Rendulic, K.D.: *Surf. Sci.* **219** (1989) L583.
- 89Att Attard, G.A., King, D.A.: *Surf. Sci.* **223** (1989) 1.
- 89Cac Cacciatore, M., Capitelli, M., Billing, G.D.: *Surf. Sci.* **217** (1989) L391.
- 89Can Cantini, P., Mattera, L., De Kieviet, M.F.M., Jalink, K., Tassistro, C., Terreni, S., Linke, U.: *Surf. Sci.* **211/212** (1989) 872.
- 89Cho Chou, M.Y., Chelikowsky, J.R.: *Phys. Rev. B* **39** (1989) 5623.
- 89Chr Christmann, K.: *Mol. Phys.* **66** (1989) 1.
- 89Cui Cui, J.H., Fain, S.C.: *Phys. Rev. B* **39** (1989) 8628.
- 89Ell Ellis, T.H., Morin, M.: *Surf. Sci.* **216** (1989) L351.
- 89Ern Ernst-Vidalis, M.-L., Bauer, E.: *Surf. Sci.* **215** (1989) 378.
- 89Fel Felter, T.E., Sowa, E.C., Van Hove, M.A.: *Phys. Rev. B* **40** (1989) 891.
- 89Fra Frank, K.H., Dudde, R., Sagner, H.J., Eberhardt, W.: *Phys. Rev. B* **39** (1989) 940.
- 89Gri Grizzi, O., Shi, M., Rabalais, J.W., Rye, R.R., Nordlander, P.: *Phys. Rev. Lett.* **63** (1989) 1408.
- 89Han Hand, M., Holloway, S.: *Surf. Sci.* **211/212** (1989) 940.
- 89Har Harris, J.: *Surf. Sci.* **221** (1989) 335.
- 89Hay Hayden, B.E., Lamont, C.L.A.: *Phys. Rev. Lett.* **63** (1989) 1823.
- 89Lam Lam, P.K., Yu, R.: *Phys. Rev. B* **39** (1989) 5035.
- 89Lau Lauth, G., Schwarz, E., Christmann, K.: *J. Chem. Phys.* **91** (1989) 3729.
- 89Leh Lehnberger, K., Nichtl-Pecher, W., Oed, W., Heinz, K., Müller, K.: *Surf. Sci.* **217** (1989) 511.
- 89Mar Marino, M.M., Ermler, W.C., Tompa, G.S., Seidl, M.: *Surf. Sci.* **208** (1989) 189.
- 89McC McCash, E.M., Parker, S.F., Pritchard, J., Chesters, M.A.: *Surf. Sci.* **215** (1989) 363.
- 89Mic Michl, M., Nichtl-Pecher, W., Oed, W., Landskron, H., Heinz, K., Müller, K.: *Surf. Sci.* **220** (1989) 59.
- 89Nor Nørskov, J.K.: *J. Chem. Phys.* **90** (1989) 7461.
- 89Paf Paffett, M.T., Campbell, C.T., Windham, R.G., Koel, B.E.: *Surf. Sci.* **207** (1989) 274.
- 89Par Parr, R.G., Yang, W.: *Density Functional Theory of Atoms and Molecules* (Oxford, New York, 1989)
- 89Puc Puchta, W., Nichtl, W., Oed, W., Bickel, N., Heinz, K., Müller, K.: *Phys. Rev. B* **39** (1989) 1020.
- 89Ren1 Rendulic, K.D., Anger, G., Winkler, A.: *Surf. Sci.* **208** (1989) 404.
- 89Ren2 Rendulic, K.D., Winkler, A.: *Int. J. Mod. Phys. B* **3** (1989) 941.
- 89Rif Riffe, D.M., Sievers, A.J.: *Surf. Sci.* **210** (1989) L215.
- 89Sin Sinniah, K., Sherman, M.G., Lewis, L.B., Weinberg, W.H., Yates Jr., J.T., Janda, K.C.: *Phys. Rev. Lett.* **62** (1989) 567.
- 89Sun Sun, Y.-K., Weinberg, W.H.: *Surf. Sci.* **214** (1989) L246.
- 89Tru Truong, T.N., Hancock, G., Truhlar, D.G.: *Surf. Sci.* **214** (1989) 523.
- 89Voi Voigtländer, B., Lehwald, S., Ibach, H.: *Surf. Sci.* **208** (1989) 113.

- 89Zho Zhou, X.-L., White, J.M.: *Surf. Sci.* **218** (1989) 201.
- 90Bar Barth, J.V., Brune, H., Ertl, G., Behm, R.J.: *Phys. Rev. B* **42** (1990) 9307.
- 90Ber Berlowitz, P.J., He, J.-W., Goodman, D.W.: *Surf. Sci.* **231** (1990) 315.
- 90Bie Biegelsen, D.K., Bringans, R.D., Northrup, J.E., Swartz, L.E.: *Phys. Rev. B* **41** (1990) 5701.
- 90Bur Burke, M.L., Madix, R.J.: *Surf. Sci.* **237** (1990) 1.
- 90Cam Campbell, C.T.: *Annu. Rev. Phys. Chem.* **41** (1990) 775.
- 90Cha Chabal, Y.J.: *Surf. Sci.* **168** (1986) 594.
- 90Chr Christmann, K.: *J. Vac. Soc. Jpn.* **33** (1990) 549.
- 90Cre Cremaschi, P., Tantardini, G.F., Muilu, J., Pakkanen, T.A.: *Vacuum* **41** (1990) 260.
- 90Dav Davenport, J.W., and Estrup, P.J.: in: *The Chemical Physics of Solid Surfaces and Heterogeneous Catalysis*, (D.A. King and D.P. Woodruff, eds.), Vol. 3A, Elsevier, Amsterdam 1990, p.1
- 90Dre Dreizler, R. M., Gross, E. K. U: *Density Functional Theory* (Springer-Verlag, Berlin 1990)
- 90Ein Einstein, T.L., Daw, M.S., Foiles, S.M.: *Surf. Sci.* **227** (1990) 114.
- 90Ern Ernst, K.-H: *Die geometrischen und elektronischen Strukturen der Adsorbatphasen von Wasserstoff auf der Kobalt(10–10)-Oberfläche*, Dissertation, Freie Universität Berlin 1990
- 90Gol Golchet, A., Poirier, G.E., White, J.M.: *Surf. Sci.* **239** (1990) 42.
- 90Gom Gomer, R.: *Prog. Surf. Sci.* **53** (1990) 917.
- 90Hal Halstead, D., Holloway, S.: *J. Chem. Phys.* **93** (1990) 2859.
- 90Ham Hamza, A.V., Kubiak, G.D., Stulen, R.H.: *Surf. Sci.* **237** (1990) 35.
- 90Hay Hayden, B.E., Lackey, D., Schott, J.: *Surf. Sci.* **239** (1990) 119.
- 90He He, J.-W., Goodman, D.W.: *J. Phys. Chem.* **94** (1990) 1502.
- 90Hig Higashi, G.S., Chabal, Y.J., Trucks, G.W., Raghavachari, K.: *Appl. Phys. Lett.* **56** (1990) 656.
- 90Hir Hira, A.S., Ray, A.K.: *Surf. Sci.* **234** (1990) 397.
- 90Kar Karimi, M., Ila, D., Dalins, I., Vidali, G.: *Surf. Sci. Lett.* **239** (1990) L505.
- 90Kir Kirsten, E., Parschau, G., Stocker, W., Rieder, K.H.: *Surf. Sci. Lett.* **231** (1990) L183.
- 90Kou Koulmann, J.J., Ringeisen, F., Alaoui, M., Bolmont, D.: *Phys. Rev. B* **41** (1990) 3878.
- 90Lie1 Liehr, M., Greenlief, C.M., Offenber, M., Kasi, S.R.: *J. Vac. Sci. Technol. A* **8** (1990) 2960.
- 90Lie2 Liepold, S., Elbel, N., Michl, M., Nichtl-Pecher, W., Heinz, K., Müller, K.: *Surf. Sci.* **240** (1990) 81.
- 90Lou Lou, L., Langreth, D.C., Nordlander, P.: *Surf. Sci.* **234** (1990) 412.
- 90Nic Nichtl-Pecher, W., Oed, W., Landskron, H., Heinz, K., Müller, K.: *Vacuum* **41** (1990) 297.
- 90Nie Nielsen, U., Halstead, D., Holloway, S., Nørskov, J.K.: *J. Chem. Phys.* **93** (1990) 2879.
- 90Nor Nørskov, J.K.: *Prog. Surf. Sci.* **53** (1990) 1253.
- 90Pap Papai, I., Salahub, D.R., Mijoule, C.: *Surf. Sci.* **236** (1990) 241.
- 90Par1 Parschau, G., Kirsten, E., Rieder, K.H.: *Surf. Sci.* **225** (1990) 367.
- 90Par2 Parker, D.H., Jones, M.E., Koel, B.E.: *Surf. Sci.* **233** (1990) 65.
- 90Rae Raeker, T.J., DePristo, A.E.: *Surf. Sci.* **235** (1990) 84.
- 90Ran Rangelov, G., Memmel, N., Bertel, E., Dose, V.: *Surf. Sci.* **236** (1990) 250.
- 90Ray Ray, K.B., Hannon, J.B., Plummer, E.W.: *Chem. Phys. Lett.* **171** (1990) 469.
- 90Sch Schmiedl, R., Nichtl-Pecher, W., Heinz, K., Müller, K., Christmann, K.: *Surf. Sci.* **235** (1990) 186.
- 90Sin Sinniah, K., Sherman, M.G., Lewis, L.B., Weinberg, W.H., Yates Jr., J.T., Janda, K.C.: *J. Chem. Phys.* **92** (1990) 5700.
- 90Spi Spitzl, R., Niehus, H., Poelsema, B., Comsa, G.: *Surf. Sci.* **239** (1990) 243.
- 90Sta Stauffer, L., Riedinger, R., Dreyssé, H.: *Surf. Sci.* **238** (1990) 83.
- 90Ste Stenzel, W., Jahnke, S.A., Song, Y., Conrad, H.: *Prog. Surf. Sci.* **35** (1990) 159.
- 90Zac Zacharias, H.: *Int. J. Mod. Phys. B* **4** (1990) 45.
- 91Ben Benziger J.B.: in: *Metal – Surface Reaction Energetics* (Shustorovich, E: ed.), Verlag Chemie Weinheim 1979, Ch. 2, p. 65
- 91Ber1 Berger, H.F., Rendulic, K.D.: *Surf. Sci.* **253** (1991) 325.
- 91Ber2 Berger, H.F., Rendulic, K.D.: *Surf. Sci.* **251/252** (1991) 882.
- 91Bol1 Boland, J.J.: *Surf. Sci.* **244** (1991) 1.

- 91Bol2 Boland, J.J.: Phys. Rev. Lett. **67** (1991) 1539.
- 91Cam Campbell, J.M., Campbell, C.T.: Surf. Sci. **259** (1991) 1.
- 91Can Canepa, M., Cantini, P., Cavanna, E., Mattera, L., Tarditi, V., Terreni, S.: Surf. Sci. **251/252** (1991) 1142.
- 91Cha Chabal, Y.J.: Chem. Phys. Lett. **181** (1991) 537.
- 91Cho Chorkendorff, I., Rasmussen, P.B.: Surf. Sci. **248** (1991) 35.
- 91Chr Christmann, K.: *Introduction to Surface Physical Chemistry*, Steinkopff-Verlag Darmstadt 199
- 91Dum Dumas, P., Chabal, Y.J.: Chem. Phys. Lett. **181** (1991) 537.
- 91Gro Groß, G., Rieder, K.H.: Surf. Sci. **241** (1991) 33.
- 91Har Hara, M., Domen, K., Onishi, T., Nozoye, H.: J. Phys. Chem. **95** (1991) 6.
- 91Hay Hayden, B.E., Lamont, C.L.A.: Surf. Sci. **243** (1991) 31.
- 91Hsu Hsu, C.-H., Larson, B.E., El-Batanouny, M., Willis, C.R.: Phys. Rev. Lett. **66** (1991) 3164.
- 91Iba Ibach, H.: *Electron Energy Loss Spectrometers – The Technology of High Performance*, Springer-Verlag Berlin, Heidelberg, New York 1991
- 91Joh Johnson, A.D., Maynard, K.J., Dayley, S.P., Yang, Q.Y., Ceyer, C.T.: Phys. Rev. Lett. **67** (1991) 927.
- 91Kir Kirsten, E., Parschau, G., Rieder, K.H.: Chem. Phys. Lett. **188** (1991) 544.
- 91Kon Kondoh, H., Nishihara, C., Nozoye, H., Hara, M., Domen, K.: Chem. Phys. Lett. **187** (1991) 466.
- 91Küc Küchenhoff, S., Brenig, W., Chiba, Y.: Surf. Sci. **245** (1991) 389.
- 91Lin Lin, T.-S., Gomer, R.: Surf. Sci. **255** (1991) 41.
- 91Mar Maruyama, T., Sikasaka, Y., Kato, H., Aiura, Y., Yanashima, H.: Surf. Sci. **253** (1991) 147.
- 91Mic Michelsen, H.A., Auerbach, D.J.: J. Chem. Phys. **94** (1991) 7502.
- 91Mij Mijoule, C., Russier, V.: Surf. Sci. **254** (1991) 329.
- 91Mit Mitsuda, Y., Yamada, T., Chuang, T.J., Seki, H., Chin, R.P., Huang, J.Y., Shen, Y.R.: Surf. Sci. Lett. **257** (1991) L633.
- 91Mor Mortensen, K., Chen, D.M., Bedrossian, P.J., Golovchenko, J.A., Besenbacher, F.: Phys. Rev. B **43** (1991) 1816.
- 91Nic1 Nichtl-Pecher, W., Stammer, W., Heinz, K., Müller, K.: Phys. Rev. B **43** (1991) 6946.
- 91Nic2 Nichtl-Pecher, W., Gossmann, J., Stammer, W., Besold, G., Hammer, L., Heinz, K., Müller, K.: Surf. Sci. **249** (1991) 61.
- 91Par Parschau, G., Kirsten, E., Rieder, K.H.: Phys. Rev. B **43** (1991) 12216.
- 91Pen1 Pennemann, B., Oster, K., Wandelt, K.: Surf. Sci. **249** (1991) 35.
- 91Pen2 Pennemann, B., Oster, K., Wandelt, K.: Surf. Sci. **251/252** (1991) 877.
- 91Per Perdew, J.P.: Physica B **172** (1991) 1.
- 91Rou Roux, C., Bu, H., Rabalais, J.W.: Surf. Sci. **259** (1991) 253.
- 91Sok Sokolowski, M., Koch, T., Pfnür, H.: Surf. Sci. **243** (1991) 261.
- 91Spr Sprunger, P.T., Plummer, E.W.: Chem. Phys. Lett. **187** (1991) 559.
- 91Ste Stenzel, W., Jahnke, S.A., Song, Y., Conrad, H.: Prog. Surf. Sci. **35** (1991) 159.
- 91Win Winkler, A., Požgainer, G., Rendulic, K.D.: Surf. Sci. **251-252** (1991) 886.
- 91Wis Wise, M.L., Koehler, B.G., Gupta, P., Coon, P.A., George, S.M.: Surf. Sci. **258** (1991) 166.
- 91Zhe Zheng, X.M., Smith, P.V.: Surf. Sci. **256** (1991) 1.
- 92AIS Al-Sarraf, N., Stuckless, J.T., King, D.A.: Nature (London) **360** (1992) 243.
- 92Ast Astaldi, C., Bianco, A., Modesti, S., Tosatti, E.: Phys. Rev. Lett. **68** (1992) 90.
- 92Atl Atli, A., Alnot, M., Ehrhardt, J.J., Bertolini, J.C., Abon, M.: Surf. Sci. **269/270** (1992) 365.
- 92Baf Baffali, R., Bell, A.T.: Surf. Sci. **278** (1992) 353.
- 92Ber1 Berger H.F., Grösslinger, E., Rendulic, K.D.: Surf. Sci. **261** (1992) 313.
- 92Ber2 Berger, H.F., Resch, Ch., Grösslinger, E., Eilmsteiner, G., Winkler, A., Rendulic, K.D.: Surf. Sci. Lett. **275** (1992) L627.
- 92Chi Chin, R.P., Huang, J.Y., Shen, Y.R., Chuang, T.J., Seki, H., Buck, M.: Phys. Rev. B **45** (1992) 1522.
- 92Cho Cho, J., Nemanich, R.J.: Phys. Rev. B **46** (1992) 12421.
- 92Eng Engdahl, C., Lundqvist, B.I., Nielsen, U., Nørskov, J.K.: Phys. Rev. B **45** (1992) 11362.

- 92Hel Held, G., Pfnür, H., Menzel, D.: *Surf. Sci.* **271** (1992) 21.
- 92Hul1 Hulpke, E., Lüdecke, J.: *Phys. Rev. Lett.* **68** (1992) 2846.
- 92Hul2 Hulpke, E., Lüdecke, J.: *Surf. Sci.* **272** (1992) 289.
- 92Kev Kevan, S.D. (ed.), *Angle-resolved Photoemission – Theory and Current Applications*, Elsevier, Amsterdam, London 1992
- 92Kna Knauff, O., Grosche, U., Wesner, D.A., Bonzel, H.P.: *Surf. Sci.* **277** (1992) 132.
- 92Kon Kondoh, H., Hara, M., Domen, K., Nozoye, H.: *Surf. Sci. Lett.* **268** (1992) L287.
- 92Lee Lee, A., Zhu, D., Deng, L., Linke, U.: *Phys. Rev B* **46** (1992) 15472.
- 92Lio Liotard, D.A.: *Int. J. Quantum Chem.* **44** (1992) 723.
- 92Lut Lutsishin, P.P., Panchenko, O.A., Shpagin, V.F.: *Surf. Sci.* **278** (1992) 218.
- 92Man Mann, S.S., Seto, T., Barnes, C.J., King, D.A.: *Surf. Sci.* **261** (1992) 155.
- 92Mor Moritz, W., Zuschke, R., Pflanz, S., Wever, J., Wolf, D.: *Surf. Sci.* **272** (1992) 94.
- 92Nic Nichtl-Pecher, W., Gossmann, J., Hammer, L., Heinz, K., Müller, K.: *J. Vac. Sci. Technol. A* **10** (1992) 501.
- 92Per Perdew, J.P., Chevary, J.A., Vosko, S.H., Jackson, K.A., Pederson, M.R., Singh, D.J., Fiolhais, C.: *Phys. Rev. B* **46** (1992) 6671; **48** (1993) 4978(E)
- 92Ren Rendulic, K.D.: *Surf. Sci.* **272** (1992) 34.
- 92Ret1 Rettner, C.T., Auerbach, D.J., Michelsen, H.A.: *Phys. Rev. Lett.* **68** (1992) 1164.
- 92Ret2 Rettner, C.T., Auerbach, D.J., Michelsen, H.A.: *Phys. Rev. Lett.* **68** (1992) 2547.
- 92Sch1 Schmidt, G., Zagel, H., Landskron, H., Heinz, K., Müller, K., Pendry, J.B.: *Surf. Sci.* **271** (1992) 416.
- 92Sch2 Schlapbach, L.: in: *Hydrogen in Intermetallic Compounds II* (L. Schlapbach, ed.), Topics in Applied Physics Vol. 67 (Springer Berlin 1992)
- 92She Shern, C.S.: *Surf. Sci.* **264** (1992) 171.
- 92Tho Thomas, R.E., Rudder, R.A., Markunas, R.J.: *J. Vac. Sci. Technol. A* **10** (1992) 2451.
- 92Zhu Zhu, X.D., Lee, A., Wong, A., Linke, U.: *Phys. Rev. Lett.* **68** (1992) 1862.
- 93Aiu Aiura, Y., Yanashima, H., Fukutani, H., Kato, H., Sakisaka, Y., Maruyama, T., Edamoto, K.: *Surf. Sci.* **283** (1993) 344.
- 93Aiz Aizawa, T., Ando, T., Kamo, M., Sato, Y.: *Phys. Rev. B* **48** (1993) 18348.
- 93All Allers, K.-H., Pfnür, H., Feulner, P., Menzel, D.: *Surf. Sci.* **286** (1993) 297.
- 93And Andersson, S., Persson, M.: *Phys. Rev. Lett.* **70** (1993) 202.
- 93Aue Auerbach D.J., Rettner, C.T., Michelsen, H.A.: *Surf. Sci.* **283** (1993) 1.
- 93Bis Bischler, U., Sandl, P., Bertel, E., Brunner, T., Brenig, W.: *Phys. Rev. Lett.* **70** (1993) 3603.
- 93Bol Boland, J.J.: *Adv. Phys.* **42** (1993) 129.
- 93DEv D'Evelyn, M.P., Cohen, S.M., Rouchouze, E., Yang, Y.L.: *J. Chem. Phys.* **98** (1993) 3560.
- 93Far Farias, D., Eckert, I., Burg, B., Rieder, K.H.: *Surf. Sci.* **297** (1993) 162.
- 93Flo Flowers, M.C., Jonathan, N.B.H., Liu, Y., Morris, A.: *J. Chem. Phys.* **99** (1993) 7038.
- 93Goe Goerge, J., Zeppenfeld, P., David, R., Büchel, M., Comsa, G.: *Surf. Sci.* **289** (1993) 201.
- 93Gru Gruyters, M., Jacobi, K.: *J. Electron Spectrosc. Relat. Phenom.* **64** (1993) 591.
- 93Ham Hammer, B., Jacobsen, K.W., Nørskov, J.K.: *Phys. Rev. Lett.* **70** (1993) 3971.
- 93Ham1 Hammer, L., Landskron, H., Nichtl-Pecher, W., Fricke, A., Heinz, K., Müller, K.: *Phys. Rev. B* **47** (1993) 15969.
- 93Ham2 Hammer, L., Nichtl-Pecher, W., Elbel, N., Stämmler, W., Heinz, K., Müller, K.: *Surf. Sci.* **287/288** (1993) 84.
- 93Hei Heitzinger, J.M., Avoyan, A., Koel, B.E.: *Surf. Sci.* **294** (1993) 251.
- 93Hul Hulpke, E., Lüdecke, J.: *Surf. Sci.* **287/288** (1993) 837.
- 93Klo Klötzer, B., Bechtold, E.: *Surf. Sci.* **295** (1993) 374.
- 93Kre1 Kresse, G., Hafner, J.: *Phys. Rev. B* **47** (1993) RC558.
- 93Kre2 Kresse, G., Hafner, J.: *Phys. Rev. B* **48** (1993) 13115.
- 93Lee Lee, S.-T., Apai, G.: *Phys. Rev. B* **48** (1993) 2684.
- 93Len Lenz, P., Christmann, K.: *J. Catal.* **139** (1993) 611.
- 93Li Li, D., Zhang, J., Dowben, P.A.: *Phys. Rev. B* **48** (1993) 5612.
- 93Lop Lopinski, G.P., Prybyla, J.A., Estrup, P.J.: *Surf. Sci.* **296** (1993) 9.
- 93Mue Müller, K.: *Prog. Surf. Sci.* **42** (1993) 245.

- 93Nyb Nyberg, C., Svensson, K., Mårtensson, A.-S., Andersson, S.: *J. Electron Spectrosc. Relat. Phenom.* **64/65** (1993) 51.
- 93Oni Onishi, H., Aruga, T., Iwasawa, Y.: *Surf. Sci.* **283** (1993) 213.
- 93Par1 Park, Y.-S., Bang, J.-S., Lee, J.: *Surf. Sci.* **283** (1993) 209.
- 93Par2 Park, Y.-S., Kim, J.-Y., Lee, J.: *J. Chem. Phys.* **98** (1993) 757.
- 93Pen del Pennino, U., Mariani, C., Amoddeo, A., Proix, F., Sébenne, C.: *J. Electron Spectrosc. Relat. Phenom.* **64/65** (1993) 491.
- 93Ras Rasmussen, P.B., Holmblad, P.M., Christoffersen, H., Taylor, P.A., Chorkendorff, I.: *Surf. Sci.* **287/288** (1993) 79.
- 93Ric Rick, S.W., Lynch, D.L., Doll, J.D.: *J. Chem. Phys.* **99** (1993) 8183.
- 93Saa Saalfrank, P., Miller, W.H.: *J. Chem. Phys.* **98** (1993) 9040.
- 93San1 Sandl, P., Bischler, U., Bertel, E.: *Surf. Sci.* **291** (1993) 29.
- 93San2 Sandhoff, M., Pfnür, H., Everts, H.-U.: *Surf. Sci.* **280** (1993) 185.
- 93Sch Schmid, M., Stadler, H., Varga, P.: *Phys. Rev. Lett.* **70** (1993) 1441.
- 93Spr Sprunger, P.T., Plummer, E.W.: *Phys. Rev. B* **48** (1993) 14436.
- 93Stu Stumpf, R., Marcus, P.M.: *Phys. Rev. B* **47** (1993) 16016.
- 93Wu Wu, C.J., Ionova, I.V., Carter, E.A.: *Surf. Sci.* **295** (1993) 64.
- 93Ye Ye, L., Freeman, A.J., Delley, B.: *Phys. Rev. B* **48** (1993) 11107.
- 94Atl Atli, A., Abon, M., Bertolini, J.C., Boudeville, Y., Fallavier, M., Benmansour, M., Thomas, J.P.: *J. Phys. Chem.* **98** (1994) 4895.
- 94Bal Balden, M., Lehwald, S., Ibach, H., Mills, D.L.: *Phys. Rev. Lett.* **73** (1994) 854.
- 94Ben Benedek, G., Toennies, J.P.: *Surf. Sci.* **299/300** (1994) 587.
- 94Bre Brenig, W., Groß, A., Russ, P.: *Z. Phys. B* **96** (1994) 231.
- 94Dai Dai, J.Q., Sheng, J., Zhang, J.Z.H.: *J. Chem. Phys.* **101** (1994) 1555.
- 94Dav Davidson, B.N., Pickett, W.E.: *Phys. Rev. B* **49** (1994) 11253.
- 94Ehr Ehrlich, G.: *Surf. Sci.* **299/300** (1994) 628.
- 94Ern Ernst, K.H., Schwarz, E., Christmann, K.: *J. Chem. Phys.* **101** (1994) 5388.
- 94Fal Fallavier, M., Benmansour, M., Hjørvarsson, B., Thomas, J.P., Abon, M., Atli, H.A., Bertolini, J.C.: *Surf. Sci.* **311** (1994) 24.
- 94Gro Groß, A., Hammer, B., Scheffler, M., and Brenig, W.: *Phys. Rev. Lett.* **73** (1994) 3121.
- 94Har Harrison, W.A.: *Surf. Sci.* **299-300** (1994) 298.
- 94Hol Holloway, S.: *Surf. Sci.* **299-300** (1994) 656.
- 94Kol Kolasinski, K.W., Nessler, W., de Meijere, A., Hasselbrink, E.: *Phys. Rev. Lett.* **72** (1994) 1356.
- 94Kra Kratzer, P., Hammer, B., Nørskov, J.K.: *Chem. Phys. Lett.* **229** (1994) 645.
- 94Kre1 Kresse, G., Hafner, J.: *Phys. Rev. B* **49** (1994) 14251.
- 94Kre2 Kreuzer, H.J., Jun, Z., Payne, S.H., Nichtl-Pecher, W., Hammer, L., Müller, K.: *Surf. Sci.* **303** (1994) 1.
- 94Kum Kumar, S., Jackson, B.: *J. Chem. Phys.* **100** (1994) 5956.
- 94Lan Landemark, E., Karlsson, C.J., Johansson, L.S.O., Uhrberg, R.I.G.: *Phys. Rev. B* **49** (1994) 16523.
- 94Lee Lee, G., Sprunger, P.T., Plummer, E.W.: *J. Vac. Sci. Technol. A* **12** (1994) 2119.
- 94Lin Linke, R., Schneider, U., Busse, H., Becker, C., Schröder, U., Castro, G.R., Wandelt, K.: *Surf. Sci.* **309** (1994) 407.
- 94Lop Lopinski, G.P., Prybyla, J.A., Estrup, P.J.: *Surf. Sci.* **315** (1994) 269.
- 94Mue Müssig, H.-J., Stenzel, W., Song, Y., Conrad, H.: *Surf. Sci.* **311** (1994) 295.
- 94Ple Plesanovas, A., Castellani Tarabini, A., Abbati, I., Kaciulis, S., Paolicelli, G., Pasquali, L., Ruocco, A., Nannarone, S.: *Surf. Sci.* **307-309** (1994) 890.
- 94Ren Rendulic, K.D., Winkler, A.: *Surf. Sci.* **299-300** (1994) 261.
- 94Rie Rieder, K.H.: *Surf. Rev. Lett.* **1** (1994) 51.
- 94Roh Rohwerder, M., Benndorf, C.: *Surf. Sci.* **307-309** (1994) 789.
- 94Shi Shi, H., Jacobi, K.: *Surf. Sci.* **313** (1994) 289.
- 94Spr Sprunger, P.T., Plummer, E.W.: *Surf. Sci.* **307-309** (1994) 118.
- 94Tho Thoms, B.D., Butler, J.E.: *Phys. Rev. B* **50** (1994) 17450.

- 94Tul Tully, J.C.: Surf. Sci. **299-300** (1994) 667.
- 94Wei van der Weide, J., Zhang, Z., Baumann, P.K., Wensell, M.G., Bernholc, J., Nemanich, R.J.: Phys. Rev. B **50** (1994) 5803.
- 94Whi White, J.A., Bird, D.M., Payne, M.C., Stich, I.: Phys. Rev. Lett. **73** (1994) 1404.
- 94Wil1 Wilke, S., Hennig, D., Löber, R., Methfessel, M., Scheffler, M.: Surf. Sci. **307-309** (1994) 76.
- 94Wil2 Wilke, S., Hennig, D., Löber, R.: Phys. Rev. B **50** (1994) 2548.
- 95Ape1 Apel, R., Farias, D., Rieder, K.H.: Surf. Rev. Lett. **2** (1995) 153.
- 95Ape2 Apel, R., Farias, D., Tröger, H., Rieder, K.H.: Surf. Sci. **331-333** (1995) 57.
- 95Ave Avery, A.R., Holmes, D.M., Sudijono, J., Jones, T.S., Joyce, B.A.: Surf. Sci. **323** (1995) 91.
- 95Beu1 Beutl, M., Riedler, M., Rendulic, K.: Chem. Phys. Lett. **247** (1995) 249.
- 95Beu2 Beutl, M., Rendulic, K., Castro, G.R.: J. Chem. Soc. Faraday Trans. **91** (1995) 3639.
- 95Bir Birkenheuer, U., Boettger, J.C., Rösch, N.: Surf. Sci. **341** (1995) 103.
- 95Bla Blaha, P., Schwarz, K., Dufek, P., Augustyn, R.: *"WIEN95" A full potential linearized Augmented Plane Wave Package for Calculating Crystal Properties*, Technical University Vienna, Austria, 1995
- 95Bra Bratu, P., Höfer, U.: Phys. Rev. Lett. **74** (1995) 1625.
- 95Cot Cottrell, C., Bowker, M., Hodgson, A., Worthy, G.: Surf. Sci. **325** (1995) 57.
- 95Cre Cremaschi, P., Yang, H., Whitten, J.L.: Surf. Sci. **330** (1995) 255.
- 95Dai Dai, D., Liao, D.W., Balasubramanian, K.: J. Chem. Phys. **102** (1995) 7530.
- 95Dan Daniels, E.A., Gomer, R.: Surf. Sci. **336** (1995) 245.
- 95Dar Darling G.R., Holloway, S.: Prog. Surf. Sci. **58** (1995) 1595.
- 95Dix Dixon-Warren, St.J., Pasteur, A.T., King, D.A.: J. Chem. Phys. **103** (1995) 2261.
- 95Fri Frieß, W., Schlichting, H., Menzel, D.: Phys. Rev. Lett. **74** (1995) 1147.
- 95Gro1 Groß, A., Wilke, S., Scheffler, M.: Phys. Rev. Lett. **75** (1995) 2718.
- 95Gro2 Groß, A.: J. Chem. Phys. **102** (1995) 5045.
- 95Ham1 Hammer, B., Scheffler, M.: Phys. Rev. Lett. **74** (1995) 3487.
- 95Ham2 Hammer, B., Nørskov, J.K.: Nature (London) **376** (1995) 238.
- 95Han Hanbicki, A.T., Baddorf, A.P., Plummer, E.W., Hammer, B., Scheffler, M.: Surf. Sci. **331-333** (1995) 811.
- 95Has Hassold, E., Löffler, U., Schmiedl, R., Grund, M., Hammer, L., Heinz, K., Müller, K.: Surf. Sci. **326** (1995) 93.
- 95Hea Healey, F., Carter, R.N., Hodgson, A.: Surf. Sci. **328** (1995) 67.
- 95Hu Hu, X., Liu, Z.: Phys. Rev. B **52** (1995) 11467.
- 95Jin Jing, Z., Whitten, J.L.: J. Chem. Phys. **102** (1995) 3867.
- 95Koh Kohler, B., Ruggerone, P., Wilke, S., Scheffler, M.: Phys. Rev. Lett. **74** (1995) 1387.
- 95Kol1 Kołasinski, K.W., Nessler, W., Bornscheuer, K.-H., Hasselbrink, E.: Surf. Sci. **331-333** (1995) 485.
- 95Kol2 Kołasinski, K.W.: Int. J. Mod. Phys. B **9** (1995) 2753.
- 95Lam Lamont, C.L.A., Persson, B.N.J., Williams, G. P.: Chem. Phys. Lett. **243** (1995) 429.
- 95Lee Lee, G., Plummer, E.W.: Phys. Rev. B **51** (1995) 7250.
- 95Lim Lim, H., Cho, K., Park, I., Joannopoulos, J.D., Kaxiras, E.: Phys. Rev. B **52** (1995) 17231.
- 95Mus Muschiol, U., Lenz, J., Schwarz, E., Christmann, K.: Surf. Sci. **331-333** (1995) 127.
- 95Pas Pasteur, A.T., Dixon-Warren, St.J., King, D.A.: J. Chem. Phys. **103** (1995) 2251.
- 95Peh Pehlke, E., Scheffler, M.: Phys. Rev. Lett. **74** (1995) 953.
- 95Qi Qi, H., Gee, P.E., Nguyen, T., Hicks, R.F.: Surf. Sci. **323** (1995) 6.
- 95Rom Romainczyk, Ch., Manson, J.R., Kern, K., Kuhnke, K., Davod, R., Zeppenfeld, P., Comsa, G.: Surf. Sci. **336** (1995) 362.
- 95Sch1 Schmiedl, R., Nichtl-Pecher, W., Hammer, L., Heinz, K., Müller, K.: Surf. Sci. **324** (1995) 289.
- 95Sch2 Scholz, S. M., Schreiner, J., Jacobi, K.: Surf. Sci. **331 – 333** (1995) 402
- 95Sta Stauffer, L., Ezzehar, H., Bolmont, D., Chelly, R., Koulmann, J.J., Minot, C.: Surf. Sci. **342** (1995) 206.
- 95Wit Witte, G., Toennies, J.P., Wöll, Ch.: Surf. Sci. **323** (1995) 228.

- 95Yos Yoshinobu, J., Tanaka, H., Kawai, M.: Phys. Rev. **B51** (1995) 4529.
- 96Ape Apel, R., Farias, D., Tröger, H., Kirsten, E., Rieder, K.H.: Surf. Sci. **364** (1996) 303.
- 96Bal Balden, M., Lehwald, S., Ibach, H.: Phys. Rev. B **53** (1996) 7479.
- 96Beu Beutl, M., Riedler, M., Rendulic, K. D.: Chem. Phys. Lett. **256** (1996) 33.
- 96Bra Bratu, P., Brenig, W., Groß, A., Hartmann, M., Höfer, U., Kratzer, P., Russ, R.: Phys. Rev. B **54** (1996) 5978.
- 96Cas Castro, G.R., Drakova, D., Grillo, M.E., Doyen, G.: J. Chem. Phys. **105** (1996) 9640.
- 96Col Colonell, J.L., Curtiss, T.J., Sibener, S.J.: Surf. Sci. **366** (1996) 19.
- 96Die Diederich, L., Küttel, O.M., Schaller, E., Schlapbach, L.: Surf. Sci. **349** (1996) 176.
- 96Eic Eichler, A., Kresse, G., Hafner, J.: Phys. Rev. Lett. **77** (1996) 1119.
- 96Gro Groß, A.: Surf. Sci. **363** (1996) 1.
- 96Han Hansen, D.A., Halbach, M.R., Seebauer, E.G.: J. Chem. Phys. **104** (1996) 7338.
- 96Hei Heinz, K., Hammer, L.: Z. Phys. Chem. **197** (1996) 173.
- 96Hoe Höfer, U.: Appl. Phys. A **63** (1996) 533.
- 96Iwa Iwai, H., Fukutani, K., Murata, Y.: Surf. Sci. **357-358** (1996) 663.
- 96Jan Janin, E., Bjorkqvist, M., Grehk, T.M., Gothelid, M., Pradier, C.M., Karlsson, U.O., Rosengren, A.: Appl. Surf. Sci. **99** (1996) 371.
- 96Kam Kampshoff, E., Waelchli, N., Menck, A., Kern, K.: Surf. Sci. **360** (1996) 55.
- 96Koh Kohler, B., Wilke, S., Scheffler, M., Kouba, R., Ambrosch-Draxl, C.: Comput. Phys. Commun. **94** (1996) 31.
- 96Kon Kondoh, H., Nozoye, H.: Surf. Sci. **364** (1996) 287.
- 96Kra Kratzer, P., Russ, R., Brenig, W.: Surf. Sci. **345** (1996) 125.
- 96Lau Lauterbach, J., Schick, M., Weinberg, W.H.: J. Vac. Sci. Technol. A **14** (1996) 1511.
- 96Lee Lee, G., Poker, D.B., Zehner, D.M., Plummer, E.W.: Surf. Sci. **357-358** (1996) 717.
- 96Mer Merrill, P.B., Madix, R.J.: Surf. Sci. **347** (1996) 249.
- 96Nog Noguez, C., Beitia, C., Preyss, W., Schkrebti, A.I., Roy, M., Borensztein, Y., Del Sole, R.: Phys. Rev. Lett. **76** (1996) 4923.
- 96Pau Paul, J.-F., Sautet, P.: Surf. Sci. **356** (1996) L403.
- 96Per Perdew, J.P., Burke, K., Ernzerhof, M.: Phys. Rev. Lett. **77** (1996) 3865.
- 96Sch Schilbe, P., Siebentritt, S., Pues, R., Rieder, K.-H.: Surf. Sci. **360** (1996) 157.
- 96Stu Stumpf, R.: Phys. Rev. B **53** (1996) R4253.
- 96Tak Takagi, N., Yasui, Y., Takaoka, T., Sawada, M., Yanagita, H., Aruga, T., Nishijima, M.: Phys. Rev. B **53** (1996) 13767.
- 96Tro Trost, J., Zambelli, T., Wintterlin, J., Ertl, G.: Phys. Rev. B **54** (1996) 17850.
- 96Whi White, J.A., Bird, D.M., Payne, M.C.: Phys. Rev. B **53** (1996) 1667.
- 96Wil Wilke, H., Scheffler, M.: Phys. Rev. B **53** (1996) 4926.
- 96Zam Zambelli, T., Trost, J., Wintterlin, J., Ertl, G.: Phys. Rev. Lett. **76** (1996) 795.
- 97Arn1 Arnold, M., Sologub, S., Frie, W., Hammer, L., Heinz, K.: J. Phys. C **9** (1997) 6481.
- 97Arn2 Arnold, M., Sologub, S., Hupfauer, G., Bayer, P., Frie, W., Hammer, L., Heinz, K.: Surf. Rev. Lett. **4** (1997) 1291.
- 97Arn3 Arnold, M., Hupfauer, G., Bayer, P., Hammer, L., Heinz, K., Kohler, B., Scheffler, M.: Surf. Sci. **382** (1997) 288.
- 97Bae Baer, R., Kosloff, R.: J. Chem. Phys. **106** (1997) 8862.
- 97Bei Beitia, C., Preyss, W., Del Sole, R., Borensztein, Y.: Phys. Rev. B **56** (1997) R4371.
- 97Cao Cao, G.X., Nabighian, B., Zhu, X.D.: Phys. Rev. Lett. **79** (1997) 3696.
- 97Don1 Dong, W., Hafner, J.: Phys. Rev. B **56** (1997) 15396.
- 97Don2 Dong, W., Ledentu, V., Sautet, P., Kresse, G., Hafner, J.: Surf. Sci. **377** (1997) 56.
- 97Eic Eichler, A., Hafner, J., Kresse, G.: Surf. Rev. Lett. **4** (1997) 1297.
- 97Far Farias, D., Siebentritt, S., Apel, R., Pues, R., Rieder, K.H.: J. Chem. Phys. **106** (1997) 8254.
- 97Gay Gayone, J.E., Pregliasco, R.G., Gómez, G.R., Sánchez, E.A., Grizzi, O.: Phys. Rev. B **56** (1997) 4186.
- 97Gos Gostein, M., Sitz, G.O.: J. Chem. Phys. **106** (1997) 7378.
- 97Gro Gross, A., Scheffler, M.: Prog. Surf. Sci. **53** (1997) 187.

- 97Iri Irigoyen, B., Ferullo, R., Castellani, N., Juan, R.: *Model. Simul. Mater. Sci. Eng.* **5** (1997) 357.
- 97Löb Löber, R., Henning, D.: *Phys. Rev. B* **55** (1997) 4761.
- 97Luh Luhmann, C.: Dissertation, Freie Universität Berlin 1997, and to be published
- 97Mat Mattsson, T.R., Wahnström, G., Bengtsson, L.: *Phys. Rev.* **B56** (1997) 2258.
- 97Men Mengel, S.K., Billing, G.D.: *J. Phys. Chem. B* **101** (1997) 10781.
- 97Nah1 Nahm, T.-U., Gomer, R.: *Surf. Sci.* **375** (1997) 281.
- 97Nah2 Nahm, T.-U., Gomer, R.: *Surf. Sci.* **380** (1997) 434.
- 97Oka Okada, M., Baddorf, A.P., Zehner, D.M.: *Surf. Sci.* **373** (1997) 145.
- 97Ols Olsen, R.A., Philipsen, P.H.T., Baerends, E.J., Kroes, G.J., Lovvik, O.M.: *J. Chem. Phys.* **106** (1997) 9286.
- 97Sti Stipe, B.C., Rezaei, M.A., Ho, W.: *J. Chem. Phys.* **107** (1997) 6443.
- 97Su Su, C., Song, K.-J., Wang, Y.L., Lu, H.-L., Chuang, T. J., Lin, J.-C.: *J. Chem. Phys.* **107** (1997) 7543.
- 97Sve Svensson, K., Andersson, S.: *Surf. Sci.* **392** (1997) L40; *Phys. Rev. Lett.* **78** (1997) 2016.
- 97Win Wintterlin, J., Trost, J., Renisch, S., Schuster, R., Zambelli, T., Ertl, G.: *Surf. Sci.* **394** (1997) 159.
- 97Yan Yanagita, H., Sakai, J., Aruga, T., Takagi, N., Nishijima, M.: *Phys. Rev. B* **56** (1997) 14952.
- 98Ali Ali, T., Walker, A.V., Klötzer, B., King, D.A.: *Surf. Sci.* **414** (1998) 304.
- 98Bae Baer, R., Zeiri, Y., Kosloff, R.: *Surf. Sci.* **411** (1998) L783.
- 98Chr Christmann, K.: in: *Electrocatalysis*, (J. Lipkowski and P. R. Ross, eds.), Wiley VCH, New York, Chichester, Weinheim 1998, Ch. 1.
- 98Doe Döll, R., Hammer, L., Heinz, K., Bedürftig, K., Muschiol, U., Christmann, K., Seitsonen, A.P., Bludau, H., Over, H.: *J. Chem. Phys.* **108** (1998) 8671.
- 98Don Dong, W., Ledentu, V., Sautet, Ph., Eichler, A., Hafner, J.: *Surf. Sci.* **411** (1998) 123.
- 98Eic Eichler, A., Kresse, G., Hafner, J.: *Surf. Sci.* **397** (1998) 116.
- 98Fri Frie, W.: *Wasserstoffadsorption auf offenen Übergangsmetalloberflächen*, Dissertation, Friedrich-Alexander-Universität Erlangen-Nürnberg, 1998
- 98Gau Gauthier, Y., Dolle, P., Baudoing-Savois, R., Hebenstreit, W., Platzgummer, E., Schmid, M., Varga, P.: *Surf. Sci.* **396** (1998) 137.
- 98Get Getzlaff, M., Bode, M., Wiesendanger, R.: *Surf. Sci.* **410** (1998) 189.
- 98Gro Groß, A.: *Appl. Phys. A* **67** (1998) 627.
- 98Ker Kern, G., Hafner, J., Kresse, G.: *Surf. Rev. Lett.* **5** (1998) 49.
- 98Led Ledentu, V., Dong, W., Sautet, P., Kresse, G., Hafner, J.: *Phys. Rev. B* **57** (1998) 12482.
- 98Lov Løvvik, O.M., Olsen, R.A.: *Phys. Rev. B* **58** (1998) 10890.
- 98Mij Mijiritskii, A.V., Wahl, U., Langelaar, M.H., Boerma, D.O.: *Phys. Rev. B* **57** (1998) 9255.
- 98Mus1 Muschiol, U., Schmidt, P.K., Christmann, K.: *Surf. Sci.* **395** (1998) 182.
- 98Mus2 Muschiol, U.: *Wechselwirkung von Wasserstoff mit der Re(10-10) und der Pd(210)-Oberfläche*, Dissertation, Freie Universität Berlin 1998
- 98Oka1 Okada, M., Baddorf, A.P., Zehner, D.M.: *Surf. Sci.* **410** (1998) 237.
- 98Oka2 Okada, M., Poker, D.B., Zehner, D.M.: *Surf. Sci.* **417** (1998) 1.
- 98Oku Okuyama, H., Siga, W., Takagi, N., Nishijima, M., Aruga, T.: *Surf. Sci.* **401** (1998) 344.
- 98Rud Rudkevich, E., Liu, F., Savage, D.E., Kuech, T.F., McCaughan, I., Lagally, M.G.: *Phys. Rev. Lett.* **81** (1998) 3467.
- 98Sch Schilbe, P., Farias, D., Rieder, K.H.: *Surf. Rev. Lett.* **5** (1998) 473.
- 98Sti Stipe, B.C., Rezaei, M.A., Ho, W.: *Science* **280** (1998) 1732.
- 98Vos Voss, M.R., Busse, H., Koel, B.E.: *Surf. Sci.* **414** (1998) 330.
- 99Arn Arnold, M., Fahmi, A., Frie, W., Hammer, L., Heinz, K.: *J. Phys. Condens. Matter* **11** (1999) 1873.
- 99Bal Balk, P.: *Microelectron. Eng.* **48** (1999) 3.
- 99Beu Beutl, M., Lesnik, J., Rendulic, K.D.: *Surf. Sci.* **429** (1999) 71.
- 99Bie Biedermann, A., Knoesel, E., Hu, Z., Heinz, T.F.: *Phys. Rev. Lett.* **83** (1999) 1810.
- 99Dar Darkrim, F., Vermesse, J., Malbrunot, P., Levesque, D.: *J. Chem. Phys.* **110** (1999) 4020.
- 99Due Dürr, M., Raschke, M.B., Höfer, U.: *J. Chem. Phys.* **111** (1999) 10411.

- 99Eic Eichler, A., Hafner, J., Groß, A., Scheffler, M.: Phys. Rev. B **59** (1999) 13297.
- 99Far Fariás, D., Schilbe, P., Patting, M., Rieder, K.-H.: J. Chem. Phys. **110** (1999) 559.
- 99Gay Gayone, J.E., Sánchez, E.A., Grizzi, O.: Surf. Sci. **419** (1999) 188.
- 99Gra Graham, A.P., Menzel, A., Toennies, J.P.: J. Chem. Phys. **111** (1999) 1676.
- 99Hag Hagedorn, C.J., Weiss, M.J., Weinberg, W.H.: Phys. Rev. B **60** (1999) R14016.
- 99Hic Hicks, R.F., Qi, H., Fu, Q., Han, B.-K., Li, L.: J. Chem. Phys. **110** (1999) 10498.
- 99Ito Ito, T., Umezawa, K., Nakanishi, S.: Appl. Surf. Sci. **147** (1999) 146.
- 99Jua Juan, A., Hoffmann, R.: Surf. Sci. **421** (1999) 1.
- 99Kis Kishi, K., Oka, A., Takagi, N., Nishijima, M., Aruga, T.: Surf. Sci. **428** (1999) 74.
- 99Kli Klinke II, D.J., Broadbelt, L.J.: Surf. Sci. **429** (1999) 169.
- 99Lui Lui, K.M., Kim, Y., Lau, W.M., Rabalais, J.W.: J. Appl. Phys. **86** (1999) 5256.
- 99Mao Mao, M.Y., Miranda, P.B., Kim, D.S., Shen, Y.R.: Appl. Phys. Lett. **75** (1999) 3357.
- 99Nie Nienhaus, H., Bergh, H.S., Gergen, B., Majumdar, A., Weinberg, W.H., McFarland, E.W.: Phys. Rev. Lett. **82** (1999) 446.
- 99Niw Niwano, M., Terashi, M., Kuge, J.: Surf. Sci. **420** (1999) 6.
- 99Ols Olsen, R.A., Kroes, G.J., Baerends, E.J.: J. Chem. Phys. **111** (1999) 11155.
- 99Our Oura, K., Lifshits, V.G., Saranin, A.A., Zotov, A.V., Katayama, M.: Surf. Sci. Rep. **35** (1999) 1.
- 99Pal Pallassana, V., Neurock, M., Hansen, L.B., Hammer, B., Nørskov, J.K.: Phys. Rev. B **60** (1999) 6146.
- 99Pay Payne, S.H., Kreuzer, H.J., Frie, W., Hammer, L., Heinz, K.: Surf. Sci. **421** (1999) 279.
- 99Pen Penev, E., Kratzer, P., Scheffler, M.: J. Chem. Phys. **110** (1999) 3986.
- 99Poh Pohl, K., Plummer, E.W.: Phys. Rev. B **59** (1999) R5324.
- 99Wan Wang, Y.M., Wong, K.W., Lee, S. T., Nishitani-Gamo, M., Sakaguchi, I., Loh, K.P., Ando, T.: Phys. Rev. B **59** (1999) 10347.
- 00Bae Bae, C., Freeman, D.L., Doll, J.D., Kresse, G., Hafner, J.: J. Chem. Phys. **113** (2000) 6926.
- 00Beu Beutl, M., Lesnik, J., Lundgren, E., Konvicka, C., Varga, P., Rendulic, K.D.: Surf. Sci. **447** (2000) 245.
- 00Car Cargnoni, F., Gatti, C., May, E., Narducci, D.: J. Chem. Phys. **112** (2000) 887.
- 00Din Diño, W.A., Kasai, H., Okiji, A.: Prog. Surf. Sci. **63** (2000) 63.
- 00Gal Gallego, S., Avila, J., Martin, M., Blase, X., Taleb, A., Dumas, P., Asensio, M.C.: Phys. Rev. B **61** (2000) 12628.
- 00Hil Hilf, M.F., Brenig, W.: J. Chem. Phys. **112** (2000) 3113.
- 00Kre1 Kresse, G.: Phys. Rev. B **62** (2000) 8295.
- 00Kre2 Kresse, G., Hafner, J.: Surf. Sci. **459** (2000) 287.
- 00Lau Lauhon, L.J., Ho, W.: Phys. Rev. Lett. **85** (2000) 4566.
- 00Lee Lee, G., Plummer, E.W.: Phys. Rev. B **62** (2000) 1651.
- 00Mor Moritani, K., Okada, M., Kasai, T., Murata, Y.: Surf. Sci. **445** (2000) 315.
- 00Pap Papoian, G., Nørskov, F.K., Hoffmann, R.: J. Am. Chem. Soc. **122** (2000) 4129.
- 00Peh Pehlke, E.: Phys. Rev. B **62** (2000) 12932.
- 00Pic Pick, S., Dreyssé, H.: Surf. Sci. **460** (2000) 153.
- 00Zim Zimmermann, F.M., Pan, X.: Phys. Rev. Lett. **85** (2000) 618.
- 01Fan Fan, C.Y., Jacobi, K.: Surf. Sci. **482-485** (2001) 21.
- 01Kae Källén, G., Wahnström, G.: Phys. Rev. B **65** (2001) 033406.
- 01Kir Kirchheim, R.: Phys. Scr. T **94** (2001) 58.
- 01Mao Mao, M.Y., Miranda, P.B., Kim, D.S., Shen, Y.R.: Phys. Rev. B **64** (2001) 035415.
- 01Nag Nagashima, A., Tazima, M., Nishimura, A., Takagi, Y., Yoshino, J.: Surf. Sci. **493** (2001) 227.
- 01Sau Sauerhammer, B., Johnson, K., Greenwood, C., Braun, W., Held, G., King, D.A.: Surf. Sci. **488** (2001) 154.
- 01Sch1 Schmidt, P.K., Christmann, K., Kresse, G., Hafner, J., Lischka, M., Groß, A.: Phys. Rev. Lett. **87** (2001) 096103.
- 01Sch2 Schmidt, P. K.: *Wechselwirkung von Wasserstoff mit einer Pd(210)-und einer Ni(210)-Oberfläche*, Dissertation, Freie Universität Berlin 2001

- 01Tok Tok, E.S., Chuan Kang, H.: J. Chem. Phys. **115** (2001) 6550.
- 01Wet Wetzig, D., Rutkowski, M., Zacharias, H., Groß, A.: Phys. Rev. B **63** (2001) 205412.
- 02Bad Badescu, Ş.C., Salo, P., Ala-Nissila, T., Ying, S.C., Jacobi, K., Wang, Y., Bedürftig, K., Ertl, G.: Phys. Rev. Lett. **88** (2002) 136101.
- 02Big Bigelow, L.K., D'Evelyn, M.P.: Surf. Sci. **500** (2002) 986.
- 02Cau Caudano, Y., Thiry, P.A., Chabal, Y.J.: Surf. Sci. **502-503** (2002) 91.
- 02Che Checchetto, R., Miotello, A., Tosello, C., Principi, G., Mengucci, P.: J. Phys. Condens. Matter **14** (2002) 6307.
- 02Due Dürr, M., Hu, Z., Biedermann, A., Höfer, U., Heinz, T.F.: Phys. Rev. Lett. **88** (2002) 0461.
- 02Jac Jacobi, K.: "Electron work function of metals and semiconductors" in *Landolt-Börnstein*, New Series, Vol. 42, subvol. A, part 2 (2002)
- 02Lis Lischka, M., Groß, A.: Phys. Rev. B **65** (2002) 075420.
- 02Nau Naumovets, A.G., Zhang, Z.: Surf. Sci. **500** (2002) 414.
- 02Oku Okuyama, H., Hossain, M.Z., Aruga, T., Nishijima, M.: Phys. Rev. B **66** (2002) 235411.
- 02Ols Olsen, R.A., Busnengo, H.F., Salin, A., Somers, M.F., Kroes, G.J., Baerends, E.J.: J. Chem. Phys. **116** (2002) 3841.
- 02Pij Pijper, E., Kroes, G.J., Olsen, R.A., Baerends, E.J.: J. Chem. Phys. **117** (2002) 5885.
- 02Ros Rosei, F., Rosei, R.: Surf. Sci. **500** (2002) 395.
- 02Smi Smit, R.H.M., Noat, Y., Untiedt, C., Lang, N.D., van Hemert, M.C., van Ruitenbeek, J.M.: Nature (London) **419** (2002) 906.
- 02Ste Steckel, J.A., Kresse, G., Hafner, J.: Phys. Rev. B **66** (2002) 155406.
- 02Zec Zecho, Th., Güttler, A., Sha, X., Jackson, B., Küppers, J.: J. Chem. Phys. **117** (2002) 8486.
- 03Bad Badescu, Ş.C., Jacobi, K., Wang, Y., Bedürftig, K., Ertl, G., Salo, P., Ala-Nissila, T., Ying, S.C.: Phys. Rev. B **68** (2003) 205401 and 209903.
- 03Che Checchetto, R., Bazzanella, N., Miotello, A., Principi, G.: J. Alloys Compounds **356** (2003) 521.
- 03Gre Greeley, J., Mavrikakis, M.: Surf. Sci. **540** (2003) 215.
- 03Gro Groß, A.: *Theoretical Surface Science*, Springer Berlin-Heidelberg 2003, p. 171
- 03Jia Jiang, D.E., Carter, E.A.: Surf. Sci. **547** (2003) 85.
- 03Lee Lee, J.Y., Maeng, J.Y., Kim, A., Cho, Y.E., Kim, A.: J. Chem. Phys. **118** (2003) 1929.
- 03Mit1 Mitsui, T., Rose, M.K., Fomin, E., Ogletree, D.F., Salmeron, M.: Surf. Sci. **540** (2003) 5.
- 03Mit2 Mitsui, T., Rose, M.K., Fomin, E., Ogletree, D.F., Salmeron, M.: Nature (London) **422** (2003) 705.
- 03Oka Okada, M., Nakamura, M., Moritani, K., Kasai, T.: Surf. Sci. **523** (2003) 218.
- 03Oku Okuyama, H., Ueda, T., Aruga, T., Nishijima, M.: Phys. Rev. B **63** (2003) 233403; 233404.
- 03Suz Suzanne, J.: "Adsorption of molecules on MgO" in: *Landolt-Börnstein*, New Series, Vol. 42, subvol. A, part 3 (2003)
- 03Tha1 Thachepan, S., Okuyama, H., Aruga, T., Nishijima, M., Ando, T., Mazur, A., Pollmann, J.: Phys. Rev. B **68** (2003) 041401R.
- 03Tha2 Thachepan, S., Okuyama, H., Aruga, T., Nishijima, M., Ando, T., Bagci, S., Tütüncü, H.M., Scrivastava, G.P.: Phys. Rev. B **68** (2003) 033310.
- 03Wie Wiechert, H.: „Adsorption of molecular hydrogen isotopes on graphite and BN“ in: *Landolt-Börnstein*, New Series, Vol. 42, subvol. A, part 3 (2003)
- 04Ale Alemozafar, A.R., Madix, R.J.: Surf. Sci. **557** (2004) 231.
- 04Kha Khatiri, A., Ripalda, J.M., Krzyzewski, T.J., Jones, T.S.: Surf. Sci. **549** (2004) 143.
- 04Kol Kolovos-Vellianitis, D., Küppers, J.: Surf. Sci. **548** (2004) 67.
- 04Kos Kostov, K.L., Widdra, W., Menzel, D.: Surf. Sci. **560** (2004) 130.
- 04Lai Lai, W., Xie, D.: Surf. Sci. **550** (2004) 15.
- 04Ogu Ogura, S., Fukutani, K., Wilde, M., Matsumoto, M., Okano, T., Okada, M., Kasai, T., Diño, W.A.: Surf. Sci. **566-568** (2004) 755.
- 04Ptu Ptushinskii, Y.G.: Low Temp. Phys. **30** (2004) 1 {Review}.
- 04Tsu Tsuboi, N., Okuyama, H., Aruga, T.: Surf. Sci. **566 - 568** (2004) 777
- 04Vin Vincent, J.K., Olsen, R.A., Kroes, G.J., Baerends, E.J.: Surf. Sci. **573** (2004) 433.
- 04Yam Yamazaki, H., Sakamoto, K., Fujii, A., Kamisawa, T.: Surf. Sci. **563** (2004) 41.

-
- 04Zha Zhang, Z., Minca, M., Deisl, C., Loerting, T., Menzel, A., Bertel, E.: Phys. Rev. **B70** (2004) 121401.
- 05Ant Antczak, G., Ehrlich, G.: Surf. Sci. **589** (2005) 52.
- 05For Ford, D.C., Xu, Y., Mavrikakis, M.: Surf. Sci. **587** (2005) 159.
- 05Luo Luo, M.F., MacLaren, D.A., Allison, W.: Surf. Sci. **586** (2005) 109.
- 05Nis Nishijima, M., Okuyama, H., Takagi N., Aruga, T., Brenig, W.: Surf. Sci. Rep. **57** (2005) 113.
- 05Per Perrier, A., Bonnet, L., Liotard, D.A., Rayez, J.-C.: Surf. Sci. **581** (2005) 189.